

Cone-like Invariant Manifolds for Nonsmooth Systems

Inaugural-Dissertation

zur

Erlangung des Doktorgrades

der Mathematisch-Naturwissenschaftlichen Fakultät

der Universität zu Köln

vorgelegt von

Hany Albadrey Hosham Bakit

aus Assiut, Ägypten

Berichterstatter: Prof. Dr. Tassilo Küpper
(Gutachter)

Prof. Dr. Rüdiger Seydel

Tag der mündlichen Prüfung: 27.06.2011

ACKNOWLEDGEMENT

I would like to express my deep and sincere gratitude to my supervisor Prof. Dr. Tassilo Küpper for his direction and guidance. He has unselfishly given his time, expertise, his dedication, and interesting discussions without which this research would not have been possible. It has been my great pleasure and honor to work closely with him.

I would like to give a special thanks to Dr. Daniel Weiss for his kindness, friendship; he has provided assistance in some way to this thesis.

I give special thanks to the staff of the mathematical institute at the university of Cologne for their assistance. Thanks are due to my friends for their moral support, good wishes and the memorable days shared together.

Abstract

This thesis deals with rigorous mathematical techniques for higher-dimensional nonsmooth systems and their applications. Motivated by various examples of nonsmooth systems in applications, we propose to explore the concept of invariant surfaces in the phase space which is separated by a discontinuity hypersurface. For such systems the corresponding Poincaré map can be determined; it turns out that under suitable conditions an invariant cone occurs which is characterized by a fixed point of the Poincaré map. The invariant cone seems to serve in a similar way as a generalisation of the classical center manifold for smooth differential systems. Hence, the stability of the whole system can be reduced to investigate the stability on the two-dimensional surface of the cone. Motivated to study the generation of invariant cones out of smooth systems, a numerical procedure to establish invariant cones and their stability is presented. It has been found that the flat degenerate cone in a smooth system develops under nonsmooth perturbations into a cone-like configuration. Also a simple example is used to explain a paradoxical situation concerning stability. Theoretical results concerning the existence of invariant cones and possible mechanisms responsible for the observed behavior for general three dimensional nonsmooth systems are discussed. These investigations reveal that the system possesses a rich dynamic behavior and new phenomena such as, for instance, the existence of multiple invariant cones for such system.

Our approach is developed to include the case when sliding motion takes place on the manifold. Sliding dynamical equations are formulated by using Filippov's method. Existence of invariant cones containing a segment of sliding orbits are given as well as stability on these cones. Different sliding bifurcation scenarios are treated by theoretical analysis and simulation.

As an application we have investigated the dynamics of an automotive brake system model under the excitation of dry friction force which has served as a motivating example to develop our concepts. This model belongs to the class of nonsmooth systems of Filippov type which is investigated from direct crossing and a sliding motion point of view. Existence of invariant cones and different types of bifurcation phenomena such as sliding periodic doubling and multiple periodic orbits are observed.

Finally, extensions to nonlinear perturbations of nonsmooth linear systems have been obtained by using the nonsmooth linear system as basic system. If the basic system possesses an attractive invariant cone without sliding motion, we have shown that locally the Poincaré map contains the necessary information with regard to attractivity of the invariant cone. The existence of a generalized center manifold reduction of nonlinear system has been proven by using Hadamard graph transformation approach. A class of nonlinear systems having a cone-like invariant "manifold" is presented to illustrate the center manifold reduction and associated bifurcation.

The scientific contributions of parts of this thesis are presented in [32, 39, 66].

Zusammenfassung

In dieser Dissertation werden mathematische Verfahren für höher dimensionale nicht-glatte Systeme und deren Anwendung behandelt. Aufgrund der Nicht-Glattheit der Systeme ist die Untersuchung des dynamischen Verhaltens keine lokale Problemstellung mehr. Angeregt durch Anwendungen von nicht-glaten Systemen untersuchen wir das Konzept von invarianten Ebenen in Phasenräumen, welche durch eine Unstetigkeitsebene getrennt sind. Für solche Systeme kann die entsprechende Poincaré-Abbildung bestimmt werden; unter geeigneten Bedingungen kann ein invarianter Kegel entstehen, welcher durch die Fixpunkte der Poincaré-Abbildung charakterisiert ist. Der invariante Kegel kann auf ähnliche Weise wie die Verallgemeinerung der klassischen Zentrumsmannigfaltigkeit für Systeme von Differentialgleichungen behandelt werden. Folglich kann die Stabilität des ganzen Systems auf die Untersuchung der Stabilität auf einer zwei-dimensionalen Ebene des Kegels reduziert werden. Um die Entstehung invarianter Kegel aus glatten Systemen heraus zu studieren, werden numerische Methoden zur Bestimmung invarianter Kegel und deren Stabilität aufgezeigt. Es wird festgestellt, dass unter nicht-glaten Störungen in glatten Systemen ein Kegel entsteht; ein einfaches Beispiel dient zur Erläuterung der paradoxen Ergebnisse bezüglich Stabilität. Theoretische Analyse der Existenz von invarianten Kegeln sowie mögliche Mechanismen, die für das beobachtete Verhalten in allgemeinen drei-dimensionalen nicht-glaten Systemen verantwortlich sind, werden diskutiert. Diese Untersuchungen brachten die Erkenntnis, dass das System ein vielfältiges dynamisches Verhalten aufweist sowie neue Phänomene, wie zum Beispiel die Existenz mehrerer invarianter Kegel in einem solchen System. Unser Ansatz berücksichtigt auch die Situation, wenn "Sliding Motion" auf der Mannigfaltigkeit stattfindet. Die "Sliding"-Bewegung des dynamischen Systems wird durch die Filippov Methode beschrieben. Neben der Existenz von invarianten Kegeln mit einem "Sliding"-Segment werden sowohl die Stabilität dieser Kegel als auch verschiedene "Sliding"-Bifurkationsszenarien anhand theoretischer Analysen und Simulationsergebnissen behandelt. Außerdem untersuchen wir das dynamische Verhalten in Kraftfahrzeugbremsystemen unter Anregung von trockener Reibung. Dieses Modell ist bei nicht-glaten Systemen der Filippov Klasse einzuordnen und wird aus der Sicht von "Direct Crossing" und "Sliding"-Motion

untersucht. Die Existenz von invarianten Kegeln und verschiedene Bifurkationsphänomene, wie beispielsweise die Sliding-Periodenverdopplung und mehrfache periodische Orbits, können beobachtet werden. Eine Erweiterung der nicht-linearen Störungen von nicht-glatten linearen Systemen wird unter Verwendung von nicht-glatten linearen Systemen als Grundsystem erreicht. Die Grundsysteme weisen einen attraktiven Kegel ohne "Sliding Motion" auf; wie bereits gezeigt, enthält die lokale Poincaré-Abbildung die wesentlichen Informationen bezüglich der Attraktivität invarianter Kegeln. Die Reduktion auf eine verallgemeinerte Zentrumsmannigfaltigkeit wird mittels Hadamard-Transformation bewiesen. Zur Veranschaulichung der Reduktion auf Zentrumsmannigfaltigkeit sowie der entsprechenden Bifurkationen wird eine Klasse von nicht-linearen Systemen, welche ein kegelartige "Mannigfaltigkeit" aufweisen, dargestellt.

Contents

1	Introduction and Objectives	1
1.1	Motivation and objectives	1
1.2	Invariant manifold concept	5
1.3	Nonsmooth dynamical systems	9
1.4	Filippov's solution concept	11
1.5	Poincaré map	12
1.6	Classification of bifurcations	13
1.6.1	Discontinuity-induced bifurcations	14
1.6.2	Generalized Hopf bifurcation	15
1.7	Outline of the thesis	16
2	Invariant cones for a class of a high-dimensional PWS	18
2.1	N-dimensional PWS	18
2.2	The basic piecewise linear problem	22
2.3	Generation of invariant cones for PWLS	25
2.3.1	Bordering algorithm	27
2.3.2	Periodic orbits via Hopf-points	29
2.3.3	Parameter dependent stability switches on invariant cones . .	31
2.4	Theoretical analysis for general situation	35
2.4.1	Existence of periodic orbits	36
2.4.2	Case I: $\alpha^\pm = \beta^\pm = \sigma^+ = 0, k^\pm = \gamma^\pm = 1, \sigma^- = -\delta$	41
2.4.3	Case II: $\alpha^\pm = -1, \beta^\pm = \lambda^\pm, k^\pm = \omega^\pm, \sigma^\pm = \mu^\pm, \gamma^\pm =$ $(\lambda^\pm)^2 + (\omega^\pm)^2$	44
2.4.4	Case III: $\alpha^+ = -1, \alpha^- = \alpha, \beta^- = \sigma^\pm = 0, \beta^+ = \lambda^+; k^\pm =$ $\gamma^\pm = 1$	45
2.4.4.1	One-parameter bifurcation for invariant cone	48
2.4.4.2	Existence of multiple cones	49
2.4.5	Mechanism to generate an invariant cone and its stability . .	50
3	Invariant cones for a class of systems with sliding motion	56
3.1	Sliding mode, dynamics on \mathcal{M}_\pm^s	56

3.2	Sliding bifurcations	58
3.2.1	Crossing-sliding Bifurcations	59
3.2.2	Grazing-sliding bifurcation	59
3.2.3	Switching-sliding bifurcation	59
3.2.4	Adding-sliding bifurcation	60
3.3	Fundamental matrix solutions	61
3.3.1	Monodromy matrix in PWS with sliding	62
3.4	Invariant cones with sliding motion for PWLS	63
3.5	Analysis of a class of 3D PWLS	65
3.5.1	Detecting sliding region	65
3.5.2	Vector field of sliding motion	66
3.5.3	Generalized Poincaré map	67
3.5.4	One-zonal invariant cone	71
3.5.5	Two-zones invariant cones (Crossing + Sliding)	73
3.5.6	Two-zones invariant cones (Sliding + Crossing)	77
3.6	Invariant cones: Sliding bifurcation	77
4	A 6-dimensional non-smooth brake-system	83
4.1	Introduction	83
4.2	General description of model	85
4.2.1	Mathematical model	85
4.2.2	Simplification and reduction	86
4.3	Smooth system	88
4.4	Non-smooth model	92
4.4.1	Detecting crossing and sliding regions	92
4.4.2	Construction of Poincaré maps	93
4.5	Case $\alpha = 0, \beta \neq 0$	94
4.6	Simulation results	97
5	Invariant manifold for PWS	104
5.1	Introduction	104
5.2	Properties of PWLS	106
5.3	The piecewise nonlinear system (PWNS)	108
5.3.1	The Poincaré map	108
5.3.2	Hadamard's Graph Transform	111
5.4	Bifurcation	117
5.5	Class of PWNS	119
5.5.1	Case I: $\alpha = \rho_- = 0$	119
5.5.2	Case II: $\delta = 0, \alpha = 1$	121
6	Summary and future work	126

7	Appendix	129
7.1	Appendix A	129
7.2	Appendix B	130

List of Figures

1.1	Pendulum with dry friction.	2
1.2	A simplified model and brake system for a bike.	3
2.1	Partitioned separation manifold: (a) and (b) are sectors of direct crossing, (c) is sector of attractive sliding motion, (c) is a sector of repulsive sliding motion.	19
2.2	Different dynamics on cones, $\mu_c < 1$, $\mu_c = 1$ and $\mu_c > 1$, respectively.	25
2.3	Attractive invariant cone consisting of periodic orbits $\beta = 1.5$, $\alpha = 0.6$, $t_- = t_+ = 3.5138$	32
2.4	Repulsive invariant cone consisting of periodic orbits $\beta = 0.01$, $\alpha = 0.0175$, $t_- = 3.0664$ $t_+ = 2.8229$	32
2.5	An attractive invariant cone with unstable orbits even though all eigenvalues of A^\pm has negative real parts.	33
2.6	Location of direct/sliding motion if $a_{12}^\pm > 0$, $a_{13}^\pm > 0$, there is no periodic orbit if $-\frac{a_{12}^-}{a_{13}^-}\xi_2 > \xi_3 > -\frac{a_{12}^+}{a_{13}^+}\xi_2$	37
2.7	Location of direct/sliding motion if $a_{12}^\pm > 0$, $a_{13}^- > 0$, $a_{13}^+ < 0$, there is no periodic orbit if $-\frac{a_{12}^-}{a_{13}^-}\xi_2 < \xi_3 < -\frac{a_{12}^+}{a_{13}^+}\xi_2$	37
2.8	Structure of invariant cone with slope transition maps	38
2.9	Attractive invariant cone consists of periodic orbits for $\lambda^+ = -\lambda^- = 1$, $\omega^\pm = 1$, $\mu^- = -1.5$, $\mu^+ = 1.2$	43
2.10	Repulsive invariant cone consists of periodic orbits for $\lambda^+ = -\lambda^- = 1.0$, $\omega^\pm = 1.0$, $\mu^- = -1.5$, $\mu^+ = 1.62$	43
2.11	Graph of $n_0(t_+)$ for parameter values $\lambda^+ = -\lambda^- = 0.6$, $\mu^+ = -1.13$, $\mu^- = 0.4266$, $\omega^\pm = 1$	49
2.12	Two attractive invariant cones, $\lambda^+ = -\lambda^- = 0.6$, $\mu^+ = -1.13$, $\mu^- = 0.4266$, $\omega^\pm = 1$ where $t_+ = \pi$ for the flat cone and $t_+ = 1.1306$ for the other.	50
2.13	An invariant cone with (center+stable focus), $\omega^\pm = \lambda^+ = 1$, $\lambda^- = 0.3338$, $\mu^+ = 0.2027$, $\mu^- = -0.1014$, $t_+ = 0.3\pi$ and $t_- = 0.6\pi$.	53

2.14	Two invariant cones where both are of (center+unstable focus), $\omega^\pm = 1, \lambda^+ = -\lambda^- = -.5, \mu^+ = -1.5, \mu^- = 1.6203, t_+ = 3.76$ and $t_- = 3.48$	53
2.15	Different dynamics on cones, Attractive/ periodic / repulsive, for $\mu^- = -1.0, \omega^+ = \omega^- = 1, \lambda^- = -0.7832, t_+ = \pi, t_- = 3\pi/4,$ (a) $\lambda^+ = 0.7768, \mu^+ = 0.7165.$ (b) $\lambda^+ = 0.8103, \mu^+ = 0.7500.$ (c) $\lambda^+ = 0.8406, \mu^+ = 0.7803.$	55
2.16	Two attractive invariant cone, $\lambda^+ = -0.5, \mu^+ = 0.1751, \omega^\pm = 1.0,$ $\lambda^- = 0.5, \mu^- = -1.0, t_+ = \pi,$ where $t_- = \pi$ for the flat cone and $t_- = 0.5505$ for the other.	55
3.1	Filippov (F) and Utkin (U) methods	58
3.2	Structures of sliding bifurcation	60
3.3	Location of attractive sliding motion \mathcal{M}_s^s	66
3.4	Invariant cone (only Sliding) with sliding segment and solution com- ponents: $\lambda^+ = 1.3, \mu^+ = -0.5, \omega^+ = 0.9, \alpha^+ = 0, \lambda^- = 1, \mu^- =$ $0.212, \omega^- = 3.0.$	72
3.5	Poincaré map structure is a composition of three maps P_\pm, P_s	74
3.6	Invariant cone (Crossing + Sliding) with sliding segment and solu- tion components: $\lambda^+ = 0.3, \mu^+ = -0.087, \omega^+ = 1.0, \alpha^+ = 0, \lambda^- =$ $1.0, \mu^- = 0.1, \omega^- = 3.0.$	75
3.7	Invariant cone (Sliding + Crossing) with sliding segment and solution components: $\lambda^+ = 1.8, \mu^+ = 10.0, \omega^+ = 28.0, \lambda^- = 0.185, \mu^- =$ $-1.0, \omega^- = 5.0.$	76
3.8	Invariant cone and solution components at the crossing-sliding bifur- cation point, $\lambda^- = 0.9654.$	79
3.9	Invariant cone and solution components after the crossing-sliding bi- furcation point, $\lambda^- = 0.95.$	79
3.10	One-zonal invariant cone and solution components at grazing-sliding bifurcation point.	80
3.11	One-zonal invariant cone and solution components after grazing-sliding bifurcation point, $\lambda^+ = \mu^+ = \alpha^+ = 0$ and $\omega^+ = 1$	80
3.12	Invariant cone and solution components at the switching-sliding bi- furcation point.	82
3.13	Invariant cone and solution components after the switching-sliding bifurcation point	82
4.1	Three-degree-of-freedom brake system model	85

4.2	Solution components behaviour with presence of damping and time increases, there is only one periodic orbit in (z_2, z_5) -plane for the coefficients as in Table 4.1	91
4.3	Invariant cone and periodic time series with fix all parameters in Table 4.1 and $\mu_2 = 0.00014$ is quite small, $c = 1.8E7$, $d = 0$ where (a)-(c) without sliding $z \in \mathcal{M}_+^c$, (d) starting point $z \in \mathcal{M}_-^s$	99
4.4	Invariant cones and solution components, existence of 4-periodic orbit due to spring parameter without sliding motion.	100
4.5	Invariant cones and solution components, existence of double-sliding periodic orbit when $d = 467.9$	101
4.6	Invariant cones and solution components, existence of 3-sliding periodic orbit when $d = 468.9$	102
4.7	Invariant cones and solution components, existence of 4-sliding periodic orbit when $\alpha \neq 0, \beta \neq 0$	103
5.1	ε -sector of the cone in \mathcal{M}	108
5.2	An attractive \mathcal{C} with invariant graph $H(y)$ of PWNS.	120
5.3	Two attractive invariant cones of PWLS for $\mu^- = \mu_0^-$	123
5.4	Two generalized center manifolds of PWNS ($\rho^- = -0.01, \rho^+ = 0.1$) for $\mu^- = \mu_0^-$	123
5.5	Stable periodic orbit of PWNS for $\mu^- = -1.06 > \mu_0^-$	124

Chapter 1

Introduction and Objectives

”Der Anfang der Erkenntnis ist die Entdeckung von etwas, das wir nicht verstehen.”

Frank Herbert (1920-1986)

In this chapter we motivate our research and give an introduction to the subject and define the objective and scope of this work.

1.1 Motivation and objectives

Common physical phenomena in engineering, biological and medical systems such as friction, impact and backlash can be described by mathematical models with some kind of discontinuity or nonsmoothness. A system model with nonsmoothness is sometimes referred to as a discontinuous differential system (*nonsmooth dynamical system* or *piecewise smooth system*). An important source for nonsmoothness is due to dry friction arising in dampers, drilling processes or rail-wheel contacts audible as creaking. A simple instance of a mechanical system is a point mass falling down to the ground with one unilateral contact. In planar nonsmooth modeling, the point mass’s two degrees of freedom are reduced to one when the point mass touches the ground. If friction is considered additionally, then the degrees of freedom are reduced to zero in the case of sticking. Thus, there are different equations of motion in minimal coordinates for these different configurations. In case of an impact, an additional impact law must be applied. Many situations can be considered in this way. Hence, we list some simple examples which have been used as model examples in the investigation of nonsmooth systems:

(i) **Pendulum with friction** [22].

The equation of motion of the system in Figure 1.1 is

$$\ddot{x} + x + a \operatorname{sgn} \dot{x} = p(t).$$

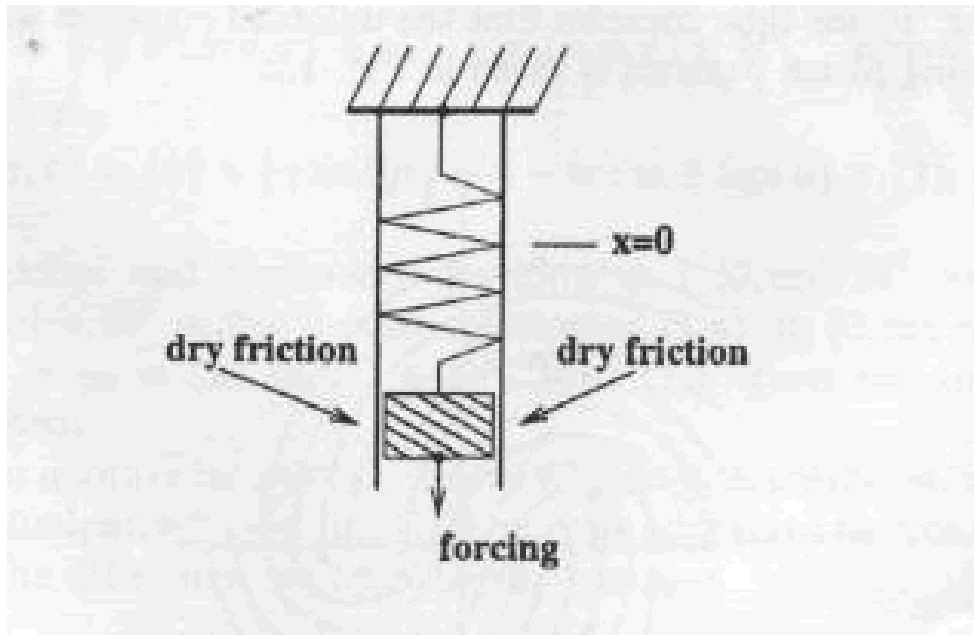


Figure 1.1: Pendulum with dry friction.

where $p(t)$ is a periodic forcing, $\text{sgn } r = r/|r|$ for all $r \in \mathbb{R} \setminus \{0\}$ and a parameter $a > 0$.

(ii) Relay control systems [70].

Relay control systems are of the most commonly used control techniques in practical applications. A single-input single-output relay feedback system is often well modeled by equations of the form

$$\begin{aligned}\dot{x} &= Ax + bu, \\ \zeta &= Cx, \\ u &= \text{sgn}(\zeta),\end{aligned}$$

where $x \in \mathbb{R}^n$ is the state vector, $A \in \mathbb{R}^{n \times n}$, $B \in \mathbb{R}^{n \times 1}$ and $C \in \mathbb{R}^{1 \times n}$ are constant matrices, ζ is the input signal to the relay element or switch, u is the output signal of the relay.

(iii) Brake system for a bike [74].

The mathematical model is a system of two differential equations:

$$\begin{aligned}m\ddot{x} + d_1\dot{x} + c_1x &= \sigma^+(x, \dot{x}, \lambda), & \text{if } x > 0 \\ m\ddot{x} + (d_1 + d_2)\dot{x} + (c_1 + c_2)x &= \sigma^-(x, \dot{x}, \lambda), & \text{if } x < 0\end{aligned}$$

where the mass rests on a smooth surface and is connected to the walls by springs c_j and dampers d_j , $j = 1, 2$, σ^\pm represent external force and λ is a free parameter,

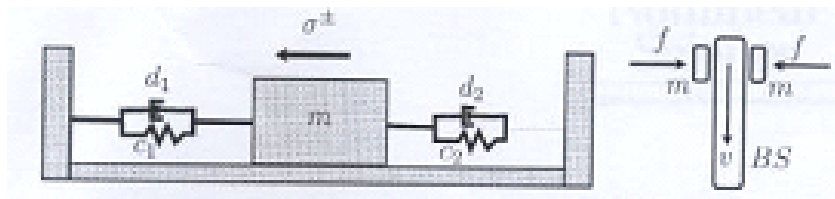


Figure 1.2: A simplified model and brake system for a bike.

see Figure 1.2.

Further applications have been investigated as nonsmooth systems such as mechanical systems including the occurrence of impact motion [7, 40, 49], vibro-impacting systems modeled by nonsmooth systems [44], stick-slip motion in oscillators with friction [56], switching in electronic circuits [5, 15] and examples of relevance to applications which are modelled by systems with nonsmooth nonlinearities [26, 27, 31, 44, 63].

Due to the nonsmoothness that appears in the system model, classical theories of differential systems are no longer applicable. Filippov's differential inclusions [24, 25, 61], evolution variational inequalities [1] and complementarity dynamical systems [30] are commonly used to study nonsmooth system. These approaches depend on the purpose of the model system at hand and the degree of nonsmoothness. The focus of this thesis is on Filippov's differential inclusions. General results concerning the theory of differential inclusions can be found in [24, 25], where in particular the standard concepts concerning existence, uniqueness, continuous dependence and stability are covered. These aspects do not address the issue of bifurcations that arise specifically from Filippov systems with nonsmooth behavior.

Filippov's differential inclusion provides a set of possible candidates for motion switching or sliding, Filippov systems can exhibit a wide range of nonlinear phenomena including bifurcations and chaos. In addition to classical bifurcations (occurring in smooth systems), nonsmooth systems can exhibit unique phenomena such as for instance *discontinuity-induced bifurcations*.

More recent investigations focus on classifying, unfolding and applying novel kinds of bifurcation that are unique to nonsmooth systems. For a review of the available results see [14–16, 44, 70]. We note that the current theory of bifurcations for nonsmooth systems is still incomplete.

In planar nonsmooth systems, existence of periodic orbits by means of Hopf-like bifurcation, existence of sliding motion with bifurcations, homoclinic or heteroclinic orbits and discontinuity-induced bifurcations of periodic orbits can be studied by taking a Poincaré section transversal to these orbits and analysing the resulting return map. In this manner, bifurcations in planar nonsmooth dynamical systems are rather well understood [14, 15, 48, 71–74], but we know of no general result valid in n -dimensions. The notation PWS refers to n -dimensional nonsmooth system, when one can identify a finite number of $(n - 1)$ -dimensional boundaries, such that the

system is locally smooth outside these boundaries.

The main objective of this thesis is to derive results concerning the dynamics, bifurcations and stability of PWS using the concept of cone-like invariant manifolds. For smooth dynamical systems the bifurcation theory is quite well developed, the reduction of smooth dynamical systems to lower dimensional center manifolds containing the essential bifurcation dynamics is a very useful approach both for theoretical investigations as well as for numerical computation. This approach and the implementation requires smoothness properties and the existence of a basic linearization at the equilibrium point; in particular the number of purely imaginary eigenvalues and the corresponding eigenvectors define the reduced space. This approach is not available in PWS. At the present time many results are already known about the dynamics of planar PWS [41, 71–74]. The occurrence of periodic orbits due to Hopf-bifurcation relies on an analytical criterium of eigenvalues crossing the imaginary axis. Since an appropriate definition of eigenvalues does not exist in the case of PWS the geometric equivalent of a change in the phase space from a stable focus to an unstable focus via a center has been used for planar systems. For planar systems the approach to split the system into a basic piecewise linear system and nonsmooth higher order terms has been successful, since a suitable Poincaré map could be derived. It has been shown that the occurrence of periodic orbits in terms of “generalized Hopf” bifurcation can be achieved. In that way, for higher dimensional smooth systems that approach goes along with a reduction to a lower dimensional system. Of course a similar result is desired for nonsmooth system as well. Of course for planar systems there is no need for any reduction of the system.

According to the researchers in PWS [10, 11, 14, 15, 45, 74], there is no result at hand on the existence of invariant manifolds for high dimensional PWS since the extension to higher dimensional systems is more complicated. This means that the reduction of a PWS from high dimension to low dimension is not available so far. First ideas for three dimensional systems have already been sketched in [38, 39].

In this work the “generalized Hopf” bifurcation for PWS in dimensions exceeding 2 will be worked out as well as the development of methods to reduce a high dimensional PWS to a low dimensional one. For such systems ($n \geq 3$) the corresponding Poincaré map can be determined; it turns out that under suitable conditions an invariant cone occurs which is characterized by an “eigenvector” ξ corresponding to an eigenvalue $\mu_c > 0$ of the Poincaré map. The invariant cone can be regarded as a generalization of the standard center manifold in smooth system which allows the reduction of the large system to an invariant two-dimensional surface on the cone. The existence of invariant cones seems to play an important role in the dynamic behaviour of PWS to characterize in particular topological type and stability

of equilibrium points.

We now address each aspect of our results in the following:

- Generation of invariant cones based on smooth systems.
- Existence of invariant cones for PWS and associated bifurcations.
- Generalized Hopf Bifurcation: Generation of periodic orbits.
- Bifurcations of sliding solutions for PWS in case of having invariant cone.
- Analysis of dynamics and bifurcation for a six-dimensional PWS brake system.
- Reduction of a PWS from high dimension to low dimension via existence of generalized center manifold.

This study is concerned with the analysis of bifurcations in n -dimensional PWS. We present detailed examples of standard and nonstandard bifurcation with the help of the notion of invariant cones.

1.2 Invariant manifold concept

Smooth dynamical systems for example occur as sets of ordinary differential equations that arise in scientific problems and engineering applications of the form

$$\dot{\xi} = f(\xi, \lambda) \tag{1.1}$$

where the function $f : \mathbb{R}^n \times \mathbb{R}^p \rightarrow \mathbb{R}^n$ is sufficiently smooth and depends on a real parameter $\lambda \in \mathbb{R}^p$, $n, p \in \mathbb{N}$. In smooth systems there exist well-developed qualitative mathematical tools to describe bifurcations and stability such as the computation of Lyapunov exponents, the reduction to lower dimensional manifolds like the center manifold or a direct determination of the bifurcation behaviour [37, 58, 67].

To understand the often complicated dynamical behaviour it is a well established tool to use the concept of invariant manifolds of the system. In this way, we briefly recall some of the background relevant to the concepts of invariant manifolds for smooth systems (1.1).

Definition 1.1. *Let \mathcal{C} be a nonempty subset of \mathbb{R}^n . \mathcal{C} is said to be invariant with respect to motions of (1.1) if for each initial value $\xi^0 \in \mathcal{C}$, the motion emanating from ξ^0 remains in \mathcal{C} for all times. For a discrete system \mathcal{C} is said to be invariant under the map $\xi \rightarrow g(\xi)$ if for any $\xi^0 \in \mathcal{C}$ we have $g^n(\xi^0) \in \mathcal{C}$ for all $n \in \mathbb{Z}$.*

If we restrict ourselves to positive times (i.e., $t \geq 0$) then we refer to \mathcal{C} as a *positively invariant* set and, for negative time as a *negatively invariant* set.

Let $\{\varphi(t)\}_{t \geq 0}$ be an operator semi-group generated by (1.1), which enjoys the following properties

- (i) $\varphi(t) : \mathbb{R}^n \rightarrow \mathbb{R}^n$,
- (ii) $\varphi(0)$ identity on \mathbb{R}^n ,
- (iii) $\varphi(t + s) = \varphi(t) \cdot \varphi(s)$, $t, s \geq 0$.

Then the solution of (1.1) can be expressed as

$$\xi(t, \xi^0) = \varphi(t)\xi^0 = \varphi(t, \xi^0), \quad \forall t \geq 0.$$

Definition 1.2. [46]. *An invariant set $\mathcal{C} \subset \mathbb{R}^n$ of (1.1) is called an attractor if \mathcal{C} is compact, and if there exists a neighborhood $U \subset \mathbb{R}^n$ of \mathcal{C} , such that for any $\xi^0 \in U$ we have*

$$\text{dist}(\varphi(t, \xi^0), \mathcal{C}) \rightarrow 0 \text{ in } \mathbb{R}^n - \text{norm as } t \rightarrow \infty. \quad (1.2)$$

The largest open set U satisfying (1.2) is called the basin of attraction of \mathcal{C} .

Definition 1.3. [14]. *A point p is an ω -limit point of a trajectory $\varphi(t, \xi^0)$ if there exists a sequence of times $t_1 < t_2 < \dots$ with $t_i \rightarrow \infty$ as $i \rightarrow \infty$ such that $\varphi(t_i, \xi^0) \rightarrow p$ as $t_i \rightarrow \infty$. If instead there exists a sequence of times with $t_1 > t_2 > \dots$ and $t_i \rightarrow -\infty$ and $\varphi(t_i, \xi^0) \rightarrow p$, then we say that p is an α -limit point of ξ^0 . The ω -(α -) limit set of ξ^0 is the set of all possible ω -(α -) limit points. The set of all such ω -limit points (or α -limit points) for all $\xi^0 \in \mathbb{R}^n$ is called the ω -limit set (or α -limit set) of the system. This set is closed and invariant.*

The smooth system (1.1) can exhibit the following kinds of invariant sets:

Equilibria. The simplest form of an invariant set of (1.1) is an equilibrium solution ξ^* which satisfies $f(\xi^*) = 0$. These are also called stationary solution of the flow since $\varphi(t, \xi^*) = \varphi(0, \xi^*)$ for all t .

Limit cycles. A periodic orbit is an invariant set, which is determined by an initial condition ξ^0 and a period T . Here T is defined as smallest time $T > 0$ for which $\varphi(T, \xi^0) = \xi^0$. By definition a limit cycle is isolated.

Invariant tori. Invariant tori are the nonlinear equivalent of two-frequency motions. Further, an invariant torus may possess a quasi-periodic solutions which can degenerate into chaotic solutions, if the tori surfaces become unstable.

Homoclinic and heteroclinic orbits. Another class of invariant sets are connecting orbits, which tend to other invariant sets as time runs to $+\infty$ and to $-\infty$, more details can be found in [37, 67].

Further interesting invariant objects are obtained for example as manifolds.

Definition 1.4. [67]. *An invariant set $\mathcal{C} \subset \mathbb{R}^n$ is said to be a \mathbf{C}^k ($k \geq 1$) invariant manifold if \mathcal{C} has the structure of a \mathbf{C}^k differential manifold. Similarly, a positively (res., negatively) invariant set $\mathcal{C} \subset \mathbb{R}^n$ is said to be a \mathbf{C}^k positively (res., negatively) invariant manifold if \mathcal{C} has the structure of a \mathbf{C}^k differential manifold.*

A manifold is a set which locally has the structure of Euclidean space. In applications, manifolds are most often met as m -dimensional surfaces embedded in \mathbb{R}^n . If the surface has no singular points, i.e., the derivative of the function representing the surface has maximal rank, then by the implicit function theorem it can locally be represented as a graph. The surface is a \mathbf{C}^k manifold if the (local) graphs representing it are \mathbf{C}^k .

We recall the smooth system (1.1) with a stationary solution $\xi^*(0) = 0$. Using linearization and transformations according to the structure of the eigenvalues of the linearization $A := Df(\xi^*)$, $D = \frac{\partial f}{\partial \xi}$ of f , equation (1.1) can be stated in the following form with $\xi = (x, y, z)^T$ and an accordingly arranged matrix A

$$A = \begin{pmatrix} A^- & 0 & 0 \\ 0 & A^0 & 0 \\ 0 & 0 & A^+ \end{pmatrix},$$

where the submatrices A^- , A^0 and A^+ correspond to the eigenvalues λ_i in the spectrum $\sigma(A) = \sigma(A^-) \cup \sigma(A^0) \cup \sigma(A^+)$ of A with negative, vanishing and positive real part respectively:

$$\widehat{\begin{pmatrix} x \\ y \\ z \end{pmatrix}} = \begin{pmatrix} A^- & 0 & 0 \\ 0 & A^0 & 0 \\ 0 & 0 & A^+ \end{pmatrix} \begin{pmatrix} x \\ y \\ z \end{pmatrix} + \begin{pmatrix} g_-(x, y, z, \lambda) \\ g_0(x, y, z, \lambda) \\ g_+(x, y, z, \lambda) \end{pmatrix}, \quad (1.3)$$

here g_- , g_0 and g_+ collect terms of higher order in x, y and z .

Theorem 1.1. [67]. *Suppose (1.3) is \mathbf{C}^k , $k \geq 2$. Then the equilibrium point 0 of (1.3) possesses a \mathbf{C}^k s -dimensional local, stable manifold, $W_{loc}^-(0)$, a \mathbf{C}^k u -dimensional local, unstable manifold, $W_{loc}^+(0)$, and a \mathbf{C}^k c -dimensional local, center manifold, $W_{loc}^0(0)$, all intersecting at 0 . These manifolds are all tangent to the respective invariant subspaces of the linear vector field $\dot{\xi} = A\xi$ at the origin, and hence, are locally representable as graphs. In particular, we have*

$$\begin{aligned} W_{loc}^-(0) &= \{(x, y, z) \in \mathbb{R}^n \mid y = H_y^-(x), z = H_z^-(x); DH_y^-(0) = 0, DH_z^-(0) = 0; \\ &\quad |x| \text{ sufficiently small}\}, \\ W_{loc}^0(0) &= \{(x, y, z) \in \mathbb{R}^n \mid x = H_x^0(y), z = H_z^0(y); DH_x^0(0) = 0, DH_z^0(0) = 0; \\ &\quad |y| \text{ sufficiently small}\}, \\ W_{loc}^+(0) &= \{(x, y, z) \in \mathbb{R}^n \mid x = H_x^+(z), y = H_y^+(z); DH_x^+(0) = 0, DH_y^+(0) = 0; \\ &\quad |z| \text{ sufficiently small}\}, \end{aligned}$$

where $H_y^-(x)$, $H_z^-(x)$, $H_x^0(y)$, $H_z^0(y)$, $H_x^+(z)$, and $H_y^+(z)$ are \mathbf{C}^k functions.

The following subsection explains as in [39] how to perform the reduction of the original system (1.1) to the center manifold using Theorem 1.1.

Since the stationary solution is already unstable if $\sigma(A^+) \neq \emptyset$, we assume for simplicity that $\sigma(A^+) = \emptyset$, hence equation (1.1) is equivalent to

$$\begin{aligned}\dot{x} &= A^-x + g^-(x, y, \lambda) \\ \dot{y} &= A^0y + g^0(x, y, \lambda).\end{aligned}\tag{1.4}$$

The center manifold approach performs a locally equivalent reduction to a system defined in the center space, i.e. there exists a function H , defined in a neighborhood of $\bar{y} = 0$ in the center space mapping into the stable space satisfying $H(0) = 0$, $\frac{\partial H}{\partial y}(0) = 0$ such that the reduced equation

$$\dot{y} = A^0y + g^0(H(y), y, \lambda),\tag{1.5}$$

is locally equivalent to (1.4).

The advantage of this approach relies on the fact that usually in relevant applications $n^0 := \dim y \ll n$, typically $n^0 = 1$ or $n^0 = 2$.

Once (1.5) has been established the dynamics, stability and bifurcation behavior of (1.1) can be obtained by studying (1.5). The underlying center manifold approach essentially depends on smoothness properties of the original problem using the properties of the linearized problem. For Piecewise smooth dynamical systems (PWS) linearization is not at hand due to a lack of smoothness. The 5th chapter is dedicated to the study of the existence of generalized center manifolds for PWS.

Further we will need the well known:

Theorem 1.2 (Implicit Function Theorem). *Let $f : D \rightarrow \mathbb{R}^n$; $D \subset \mathbb{R}^n \times \mathbb{R}^p$ be a function of class \mathbf{C}^k ($k \geq 1$) on an open neighborhood $D_0 \subset D$ of a point (x^0, y^0) for which $f(x^0, y^0) = 0$. Assume that $D_x f$ exists in a neighborhood of (x^0, y^0) and is continuous at (x^0, y^0) , and that $D_x f(x^0, y^0)$ is nonsingular. Then there exist open sets $S_1 \subset \mathbb{R}^n$ and $S_2 \subset \mathbb{R}^n$ of x^0 and y^0 , respectively, such that,*

- For any $y \in \bar{S}_2$, there exists a unique solution $x = H(y) \in \bar{S}_1$ for $f(x, y) = 0$.
- The function $H : S_2 \rightarrow \mathbb{R}^n$, defined above, is \mathbf{C}^k .
- If $D_y f(x^0, y^0) \neq 0$ then $D_y H(y^0) = -[D_x f(x^0, y^0)]^{-1} D_y f(x^0, y^0)$.

Proof. See [51].

1.3 Nonsmooth dynamical systems

Dynamical systems with discontinuous events fall into a wide group of systems that are often referred to as discontinuous or nonsmooth dynamical systems. In various applications physical systems can operate in different modes separated by boundaries; in electrical networks if nonsmooth characteristics are used to represent switches; further systems involving Coulomb friction [3, 4, 26, 27, 64], impacts [7, 15, 40, 49] and mechanical systems subjected to unilateral constraints [7, 53]. Mathematical models of physical systems may lead to dynamical systems whose righthand sides are not continuous or not differentiable due to switches between different modes. In such cases the existence of solutions is not guaranteed further in general the study of bifurcations for those systems is not yet completed.

Piecewise smooth dynamical systems occur as discrete or continuous-time dynamical system whose phase space is partitioned in different regions, each associated to a different functional form of the system vector field.

PWS can be classified into three different types according to their degree of non-smoothness

- Piecewise smooth continuous systems (PWCS): These systems have a continuous vector field but the Jacobian of the vector field is discontinuous. Examples include mechanical systems with bilinear elastic support [59] and systems modelling electrical circuits [10].
- Filippov systems: The vector field of these systems is bounded but discontinuous on certain hypersurfaces in the state-space. As examples we refer to systems with viscoelastic supports and dry friction [64, 74] and discontinuity induced bifurcations [14, 15].
- Impact systems: Here the discontinuous surface acts as a boundary between allowed and forbidden regions of the phase space such that there is a jump of the state at this boundary, for example mechanical systems with velocity jumps due to impacts [7, 40, 49].

The first two groups are called PWS and can be described as a dynamical system such that the state space splits into various components \mathcal{D}_i separated by manifolds \mathcal{M}_j , i.e.

$$\dot{\xi} = f_i(\xi, \lambda), \quad \xi \in \mathcal{D}_i \subset \mathbb{R}^n, \quad \mathbb{R}^n = (\cup_i \mathcal{D}_i) \cup (\cup_j \mathcal{M}_j) \quad (1.6)$$

where \mathcal{D}_i , $i = 1, 2, \dots, N$ are finitely many open domains of an n -dimensional state space, \mathcal{M}_j are $(n - 1)$ -dimensional manifolds \mathcal{M}_j separating the domains \mathcal{D}_j .

Suppose that $\xi^0 \in \mathcal{D}_i$ and that the solution trajectory stays inside the same domain \mathcal{D}_i and does not reach any \mathcal{M}_j . Then the dynamics behaves as in a conventional

smooth system which is sufficiently understood. The interesting case occurs when there exists a finite time at which the solution trajectory reaches any particular manifold M_j . *What will happen at such a point?*. Several forms of interaction may occur, some of them giving birth to new dynamical phenomena. Such interactions may be: direct crossing [39, 41, 71, 74], sliding [14], grazing [15], and jumping [40], each with single or multiple interactions.

For simplicity we restrict our attention to PWS consisting of two components separated by a hyperplane

$$\mathcal{M}(\lambda) := \{\xi \in \mathbb{R}^n \mid h(\xi, \lambda) = 0\}, \quad (1.7)$$

Although the separation manifold may depend in general on time, we have restricted our consideration to the case of a static separation manifold with nonvanishing gradient $\nabla h(\xi, \lambda) \neq 0$, ($\nabla = \nabla_\xi$) on \mathcal{M} . The normal vector $n(\xi, \lambda)$ perpendicular to the manifold \mathcal{M} is given by $n(\xi, \lambda) = \frac{\nabla h(\xi, \lambda)}{|\nabla h(\xi, \lambda)|_2}$, $\|n(\xi, \lambda)\| = 1$.

System (1.6) can be written as a n -dimensional nonlinear system with right-hand side

$$\dot{\xi} = \begin{cases} f_+(\xi, \lambda), & \xi \in \mathbb{R}_+^n, \\ f_-(\xi, \lambda), & \xi \in \mathbb{R}_-^n, \end{cases} \quad (1.8)$$

here $f_\pm : \mathbb{R}^n \times \mathbb{R} \rightarrow \mathbb{R}^n$ are sufficiently smooth functions and \mathbb{R}^n is split into two regions \mathbb{R}_+^n and \mathbb{R}_-^n by the separation manifold \mathcal{M} such that $\mathbb{R}^n = \mathbb{R}_+^n \cup \mathcal{M} \cup \mathbb{R}_-^n$. The regions $\mathbb{R}_+^n(\lambda)$ and $\mathbb{R}_-^n(\lambda)$ are defined as

$$\mathbb{R}_+^n(\lambda) = \{\xi \in \mathbb{R}^n \mid h(\xi, \lambda) > 0\},$$

$$\mathbb{R}_-^n(\lambda) = \{\xi \in \mathbb{R}^n \mid h(\xi, \lambda) < 0\}.$$

Definition 1.5 (Direct crossing). *Let $\rho(\xi, \lambda) = (n^T(\xi, \lambda)f_+(\xi, \lambda))(n^T(\xi, \lambda)f_-(\xi, \lambda))$. The direct crossing set is the set of all points $(\xi, \lambda) \in \mathcal{M}$, such that both vectors $f_\pm(\xi, \lambda)$ have nontrivial projections on $n^T(\xi, \lambda)$ in the same direction, hence*

$$\mathcal{M}^c = \{(\xi, \lambda) \in \mathcal{M} \mid \rho(\xi, \lambda) > 0\}.$$

Direct crossing implies that all trajectories of (1.8) approaching the hyperspace \mathcal{M} cross it immediately. Thus, for such initial condition, there is a unique absolutely continuous solution.

Definition 1.6 (Sliding mode). *The sliding mode set is the complement of \mathcal{M}^c in \mathcal{M} , i.e.*

$$\mathcal{M}^s = \{(\xi, \lambda) \in \mathcal{M} \mid \rho(\xi, \lambda) \leq 0\}.$$

where the vector fields are both pointing towards or away from \mathcal{M} .

This situation is further classified as attracting or repulsive, depending on the following cases.

An attracting sliding mode for \mathcal{M}^s occurs if the following conditions are satisfied at $\xi \in \mathcal{M}^s$

$$[n^T(\xi, \lambda)f_+(\xi, \lambda)] < 0 \text{ and } [n^T(\xi, \lambda)f_-(\xi, \lambda)] > 0, \quad (1.9)$$

hence a flow of (1.8) reaching \mathcal{M}^s has to stay in \mathcal{M}^s until it reaches the boundary of \mathcal{M}^s . Since the righthand sides f^\pm are smooth the flow is uniquely defined in forward time.

A repulsive sliding mode at \mathcal{M}^s occurs if the following conditions are satisfied at $\xi \in \mathcal{M}^s$

$$[n^T(\xi, \lambda)f_+(\xi, \lambda)] > 0 \text{ and } [n^T(\xi, \lambda)f_-(\xi, \lambda)] < 0, \quad (1.10)$$

meaning that trajectories starting in \mathcal{M}^s are directed away from the surface in both into \mathbb{R}_+^n and \mathbb{R}_-^n , hence the flow can not be continued uniquely.

1.4 Filippov's solution concept

Due do (1.8), $f(\xi, \lambda)$ is not yet defined if ξ is on \mathcal{M} . In order to overcome this difficulty Filippov [24, 25] has extended the notion of solutions by means of differential inclusions

$$\dot{\xi} \in F(\xi, \lambda) = \begin{cases} \{f_+(\xi, \lambda)\}, & \xi \in \mathbb{R}_+^n, \\ \{q(\xi, \lambda)f_+(\xi, \lambda) + (1 - q(\xi, \lambda))f_-(\xi, \lambda), \forall q \in [0, 1]\}, & \xi \in M, \\ \{f_-(\xi, \lambda)\}, & \xi \in \mathbb{R}_-^n. \end{cases} \quad (1.11)$$

Existence of solutions of (1.11) can be guaranteed with the notion of upper semi-continuity of set-valued functions. General results can be found in [24, 25].

Definition 1.7 (Filippov solution). *An absolutely continuous function $\xi : [a, b] \rightarrow \mathbb{R}^n$, $a, b \in \mathbb{R}^n$, $a < b$ is a solution of (1.11) if for almost all $t \in [a, b]$ it holds that*

$$\dot{\xi}(t) \in F(\xi(t)).$$

Theorem 1.3. *Let f_\pm be C^1 in $\mathbb{R}_+^n \cup M$ and $\mathbb{R}_-^n \cup M$, respectively, and $h(\xi)$ be C^2 on M . If at any point $\xi \in M$ we have that at least one of the conditions $n^T(\xi)f_+(\xi) < 0$ and $n^T(\xi)f_-(\xi) > 0$ holds, then there exists a unique Filippov solution for each initial condition [25].*

The parameter q will be selected such that the vector field is tangential to the separation manifold, i.e., $n^T(\xi)F(\xi, \lambda) = 0$, $\xi \in \mathcal{M}$ and therefore q is determined as

$$q(\xi, \lambda) = \frac{n^T(\xi, \lambda)f_-(\xi, \lambda)}{n^T(\xi, \lambda)(f_-(\xi, \lambda) - f_+(\xi, \lambda))}.$$

Therefore, we have an explicit form of the sliding vector field, i.e.

$$F_s(\xi, \lambda) = \frac{n^T(\xi, \lambda)f_-(\xi, \lambda) \cdot f_+(\xi, \lambda) - n^T(\xi, \lambda)f_+(\xi, \lambda) \cdot f_-(\xi, \lambda)}{n^T(\xi, \lambda)(f_-(\xi, \lambda) - f_+(\xi, \lambda))}. \quad (1.12)$$

If for some $\xi \in \mathcal{M}$, $n^T(\xi, \lambda)(f_-(\xi, \lambda) - f_+(\xi, \lambda)) = 0$, then we say that ξ is a singular sliding point. In terms of Filippov's notion, the boundary of the sliding mode region is defined as

$$\begin{aligned} \partial M_+^s &= \{\xi \in \mathcal{M} : q(\xi, \lambda) = 1, \text{ i.e. } n^T(\xi, \lambda)f_+(\xi, \lambda) = 0\}, \\ \partial M_-^s &= \{\xi \in \mathcal{M} : q(\xi, \lambda) = 0, \text{ i.e. } n^T(\xi, \lambda)f_-(\xi, \lambda) = 0\}. \end{aligned}$$

We assume that the separating manifold is flat; i.e. $\nabla n(\xi, \lambda) = 0$; locally this can be achieved after a series of appropriate near-identity transformation.

In that case we obtain:

$$\begin{aligned} \nabla q(\xi, \lambda) &= \left[n^T(\xi, \lambda)\nabla f_-(\xi, \lambda) n^T(\xi, \lambda)(f_-(\xi, \lambda) - f_+(\xi, \lambda)) - n^T(\xi, \lambda)f_-(\xi, \lambda) \right. \\ &\quad \left. n^T(\xi, \lambda)(\nabla f_-(\xi, \lambda) + \nabla f_+(\xi, \lambda)) \right] / \left[n^T(\xi, \lambda)(f_-(\xi, \lambda) - f_+(\xi, \lambda)) \right]^2. \end{aligned}$$

At the boundary ($q(\xi, \lambda) = 1$), since $F(\xi, \lambda) = \{f_+(\xi, \lambda)\}$, we get

$$\nabla q(\xi, \lambda) = \frac{n^T(\xi, \lambda)\nabla f_+(\xi, \lambda)}{n^T(\xi, \lambda)f_-(\xi, \lambda)}, \quad (1.13)$$

and at the boundary ($q(\xi, \lambda) = 0$), since $F(\xi, \lambda) = \{f_-(\xi, \lambda)\}$, we get

$$\nabla q(\xi, \lambda) = -\frac{n^T(\xi, \lambda)\nabla f_-(\xi, \lambda)}{n^T(\xi, \lambda)f_+(\xi, \lambda)}. \quad (1.14)$$

System (1.11) can exhibit so-called sliding bifurcation which has been observed to cause dramatic transitions in the dynamics of several systems relevant for applications [14, 15, 19]. Sliding bifurcations occur in four fundamental scenarios: grazing-sliding, crossing-sliding, adding-sliding and switching-sliding. We will present a brief description and the analytical conditions that must hold for each case of four possible scenarios in Chapter 3.

1.5 Poincaré map

For smooth systems a Poincaré section \mathcal{M} is a $(n - 1)$ -dimensional a manifold such that the flow crosses \mathcal{M} transversally. The Poincaré map \mathcal{P} is defined by the property that it assigns to $\xi^0 \in \mathcal{M}$ the point of the first return map under the flow $\xi(t; \xi^0)$ of (1.1). In that way the dynamical system (1.1) can be replaced by a discrete system given by \mathcal{P} . Then, a fixed point $\bar{\xi}$ of \mathcal{P} corresponds to a periodic orbit of (1.1), i.e., a trajectory starting at $\bar{\xi}$ returns to $\bar{\xi}$ after some time T . By looking at the behavior of \mathcal{P} near a fixed point we can determine the stability of an periodic orbit.

Topological changes of the Poincaré map can be brought about either by changing

a system parameter so that an invariant object changes in such a way that its intersection with the section is affected, or equivalently by changing the position of the section in the flow, [37, 67].

It appears as a natural choice to define a Poincaré map for nonsmooth systems by choosing the separating manifold as (local) Poincaré section. For a proper definition we consider 3 types of sub-maps:

- \mathcal{P}_- associated to the flow of $\dot{\xi} = f_-(\xi, \lambda)$.
- \mathcal{P}_+ associated to the flow of $\dot{\xi} = f_+(\xi, \lambda)$.
- \mathcal{P}_s associated to the flow of $\dot{\xi} = F_s(\xi, \lambda)$.

From a local point of view, the first return map \mathcal{P} is an unknown combination of the maps \mathcal{P}_+ , \mathcal{P}_- and \mathcal{P}_s ; and it can be equal to $\mathcal{P} = \mathcal{P}_+ \circ \mathcal{P}_-$, $\mathcal{P} = \mathcal{P}_- \circ \mathcal{P}_s$ or $\mathcal{P} = \mathcal{P}_+ \circ \mathcal{P}_- \circ \mathcal{P}_s$ or another combination of maps. A precise definition of those maps is given in Chapter 2.

1.6 Classification of bifurcations

Due to the presence of discontinuities on the manifold, PWS present a wide variety of standard and nonstandard bifurcations. If the behavior of PWS does not involve the dynamics of separation boundaries, we speak about standard bifurcations. That is, all the bifurcation which may occur in smooth system [37]. If the behavior of PWS relies on the dynamics of the separation boundaries, we deal with nonstandard bifurcations.

In other way, we can classify bifurcation of PWS according to the following:

- (i) Bifurcations that rely on the collapse or change of stability of equilibrium points (Saddle-node, Pitchfork, Hopf, etc.);
- (ii) Bifurcations related to the change of the real/virtual character of equilibrium points;
- (iii) Vanishing or appearing of a sliding mode domain (Sliding bifurcation).

Examples are given by the following situation:

If a limit cycle or a flow becomes sliding leads to *sliding bifurcation* [14, 44], if limit cycle becomes tangent to the separation boundary leads to *grazing bifurcation* [49] and bifurcations due to the existence of corners when \mathcal{M} has more than 2 crosses; for instance the corners formed by the intersections of two smooth surfaces \mathcal{M}_1 and \mathcal{M}_2 [15, 72, 73]. Further bifurcation of equilibria leading to nonsmooth bifurcation such as multiple crossing bifurcations [45], or discontinuity-induced bifurcations [14, 15]. Next, our attention is particularly focused on two of the phenomena that can occur for PWS, namely, discontinuity-induced bifurcation and Hopf-bifurcation.

1.6.1 Discontinuity-induced bifurcations

Generic equilibria of (1.8) can be standard equilibria of f_{\pm} in \mathbb{R}_{\pm}^n or equilibria of the Filippov vector field F_s in \mathcal{M} . Hence, we review the following definitions [14, 15].

Definition 1.8 (Standard equilibrium).

(i) A point ξ^* is a standard equilibrium point if $\xi^* \in \mathbb{R}^n$ such that either

$$f_-(\xi^*, \lambda) = 0, \quad h(\xi^*, \lambda) < 0, \quad \text{or} \quad f_+(\xi^*, \lambda) = 0, \quad h(\xi^*, \lambda) > 0.$$

(ii) A point $\xi^* \in \mathbb{R}^n$ is a virtual equilibrium if either

$$f_-(\xi^*, \lambda) = 0, \quad h(\xi^*, \lambda) > 0, \quad \text{or} \quad f_+(\xi^*, \lambda) = 0, \quad h(\xi^*, \lambda) < 0.$$

For sliding vector fields F_s there are equilibrium points which are not equilibria for the vector fields f_{\pm} (f_{\pm} are nonzero and anticollinear).

Definition 1.9 (Pseudo-equilibrium). A point ξ^* is a pseudo-equilibrium point if $\xi^* \in \mathcal{M}$ such that

$$\begin{aligned} h(\xi^*, \lambda) &= 0, \\ q(\xi^*, \lambda)f_+(\xi^*, \lambda) + (1 - q(\xi^*, \lambda))f_-(\xi^*, \lambda) &= 0, \end{aligned}$$

(i) A Pseudo-equilibrium is called *admissible* if $0 \leq q(\xi^*, \lambda) \leq 1$,

(ii) A pseudo-equilibrium is *virtual* if $q(\xi^*, \lambda) < 0$ or $q(\xi^*, \lambda) > 1$.

Definition 1.10 (Boundary equilibrium). A point ξ^* is a boundary equilibrium point if $\xi^* \in \mathcal{M}$ such that

$$\begin{aligned} h(\xi^*, \lambda) &= 0, \\ f_+(\xi^*, \lambda) = 0, \quad \text{or} \quad f_-(\xi^*, \lambda) &= 0, \end{aligned}$$

hence it is an equilibrium on the manifold and it is on the boundary between standard and virtual versions of both standard and pseudo-equilibria.

Definition 1.11 (Boundary equilibrium bifurcation). PWS (1.8) has a boundary equilibrium bifurcation at the point (ξ^*, λ^*) if a equilibrium collides with the discontinuity boundary such that:

- ξ^* is a boundary equilibrium; $f_-(\xi^*, \lambda^*) = 0$ and $h(\xi^*, \lambda^*) = 0$.
- $D_{\xi}f_-(\xi^*, \lambda^*) \neq 0$; ξ^* is a non-singular boundary equilibrium.
- (ξ^*, λ^*) is an isolated equilibrium to vector field f_- (non-degeneracy condition): $h_{\lambda}(\xi^*, \lambda^*) - h_{\xi}(\xi^*, \lambda^*)(D_{\xi}f_-(\xi^*, \lambda^*))^{-1}D_{\lambda}f_-(\xi^*, \lambda^*) \neq 0$.

Note that, similar definition if (ξ^*, λ^*) is a boundary equilibrium of $f_-(\xi, \lambda)$.

Discontinuity induced bifurcations can be classified into two generic scenarios, namely, persistence of an equilibrium for the Filippov system or nonsmooth-fold of equilibria for the Filippov system. *Persistence* (or border crossing) bifurcation is said to take place if a standard equilibrium point on one side of \mathcal{M} becomes a boundary equilibrium at the bifurcation point and turns into a virtual equilibrium due to variation of the parameter or if a virtual pseudo-equilibrium of one side of \mathcal{M} in a Filippov system becomes admissible. In the case of *Nonsmooth-fold* bifurcation the two branches of an admissible equilibria collide on the manifold \mathcal{M} at the bifurcation point, becoming a boundary equilibrium, and then both turn into two branches of virtual equilibria. For more details and applications [14, 15].

1.6.2 Generalized Hopf bifurcation

A smooth system undergoes a Hopf-bifurcation if the equilibrium point loses stability via a pair of purely imaginary eigenvalues, giving rise to the birth of a periodic motion called a limit cycle [37, 58].

A similar phenomenon in PWS is called generalized Hopf bifurcation due to a combination of the eigenstructure of the smooth subsystems together with the behavior of the vector field on the manifold \mathcal{M} and relevant to the switching laws or transition laws between the subsystems. For nonsmooth systems we are interested to discuss extension of Hopf-bifurcation to high dimensional systems. In recent works [41, 71, 74] the bifurcation of periodic orbits for planar PWS of the form (1.8) has been studied, we briefly recall the results for two-dimensional problems.

We assume that the right-hand side of PWS (1.8) is of the form

$$\dot{\xi} = f_{\pm}(\xi, \lambda) = \underbrace{A^{\pm}(\lambda)\xi}_{\text{basic linear term}} + \underbrace{g_{\pm}(\xi, \lambda)}_{\text{nonlinear term}}, \quad \lambda \in \mathbb{R}, \xi \in \mathbb{R}^2, \quad (1.15)$$

where λ is a parameter and the separation manifold is defined by $\mathcal{M} = \{\xi \in \mathbb{R}^2 | \xi_1 = 0\}$.

In this case the Poincaré map for the two-dimensional linear piecewise linear system $\dot{\xi} = A^{\pm}(\lambda)\xi$ turns out to be of the form

$$P(\xi_2, \lambda) = e^{\pi b(\lambda)} \xi_2, \quad b(\lambda) = \alpha^+(\lambda)/\omega^+(\lambda) + \alpha^-(\lambda)/\omega^-(\lambda).$$

We consider the following assumptions:

(H1) $f_{\pm}(\xi, \lambda)$ are \mathbf{C}^k -smooth ($k \geq 2$) for $(\xi, \lambda) \in \mathbb{R}_2^{\pm} \times \mathbb{R}$.

(H2) $f_{\pm}(0, \lambda) \equiv 0$ for $\lambda \in \mathbb{R}$.

(H3) The spectrum of $A^{\pm}(\lambda)$ consists of a pair of complex conjugate eigenvalues $\alpha^{\pm}(\lambda) \pm i\omega^{\pm}(\lambda)$, $\omega(\lambda) > 0$ for $\lambda \in \mathbb{R}$.

(H4) $a_{12}^{\pm} > 0$ or $a_{12}^{\pm} < 0$.

(H5) transversality condition, $b(0) = 0$, $\frac{db}{d\lambda} \neq 0$.

Under the previous assumptions, the main results are given in the following theorem [74].

Theorem 1.4. *Suppose that (H1) – (H5) hold, then there bifurcates a continuous branch of periodic orbits for the planar PWS (1.15) from the origin at $\lambda = 0$.*

The stability of stationary solution of piecewise linear system (i.e., $g^{\pm}(\xi, \lambda) = 0$ in (1.15)) can be determined by the sign of $b(\lambda)$. For planar systems there is of course no need for any reduction of the system, since the Poincaré map is essentially one-dimensional and it contains all necessary information. Various cases are investigated in [41, 71, 74].

The situation of high dimensional systems is significantly more complicated. There are examples of three-dimensional piecewise linear system (PWLS) when A^{\pm} are stable (i.e., A^{\pm} have eigenvalues with negative real parts) and the stability of stationary solutions is not a simple problem. Hence, that stationary solution of a composite problem may be unstable even if both subsystems are stable. The first example of this surprising result has been given in [10]; in Chapter 2, we will present more examples.

1.7 Outline of the thesis

This thesis is a contribution to the field of nonsmooth dynamical systems with particular application to a brake system with dry friction. Each chapter is structured in five sections and the content is revised as follows:

Chapter 2: This chapter is concerned with a class of n -dimensional PWS involving invariant cones with discontinuity surface. Specifically, we will study direct crossing from one half-space \mathbb{R}_+^n (or \mathbb{R}_-^n) to the other \mathbb{R}_-^n (or \mathbb{R}_+^n) via \mathcal{M}^c and only one equilibrium at the origin lying on the discontinuity manifold and for the important case where both matrices for basic PWLS have complex eigenvalues. We obtain results by direct composition of Poincaré maps which will help to establish the existence of invariant cones, stability of equilibrium point and generalized Hopf bifurcation. We will also describe numerical procedures to compute the dynamics of invariant cones in the case of PWS seen as a perturbation of smooth systems. Part of this Chapter has already been published in [39]

Chapter 3: If both vector fields $f_-(\xi, \lambda)$ and $f_+(\xi, \lambda)$ are locally pointing away from or towards the manifold \mathcal{M} , then a sliding mode may occur. In other words, once a trajectory reaches the sliding surface, it will stay on it. In this chapter we investigate necessary and sufficient conditions for the existence of cones consisting

of periodic orbits for a class of PWS including sliding motion. The stability of the cones consisting of sliding motion is the topic of this chapter. This topic will be studied by either considering the stability of stationary solution or the bifurcation of limit cycles such as *sliding bifurcation*. Again we prove a generalization concerning invariant cones for a class of PWS.

Chapter 4: In this chapter we study a mechanical model for investigating different aspects of bifurcations in PWS of a six -dimensional brake system. We will pay attention to reduction from high dimension to low dimension. Instead of considering the six-dimensional phase space a reduction to the invariant two-dimensional surface of the cone will be formulated and analyzed. In that way mathematical investigations about the existence of self-sustained oscillations caused by variation of parameters are carried out. Furthermore we show the existence of a sliding motion within the separating manifold and we show which parameters have the strongest influence on the self-induced oscillations.

Chapter 5: We continue to extend the concept of dimension reduction via a generalized center manifold analysis for nonlinear PWS. The reduction procedure has been established for nonlinear PWS allowing a bifurcation and stability analysis of a reduced system. The proof of existence of generalized center manifold is based on Hadamard's graph transform and the Poincaré map approach. Finally, we present the explicit construction of lower dimensional invariant manifolds for a class of nonlinear PWS having a cone-like invariant "manifold" carrying the essential dynamics of the full system under appropriate conditions and determine the leading coefficients of the function generating the invariant surface. The results in this Chapter have been published in [66].

Chapter 6: Here the conclusions of the thesis are presented and several open problems are outlined for further research.

Chapter 2

Invariant cones for a class of a high-dimensional PWS

Part I: In the first part of this Chapter, we discuss various aspects for n -dimensional PWS such as: the manifold can be partitioned into sectors allowing the existence of direct transition and sliding motion regions, Poincaré map, times intersection, fundamental matrix solution associated to PWS and monodromy matrix whose eigenvalues, the Floquet multipliers, determine the stability of limit cycles. The concept of invariant cones for PWLS is established to understand the often complicated dynamical behaviour. A nonsmooth perturbation approach is introduced for the generation of invariant cones and stability of the bifurcating limit cycle. Finally we show a paradoxical situation where the behavior of a simple PWLS can be rather complex even if all of its subsystems are stable.

2.1 N-dimensional PWS

Define an n -dimensional two region PWS consisting of \mathbb{R}_{\pm}^n and fixed λ . Thus, we rewrite PWS (1.8) in the form

$$\dot{\xi} = \begin{cases} f_+(\xi), & h(\xi) > 0, \\ f_-(\xi), & h(\xi) < 0. \end{cases} \quad (2.1)$$

An important observation in the study of (2.1) is that there are two main types of motion namely, direct crossing between \mathbb{R}_-^n and \mathbb{R}_+^n through \mathcal{M}^c and sliding motion in \mathcal{M}^s , see Figure 2.1. Thus, in order to understand the behavior of the composed motion we will first discuss the vector field on $\mathcal{M} = \mathcal{M}^c \cup \mathcal{M}^s$

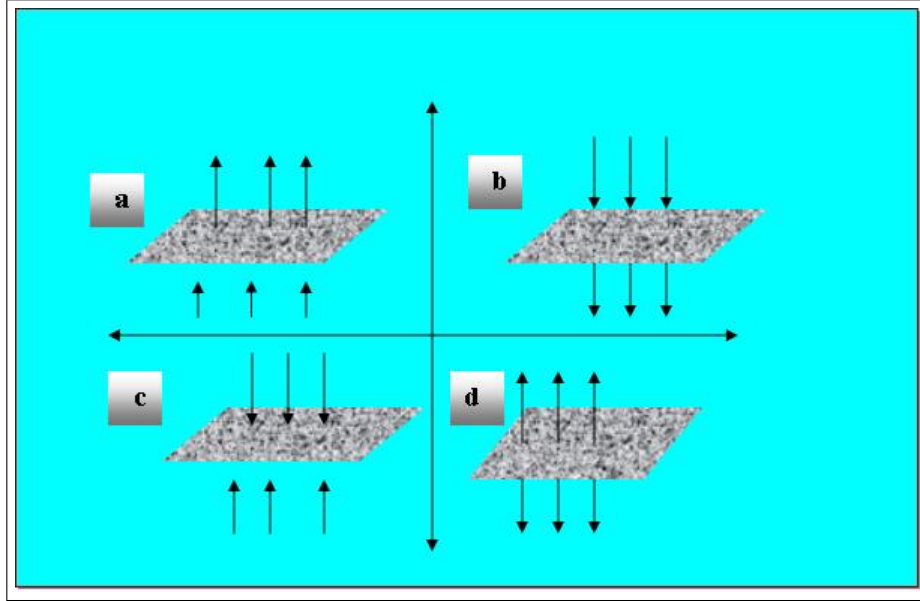


Figure 2.1: Partitioned separation manifold: (a) and (b) are sectors of direct crossing, (c) is sector of attractive sliding motion, (c) is a sector of repulsive sliding motion.

where the separation manifold can be partitioned into sectors defined as:

$$\begin{aligned}
 \mathcal{M}_-^c &= \{\xi \in \mathcal{M}^c \mid n^T(\xi)f_-(\xi) < 0\} \\
 \mathcal{M}_+^c &= \{\xi \in \mathcal{M}^c \mid n^T(\xi)f_-(\xi) > 0\} \\
 \mathcal{M}_-^s &= \{\xi \in \mathcal{M}^s \mid n^T(\xi)f_-(\xi) > 0\} \\
 \mathcal{M}_+^s &= \{\xi \in \mathcal{M}^s \mid n^T(\xi)f_-(\xi) < 0\}
 \end{aligned} \tag{2.2}$$

Remark 2.1.

1. For $\xi \in \mathcal{M}_-^c$ or $\xi \in \mathcal{M}_+^c$ there is a direct crossing of the flow of (2.1) through the sector \mathcal{M}_-^c or \mathcal{M}_+^c , respectively.
2. For $\xi \in \mathcal{M}_-^s$ or $\xi \in \mathcal{M}_+^s$ the flow near ξ is restricted to \mathcal{M}_-^s (attractive sliding motion) or \mathcal{M}_+^s (repulsive sliding motion), respectively. The flow in \mathcal{M}^s is generated by (1.12).

Here, we restrict our attention to trajectories with immediate transition between the half spaces; for any initial value trajectories never slide or jump on the manifold leading to the existence of a unique absolutely continuous solution of (2.1). Let us start from the initial position $\xi \in \mathcal{M}_-^c$ or $\xi \in \mathcal{M}_+^c$, then the solutions respectively are denoted by $\varphi^-(\tau_-, \xi)$ or $\varphi^+(\tau_+, \xi)$, which both are \mathbf{C}^k , $k \geq 1$. Assume that $\varphi^-(\tau_-, \xi)$ reaches \mathcal{M}_+^c of the minimum return time $\tau_-(\xi)$ at $\eta = \varphi^-(\tau_-, \xi) \in \mathcal{M}_+^c$, hence there exists the first intersection time

$$\tau_-(\xi) = \inf\{\tau > 0 \mid n^T(\xi)\varphi^-(\tau, \xi) = 0\}. \tag{2.3}$$

In a similar way we can define $\tau^+(\eta)$ as

$$\tau_+(\eta) = \inf\{\tau > 0 \mid n^T(\xi)\varphi^+(\tau, \eta) = 0\}. \quad (2.4)$$

Poincaré map: without loss of generality we will assume that $\xi \in \mathcal{M}_-^c$ and $\varphi^-(\tau_-, \xi)$ reaches \mathcal{M}_+^c transversally at time $\tau_-(\xi)$. Thus, we can define the map

$$\begin{aligned} \mathcal{P}_-(\xi) &: \mathcal{M}_-^c \rightarrow \mathcal{M}_+^c, \\ \xi &\rightarrow \varphi^-(\tau_-, \xi) = \mathcal{P}_-(\xi), \end{aligned}$$

Similarly the flow $\varphi^+(\tau_+, \eta)$ reaches \mathcal{M}_-^c at the time $\tau_+(\eta)$

$$\begin{aligned} \mathcal{P}_+(\eta) &: \mathcal{M}_+^c \rightarrow \mathcal{M}_-^c, \\ \eta &\rightarrow \varphi^+(\tau_+, \eta) = \mathcal{P}_+(\eta). \end{aligned}$$

Consequently, PWS (2.1) yields a $(n-1)$ -dimensional map defined by

$$\begin{aligned} \mathcal{P}(\xi) &: \mathcal{M}_-^c \rightarrow \mathcal{M}_-^c \\ \mathcal{P}(\xi) &:= \mathcal{P}_+ \circ \mathcal{P}_-(\xi) = \varphi^+(\tau_+(\eta), \eta), \quad \eta = \varphi^-(\tau_-(\xi), \xi). \end{aligned}$$

Note that \mathcal{P} is a nonlinear map due to the nonlinearity contained in (2.1) and the nonlinear return times.

Lemma 2.1.

(i) For all $\hat{\xi} \in \mathcal{M}_-^c$, $\mathcal{P}_-(\hat{\xi}) \in \mathcal{M}_+^c$ and $\varphi^-(\tau, \hat{\xi}) \in \mathbb{R}^n$, ($0 < \tau < \tau_-(\hat{\xi})$):

(a) The function $\tau_-(\xi)$ is differentiable in $\hat{\xi}$.

(b) \mathcal{P}_- is differentiable in $\hat{\xi}$ and $\frac{\partial \mathcal{P}_-}{\partial \xi}(\hat{\xi}) = \left(\frac{\partial \varphi^-}{\partial \xi} + f_-(\xi) \frac{\partial \tau_-}{\partial \xi} \right)(\hat{\xi})$.

(ii) For all $\hat{\eta} \in \mathcal{M}_+^c$, $\mathcal{P}_+(\hat{\eta}) \in \mathcal{M}_-^c$ and $\varphi^+(\tau, \hat{\eta}) \in \mathbb{R}^n$, ($0 < \tau < \tau_+(\hat{\eta})$):

(a) The function $\tau_+(\eta)$ is differentiable in $\hat{\eta}$.

(b) \mathcal{P}_+ is differentiable in $\hat{\eta}$ and $\frac{\partial \mathcal{P}_+}{\partial \xi}(\hat{\eta}) = \left(\frac{\partial \varphi^+}{\partial \xi} + f_+(\xi) \frac{\partial \tau_+}{\partial \xi} \right)(\hat{\eta})$.

(iii) For $\hat{\xi} \in \mathcal{M}_-^c$, $\hat{\eta} \in \mathcal{M}_+^c$:

(a) $\mathcal{P}(\hat{\xi}) = \mathcal{P}_+(\mathcal{P}_-(\hat{\xi}))$ is differentiable in $\hat{\xi}$ and

$$\frac{\partial \mathcal{P}}{\partial \xi}(\hat{\xi}) = \left(\frac{\partial \varphi^+}{\partial \eta} + f_+(\eta) \frac{\partial \tau_+}{\partial \eta} \right) \cdot \left(\frac{\partial \varphi^-}{\partial \xi} + f_-(\xi) \frac{\partial \tau_-}{\partial \xi} \right)(\hat{\xi}).$$

To determine the stability properties of the limit cycle for a smooth system (1.1), we consider the solutions of the variational equation for trajectories. Specifically, let $\varphi(t, \tilde{\xi})$, $t > 0$ denote the solution of (1.1) with initial condition $\tilde{\xi} \in \mathbb{R}^n$. The fundamental matrix solution is the derivative of the solution with

respect to $\tilde{\xi}$. Then the matrix $Y = \frac{\partial}{\partial \xi} \varphi(t, \tilde{\xi})$ is a solution of the variational system [58]

$$\dot{Y} = \frac{\partial}{\partial \xi} f(\tilde{\xi})Y, \quad Y(0) = I.$$

For PWS (2.1) the effects of the discontinuity surface must be taken into account when calculating the monodromy matrix.

Definition 2.1. For PWS (2.1) the two matrices $Y_- = \Phi^-(\tau_-, \xi_0)$ and $Y_+ = \Phi^+(\tau_+, \eta_0)$ are called fundamental matrix solutions of (2.1) where $\tilde{\xi} \in \mathbb{R}_-^n$ and $\tilde{\eta} \in \mathbb{R}_+^n$ related to

$$\begin{cases} \dot{\xi} = f_-(\xi), & \xi(0) = \tilde{\xi}: \quad \dot{Y}_- = \frac{\partial}{\partial \xi} f_-(\tilde{\xi})Y_-, Y_-(0) = I, \quad 0 \leq \tau_- \leq \tilde{\tau}_-; \\ \dot{\eta} = f_+(\eta), & \eta(\tilde{\tau}_-) = \tilde{\eta}: \quad \dot{Y}_+ = \frac{\partial}{\partial \eta} f_+(\tilde{\eta})Y_+, \quad \tilde{\tau}_- \leq \tau_+ \leq \tilde{\tau}_+. \end{cases}$$

Theorem 2.1. If $\rho(\xi) > 0$ and $\tilde{\xi} \in \mathcal{M}_-^c$ the flow given by $\varphi^-(\tau, \xi)$ crosses the manifold \mathcal{M}^c at the time $\tilde{\tau}_-$. Then for Y_- and Y_+ at the time $\tilde{\tau}_-$ we have

$$Y_+ = J_- Y_-, \quad J_- = I + \frac{(f_+(\tilde{\tau}_-, \tilde{\eta}) - f_-(\tilde{\tau}_-, \tilde{\eta}))n^T(\tilde{\eta})}{n^T(\tilde{\eta})f_-(\tilde{\tau}_-, \tilde{\eta})}$$

where I is the identity matrix of the same order as the number of state variables and J_- is called jump or saltation matrix [21, 25, 44].

Proof: if $\xi \in \mathcal{M}_-^c$, and $\varphi^+(\tau_+, \eta)$ is a solution of \oplus -system of (2.1), we obtain

$$\varphi^+(\tau_+, \eta) = \eta + \int_{\tau_-}^{\tau_+} f_+(s, \eta) ds, \quad \eta = \varphi^+(\tau_-, \xi), \quad \xi \in \mathcal{M}_+^c.$$

Differentiate with respect to ξ and set $(\tilde{\tau}_-, \tilde{\eta})$ are boundary points that satisfy $h(\tilde{\eta}) = 0$ and (2.3),

$$\begin{aligned} \frac{\partial}{\partial \xi} \varphi^+(\tau_+, \eta) &= \frac{\partial \eta}{\partial \xi} - f_+(\tau_-, \eta) \frac{\partial \tau_-}{\partial \xi} + \int_{\tilde{\tau}_-}^{\tau_+} \frac{\partial}{\partial \xi} f_+(s, \eta) ds, \\ \frac{\partial \eta}{\partial \xi} &= \frac{\partial}{\partial \xi} \varphi^-(\tau_-, \xi) + f_-(\xi, \tau_-) \frac{\partial \tau_-}{\partial \xi}, \quad n^T \varphi(\tilde{\tau}_-, \tilde{\eta}) = 0. \end{aligned}$$

Since $\varphi^-(\tau_-, \xi) \in \mathcal{M}_-^c$, we have

$$h(\varphi^-(\tau_-, \xi)) = 0 \Rightarrow \frac{\partial \tau_-}{\partial \xi} = -\frac{n^T \frac{\partial \varphi^-}{\partial \xi}(\tau_-, \xi)}{n^T f_-(\tau_-, \xi)}.$$

Therefore, we get

$$\frac{\partial}{\partial \xi} \varphi^+(\tau_+, \eta) = \left(I + \frac{(f_+(\tau_-, \eta) - f_-(\tau_-, \xi))n^T(\xi)}{n^T(\xi)f_-(\tau_-, \xi)} \right) \frac{\partial}{\partial \xi} \varphi^-(\tau_-, \xi) + \int_{\tilde{\tau}_-}^{\tau_+} \frac{\partial}{\partial \xi} f_+(s, \eta) ds.$$

At the first exact intersection time $\tilde{\tau}_-$ substituting $\tilde{\tau}_-$ into (τ_-, τ_+) and $\tilde{\eta}$ into (ξ, η) , thus

$$\frac{\partial}{\partial \xi} \varphi^+(\tilde{\tau}_-, \tilde{\eta}) = \underbrace{\left(I + \frac{(f_+(\tilde{\tau}_-, \tilde{\eta}) - f_-(\tilde{\tau}_-, \tilde{\eta}))n^T(\tilde{\eta})}{n^T(\tilde{\eta})f_-(\tilde{\tau}_-, \tilde{\eta})} \right)}_{J_-} \frac{\partial}{\partial \xi} \varphi^-(\tilde{\tau}_-, \tilde{\xi}).$$

Remark 2.2. For $\xi \in \mathcal{M}_+^c$ there is an analogous result of Theorem 2.1, for this case we get the jump matrix as $J_+ = I + \frac{(f_-(\tilde{\tau}_+, \tilde{\eta}) - f_+(\tilde{\tau}_+, \tilde{\eta}))n^T(\tilde{\eta})}{n^T(\tilde{\eta})f_+(\tilde{\tau}_+, \tilde{\eta})}$.

In order to examine the structural behaviour of limit cycle arise from trajectory of (2.1), where ξ is a closed trajectory of limit cycle, we examine the eigenvalues of the monodromy matrix which has the form

$$Y(T, \xi) = J_+ Y_+(\tilde{\tau}_+, \xi(\tilde{\tau}_-)) J_- Y_-(\tilde{\tau}_-, \xi), \quad T = \tilde{\tau}_+ + \tilde{\tau}_-,$$

The eigenvalues of $Y(T, \xi)$ are also called the Floquet multipliers. If all the eigenvalues are inside the unit circle, the system is stable.

2.2 The basic piecewise linear problem

We assume that the right-hand side of (2.1) is of the form

$$\begin{aligned} f_+(\xi) &= A^+ \xi + g_+(\xi), \\ f_-(\xi) &= A^- \xi + g_-(\xi), \end{aligned}$$

where A^\pm are constant matrices representing the basic piecewise linear part and g_\pm are nonlinear perturbations of higher order. Here we restrict our attention to trajectories with immediate transition between the half spaces for PWLS defined as:

$$\dot{\xi} = \begin{cases} A^+ \xi, & h(\xi) > 0, \\ A^- \xi, & h(\xi) < 0, \end{cases} \quad (2.5)$$

where $\xi \in \mathbb{R}^n$ and A^\pm are $n \times n$ real matrices, the stationary solution is always an equilibrium point. System (2.5) is a general form of PWLS which can be divided into two main categories: first, continuous PWLS where both matrices satisfy the continuity relation $A^+ - A^- = (A^+ - A^-)e_1^T e_1$, e_1 is the first vector of the standard basis \mathbb{R}^n . Note that A^+ and A^- share the same structures and are only different in the first column [8,10,11]. Second, for the general PWLS, the two vector fields $A^\pm \xi$ are not necessarily continuously on \mathcal{M} [38,39].

In order to study the local bifurcation for the continuous PWLS it is often helpful to obtain a normal form first. Therefore, we extend the notions of observability and controllability from control theory [6,8,60].

Definition 2.2. The observability matrix is defined as

$$Ob = \begin{pmatrix} e^T \\ e^T A^- \\ e^T (A^-)^2 \\ \vdots \\ e^T (A^-)^{n-1} \end{pmatrix}, \quad Co = \begin{pmatrix} b \\ A^- b \\ (A^-)^2 b \\ \vdots \\ (A^-)^{n-1} b \end{pmatrix},$$

where $b = (A^+ - A^-)e$, the continuous PWLS (2.5) is said to be observable or controllable if $\text{rank}(Ob) = n$ or $\text{rank}(Co) = n$, respectively.

The following lemma provides a geometric interpretation of the notion of observability.

Lemma 2.2. [6, 8, 60]

The continuous PWLS (2.5) is observable if and only if A^- has no eigenspace orthogonal to e and when continuous PWLS (2.5) is not observable, then the system can be decomposed into two, one of them decoupled from the other.

This lemma explains why the canonical form may only be obtained when A^\pm has no eigenspace tangent to the switching manifold at the bifurcation point. Furthermore, the continuous PWLS (2.5) can be transformed by a linear change of variables into the observability canonical form, some canonical form for specific cases of continuous PWLS (2.5) introduced in [8, 10].

Let us consider the general form of (2.5) (continuous or discontinuous PWLS). If $\xi \in \mathcal{M}_-^c$ and $\varphi(t_-, \xi) \in \mathcal{M}_+^c$ in forward time, then we can define the Poincaré map for the full system (2.5) as:

$$\begin{aligned} P^-(\xi) &: \mathcal{M}_-^c \rightarrow \mathcal{M}_+^c := e^{t_-(\xi)A^-} \xi \\ P^+(\eta) &: \mathcal{M}_+^c \rightarrow \mathcal{M}_-^c := e^{t_+(\eta)A^+} \eta \\ P(\xi) &:= P^+(P^-(\xi)) = e^{t_+(\eta)A^+} e^{t_-(\xi)A^-} \xi, \end{aligned}$$

where $t_-(\xi)$ and $t_+(\eta)$ are determined as smallest positive root, i.e.

$$t_-(\xi) = \inf\{t > 0 \mid n^T(\xi)e^{t(\xi)A^-} \xi = 0\}, \quad (2.6)$$

$$t_+(\eta) = \inf\{t > 0 \mid n^T(\eta)e^{t(\eta)A^+} \eta = 0\}, \quad (2.7)$$

respectively. Note that t_- and t_+ are constant on rays in \mathcal{M}_-^c and \mathcal{M}_+^c and thus provide useful (linearity) properties which we collect in:

Lemma 2.3. [39]

(i) For $\hat{\xi} \in \mathcal{M}_-^c$, and all $\lambda > 0$:

(a) $\lambda \hat{\xi} \in \mathcal{M}_-^c$, $t_-(\lambda \hat{\xi}) = t_-(\hat{\xi})$ and $P_-(\lambda \hat{\xi}) = \lambda P_-(\hat{\xi})$.

(b) t_- is differentiable in $\hat{\xi}$ and $\nabla t_-(\hat{\xi}) \cdot \hat{\xi} = 0$.

(c) P_- is differentiable in $\hat{\xi}$ and $\frac{\partial P_-}{\partial \xi} \hat{\xi} = e^{t_-(\hat{\xi})A^-} [A^- \hat{\xi} \nabla t_-(\hat{\xi}) + I]$.

(ii) For $\hat{\eta} \in \mathcal{M}_+^c$, and each $\lambda > 0$:

- (a) $\lambda\hat{\eta} \in \mathcal{M}_+^c$, $t_+(\lambda\hat{\eta}) = t_+(\hat{\eta})$ and $P_+(\lambda\hat{\eta}) = \lambda P_+(\hat{\eta})$.
- (b) t_+ is differentiable in $\hat{\eta}$ and $\nabla t_+(\hat{\eta}) \cdot \hat{\eta} = 0$.
- (c) P_+ is differentiable in $\hat{\eta}$ and $\frac{\partial P_+}{\partial \eta} \hat{\eta} = e^{t_+(\hat{\eta})A^+} [A^+ \hat{\eta} \nabla t_+(\hat{\eta}) + I]$.

(iii) For $\hat{\xi} \in \mathcal{M}_-^c$, $\hat{\eta} \in \mathcal{M}_+^c$, and all $\lambda > 0$:

- (a) $P(\hat{\xi}) = P_+(P_-(\hat{\xi}))$ is differentiable in $\hat{\xi}$ and $\frac{\partial P}{\partial \xi}(\hat{\xi}) = e^{t_+(\hat{\eta})A^+} [A^+ \hat{\eta} \nabla t_+(\hat{\eta}) + I] \cdot e^{t_-(\hat{\xi})A^-} [A^- \hat{\xi} \nabla t_-(\hat{\xi}) + I]$.
- (b) $\frac{\partial P_-}{\partial \xi}(\hat{\xi}) \cdot \hat{\xi} = P(\hat{\xi})$.
- (c) $P(\lambda\hat{\xi}) = \lambda P(\hat{\xi})$.

- (iv) (a) $t_-^{(j)}(\lambda\hat{\xi})\lambda^{(j)} = t_-^{(j)}(\hat{\xi})$ and $t_-^{(j)}(\lambda\hat{\xi})\hat{\xi} = 0$ for all $\hat{\xi} \in \mathcal{M}_-^c$ and $j \geq 1$.
- (b) $t_+^{(j)}(\lambda\hat{\eta})\lambda^{(j)} = t_+^{(j)}(\hat{\eta})$ and $t_+^{(j)}(\lambda\hat{\eta})\hat{\eta} = 0$ for all $\hat{\eta} \in \mathcal{M}_+^c$ and $j \geq 1$.

Invariant cone: We assume that $\bar{\xi} \in \mathcal{M}^c$, then the trajectory of the considered system (2.5) through $\bar{\xi}$ crosses immediately \mathcal{M} and never slides on \mathcal{M} . Both Poincaré half maps P_+ and P_- transform half rays contained in \mathcal{M}^c and passing through the origin into half rays contained in \mathcal{M}^c again and passing through the origin. Then the first return Poincaré map P has an invariant half straight line if $P(\bar{\xi}) = \mu_c \bar{\xi}$. A manifold \mathcal{C} formed by P such that for all $P(\bar{\xi}) \in \mathcal{C}$ we have that $P(\lambda\bar{\xi}) \in \mathcal{C}$ for every $\lambda \geq 0$ is called a two-zonal invariant cone. Furthermore if the flow has no intersection with \mathcal{M}^c , \mathcal{C} will be called one-zonal invariant cone.

The following theorem explains the stability of the origin in the presence of invariant cones with two-zones. Further, it can be understood as a generalization of the center manifold concept besides the lack of smoothness.

Theorem 2.2. [38]

If there exists $\bar{\xi} \in \mathcal{M}_-^c$ and $\mu_c > 0$ such that

$$P(\bar{\xi}) = \mu_c \bar{\xi},$$

then $\bar{\xi}$ generates an invariant cone under the flow of (2.5) due to $P(\lambda\bar{\xi}) = \lambda P(\bar{\xi}) = \lambda \mu_c \bar{\xi}$; moreover,

- (a) If $\mu_c > 1$, then the stationary solution 0 is unstable
- (b) If $\mu_c = 1$, then the cone consists of periodic orbits
- (c) If $\mu_c < 1$, then the stability of 0 depends on the stability of P with respect to the complementary directions.

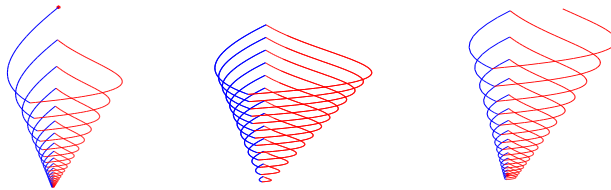


Figure 2.2: Different dynamics on cones, $\mu_c < 1$, $\mu_c = 1$ and $\mu_c > 1$, respectively.

These three possible situations are drawn in Figure 2.2.

Note that the above theorem indicates the difficult task to determine μ_c and to characterize the attractivity of \mathcal{C} , because μ_c depends on t_{\pm} in a nonlinear way.

To explain the attractivity of \mathcal{C} [66], we assume that the remaining $(n - 2)$ eigenvalues μ_1, \dots, μ_{n-2} of $\frac{\partial P}{\partial \xi}(\bar{\xi})$ satisfy

$$|\mu_j| \leq \tilde{\alpha} < \min\{1, \mu_c\}, \quad (j = 1, \dots, n - 2). \quad (2.8)$$

Then the invariant cone is attractive under the flow of (2.5) while the dynamics on the cone is determined by $\mu_c < 1$, $\mu_c = 1$ or $\mu_c > 1$. In that way the investigation of the dynamical behavior of the original problem can be reduced to the dynamics on a 2-dimensional surface.

Remark 2.3. *The attractivity condition (2.8) guarantees that all solutions with initial values close to \mathcal{C} are attracted to the cone. In case of contracting spiraling on \mathcal{C} itself these solutions converge faster to the cone than to the origin. These statements will be discussed in more detail in Chapter 5.*

2.3 Generation of invariant cones for PWLS

In this section, we present a procedure to establish the invariant cone and stability of the bifurcating limit cycle of PWLS (2.5) born from a smooth system which has been set up in [38].

In a smooth system [37, 46, 58] $\dot{\xi} = A(\alpha)\xi + g(\xi, \alpha)$, $\xi \in \mathbb{R}^n$, $g \in \mathbf{C}^k$, $\alpha \in \mathbb{R}$: if 0 is an isolated stationary point and $A(\alpha)$ has one pair of complex eigenvalues $\lambda(\alpha) \pm i\omega(\alpha)$ that becomes purely imaginary when $\alpha = 0$, i.e., $\lambda(0) = 0$ and $\omega(0) > 0$, and if moreover, all other eigenvalues of $A(\alpha)$ have negative real part, then, generically, we get a Hopf bifurcation. As α passes through $\alpha = 0$, the dynamics of 0 changes stability, and the system will exhibit limit cycle behavior. Furthermore, the interesting feature occurs of according to the center manifold theorem any system undergoing Hopf bifurcation can be reduced to

a two-dimension dynamical system.

The generation of invariant cones plays a similar role for PWLS as the presence of purely imaginary eigenvalues of the linearization of smooth systems with respect to the generation of bifurcation of periodic orbits for nonlinearly perturbed systems. Seen from the perspective of PWLS the periodic orbits of a smooth linear system might be seen as a degenerate (flat) cone. It appears as a natural approach to investigate how a (flat) cone for a smooth system develops under non-smooth perturbations.

Starting from the vector $\xi \in \mathcal{M}_-^c$ we want to determine an invariant cone given by

$$P(\xi) = \mu_c \xi.$$

Following [38] we can transform this nonlinear eigenvalue problem into a nonlinear set of $(n+3)$ equations for the $(n+3)$ variables $X = (\xi, t_-(\xi), t_+(P_-(\xi), \mu_c))^T$:

$$0 = F(X) = \begin{bmatrix} e^{t_+ A^+} e^{t_- A^-} \xi - \mu_c \xi \\ n^T e^{t_+ A^+} \xi \\ n^T \xi \\ \xi^T \xi - 1 \end{bmatrix}, \quad (2.9)$$

The Jacobian matrix is evaluated at a special solution $X_0 = (\bar{\xi}, s^-, s^+, \bar{\mu}_c)^T$:

$$J = \begin{pmatrix} e^{s^+ A^+} e^{s^- A^-} - \bar{\mu}_c I & e^{s^+ A^+} e^{s^- A^-} A^- \bar{\xi} & \bar{\mu}_c A^+ \bar{\xi} & -\bar{\xi} \\ n^T e^{s^- A^-} & n^T e^{s^- A^-} A^- \bar{\xi} & 0 & 0 \\ n^T & 0 & 0 & 0 \\ 2\bar{\xi}^T & 0 & 0 & 0 \end{pmatrix} = \left(\begin{array}{ccc|c} & & & -\bar{\xi} \\ & J_1 & & 0 \\ & & & 0 \\ \hline 2\bar{\xi}^T & 0 & 0 & 0 \end{array} \right).$$

Note that A^+ , $e^{s^+ A^+}$ commute. Newton's method can be applied to determine X as:

$$J \Delta X^\nu = -F(X^\nu), \quad X^{\nu+1} = X^\nu + \Delta X^\nu, \quad (2.10)$$

if J is nonsingular at X_0 . To check regularity the bordering lemma is helpful.

Lemma 2.4. [33, 35]

Assume that $J = \begin{pmatrix} J_1 & b \\ c^T & d \end{pmatrix}$. Then

- i- If J_1 is nonsingular $\Rightarrow J$ is nonsingular if and only if $d - c^T J_1^{-1} b \neq 0$
- ii- If J_1 is singular with $\dim \mathcal{N}(J_1) = \dim \mathcal{N}(J_1^T) = 1$, then J is nonsingular if and only if $b \notin \mathcal{R}(J_1)$ and $c \notin \mathcal{R}(A^T)$
- iii- If J_1 is singular with $\dim \mathcal{N}(J_1) \geq 2$ then J is singular.

2.3.1 Bordering algorithm

The following algorithm is valid if J or J_1 are nonsingular [33, 35].

We write the coefficient of the linear system in Newton's method (2.10) in the form

$$\begin{pmatrix} J_1 & b \\ c^T & d \end{pmatrix} \begin{pmatrix} x \\ z \end{pmatrix} = \begin{pmatrix} f \\ h \end{pmatrix}, \quad (2.11)$$

where J_1 is $n \times n$ matrix, $b, c \in \mathbb{R}^n$ and $d \in \mathbb{R}$, then the following bordered LU -decomposition will be efficient:

$$\begin{pmatrix} J_1 & b \\ c^T & d \end{pmatrix} = \begin{pmatrix} L & 0 \\ \beta^T & 1 \end{pmatrix} \begin{pmatrix} U & \gamma \\ 0^T & \delta \end{pmatrix},$$

we compute γ, β and δ from

$$L\gamma = b, \quad U^T\beta = c, \quad \delta = d - \beta^T\gamma.$$

The linear system can than be written as

$$\begin{pmatrix} L & 0 \\ \beta^T & 1 \end{pmatrix} \begin{pmatrix} U & \gamma \\ 0^T & \delta \end{pmatrix} \begin{pmatrix} x \\ z \end{pmatrix} = \begin{pmatrix} f \\ h \end{pmatrix},$$

Defining

$$\begin{pmatrix} \tilde{f} \\ \tilde{h} \end{pmatrix} = \begin{pmatrix} U & \gamma \\ 0^T & \delta \end{pmatrix} \begin{pmatrix} x \\ z \end{pmatrix},$$

we obtain the solution (x, z) by the following steps:

$$L\tilde{f} = f, \quad \tilde{h} = h - \beta^T\tilde{f}, \quad z = \tilde{h}/\delta, \quad Ux = \tilde{f} - z\gamma.$$

If J is nonsingular and J_1 is singular we assume that

$$\mathcal{N}(J_1) = \text{span}\{\phi\}, \quad \mathcal{N}(J_1^T) = \text{span}\{\psi\}, \quad b \notin \mathcal{R}(J_1) \text{ and } c \notin \mathcal{R}(J_1^T)$$

Conditions in (ii) Lemma 2.4 are equivalent to

$$\psi^T b \neq 0, \quad c^T \phi \neq 0,$$

where ϕ and ψ are nontrivial solutions of

$$J_1\phi = 0, \quad J_1^T\psi = 0.$$

Multiplying the first equation of (2.11) by ψ^T , we get

$$z = \frac{\psi^T f}{\psi^T b}.$$

Therefore x is a solution of

$$J_1 x = f - \frac{\psi^T f}{\psi^T b} b \in \mathcal{R}(J_1).$$

Therefore, the previous equation says, all solutions of x have the form

$$x = x_p + \alpha \phi,$$

where x_p is a particular solution and α is obtain by $\alpha = \frac{h-dz-c^T x_p}{c^T \phi}$. To evaluate this solution we need the vectors ψ , ϕ and x_p . Next, we will show how to compute ψ , and ϕ efficiently (left and right null vectors of J_1).

Assume that J_1 has been decomposed into $J_1 = P\tilde{L}\tilde{U}Q$, where P and Q are permutation matrices and

$$\tilde{L} = \begin{pmatrix} L & 0 \\ l^T & 1 \end{pmatrix}, \quad \tilde{U} = \begin{pmatrix} U & u \\ 0^T & 0 \end{pmatrix},$$

where L and U are lower and triangular matrices, respectively, of order $(n-1) \times (n-1)$ and $\tilde{L}, \tilde{U} \in \mathbb{R}^{n-1}$. Thus, ϕ is a solution of $J_1 \phi = 0$, or equivalently, since P and Q are nonsingular, of

$$\begin{pmatrix} U & u \\ 0 & 0 \end{pmatrix} \begin{pmatrix} \nu \\ \mu \end{pmatrix} = \begin{pmatrix} 0 \\ 0 \end{pmatrix}, \quad \begin{pmatrix} \nu \\ \mu \end{pmatrix} \equiv Q\phi.$$

Choose $\mu = -1$. Then find ν from

$$U\nu = u.$$

Since Q is a permutation matrix we have $\phi = Q^T \begin{pmatrix} \nu \\ \mu \end{pmatrix}$. we can also find ψ by just one backsolve: Form $J_1^T \psi = 0$, we have $Q^T \tilde{L}^T \tilde{U}^T P^T \psi = 0$, or equivalently, since Q is nonsingular

$$\begin{pmatrix} U^T & 0 \\ u^T & 0 \end{pmatrix} \begin{pmatrix} L^T & l \\ 0^T & 1 \end{pmatrix} \begin{pmatrix} w \\ \nu \end{pmatrix}, \quad \text{where } \begin{pmatrix} w \\ \nu \end{pmatrix} \equiv P^T \psi.$$

Since U is nonsingular, we must have

$$\begin{pmatrix} L^T & l \\ 0^T & 1 \end{pmatrix} \begin{pmatrix} w \\ \nu \end{pmatrix} = \begin{pmatrix} 0 \\ \nu \end{pmatrix},$$

where $\nu \neq 0$ is arbitrary (e.g., $\nu = -1$). Then w is found from

$$L^T w = l, \quad \psi = P \begin{pmatrix} w \\ -1 \end{pmatrix}.$$

To compute a particular solution x_p of $J_1 x_p = \tilde{f}$, when $\mathcal{N}(J_1) = \text{span}\{\phi\}$, $\tilde{f} \in \mathcal{R}(J_1)$, we have the LU decomposed from

$$P \begin{pmatrix} L & 0 \\ l^T & 1 \end{pmatrix} \begin{pmatrix} U & u \\ 0^T & 0 \end{pmatrix} Q x_p = \tilde{f}.$$

First solve

$$\begin{pmatrix} L & 0 \\ l^T & 1 \end{pmatrix} \begin{pmatrix} \hat{f} \\ \hat{h} \end{pmatrix} = P^T \tilde{f}.$$

Followed by

$$\begin{pmatrix} U & u \\ 0^T & 0 \end{pmatrix} Q x_p = \begin{pmatrix} \hat{f} \\ \hat{h} \end{pmatrix},$$

where $\hat{h} = 0$ because $\hat{f} \in \mathcal{R}(J_1)$ (the system must be solvable). Write

$$\begin{pmatrix} y_p \\ z_p \end{pmatrix} \equiv Q x_p.$$

Note that z_p can be have any value (e.g., $z_p = 0$). Now find y_p from

$$U y_p = \hat{f}, \quad x_p = Q^T \begin{pmatrix} y_p \\ z_p \end{pmatrix}.$$

2.3.2 Periodic orbits via Hopf-points

The eigenvectors in the Hopf point allow one to find the periodic orbit in the phase space. Then a continuation technique with linear prediction is used to further trace behavior of the observed periodic orbit. In our approach we use this notion and replace the basic linear system by a basic piecewise linear system. Therefore, we consider the PWLS (2.5) dependent on two parameters and given in the following form with two perturbation matrices B^\pm and C^\pm as:

$$A^\pm(\alpha, \beta) = A_0^\pm + \alpha B^\pm + \beta C^\pm. \quad (2.12)$$

without loss of generality, the two matrices A_0^+ and A_0^- share the eigenvectors to the same two purely imaginary eigenvalues. Then a periodic orbit can be started from the Hopf bifurcation point for the system $\dot{\xi} = A_0^\pm \xi$ and develops or grow under nonsmooth perturbation.

To simplify the computation, we take $A_0^+ = A_0^- = A_0$, where the matrix A_0 has exactly two purely imaginary eigenvalues. We assume $\bar{\xi}$ is a fixed point of the Poincaré map if and only if $\alpha = \beta = 0$. To determine periodic orbits we set $\mu_c = 1$ and $\mathcal{M} = \{\xi \in \mathbb{R}^n | h(\xi) = e_1^T \xi = 0\}$. For this special situation we try to parameterize the solution by the parameter β . The system to determine the unknown $(n + 4)$ quantities $\xi, t_-(\xi), t_+(\xi), \alpha, \beta$ is given by (2.9) after setting

$$A^\pm = A^\pm(\alpha, \beta).$$

The Jacobian matrix at a special solution $\bar{X} = (\bar{\xi}, s^-, s^+, 0)$ for $\beta = 0$ can be written in the form

$$J = \begin{pmatrix} e^{(s^++s^-)A_0} - I & A_0\bar{\xi} & A_0\bar{\xi} & \frac{\partial F_1}{\partial \alpha}(\bar{X}) \\ n^T e^{s^-A_0} & n^T e^{s^-A_0} A_0 - \bar{\xi} & 0 & n^T s^- e^{s^-A_0} B^- \bar{\xi} \\ n^T & 0 & 0 & 0 \\ 2\bar{\xi}^T & 0 & 0 & 0 \end{pmatrix} = \left(\begin{array}{ccc|c} & & & b \\ & J_1 & & 0 \\ & & & 0 \\ \hline 2\bar{\xi}^T & 0 & 0 & 0 \end{array} \right),$$

where

$$\frac{\partial F_1}{\partial \alpha} \bar{X} = e^{s^+A_0} \left(s^+ B^+ e^{s^-A_0} + s^- e^{s^-A_0} B^- \right) (\bar{\xi}).$$

Regularity of J leads to the existence of nontrivial solutions $X(\beta)$ with $X(0) = (\bar{\xi}, s^-, s^+, 0)$.

In this case J_1 is singular because of the $J_1(\bar{\xi}, 0, 0, 0)^T = 0$.

We assume that the leading matrix of the smooth system where A_0 has exactly two purely imaginary eigenvalues $\pm i\omega$ with corresponding ξ_0 and $\bar{\xi}_0$ where $\bar{\xi} = \xi_0 + \bar{\xi}_0$ generates a degenerate (flat) cone under the flow given by e^{tA_0} . Since the vector fields depends on two parameters, we obtain that there is a function $X(\beta) = (\xi(\beta), t_-(\beta), t_+(\beta), \alpha(\beta))$ satisfying $X_0 = (\bar{\xi}, \frac{\pi}{\omega}, \frac{\pi}{\omega}, 0)$ such that

$$F(X(\beta), \beta) = 0.$$

Existence of invariant periodic cones corresponds to existence of solutions for the above system with $\mu_c = 1$. The stability analysis of these cones consists of computing the other eigenvalues of P at the periodic orbits.

As specific example we choose A_0 , B^\pm and C^\pm in the following form:

$$A_0 = \begin{pmatrix} 0 & -w & 0 \\ w & 0 & 0 \\ 0 & 0 & \mu \end{pmatrix}, \quad B^\pm = \begin{pmatrix} 0 & 0 & 0 \\ 0 & b_{22}^\pm & 0 \\ 0 & 0 & 0 \end{pmatrix}, \quad C^\pm = \begin{pmatrix} 0 & c_{12}^\pm & 0 \\ 0 & c_{22}^\pm & 0 \\ 0 & c_{32}^\pm & 0 \end{pmatrix}.$$

In order to analyze what happens with such periodic orbits as the parameter β varies in the neighborhood of X_0 , we use the fixed-point system (2.9). The solutions of system (2.9) are functions of β at 0 if $-2\pi\omega(e^{2\pi\mu/\omega} - 1)(b_{22}^- + b_{22}^+) \neq 0$ which is equivalent to $\mu \neq 0, b_{22}^- \neq -b_{22}^+$, hence the solution is of the form

$$\begin{aligned}\xi(\beta)^T &= \left(0, 1, \frac{\pi}{\omega} (e^{\pi\mu/\omega} c_{32}^+ - e^{2\pi\mu/\omega} c_{32}^-) \beta / (e^{2\pi\mu/\omega} - 1)\right)^T + O(\beta^2), \\ \alpha(\beta) &= -\frac{c_{22}^- + c_{22}^+}{b_{22}^- + b_{22}^+} \beta + O(\beta^2), \\ t_-(\beta) &= \frac{\pi}{\omega} + \frac{\pi}{\omega^2} c_{12}^- \beta + O(\beta^2), \\ t_+(\beta) &= \frac{\pi}{\omega} + \frac{\pi}{\omega^2} c_{12}^+ \beta + O(\beta^2).\end{aligned}$$

It is obvious that solution of (2.9) are verified by the existence of intersection times of every periodic solution living in the two regions such that $\xi(\beta) \in \mathcal{M}_-^c$.

Remark 2.4. All system parameters should be determined such that $\xi(\beta) \in \mathcal{M}_-^c$, i.e. $\left(-\omega + \beta c_{12}^\pm + O(\beta^2)\right) < 0$, since it is possible that the vector $\xi(\beta)$ leaves the admissible range so that sliding motion may occur.

As specific values for the coefficients we choose

(a) $\omega = 1.0$, $\mu = -1.0$, $b_{22}^+ = -1$, $b_{22}^- = 0.5$, $c_{12}^\pm = c_{22}^\pm = 0.1$, $c_{32}^+ = 0.5$ and $c_{32}^- = -1$. Newton's Method is used to compute the roots of $F(X(\beta), \beta) = 0$. Figure 2.3 shows an attractive invariant cone consisting of periodic orbits.

We also take an example of the form treated in [10] where we choose C^\pm as

$$C^\pm = \begin{pmatrix} c_{11}^\pm & -1 & 0 \\ c_{21}^\pm & 0 & -1 \\ c_{31}^\pm & 0 & 0 \end{pmatrix}.$$

As specific values of the coefficients we choose

(b) $\omega = 1$, $\mu = 0.1$, $b_{22}^\pm = 1$, $c_{11}^+ = -3.2$, $c_{21}^+ = 25.61$, $c_{13}^+ = -75.03$, $c_{11}^- = -1.0$, $c_{21}^- = 1.28$ and $c_{31}^- = -0.624$, Figure 2.4. shows a repulsive invariant cone consisting of periodic orbits.

2.3.3 Parameter dependent stability switches on invariant cones

We assume that

$$A^\pm(\epsilon) = A_0 + B^\pm(\epsilon); \quad (2.13)$$

where

$$A_0 = \begin{pmatrix} \lambda_0 & -\omega_0 & 0 \\ \omega_0 & \lambda_0 & 0 \\ 0 & 0 & \mu_0 \end{pmatrix}, \quad B^\pm(\epsilon) = \epsilon \begin{pmatrix} 0 & 0 & b_{13}^\pm \\ 0 & b_{22}^\pm & 0 \\ b_{31}^\pm & 0 & 0 \end{pmatrix}. \quad (2.14)$$

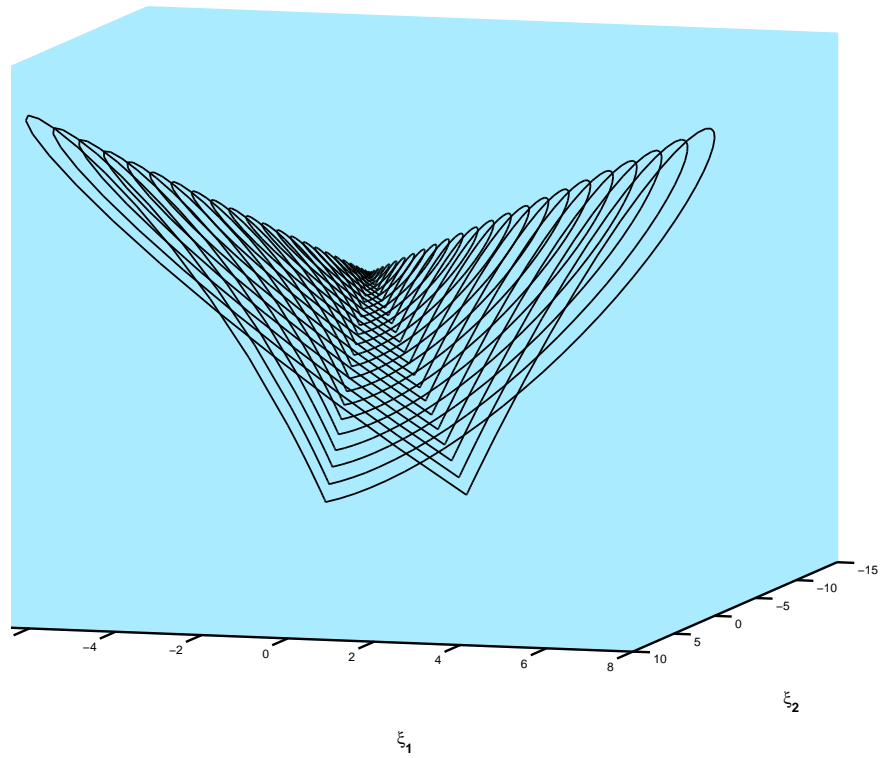


Figure 2.3: Attractive invariant cone consisting of periodic orbits $\beta = 1.5$, $\alpha = 0.6$, $t_- = t_+ = 3.5138$.

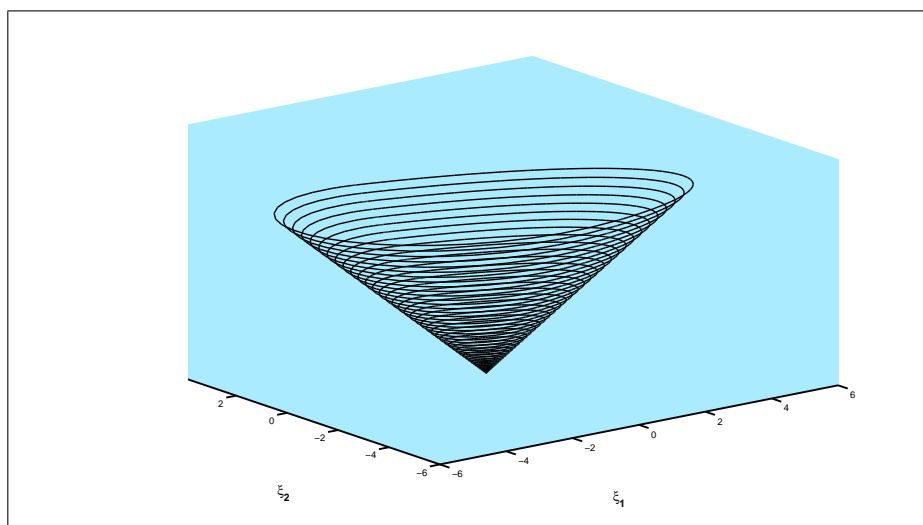


Figure 2.4: Repulsive invariant cone consisting of periodic orbits $\beta = 0.01$, $\alpha = 0.0175$, $t_- = 3.0664$, $t_+ = 2.8229$.

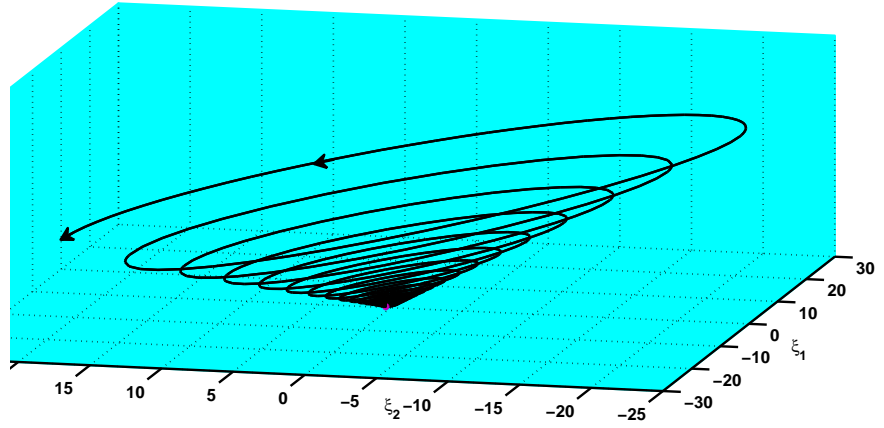


Figure 2.5: An attractive invariant cone with unstable orbits even though all eigenvalues of A^\pm has negative real parts.

We consider the system

$$0 = F(X(\epsilon), \epsilon) = \begin{bmatrix} e^{t_+ A^+(\epsilon)} e^{t_- A^-(\epsilon)} \xi - \mu_c \xi \\ n^T e^{t_- A^-(\epsilon)} \xi \\ n^T \xi \\ \xi^T \xi - 1 \end{bmatrix}, \quad X(\epsilon) = (\xi(\epsilon), t_-(\epsilon), t_+(\epsilon), \bar{\mu}_c(\epsilon))^T, \quad (2.15)$$

The Jacobian matrix is

$$J = \begin{pmatrix} e^{2\pi\lambda_0/\omega_0} - \bar{\mu}I & 0 & 0 & -\omega_0 e^{2\pi\lambda_0/\omega_0} & -\omega_0 e^{2\pi\lambda_0/\omega_0} & 0 \\ 0 & e^{2\pi\lambda_0/\omega_0} - \bar{\mu}I & 0 & \lambda_0 e^{2\pi\lambda_0/\omega_0} & \lambda_0 e^{2\pi\lambda_0/\omega_0} & -1 \\ 0 & 0 & e^{2\pi\mu_0/\omega_0} - \bar{\mu}I & 0 & 0 & 0 \\ -e^{\pi\lambda_0/\omega_0} & 0 & 0 & -\omega_0 e^{2\pi\lambda_0/\omega_0} & 0 & 0 \\ 1 & 0 & 0 & 0 & 0 & 0 \\ 0 & 2 & 0 & 0 & 0 & 0 \end{pmatrix}.$$

We consider the special situation of the discontinuity surface, which may be defined as $\mathcal{M} = \{\xi \in \mathbb{R}^n | h(\xi) = e_1^T \xi = 0\}$.

For *smooth system* (2.13) with $(\epsilon = 0)$, the origin is the only equilibrium point of the system. The stability of the origin with $\mu_0 < 0$ is determined by the sign of the parameter λ_0 . Then, $\lambda_0 = 0$ is a bifurcation point of the system. For $\lambda_0 < 0$, the origin is an asymptotically equilibrium solution of the system and for $\lambda_0 > 0$, the origin is an unstable equilibrium solution of the system.

A *nonsmooth* perturbation (2.13) with $\epsilon \neq 0$ sufficiently small leads to quite different dynamics of the system due to the ratio of deformation of eigenvalues

and eigenvectors of the system and the interaction between the trajectory and the discontinuity surface.

We compute eigenvalues and eigenvectors as polynomials of ϵ as:

$$\begin{aligned}\lambda(\epsilon) &= \lambda_0 \pm i\omega + \frac{1}{2}b_{22}^{\pm}\epsilon + O(\epsilon^2), \\ \mu(\epsilon) &= \mu_0 + O(\epsilon^2),\end{aligned}$$

corresponding to eigenvectors

$$\begin{aligned}\Xi_{\lambda(\epsilon)} &= e_1 \mp i e_2 + \left[(0, -b_{22}^{\pm}/\omega_0, (\lambda_0 - \mu_0)b_{31}^{\pm}/(\omega_0^2 + (\lambda_0 - \mu_0)^2)) \right. \\ &\quad \left. \mp i (b_{22}^{\pm}/(2\omega_0), 0, \omega b_{31}^{\pm}/(\omega_0^2 + (\lambda_0 - \mu_0)^2)) \right]^T \epsilon + O(\epsilon^2), \\ \Xi_{\mu(\epsilon)} &= e_3 + \frac{\epsilon}{(\omega_0^2 + (\lambda_0 - \mu_0)^2)} ((\mu_0 - \lambda_0)b_{13}^{\pm}, \omega_0 b_{13}^{\pm}, 0)^T + O(\epsilon^2).\end{aligned}$$

Clearly, in a generic system (2.13) we may encounter that stability cannot be gained from the stability properties of the subsystems alone. For example, an equilibrium of (2.13) on \mathcal{M}^c may be unstable even if all eigenvalues of both $A^{\pm}(\epsilon)$ have negative real part. To detect this situation consider specific values of the coefficient of A^{\pm} ; $w_0 = 1$, $\mu_0 = \lambda_0 = -\epsilon = -0.01$, $b_{13}^- = -11.0$, $b_{22}^- = -0.01$, $b_{31}^- = -95.0$, $b_{13}^+ = -1.0$, $b_{22}^+ = 0$, and $b_{31}^+ = -75.0$. Using the above algorithm to compute the roots of $F(X(\epsilon), \epsilon) = 0$. We explain this situation by means of invariant cone as: Figure 2.5 shows the corresponding invariant cone which is attracting under the Poincaré map while the motion on \mathcal{C} itself or outside \mathcal{C} is unstable (orbits spiraling “out” of zero). Furthermore, the dynamics on the cone can be stabilized by moving the parameter ϵ and keeping all the parameters fixed.

Part II: The second part of the Chapter will address the general situation of three-dimensional PWLS which may be continuous PWLS or discontinuous. First, a sufficient condition for the non-existence of invariant cones is given. Next, we give an analytical proof of the existence of invariant cones which depends crucially on an explicit construction of a Poincaré map and its relation with a slope transition map. Through the present investigation several case studies are considered, such as; continuous PWLS; existence of multiple invariant cones for discontinuous PWLS.

2.4 Theoretical analysis for general situation

In this section, we provide a systematic analysis and a bifurcation analysis for general PWLS. We will consider a general 3-dimensional PWLS described as

$$\dot{\xi} = \begin{cases} A^+\xi, & e_1^T \xi > 0, \\ A^-\xi, & e_1^T \xi < 0. \end{cases} \quad (2.16)$$

where $h(\xi) = \xi_1$ and A^\pm are 3×3 real matrices both having complex eigenvalues with non-vanishing imaginary part; hence the spectrum of A^\pm is of the form μ^\pm and $\lambda^\pm \pm i\omega^\pm$, $\omega^\pm > 0$.

To state our results we consider the general case and the specific subcases (a) without sliding motion and (b) with continuous vector fields

(a) 3D PWLS without sliding motion

$$A^\pm = \begin{pmatrix} a_{11}^\pm & a_{12} & a_{13} \\ a_{21}^\pm & a_{22}^\pm & a_{23}^\pm \\ a_{31}^\pm & a_{32}^\pm & a_{33}^\pm \end{pmatrix}.$$

According to (2.2) and Figure 2.1, there is no of a sliding motion possible.

(b) 3D PWLS with continuous vector fields

$$A^\pm = \begin{pmatrix} a_{11}^\pm & a_{12} & a_{13} \\ a_{21}^\pm & a_{22} & a_{23} \\ a_{31}^\pm & a_{32} & a_{33} \end{pmatrix}.$$

Again, there is no attractive or repulsive sliding motion possible. In this situation, the existence of invariant cones for a special form of the above 3D continuous PWLS has already been discussed in [10].

In the following study, we first consider the general situation of homogeneous 3D PWLS which is given by

$$A^\pm = \begin{pmatrix} a_{11}^\pm & a_{12}^\pm & a_{13}^\pm \\ a_{21}^\pm & a_{22}^\pm & a_{23}^\pm \\ a_{31}^\pm & a_{32}^\pm & a_{33}^\pm \end{pmatrix}. \quad (2.17)$$

Let us start from the initial position $\xi \in \mathcal{M}_-^c$ or $\xi \in \mathcal{M}_+^c$, then the solutions respectively are denoted by $\varphi^-(t_-, \xi)$ or $\varphi^+(t_+, \xi)$, which are both \mathbf{C}^k ,

2.4.1 Existence of periodic orbits

Depending on the sign of a_{12}^\pm and a_{13}^\pm of (2.17), we obtain a classification for *direct crossing* and *sliding motion* showing the regions where different types of bifurcations occur.

Lemma 2.5. *If $\xi \in \mathcal{M}$, $\xi \neq 0$ and if the coefficients of A^\pm satisfy one of the following conditions (i) or(ii) or (iii) there is no periodic orbit through ξ*

- (i) $a_{13}^\pm \geq 0$, $-\frac{a_{12}^-}{a_{13}^-} \xi_2 \geq \xi_3 \geq -\frac{a_{12}^+}{a_{13}^+} \xi_2$,
- (ii) $a_{13}^+ = 0$, $a_{12}^+ \leq 0$, $\xi_2 \leq 0$, $a_{13}^- \geq 0$, $\xi_3 \leq -\frac{a_{12}^-}{a_{13}^-} \xi_2$,
- (iii) $a_{13}^- = 0$, $a_{12}^- \leq 0$, $\xi_2 \geq 0$, $a_{13}^+ \geq 0$, $\xi_3 \geq -\frac{a_{12}^+}{a_{13}^+} \xi_2$,

Proof:

By observation and study of the location and the dynamic properties of the vector field, i.e., by means of a vectors field evaluation on the four sectors which are defined in (2.2), where the \mathcal{M} is a two-dimensional space such that horizontal axis is the ξ_2 -axis and vertical axis is ξ_3 -axis on a graph. For instance, appropriate specification of these quantities will lead to the various situations, see Figures 2.6 and 2.7. It is interesting to study the changes from one constellation to another.

Remark 2.5. *To obtain nontrivial invariant cones or periodic orbits none of the conditions in Lemma 2.5 should hold.*

Next, we will establish slope transition maps by means of Poincaré map techniques and based on some topological characterization of the fixed points of P . The point $\xi^0 = (0, \xi_2^0, \xi_3^0)$ will be transformed into $\xi^1 = (0, \xi_2^1, \xi_3^1)$ by the Poincaré half map P_- . Analogously the point ξ^1 will be transformed into $\xi^2 = (0, \xi_2^2, \xi_3^2)$ by P_+ , see Figure 2.8. Note that if the composite map $P(\xi^0) = \xi^2$ has a fixed points, then, system (2.16) has a two-zonal invariant cone.

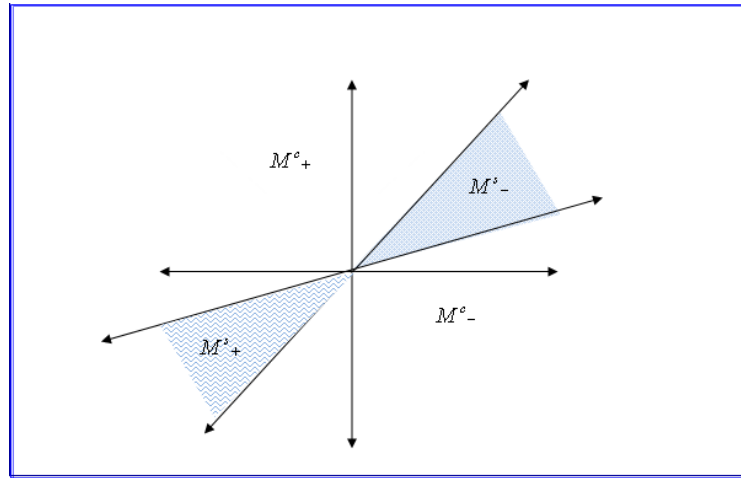


Figure 2.6: Location of direct/sliding motion if $a_{12}^{\pm} > 0$, $a_{13}^{\pm} > 0$, there is no periodic orbit if $-\frac{a_{12}^-}{a_{13}^-} \xi_2 > \xi_3 > -\frac{a_{12}^+}{a_{13}^+} \xi_2$.

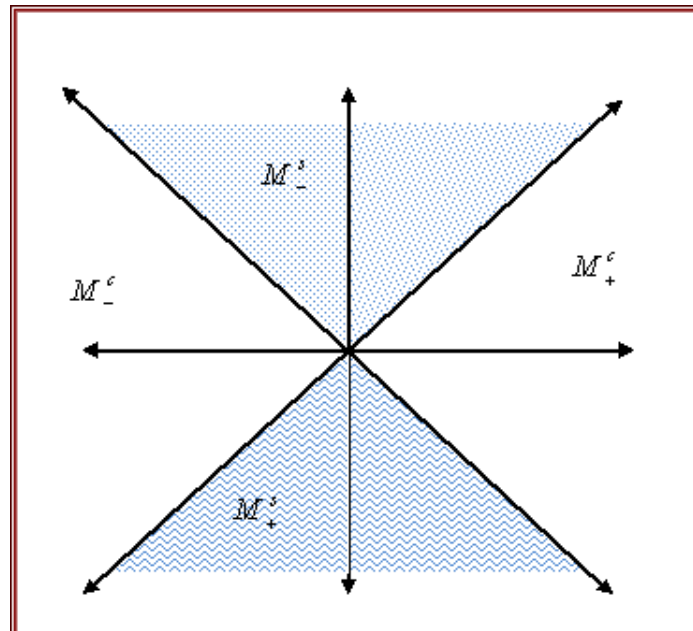


Figure 2.7: Location of direct/sliding motion if $a_{12}^{\pm} > 0$, $a_{13}^- > 0$, $a_{13}^+ < 0$, there is no periodic orbit if $-\frac{a_{12}^-}{a_{13}^-} \xi_2 < \xi_3 < -\frac{a_{12}^+}{a_{13}^+} \xi_2$.

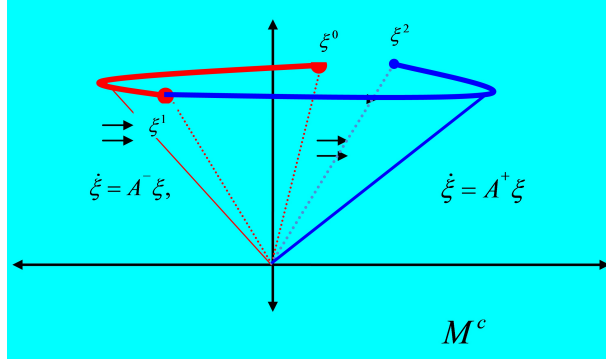


Figure 2.8: Structure of invariant cone with slope transition maps

Definition 2.3. Using the Poincaré half maps P_{\pm} and where $\mathcal{M} = \{\xi \in \mathbb{R}^3 \mid e_1^T \xi = 0\}$, Figure 2.8. Then by $\{\xi \in \mathbb{R}^3 \mid e_1^T \varphi^{\pm}(t_{\pm}, \xi) = 0\}$ we can define two slope transition maps $S_{\pm} : \mathbb{R} \rightarrow \mathbb{R}$, $m_1 = S_-(m_0)$ and $n_1 = S_+(n_0)$, respectively

- $m_0 = \frac{\xi_3^0}{\xi_2^0}$, i.e., the slope of the line $\xi_3^0 = m_0 \xi_2^0$, $(\xi_2^0, \xi_3^0) \in \mathcal{M}_-$ through P_- and $m_1 = \frac{\xi_3^1}{\xi_2^1}$ is the image of m_0 which passes through the point $(\xi_2^1, \xi_3^1) = P_-(\xi_2^0, \xi_3^0)$, $(\xi_2^1, \xi_3^1) \in \mathcal{M}_+$.
- n_0 is the slope of line $\xi_3^1 = n_0 \xi_2^1$, $(\xi_2^1, \xi_3^1) \in \mathcal{M}_+$ through P_+ and $n_1 = \frac{\xi_3^2}{\xi_2^2}$ is the image of n_0 which passes through the point $(\xi_2^2, \xi_3^2) = P_+(\xi_2^1, \xi_3^1)$, $(\xi_2^2, \xi_3^2) \in \mathcal{M}_-$.

Lemma 2.6. Let μ^{\pm} and $\lambda^{\pm} \pm i\omega^{\pm}$, $\omega^{\pm} > 0$ be eigenvalues of A^{\pm} of (2.17). The following statements hold with quantities $\mathcal{A}_1, \mathcal{B}_1, \dots$ given below.

- (i) For an initial value $\xi^0 \in \mathcal{M}_-$, the trajectory given by the Poincaré halfmap P_- transforms the point ξ^0 into the point $\xi^1 \in \mathcal{M}_+$, with $(\xi^0)^T \xi^1 \neq 0$ for the first positive time $t_- > 0$ which can be defined from $e_1^T \varphi^-(t_-, \xi^0) = 0$, so that

$$m_0(t_-) = -\frac{\alpha \mathcal{A}_1 \mathcal{B}_1 + 2\mathcal{A}_2 \mathcal{B}_2 - \sigma \mathcal{A}_3 \mathcal{B}_3}{2\alpha \mathcal{A}_1 \mathcal{R}_1 - 2\mathcal{A}_2 \mathcal{R}_2 + \mathcal{A}_3 \mathcal{R}_3},$$

$$m_1(t_-) = \frac{\alpha \mathcal{K}_4 \mathcal{B}_1 - 2\mathcal{K}_3 \mathcal{B}_2 + \sigma \gamma E \mathcal{B}_3 + (2\alpha \mathcal{K}_4 \mathcal{R}_1 + 2\mathcal{K}_3 \mathcal{R}_2 - \gamma E \mathcal{R}_3)m_0(t_-)}{\alpha \mathcal{K}_1 \mathcal{B}_1 - 2\mathcal{K}_2 \mathcal{B}_2 + 2\beta \sigma E \mathcal{B}_3 + (2\alpha \mathcal{K}_1 \mathcal{R}_1 + 2\mathcal{K}_2 \mathcal{R}_2 - 2\beta E \mathcal{R}_3)m_0(t_-)}.$$

Furthermore, we can also get

$$\frac{\xi_2^1}{\xi_2^0} = \frac{1}{\Delta} \left[e^{\lambda^- t_-} (\alpha \mathcal{K}_1 \mathcal{B}_1 - 2\mathcal{K}_2 \mathcal{B}_2) + 2\beta \sigma \mathcal{B}_3 e^{\mu^- t_-} + \left(e^{\lambda^- t_-} (2\alpha \mathcal{K}_1 \mathcal{R}_1 + 2\mathcal{K}_2 \mathcal{R}_2) - 2\beta \mathcal{R}_3 e^{\mu^- t_-} \right) m_0(t_-) \right],$$

$$\frac{\xi_3^1}{\xi_3^0} = \frac{1}{\Delta} \left[\frac{e^{\lambda^- t_-} (\alpha \mathcal{K}_4 \mathcal{B}_1 - 2\mathcal{K}_3 \mathcal{B}_2) + \sigma \gamma \mathcal{B}_3 e^{\mu^- t_-}}{m_0(t_-)} + e^{\lambda^- t_-} (2\alpha \mathcal{K}_4 \mathcal{R}_1 + 2\mathcal{K}_3 \mathcal{R}_2) - \gamma \mathcal{R}_3 e^{\mu^- t_-} \right].$$

The above parameters only refer to \ominus -system with the matrix A^- .

- (ii) In a similar way, the point $\xi^1 \in \mathcal{M}_+^c$ is transformed into $\xi^2 \in \mathcal{M}_-^c$ via Poincaré halfmap P_+ , with $(\xi^1)^T \xi^2 \neq 0$ for the first positive time $t_+ > 0$ which can be defined from $e_1^T \varphi^-(t_-, \xi^1) = 0$, so that

$$n_0(t_+) = -\frac{\alpha \mathcal{A}_1 \mathcal{B}_1 + 2\mathcal{A}_2 \mathcal{B}_2 - \sigma \mathcal{A}_3 \mathcal{B}_3}{2\alpha \mathcal{A}_1 \mathcal{R}_1 - 2\mathcal{A}_2 \mathcal{R}_2 + \mathcal{A}_3 \mathcal{R}_3},$$

$$n_1(t_+) = \frac{\alpha \mathcal{K}_4 \mathcal{B}_1 - 2\mathcal{K}_3 \mathcal{B}_2 + \sigma \gamma E \mathcal{B}_3 + (2\alpha \mathcal{K}_4 \mathcal{R}_1 + 2\mathcal{K}_3 \mathcal{R}_2 - \gamma E \mathcal{R}_3) n_0(t_+)}{\alpha \mathcal{K}_1 \mathcal{B}_1 - 2\mathcal{K}_2 \mathcal{B}_2 + 2\beta \sigma E \mathcal{B}_3 + (2\alpha \mathcal{K}_1 \mathcal{R}_1 + 2\mathcal{K}_2 \mathcal{R}_2 - 2\beta E \mathcal{R}_3) n_0(t_+)}.$$

Furthermore, we can also get

$$\frac{\xi_2^2}{\xi_2^1} = \frac{1}{\Delta} \left[e^{\lambda^+ t_+} (\alpha \mathcal{K}_1 \mathcal{B}_1 - 2\mathcal{K}_2 \mathcal{B}_2) + 2\beta \sigma \mathcal{B}_3 e^{\mu^+ t_+} + \left(e^{\lambda^+ t_+} (2\alpha \mathcal{K}_1 \mathcal{R}_1 + 2\mathcal{K}_2 \mathcal{R}_2) - 2\beta \mathcal{R}_3 e^{\mu^+ t_+} \right) n_0(t_+) \right],$$

$$\frac{\xi_3^2}{\xi_3^1} = \frac{1}{\Delta} \left[\frac{e^{\lambda^+ t_+} (\alpha \mathcal{K}_4 \mathcal{B}_1 - 2\mathcal{K}_3 \mathcal{B}_2) + \sigma \gamma \mathcal{B}_3 e^{\mu^+ t_+}}{n_0(t_+)} + e^{\lambda^+ t_+} (2\alpha \mathcal{K}_4 \mathcal{R}_1 + 2\mathcal{K}_3 \mathcal{R}_2) - \gamma \mathcal{R}_3 e^{\mu^+ t_+} \right].$$

Currently, the above parameters only refer to \oplus -system with the matrix A^+ .

- iii- A similar result holds for $\xi^0 \in \mathcal{M}_+^c$ and $\xi^1 \in \mathcal{M}_-^c$.

Proof:

If $\xi^0 \in \mathcal{M}_-^c$ and assuming that A_N^\pm are given in Jordan normal form and $(\mathbf{S}^\pm)^{-1}$ denote the inverse of transformation matrix as:

$$A_N^\pm = \begin{pmatrix} \lambda^\pm & -w^\pm & 0 \\ w^\pm & \lambda^\pm & 0 \\ 0 & 0 & \mu^\pm \end{pmatrix}, \quad (\mathbf{S}^\pm)^{-1} = \begin{pmatrix} 1 & \frac{-\alpha^\pm(\alpha^\pm+1)}{2} & -\alpha^\pm \\ \beta^\pm + \sigma^\pm & k^\pm & 2\beta^\pm \\ \beta^\pm \sigma^\pm & k^\pm \sigma^\pm & \gamma^\pm \end{pmatrix}.$$

Thus, we can replace (2.17) by the following form:

$$A^\pm = (\mathbf{S}^\pm)^{-1} A_N^\pm \mathbf{S}^\pm.$$

Note that this transformation does not perturb the separation manifold \mathcal{M} .

Then the general solution of (2.16) is given by

$$\begin{aligned} \xi(t_\pm) = & e^{\lambda^\pm t_\pm} \{ (\cos(\omega^\pm t_\pm) (\mathbf{S}^\pm)^{-1} e_1 + \sin(\omega^\pm t_\pm) (\mathbf{S}^\pm)^{-1} e_2) \bar{\xi}_1 \\ & + (\cos(\omega^\pm t_\pm) (\mathbf{S}^\pm)^{-1} e_2 - \sin(\omega^\pm t_\pm) (\mathbf{S}^\pm)^{-1} e_1) \bar{\xi}_2 \} + e^{\mu^\pm t_\pm} (\mathbf{S}^\pm)^{-1} e_3 \bar{\xi}_3, \end{aligned} \quad (2.18)$$

where

$$\mathbf{S}^\pm \xi(0) = \bar{\xi}, \quad \xi(0) = (0, \xi_2^0, \xi_3^0)^T \in M^c.$$

The general solution (2.18) allows us to construct Poincaré halfmaps P_\pm for \ominus and \oplus -systems; the flow starts from the initial point $\xi^0 \in \mathcal{M}_-^c$ and spends a time t_- before it returns to $\xi^1(t_-) \in \mathcal{M}_-^c$. At that point, the flow starts once again and spends a time t_+ before it reaches $\xi^2(t_+) \in \mathcal{M}_-^c$, see Figure 2.8. The return times $t_\pm(\xi)$ depend on ξ and are determined as smallest positive root of $e_1^T \xi(t_\pm) = 0$. Consequently, by solving $\xi^1(t_-) = \xi^0$ and $\xi^2(t_+) = \xi^1$ we can get the coordinate ratios for the initial and end values in terms of the parameters as (i) and (ii).

Following, we give a list of assignments for parameters that are used in this Lemma. Note that for simplicity, we omit superscripts (\pm) in the following parameters.

$$\begin{aligned} \mathcal{A}_1 &= (c - \frac{\alpha(\alpha+1)}{2}s), & \mathcal{A}_2 &= (\frac{\alpha(\alpha+1)}{2}c + s), & \mathcal{A}_3 &= \alpha E, \\ \mathcal{B}_1 &= (2k\sigma - \gamma(1+\alpha)), & \mathcal{B}_2 &= (\gamma + \alpha\beta\sigma), & \mathcal{B}_3 &= (2k + \alpha\beta(1+\alpha)), \\ \mathcal{R}_1 &= \beta(1+\alpha) - k, & \mathcal{R}_2 &= ((2+\alpha)\beta + \alpha\sigma), & \mathcal{R}_3 &= (2k + \alpha(\beta + \sigma)(1+\alpha)), \\ \mathcal{K}_1 &= sk + c(\beta + \sigma), & \mathcal{K}_2 &= ck - s(\beta + \sigma), & \mathcal{K}_3 &= ck\sigma - s\beta\sigma, & \mathcal{K}_4 &= c\beta\sigma + sk\sigma, \\ \Delta &= (1+\alpha)(2\beta^2\sigma\alpha - \alpha\gamma(\sigma + \beta)) + k(2\sigma(2\beta + \alpha\sigma) - 2\gamma), \\ E &= e^{(\mu-\lambda)t}, & s &= \sin(\omega t), & c &= \cos(\omega t). \end{aligned}$$

If the initial point $\xi^0 \in \mathcal{M}_+^c$ and $\xi^1 \in \mathcal{M}_-^c$, i.e. $P_+(\xi^0) = \xi^1$, and $P_-(\xi^1) = \xi^2$, $\xi^2 \in \mathcal{M}_+^c$. Then property (iii) is seen immediately as analogous scenario.

Theorem 2.3. *Suppose the eigenvalues of A^\pm are $\lambda^\pm \pm i\omega^\pm$, μ^\pm with $\omega^\pm > 0$, corresponding eigenvectors $(\mathbf{S}^\pm)^{-1}e_1 \pm i(\mathbf{S}^\pm)^{-1}e_2$, $(\mathbf{S}^\pm)^{-1}e_3$ and Υ_i satisfies $\det(P' - \Upsilon_j I) = 0, j = 1, 2$. Then system (2.16) has an invariant cone \mathcal{C} if and only if there exist $t_\pm > 0$ such that*

- (i) $n_0(t_+) = m_1(t_-)$,
- (i) $n_1(t_+) = m_0(t_-)$.

The dynamics on the invariant cone \mathcal{C} is determined by the following rules:

- If $|\Upsilon_1| > 1$ or $|\Upsilon_2| > 1$, then \mathcal{C} is an unstable focus.
- If $|\Upsilon_1| \leq 1$ and $|\Upsilon_2| \leq 1$, then \mathcal{C} is a stable focus.
- If $(\Upsilon_1 = 1$ and $|\Upsilon_2| \leq 1)$ or $(\Upsilon_2 = 1$ and $|\Upsilon_1| \leq 1)$ then \mathcal{C} is attractive and consists of periodic orbits (center+stable focus).

- If $(\gamma_1 = 1 \text{ and } |\gamma_2| > 1)$ or $(\gamma_2 = 1 \text{ and } |\gamma_1| > 1)$ then \mathcal{C} is repulsive and consists of periodic orbits (center+unstable focus).

In other words, the dynamics on \mathcal{C} can be monitored simply by measuring the ratio of the distance between start and end points on the invariant straight line as:

$$D = \sqrt{\frac{(\xi_2^2)^2 + (\xi_3^2)^2}{(\xi_2^0)^2 + (\xi_3^0)^2}} = \sqrt{\frac{(\xi_2^2)^2(1 + n_1^2)}{(\xi_2^0)^2(1 + m_0^2)}} = \frac{\xi_2^2}{\xi_2^0},$$

hence, \mathcal{C} is a stable focus (center focus or unstable focus) if $D < 1$ ($D = 1$ or $D > 1$).

Note that, using Lemma 2.6, we can explicitly compute D .

Lemma 2.7. Considering PWLS (2.16) with $\alpha^\pm = \beta^\pm = 0$ in \mathbf{S}^\pm , then both intersection times are constant $t_\pm = \frac{\pi}{\omega^\pm}$ and sliding motion occurs if k^+ and k^- have opposite signs.

Proof:

If $\alpha^\pm = \beta^\pm = 0$, then the both subsystems given as:

$$A^\pm = \begin{pmatrix} \frac{\lambda k + \omega \sigma}{k} & \frac{-\omega}{k} & 0 \\ \frac{\omega(\sigma^2 + k^2)}{k} & \frac{\lambda k - \omega \sigma}{k} & 0 \\ \sigma(\omega k - \sigma(\lambda - \mu)) & \sigma(\lambda - \mu) & \mu \end{pmatrix}^\pm, \text{ where } (\mathbf{S}^\pm)^{-1} = \begin{pmatrix} 1 & 0 & 0 \\ \sigma^\pm & k^\pm & 0 \\ 0 & k^\pm \sigma^\pm & \gamma^\pm \end{pmatrix}.$$

The return times $t_\pm(\xi)$ are determined as smallest positive root of $e_1^T \xi(t_\pm) = 0$. Then, we have $2s^\pm \gamma^\pm \xi_2 = 0$ leads to $t_\pm = \frac{\pi}{\omega^\pm}$ and $\xi_2 \neq 0$. According to the definition of \mathcal{M}_\pm^s in (2.2), sliding motion is possible if k^+ and k^- have opposite signs.

2.4.2 Case I: $\alpha^\pm = \beta^\pm = \sigma^+ = 0, k^\pm = \gamma^\pm = 1, \sigma^- = -\delta$.

In this case, PWLS (2.16) allows to ensure that a simple situation will be considered, where $A^+ = A_N^+$ and

$$A^- = \begin{pmatrix} \lambda^- - \delta \omega^- & -\omega & 0 \\ \omega(\delta^2 + 1) & \lambda^- + \delta \omega^- & 0 \\ -\delta(\omega^- + \delta(\lambda^- - \mu^-)) & -\delta(\lambda^- - \mu^-) & \mu^- \end{pmatrix}.$$

Then there are two invariant half-planes for the \oplus and \ominus -system respectively, spanned by $\langle e_1, e_2 \rangle$ for the \oplus -system and $\langle (1, -\delta, 0)^T, (0, 1, -\delta)^T \rangle$ for the \ominus -system. For both systems we obtain $\mathcal{M}_\mp^c = \{\xi \in \mathbb{R}^3 | \xi_1 = 0, \pm \xi_2 > 0\}$ and $\mathcal{M}_\mp^s = \{\emptyset\}$, hence there is no *sliding motion*. Note that $\xi = (0, 0, 1)^T$ is an eigenvector representing the z-axis which can be considered as a degenerated

invariant cone although ξ is not contained in \mathcal{M}_\pm^c . According to Theorem 2.3 and Lemma 2.7 we obtain $t_\pm = \frac{\pi}{\omega^\pm}$ as solution of $e_1^T \psi(t_\pm, \xi) = 0$, hence the Poincaré map is linear in ξ on \mathcal{M}_-^c . The explicit Poincaré map P mapping $\langle \xi_2, \xi_3 \rangle$ -plane into itself is given by

$$P = \begin{pmatrix} e^{(\lambda^+/\omega^+ + \lambda^-/\omega^-)\pi} & 0 \\ \delta e^{\mu^+\pi/\omega^+} (e^{\lambda^-\pi/\omega^-} + e^{\mu^-\pi/\omega^-}) & e^{(\mu^+/\omega^+ + \mu^-/\omega^-)\pi} \end{pmatrix} \begin{pmatrix} \xi_2 \\ \xi_3 \end{pmatrix}.$$

There are 2 cases to obtain an invariant cone of periodic orbits: Since an invariant cone requires that either Υ_1 or Υ_2 equals 1 where

$$\Upsilon_1 = e^{(\lambda^+/\omega^+ + \lambda^-/\omega^-)\pi}, \Upsilon_2 = e^{(\mu^+/\omega^+ + \mu^-/\omega^-)\pi}.$$

(i) We get: $\Upsilon_1 = 1$, (i.e. $\lambda^+/\omega^+ + \lambda^-/\omega^- = 0$) and $\Upsilon_2 \neq 1$.

The corresponding eigenvector is calculated as

$$\bar{\xi} = \begin{pmatrix} 1 \\ \delta \frac{e^{\mu^+\pi/\omega^+} (e^{\lambda^-\pi/\omega^-} + e^{\mu^-\pi/\omega^-})}{1 - \Upsilon_2} \end{pmatrix},$$

the corresponding cone is attractive if $\mu^+/\omega^+ + \mu^-/\omega^- < 0$ and repulsive if $\mu^+/\omega^+ + \mu^-/\omega^- > 0$, hence stability is determined by the time spent in each half-space, which is measured by ω^- and ω^+ . For example see Figure 2.10 and Figure 2.9.

For $\delta = 0$ (the smooth case i.e. $A^\pm = A_N^\pm$) there is a degenerate (flat) cone within the (ξ_1, ξ_2) -plane, for $\delta \neq 0$ a nontrivial cone tending to the positive z-axis for $\delta(1 - \Upsilon_2) \rightarrow \infty$ and to the negative z-axis for $\delta(1 - \Upsilon_2) \rightarrow -\infty$.

For fixed $\delta \neq 0$, variation of μ^+ for example from $-\infty$ to ∞ corresponds to an attractive cone developing out of the (ξ_1, ξ_2) -plane approaching the ξ_3 -axis for $\mu^+ \rightarrow -\mu^-\omega^-/\omega^+$; for $\mu^+ = -\mu^-\omega^-/\omega^+$ there is no invariant cone; for $\mu^+ > -\mu^-\omega^-/\omega^+$ there is an repulsive cone.

(ii) $\Upsilon_2 = 1$, (i.e. $\mu^+/\omega^+ + \mu^-/\omega^- = 0$) implies $\delta \xi_2 = 0$, and $e^{(\lambda^+/\omega^+ + \lambda^-/\omega^-)\pi} \xi_2 = \xi_2$, hence either $\xi_2 = 0$ or $\delta = 0$, $\lambda^+/\omega^+ + \lambda^-/\omega^- = 0$. The case $\delta \xi_2 = 0$ corresponds to an invariant z-axis. Iterations of the Poincaré map starting in $(\xi_2^0, \xi_3^0) \in \mathcal{M}_-^c$ give

$$\xi_2^{n+1} = \Upsilon_1 \xi_2^n = \Upsilon_1^{n+1} \xi_2^0,$$

$$\xi_3^{n+1} = \delta (e^{(\mu^+/\omega^+ + \lambda^-/\omega^-)\pi} + 1) \xi_2^n + \xi_3^n,$$

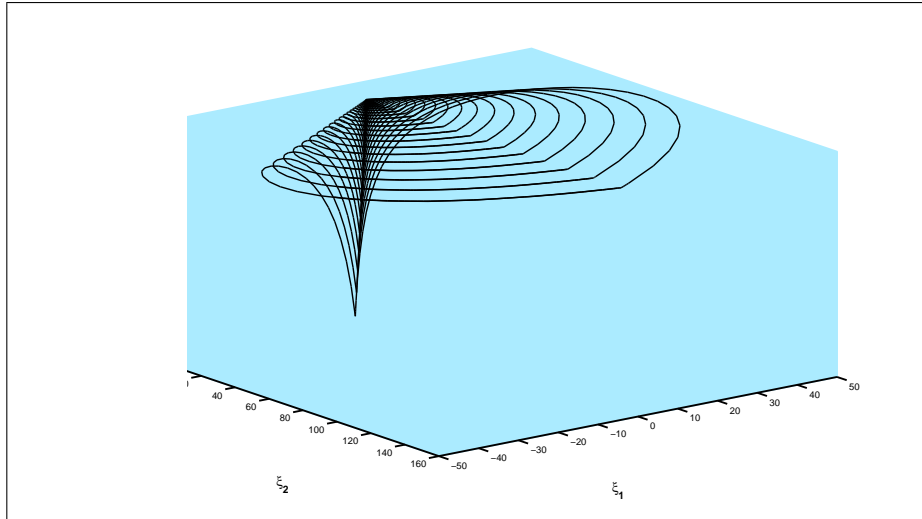


Figure 2.9: Attractive invariant cone consists of periodic orbits for $\lambda^+ = -\lambda^- = 1$, $\omega^\pm = 1, \mu^- = -1.5, \mu^+ = 1.2$.

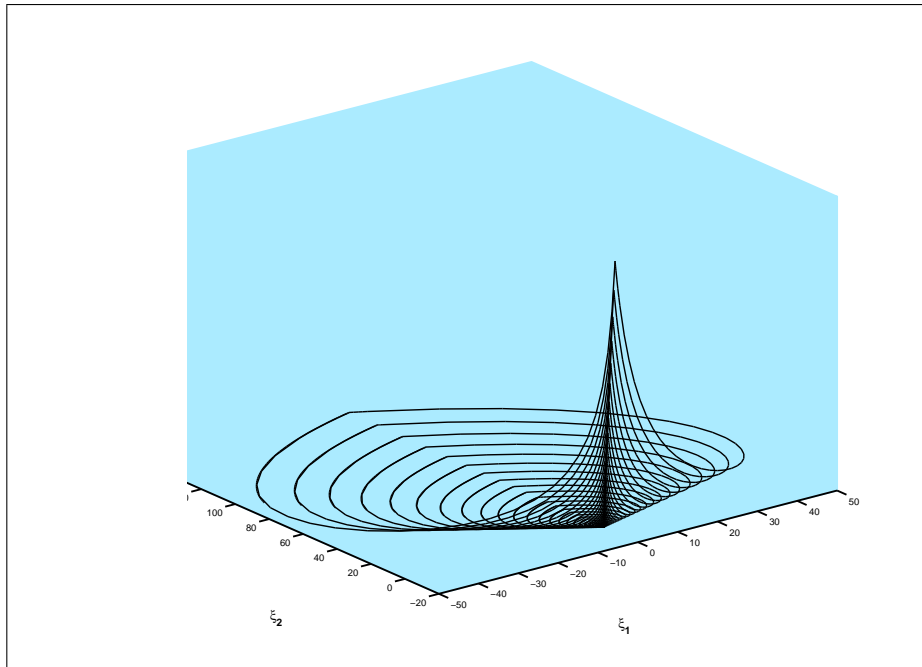


Figure 2.10: Repulsive invariant cone consists of periodic orbits for $\lambda^+ = -\lambda^- = 1.0$, $\omega^\pm = 1.0, \mu^- = -1.5, \mu^+ = 1.62$.

hence

$$\begin{aligned}
\xi_2^{n+1} &= \Upsilon_1^{n+1} \xi_2^0, \\
\xi_3^{n+1} &= \sum_{i=0}^n \delta(e^{(\mu^+/\omega^+ + \lambda^-/\omega^-)\pi} + 1) \xi_2^i + \xi_3^0, \\
&= \delta(e^{(\mu^+/\omega^+ + \lambda^-/\omega^-)\pi} + 1) \sum_{i=0}^n \xi_2^i + \xi_3^0, \\
&= \delta(e^{(\mu^+/\omega^+ + \lambda^-/\omega^-)\pi} + 1) \sum_{i=0}^n \Upsilon_1^i \xi_2^0 + \xi_3^0, \\
&= \delta(e^{(\mu^+/\omega^+ + \lambda^-/\omega^-)\pi} + 1) \xi_2^0 \sum_{i=0}^n \Upsilon_1^i + \xi_3^0,
\end{aligned}$$

hence

$$\xi_2^n \rightarrow \begin{cases} 0, & \Upsilon_1 < 1 \\ \equiv \xi_2^0, & \Upsilon_1 = 1 \\ \infty, & \Upsilon_1 > 1 \end{cases}$$

$$\xi_3^n \rightarrow \begin{cases} \delta(e^{(\mu^+/\omega^+ + \lambda^-/\omega^-)\pi} + 1) \xi_2^0 \frac{1}{1-\Upsilon_1}, & \Upsilon_1 < 1. \\ \infty, & \Upsilon_1 \geq 1 \end{cases}$$

Since $t_- = \pi/\omega^-$ the relation $\Upsilon_1 = 1$ is equivalent to $\lambda^+/\omega^+ + \lambda^-/\omega^- = 0$.

In any case there is no periodic cone.

2.4.3 Case II: $\alpha^\pm = -1, \beta^\pm = \lambda^\pm, k^\pm = \omega^\pm, \sigma^\pm = \mu^\pm, \gamma^\pm = (\lambda^\pm)^2 + (\omega^\pm)^2$

In this case, we have a *continuous* PWLS such that:

$$A^\pm = \begin{pmatrix} \mu^\pm + 2\lambda^\pm & -1 & 0 \\ 2\mu^\pm\lambda^\pm + (\lambda^\pm)^2 + (\omega^\pm)^2 & 0 & -1 \\ \mu^\pm((\lambda^\pm)^2 + (\omega^\pm)^2) & 0 & 0 \end{pmatrix}, \quad (2.19)$$

where

$$(\mathbf{S}^\pm)^{-1} = \begin{pmatrix} 1 & 0 & 1 \\ \lambda^\pm + \mu^\pm & \omega^\pm & 2\lambda^\pm \\ \lambda^\pm\mu^\pm & \mu^\pm\omega^\pm & (\lambda^\pm)^2 + (\omega^\pm)^2 \end{pmatrix}.$$

Clearly no sliding motion can occur on \mathcal{M} . Hence, there is only a direct crossing between the half spaces. The existence of invariant cones and the stability of the origin for the above system has already been investigated in [9, 11] by using the properties of the auxiliary function and transferring (2.19) to a continuous piecewise cubic system.

Here, we give some direct results concerning the existence of \mathcal{C} based on existence of solutions of (i),(ii) in Theorem 2.3. Hence, from Lemma (2.6) we can rewrite quantities in (i) and (ii) as follows :

$$m_0(t_-) = \frac{\mu^- \omega^- (E^- - c^-) + s^- ((\lambda^-)^2 + (\omega^-)^2 - \lambda^- \mu^-)}{\omega^- (E^- - c^-) + s^- (\lambda^- - \mu^-)},$$

$$\begin{aligned}
m_1(t_-) &= \frac{\omega^- \mu^- (c^- E^- - 1) + s^- E^- ((\lambda^-)^2 + (\omega^-)^2 - \lambda^- \mu^-)}{\omega^- (c^- E^- - 1) + s^- E^- (\lambda^- - \mu^-)}, \\
n_0(t_+) &= \frac{\mu^+ \omega^+ (E^+ - c^+) + s^+ ((\lambda^+)^2 + (\omega^+)^2 - \lambda^+ \mu^+)}{\omega^+ (E^+ - c^+) + s^+ (\lambda^+ - \mu^+)}, \\
n_1(t_+) &= \frac{\omega^+ \mu^+ (c^+ E^+ - 1) + s^+ E^+ ((\lambda^+)^2 + (\omega^+)^2 - \lambda^+ \mu^+)}{\omega^+ (c^+ E^+ - 1) + s^+ E^+ (\lambda^+ - \mu^+)}.
\end{aligned}$$

Further

$$D = \frac{F(\omega^+(c^+ E^+ - 1) - s^+ E^+(\mu^+ - \lambda^+))(\omega^-(c^- E^- - 1) - s^- E^-(\mu^- - \lambda^-))}{(\omega^+(E^+ - c^+) + s^+(\lambda^+ - \mu^+))(\omega^-(E^- - c^-) + s^-(\lambda^- - \mu^-))}.$$

Lemma 2.8. *For the continuous PWLS (2.16) where A^\pm are given by (2.19), the following statements hold:*

(c₁) $n_0(\frac{\pi}{\omega^+}) = n_1(\frac{\pi}{\omega^+}) = \mu^+$, $m_0(\frac{\pi}{\omega^-}) = m_1(\frac{\pi}{\omega^-}) = \mu^-$,

$$\lim_{t \rightarrow 0} m_0(t) = \lim_{t \rightarrow 0} n_0(t) = \infty, \quad \lim_{t \rightarrow 0} m_1(t) = \lim_{t \rightarrow 0} n_1(t) = -\infty.$$

(c₂) *If $\lambda^+ = \lambda^- = \hat{\mu}$, $\hat{\mu} \in \mathbb{R}$, then the continuous PWLS has only one invariant cone for $t_\pm = \pi/\omega^\pm$, which is stable focus (center focus or unstable focus) if $\hat{\mu} < 0$ ($\hat{\mu} = 0$ or $\hat{\mu} > 0$).*

(c₃) *If $\lambda^\pm = \mu^\pm = \hat{\mu}$, $\hat{\mu} \in \mathbb{R}$, then the continuous PWLS has only one invariant cone if and only if $t_\pm = \pi/\omega^\pm$, which is stable focus (center focus or unstable focus) if $\hat{\mu} < 0$ ($\hat{\mu} = 0$ or $\hat{\mu} > 0$).*

(c₄) *If the continuous PWLS (2.19) has no invariant cones, then the origin is asymptotically stable if $\lambda^\pm < 0, \mu^\pm < 0$.*

(c₅) *If $\lambda^\pm = \lambda < 0, \omega^\pm = \omega > 0$, then the origin is asymptotically stable if $\mu^\pm < 0$.*

To display more results on the existence of \mathcal{C} and stability of continuous PWLS (2.19), see [9, 10].

2.4.4 Case III: $\alpha^+ = -1, \alpha^- = \alpha, \beta^- = \sigma^\pm = 0, \beta^+ = \lambda^+; k^\pm = \gamma^\pm = 1$.

In this case we get

$$\begin{aligned}
A^- &= \begin{pmatrix} \lambda^- - \frac{\alpha}{2}(\alpha + 1)\omega^- & -\omega^- - \frac{\omega^-}{4}(\alpha + \alpha^2)^2 & \alpha(\lambda^- - \mu^- - \frac{\alpha}{2}(\alpha + 1)\omega^-) \\ \omega^- & \lambda^- + \frac{\alpha}{2}(\alpha + 1)\omega & \alpha\omega^- \\ 0 & 0 & \mu^- \end{pmatrix}, \\
A^+ &= \begin{pmatrix} \lambda^+(1 + \omega^+) & -\omega^+ & \lambda^+(\omega^+ - 1) + \mu^+ \\ \omega^+(\lambda^{+2} + 1) & \lambda^+(1 - \omega^+) & \lambda^{+2}(\omega^+ - 2) + 2\lambda^+\mu^+ - \omega^+ \\ 0 & 0 & \mu^+ \end{pmatrix},
\end{aligned} \tag{2.20}$$

where α is a free parameter.

Because $\xi \in \mathcal{M}_-^c$ we get (according to Lemma 2.5)

$$\frac{\xi_3}{\xi_2} < \frac{w^-(1 + (\alpha + \alpha^2)^2/4)}{\alpha(\lambda^- - \mu^-) - \alpha^2(\alpha + 1)\omega^-/2}, \quad \text{if } \alpha(\lambda^- - \mu^-) - \alpha^2(\alpha + 1)\omega^-/2 > 0,$$

$$\frac{\xi_3}{\xi_2} > \frac{w^-(1 + (\alpha + \alpha^2)^2/4)}{\alpha(\lambda^- - \mu^-) - \alpha^2(\alpha + 1)\omega^-/2}, \quad \text{if } \alpha(\lambda^- - \mu^-) - \alpha^2(\alpha + 1)\omega^-/2 < 0,$$

and

$$\frac{\xi_3}{\xi_2} < \frac{\omega^+}{\lambda^+(\omega^+ - 1) + \mu^+}, \quad \text{if } \lambda^+(\omega^+ - 1) + \mu^+ > 0,$$

$$\frac{\xi_3}{\xi_2} > \frac{\omega^+}{\lambda^+(\omega^+ - 1) + \mu^+}, \quad \text{if } \lambda^+(\omega^+ - 1) + \mu^+ < 0.$$

For the \ominus -system we obtain via (2.6) and (2.18) a representation of the return time as solution of

$$(4 + \alpha^2 + 2\alpha^3 + \alpha^4)s^-\xi_2 + 2\alpha(2(E^- - c^-) + \alpha s^-(1 + \alpha))\xi_3 = 0, \quad (2.21)$$

and from Lemma 2.6 we get the following

$$m_0(t_-) = -\frac{1}{2} \frac{s^-(4 + \alpha^2 + 2\alpha^3 + \alpha^4)}{\alpha(2(E^- - c^-) + \alpha s^-(1 + \alpha))},$$

$$m_1(t_-) = -\frac{1}{2} \frac{s^-E^-(4 + \alpha^2 + 2\alpha^3 + \alpha^4)}{\alpha[(\alpha s^-(1 + \alpha) + 2c^-)E^- - 2]},$$

$$\frac{\xi_2^1}{\xi_2^0} = \frac{e^{\lambda^- t_-} [(\alpha s^-(1 + \alpha) + 2c^-)E^- - 2]}{2(E^- - c^-) + \alpha s^-(1 + \alpha)},$$

$$\frac{\xi_3^1}{\xi_3^0} = e^{\mu^- t_-}.$$

For the \oplus -system we get

$$-s^+\xi_2 + (\lambda^+s^+ - c^+ + E^+)\xi_3 = 0, \quad (2.22)$$

and from Lemma 2.6 we get the following

$$n_0(t_+) = \frac{s^+}{\lambda^+s^+ - c^+ + E^+},$$

$$n_1(t_+) = \frac{s^+E^+}{(c^+ + \lambda^+s^+)E^+ - 1},$$

$$\frac{\xi_2^2}{\xi_2^1} = \frac{e^{\lambda^+ t_+} ((c^+ + \lambda^+s^+)E^+ - 1)}{\lambda^+s^+ - c^+ + E^+}, \quad \frac{\xi_3^2}{\xi_3^1} = e^{\mu^+ t_+}.$$

$$\gamma_1 = \frac{F(E^+(c^+ + \lambda^+s^+) - 1)(E^-s^-\alpha^-(1 + \alpha^-) + 2E^-c^- - 2)}{(\lambda^-s^+ - c^+ + E^+)(\alpha^-s^-(\alpha^- + 1) + 2E^- - 2c^-)},$$

$$\gamma_2 = FE^+E^-, \quad F = e^{\lambda^+ t_+ + \lambda^- t_-}.$$

Since there are still many parameters involved we illustrate various situations for a special choice of parameters.

In the case $\alpha = 0$, the \ominus -system possesses an invariant plane $\xi_3 = 0$ with $t_-(\xi) = \pi/\omega^-$. In this situation we assume that the starting point $\xi \in \mathcal{M}_+^c$, hence $\xi_2 < 0$ from (2.2), and we get

$$\frac{\xi_3}{\xi_2} < n_0(0); \quad \text{if } n_0(0) > 0, \quad (2.23a)$$

$$\frac{\xi_3}{\xi_2} > n_0(0); \quad \text{if } n_0(0) < 0, \quad (2.23b)$$

where $n_0(0) = \frac{\omega^+}{\lambda^+(\omega^+-1)+\mu^+}$. Geometrically the line $\xi_3 = n_0(0)\xi_2$ determines the boundary of the sliding motion area in the (ξ_2, ξ_3) -plane.

The Poincaré map $P = P^- \circ P^+(\xi)$ mapping $\langle \xi_2, \xi_3 \rangle$ -plane into itself (i.e., $P(\xi) : \mathcal{M}_+^c \rightarrow \mathcal{M}_+^c$) is given by

$$P = \begin{pmatrix} F(\lambda^+s^+ - c^+) & F(s^+(1 - \lambda^+) + \lambda^+(c^+ - 2E^+)) \\ 0 & FE^+E^- \end{pmatrix} \begin{pmatrix} \xi_2 \\ \xi_3 \end{pmatrix}.$$

For $t_+(\xi)$ defined by (2.22) we can determine an invariant cone spanned by invariant line $\xi_3 = n_0(t_+)\xi_2$ provided (2.23) and the fixed point equation $P(\xi) = \xi$ is satisfied. In this case P is a triangular matrix which will allow easy access to eigenvalues and eigenvectors; note that the map P depends through $t_+(\xi)$ in a nonlinear way on ξ .

The eigenvalues of P can be obtained as follows:

$$\gamma_1 = F(\lambda^+s^+ - c^+), \gamma_2 = FE^+E^-.$$

Then there are 2 cases to obtain an invariant cone consisting of periodic orbit.

(a) If $\lambda^+/\omega^+ + \lambda^-/\omega^- = 0$ and $t_+ = \pi/\omega^+$. Then system (2.16) has invariant cone if and only if $\mu^+/\omega^+ + \mu^-/\omega^- \neq 0$. Furthermore the dynamics of the system can be established by observing the sign of $(\frac{\mu^+}{\omega^+} + \frac{\mu^-}{\omega^-})$. To see this note that the fixed point equation yields $(FE^+E^- - 1)\xi_3 = 0$ if $F(\lambda^+s^+ - c^+) = 1$

If $\xi_3 = 0$ then $s^+ = 0$, hence $t_+ = \pi/\omega^-$ and $c^+ = -1$, corresponding to a flat cone for which of course $\xi \in \mathcal{M}_+^c$.

If $\xi_3 \neq 0$ then $FE^+E^- = 1$. The first part of the fixed point equation requires $s^+(1-\lambda^+)+\lambda^+(c^+-2E^+) = 0$ which means that the solution does not exist on the interval $(0, \pi)$ where $\xi \in \mathcal{M}_+^c$ (i.e. $\lambda^+(\omega^+ - 1) + \mu^+ < 0$), hence $\xi_3 = 0$.

In this case we obtain a flat cone given as the invariant plane. The cone

corresponding to $\lambda^+/\omega^+ + \lambda^-/\omega^- = 0$ is attractive if $\mu^+/\omega^+ + \mu^-/\omega^- < 0$ and repulsive if $\mu^+/\omega^+ + \mu^-/\omega^- > 0$.

(b) If $FE^+E^- = 1$ hence $\mu^+t_+ + \mu^-t_- = 0$.

The corresponding eigenvector is calculated as

$$\bar{\xi} = \begin{pmatrix} -1 \\ -\frac{1+F(\lambda^+s^+-c^+)}{F(s^+(1-\lambda^+)+\lambda^+(c^+-2E^+))} \end{pmatrix}$$

Since t_+ must satisfy $t_+ = -(\mu^-/\mu^+)\pi/\omega^-$ we can check by considering the graph of $n_0(t_+)$ for which parameters (2.23) holds, that is for $t_+ = -(\mu^-/\mu^+)\pi/\omega^-$, $\xi_2 = -1$. We have to check if $\xi_3 = -n_0(t_+)$ satisfies (2.23).

Let $(T_0, T_1) \subseteq (0, \infty)$ denote the interval such that for $t_+ \in (T_0, T_1)$, $\xi_3 = -n_0(t_+)$ satisfies (2.23). Let T^* denote the smallest positive root of $h_1(t_+)$ where $h_1(t_+) = \lambda^+s^+ - c^+ + E^+$, then $h_1(0) = 0$ and $h'_1(0) = \omega^+/n_0(0)$.

In the case $0 > n_0(0)$ we obtain $T_0 = T^*$ and T_1 as the smallest positive root of $n_0(t_+) - n_0(0) = 0$. The typical graph of $n_0(t_+)$ in case (2.23b) is given in Figure 2.11.

In the case $0 < n_0(0)$ we obtain $T_0 = 0$ and $T_1 = T^*$. Note that both T_0 and T_1 depend on the parameters w^- , λ^- , μ^- , and may be fixed point exists only at $t_+ = \pi/\omega^+$

Based on this construction, we are able to consider a variety of special cases:

2.4.4.1 One-parameter bifurcation for invariant cone

In order to illustrate the three possible situations of dynamics on the cone as described in Theorem 2.3, we consider a parameter dependent example to control switching of stability for the invariant cone from a stable focus type to an unstable focus type via a center. We can arrange that $\lambda^+s^+ - c^+ = 0$ for $\lambda^+ = -1$, $-\frac{\mu^-\pi}{\mu^+\omega^-} = t^+ = \frac{3\pi}{4\omega^+}$ and take

$$A^- = \begin{pmatrix} 0.4259 & -1 & 0 \\ 1 & 0.4259 & 0 \\ 0 & 0 & -3\mu^+/4 \end{pmatrix}, A^+ = \begin{pmatrix} -2 & -1 & \mu^+ \\ 2 & 0 & -2 - 2\mu^+ \\ 0 & 0 & \mu^+ \end{pmatrix}$$

where $\omega^\pm = -\lambda^\pm = 1$, $\lambda^- = 0.4259$ and varying μ^+ as parameter. Thus, for $\mu^+ = -1.3$ the corresponding system has one invariant cone and the dynamics on it is of stable focus type. By moving the real value μ^+ and keeping fixed all the remaining eigenvalues, a dynamics of center type is obtained on the

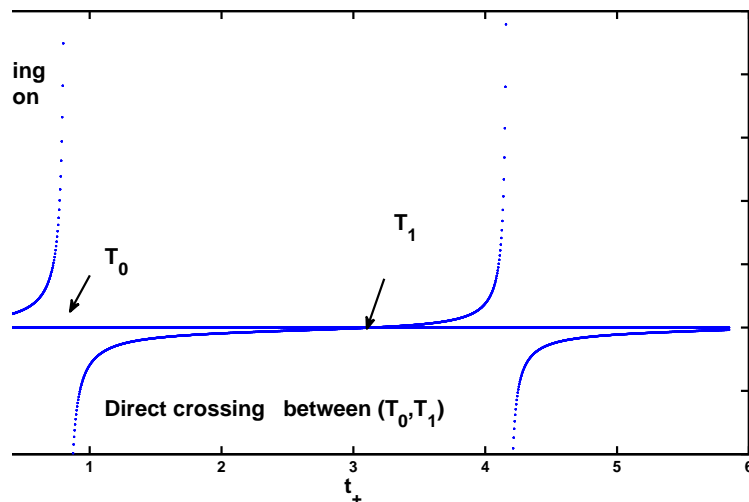


Figure 2.11: Graph of $n_0(t_+)$ for parameter values $\lambda^+ = -\lambda^- = 0.6$, $\mu^+ = -1.13$, $\mu^- = 0.4266$, $\omega^\pm = 1$

invariant cone for $\mu^+ = -1.13$, and being the the dynamics of unstable focus type for $\mu^+ > -1.13$.

2.4.4.2 Existence of multiple cones

Here we face a situation which is more complicated in smooth system if there exist two limit cycles such that one of these is unstable, located inside the stable one, for instance this scenario has been observed in [54]. The question considered here is this: *Is it possible to get the same scenario for PWLS?*

Lemma 2.9. *If $\xi \in M_\pm^c$ and $\lambda^+/\omega^+ + \lambda^-/\omega^- = 0$, then the system (2.16) has, at least, two invariant cones with periodic orbits. One of them can be asymptotically stable and the other unstable or both can be unstable focus; but there is also the situation where both invariant cones are asymptotically stable.*

Remark 2.6. *It should be noted that the existence of multiple attractive invariant cones is not possible in continuous PWLS, see Theorem 2 in [10].*

The following situation establishes the existence of attractive multiple invariant cones.

If $\xi \in \mathcal{M}_+^c$ and $\lambda^+/\omega^+ + \lambda^-/\omega^- = 0$ and $\mu^+ + \mu^- < 0$, then by (a) there exists an attractive invariant flat cone with $t_\pm = \pi/\omega^\pm$.

We use this constellation to construct another invariant cone by using case (b) for a different $t_+ = -\frac{\mu^-}{\mu^+} \frac{\pi}{\omega^-}$; that cone is attractive as well if $|F(\lambda^+ s^+ - c^+)| < 1$

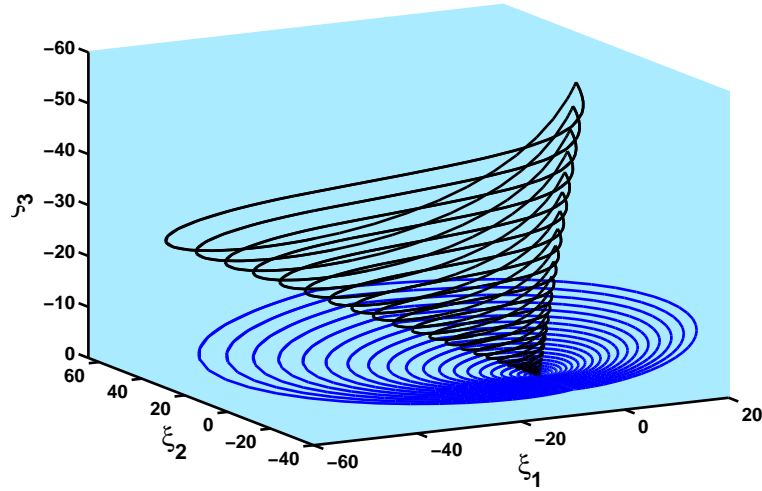


Figure 2.12: Two attractive invariant cones, $\lambda^+ = -\lambda^- = 0.6$, $\mu^+ = -1.13$, $\mu^- = 0.4266$, $\omega^\pm = 1$ where $t_+ = \pi$ for the flat cone and $t_+ = 1.1306$ for the other.

for this choice of t_+ . For example this situation holds for the special choice of parameters used in Figure 2.12.

2.4.5 Mechanism to generate an invariant cone and its stability

In view of the previous results, we will show the mechanism which is responsible to generate invariant cones and to determine the stability of the origin for most general PWLS (2.16) where A^\pm are given in (2.20) by the following steps:

step 1: Lemma 2.5 indicates the possibility of obtaining an invariant cone with periodic orbit. Without loss of generality, one can assume that $\xi \in \mathcal{M}_-^c$ and $\xi_2 > 0$ and $\alpha \neq 0$ requires essentially the following conditions:

$$\frac{\xi_3}{\xi_2} < m_0(0); \quad \text{if } m_0(0) > 0, \quad (2.24a)$$

$$\frac{\xi_3}{\xi_2} > m_0(0); \quad \text{if } m_0(0) < 0, \quad (2.24b)$$

with (2.23) where $m_0(0) = \frac{\omega^-(1+(\alpha+\alpha^2)^2/4)}{\alpha(\lambda^- - \mu^-) - \alpha^2(\alpha+1)\omega^-/2}$.

step 2: Construction of Poincaré map via (2.18). In this case, we consider $P = P^+ \circ P^-(\xi)$ mapping $\langle \xi_2, \xi_3 \rangle$ -plane into itself (i.e., $P(\xi) : \mathcal{M}_-^c \rightarrow \mathcal{M}_-^c$) is

given by

$$P = F \begin{pmatrix} (c^+ - \lambda^+ s^+) (c^- + \frac{\alpha(1+\alpha)s^-}{2}) & (c^+ - \lambda^+ s^+) \alpha s^- + 2\lambda^+ E^+ E^- \\ & + E^-(\lambda^{+2} s^+ - s^+ - 2\lambda^+ c^+) \\ 0 & E^+ E^- \end{pmatrix} \begin{pmatrix} \xi_2 \\ \xi_3 \end{pmatrix}. \quad (2.25)$$

If there exists $\bar{\xi}$ such that $P^+ \circ P^-(\bar{\xi}) = \bar{\xi}$, then the existence of an invariant half straight line which defines a two-zonal invariant cone is concluded.

The eigenvalues of P can be obtained as follows:

$$\gamma_1 = F(c^+ - \lambda^+ s^+) (c^- + \frac{\alpha(1+\alpha)s^-}{2}), \gamma_2 = FE^+ E^-.$$

step 3: We emphasize that, according to Lemma 2.3, t_- and t_+ are constant on rays in \mathcal{M}_-^c and \mathcal{M}_+^c . Furthermore the relations (i-ii) in Theorem 2.3 allow to define in parameter form a slope of two straight lines, hence t_{\pm} is a unique solution of the following system

$$-\frac{1}{2} \frac{s^- E^- (4 + \alpha^2 + 2\alpha^3 + \alpha^4)}{\alpha [(\alpha s^- (1 + \alpha) + 2c^-) E^- - 2]} = \frac{s^+}{\lambda^+ s^+ - c^+ + E^+} \quad (2.26a)$$

$$-\frac{1}{2} \frac{s^- (4 + \alpha^2 + 2\alpha^3 + \alpha^4)}{\alpha (2(E^- - c^-) + \alpha s^- (1 + \alpha))} = \frac{s^+ E^+}{(c^+ + \lambda^+ s^+) E^+ - 1}. \quad (2.26b)$$

In other words, the existence of solutions for this system, provides necessary conditions for the existence of two invariant straight lines which in turn leads to two-zonal invariant cone. Note that the above system of equations has a trivial solution at $t_{\pm} = \pi/\omega^{\pm}$.

step 4: In general the existence of an attractive invariant cone with periodic orbits requires solution of a fixed point equation $P(\xi) = \xi$ with exactly one eigenvalue equal to 1 and all of the other eigenvalues with modulus less than 1. The current example requires that only one of the two eigenvalues of P equals 1, hence we distinguish two cases to obtain invariant cones:

a- $F(c^+ - \lambda^+ s^+) (c^- + \frac{\alpha^-(1+\alpha^-)s^-}{2}) = 1$. The fixed point equation $P(\xi) = \xi$, where P is given by (2.25) requires either $\xi_3 = 0$ or $\xi_3 \neq 0$.

(i) $\xi_3 = 0$ is invariant plane such that $FE^+ E^- \neq 1$. Therefore, we obtain an invariant flat cone with trivial solution of (2.26) at $t_{\pm} = \pi/\omega^{\pm}$. The stability of the origin depends on the sign of the quantity $(\frac{\mu^+}{\omega^+} + \frac{\mu^-}{\omega^-})$.

(ii) $\xi_3 \neq 0$ leading to $\mu^+ t_+ + \mu^- t_- = 0$ where t_{\pm} satisfies (2.26) with investigate the existence of solutions for $F(c^+ - \lambda^+ s^+) \alpha^- s^- + 2\lambda^+ + FE^-(\lambda^{+2} s^+ - s^+ - 2\lambda^+ c^+) = 0$.

b- $FE^+E^- = 1$. For t_{\pm} satisfying (2.26) we can determine an invariant cone spanned by

$$\xi_2 = 1, \quad \xi_3 = \frac{1 - F(c^+ - \lambda^+ s^+)(c^- + \frac{\alpha^-(1+\alpha^-)s^-}{2})}{F(c^+ - \lambda^+ s^+)\alpha^- s^- + 2\lambda^+ + FE^-(\lambda^{+2}s^+ - s^+ - 2\lambda^+ c^+)}.$$

The same idea can be used if $\xi \in \mathcal{M}_+^c$.

For illustration a few examples of PWLS (2.16) are given below:

Example I: A typical example illustrate the previous mechanism.

Consider PWLS (2.16) where A^{\pm} are given in (2.20), we take $\alpha = 1$, get $m_0(0) = \frac{2\omega^-}{\lambda^- - \mu^- - \omega^-}$ and $n_0(0) = \frac{\omega^+}{\lambda^+ (\omega^+ - 1) + \mu^+}$ where (2.23) and (2.24) have been taken into account. The system (2.26) is reduced to the following expression

$$2s^- E^-(\lambda^+ s^+ - c^+ + E^+) - s^+(1 - (s^- + c^-)E^-) = 0, \quad (2.27a)$$

$$2s^- ((c^+ + \lambda^+ s^+)E^+ - 1) - s^+ E^+(c^- - s^- - E^-) = 0. \quad (2.27b)$$

Here t_{\pm} must be computed numerically. Regarding Step 4 we get the eigenvector ξ in two cases which is responsible to generate invariant cones with periodic orbits as well as dynamics on \mathcal{C} can be achieved. Keeping $(\frac{\mu^+}{\omega^+} + \frac{\mu^-}{\omega^-}) < 0$ and $t_{\pm} = \frac{\pi}{\omega^{\pm}}$, the dynamics on the planar invariant cone is of a center (unstable/stable focus) if and only if $(\frac{\lambda^+}{\omega^+} + \frac{\lambda^-}{\omega^-}) = 0 (> 0 / < 0)$. By perturbing this situation corresponding $\mu^+ t_+ + \mu^- t_- = 0$, it is immediate to get a similar dynamics on a nonplanar invariant cone. To show the existence of stable dynamics on the invariant cone, let us choose $\omega^{\pm} > \lambda^- > \mu^+ > 0$ and $\mu^- < 0$. Then if $\lambda^+ = 1$ and $0 < t_{\pm} < \pi$, we get an invariant cone with periodic orbit and the dynamics on the cone is of (center+stable focus), for example see Figure 2.13. By increasing $\lambda^+ \cong 1.12$ the dynamics on the cone is of (center+unstable focus).

Example II: The next result is concerned with the existence of multiple cones of (2.16) where A^{\pm} are given in (2.20). Note that we are still under the same constraints as in I. It becomes evident from Lemma 2.9 that the existence of multiple cones requires $\lambda^+/\omega^+ + \lambda^-/\omega^- = 0$. Taken into account the above four steps. Hence, for $\xi \in \mathcal{M}_-^c$, we have a fairly complete analysis of the orbit structure of the Poincaré map and existence of solutions of the system (3.14). For example this situation holds for the special choice of parameters used in Figure 2.14. Both locally repulsive invariant cones are separated by an attractive manifold. Notice that the same situation holds if $\xi \in \mathcal{M}_+^c$.

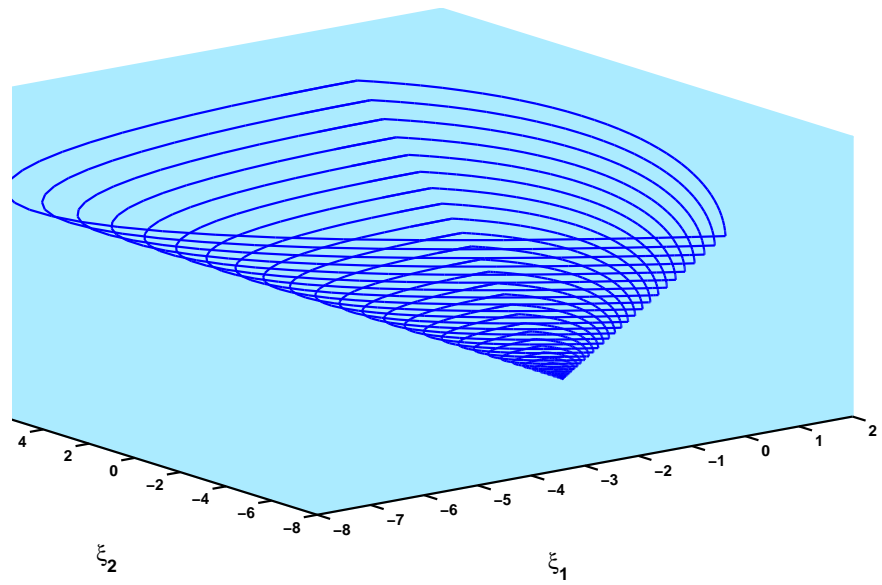


Figure 2.13: An invariant cone with (center+stable focus), $\omega^\pm = \lambda^+ = 1$, $\lambda^- = 0.3338$, $\mu^+ = 0.2027$, $\mu^- = -0.1014$, $t_+ = 0.3\pi$ and $t_- = 0.6\pi$.

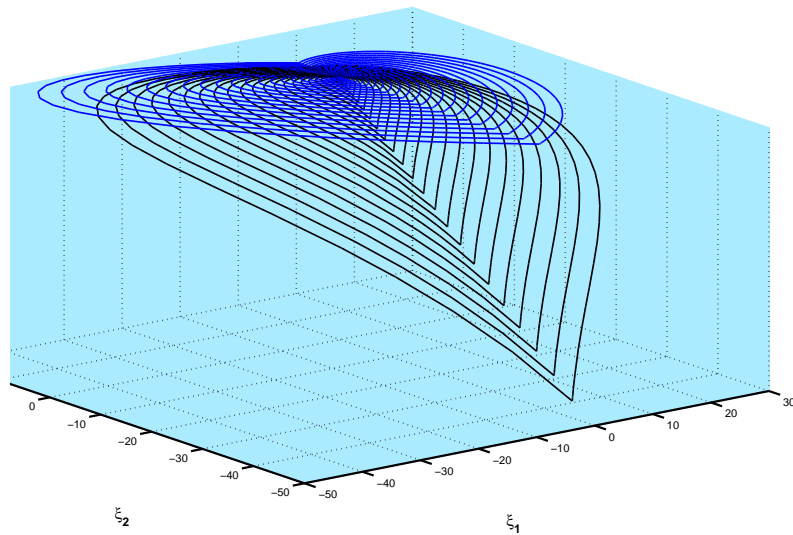


Figure 2.14: Two invariant cones where both are of (center+unstable focus), $\omega^\pm = 1$, $\lambda^+ = -\lambda^- = -.5$, $\mu^+ = -1.5$, $\mu^- = 1.6203$, $t_+ = 3.76$ and $t_- = 3.48$.

Example III: Coming back now to the case 2.4.4 posed at the beginning of this section. Without restriction we can assume that the \oplus -system of (2.16) can be considered as classical Jordan normal form [39]; i.e. to be in

$$A^+ = \begin{pmatrix} \lambda^+ & -\omega^+ & 0 \\ \omega^+ & \lambda^+ & 0 \\ 0 & 0 & \mu^+ \end{pmatrix},$$

by setting $\alpha^+ = \beta^+ = 0$ and fixing all other parameters as in case 2.4.4. Hence, the \ominus -system is under the same constraints, i.e., A^- is given in (2.20). To see different dynamics on invariant cone corresponding to Theorem 2.3, let us begin to study the existence of t_- for (2.21) where $\alpha = 1$ and $m_0(t_-) = -\frac{2s^-}{E^- + s^- - c^-}$. Since $0 < t_- \leq \pi$ we can always arrange that $s^- + c^- = 0$ for $-\frac{\mu^+ \pi}{\mu^- \omega^+} = t_- = \frac{3\pi}{4\omega^-}$. The matrix associated with the Poincaré map (2.25) has one eigenvalue equal to zero and the stability on the cone is determined by the quantity $(\mu^+ + 3\mu^-/4)$. This situation can be classified as follows [39]:

If $\xi \in \mathcal{M}_-^c$ and according to (2.24a) require $m_0(0) = \lambda^- - \mu^- - \omega^- > 0$ and $t_- = 3t_+/4$ with $\omega^+ = \omega^-$, thus, existence of center (unstable/stable focus) dynamics on the invariant cone if $4\mu^+ + 3\mu^- = 0 (> 0 / < 0)$ without any restriction on λ^+ . The three possible situations with specific parameters are illustrated in Figure 2.15

Further, according to Lemma 2.9 and the same way of analysis, we can get two invariant cones separated by a repulsive manifold [39] on which solutions converge towards the origin. An example with specific values of parameters is shown in Figure 2.16. An interpretation of the existence of multiple cones in term of generalized center manifolds provides a situation that there are locally multiple generalized center manifolds at the same time, hence there is a chance of bifurcation of multiple separate periodic orbits if nonlinear terms are added. The class of nonlinear PWS will be investigated in Chapter 5.

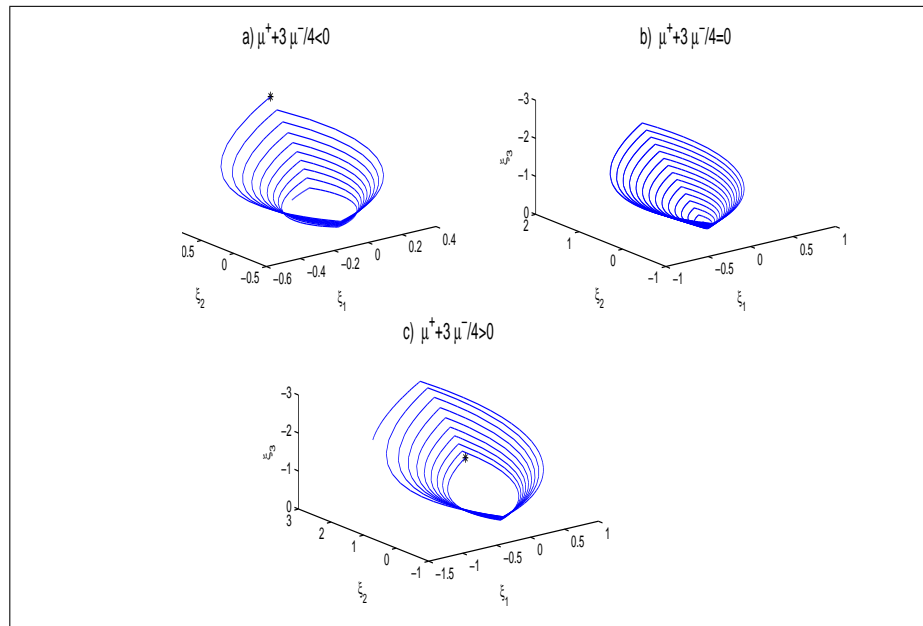


Figure 2.15: Different dynamics on cones, Attractive/ periodic / repulsive, for $\mu^- = -1.0, \omega^+ = \omega^- = 1, \lambda^- = -0.7832, t_+ = \pi, t_- = 3\pi/4$, **(a)** $\lambda^+ = 0.7768, \mu^+ = 0.7165$. **(b)** $\lambda^+ = 0.8103, \mu^+ = 0.7500$. **(c)** $\lambda^+ = 0.8406, \mu^+ = 0.7803$.

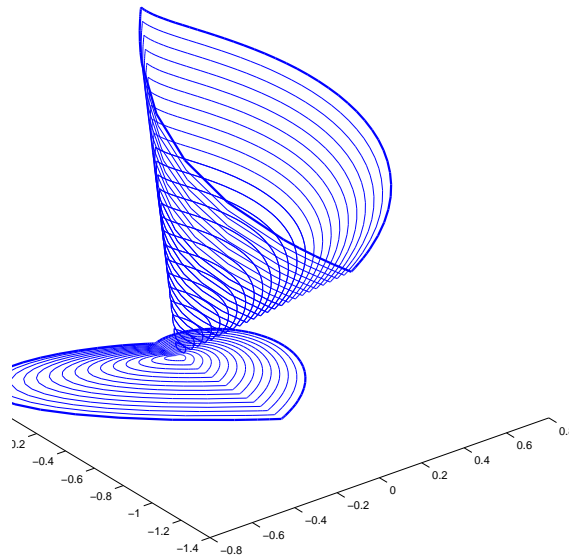


Figure 2.16: Two attractive invariant cone, $\lambda^+ = -0.5, \mu^+ = 0.1751, \omega^\pm = 1.0, \lambda^- = 0.5, \mu^- = -1.0, t_+ = \pi$, where $t_- = \pi$ for the flat cone and $t_- = 0.5505$ for the other.

Chapter 3

Invariant cones for a class of systems with sliding motion

Over the past few years, many problems of interest have been treated as Filippov models [13, 42, 43, 57]. In this chapter, we analyse the case of limit cycles interacting for such systems, presenting sliding bifurcations as well as an investigation of necessary and sufficient conditions for the existence of periodically invariant cones for a class of PWS including sliding motion. These investigations are based on a constructive approach which is a combination of theoretical analysis and numerical computation. This approach allows us to prove the existence of some sliding bifurcations for a class of PWS related to invariant cones. The stability of invariant cones containing sliding motion can be studied by either considering the stability of stationary solutions or the bifurcation of limit cycles. Further, we prove a generalization concerning invariant cones of class of PWS.

3.1 Sliding mode, dynamics on \mathcal{M}_{\pm}^s

In PWS there are many bifurcation phenomena that cannot be explained by classical bifurcation theory for smooth systems. A special phenomena for example occurs for PWS if the trajectories reach one or more discontinuity surfaces and stay on it. Sliding bifurcation has been shown to give rise to complex phenomena including deterministic chaos and it can be used to explain the formation and metamorphosis of stick-slip oscillations in friction oscillators [15, 16, 52]. We wish to emphasize that, the practically interests case is when the sliding region is attractive (i.e. $\xi \in \mathcal{M}_{-}^s$). This means that trajectories in \mathcal{M}_{-}^s stay within this region until the boundary is reached. The other case when the sliding region is repulsive (i.e. $\xi \in \mathcal{M}_{+}^s$) leads solutions of the

sliding system that can not be continued uniquely. Thus, we will not further consider repulsive sliding motion during this work.

Consider a trajectory of (2.1), and suppose that $\xi \in \mathcal{M}^s$. Two formalisms exist in the literature for deriving the equations for flows governing the dynamics within the sliding region. These are Utkin's equivalent control method [61] and Filippov's convex method [25]. To describe Utkin's approach, we consider systems where the discontinuity is due to effects of control. The system considered then is of the form:

$$\dot{\xi} = f(\xi, u), u(\xi) = \begin{cases} u^-(\xi), & h(\xi) < 0, \\ u^+(\xi), & h(\xi) > 0, \end{cases}$$

where u^- and u^+ are \mathbf{C}^k function of ξ . The system defined above presents a sliding motion when $\xi \in \mathcal{M}^s$. Therefore, the sliding dynamics is determined by replacing the discontinuous function u by an equivalent control [61]. Then, the dynamic of the sliding mode is given by the equivalent system

$$\dot{\xi} = F_s(\xi, u_{eq}),$$

where u_{eq} is the equivalent control which makes the surface invariant. For $\xi \in \mathcal{M}^s$, u_{eq} satisfies the following inequality

$$\min(u^-(\xi), u^+(\xi)) < u_{eq} < \max(u^-(\xi), u^+(\xi)).$$

Remark 3.1. *The dynamics of Filippov and Utkin methods are generally different. Utkin method corresponds to systems which are made discontinuous by the choice of discontinuous control. Filippov's method is derived corresponding to a situation when we deal with discontinuous vector field.*

In [20,61], there are some special cases where the two methods lead to different results.

Next, we show that both methods are equivalent in special situation . In Utkin's method we can derive the vector field $F_s(\xi)$ as an average of the two vector fields $f_-(\xi)$ and $f_+(\xi)$ plus a control $\beta(\xi) \in [-1, 1]$ in the direction of the difference between the vector fields [14]:

$$F_s(\xi) = \frac{f_+(\xi) + f_-(\xi)}{2} + \frac{f_-(\xi) - f_+(\xi)}{2}\beta(\xi). \quad (3.1)$$

Since $F_s(\xi)$ must be tangent to \mathcal{M}^s , which yields

$$\beta(\xi) = -\frac{n^T(\xi)f_+(\xi) + n^T(\xi)f_-(\xi)}{n^T(\xi)f_-(\xi) - n^T(\xi)f_+(\xi)}.$$

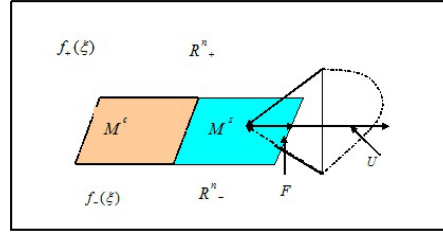


Figure 3.1: Filippov (**F**) and Utkin (**U**) methods .

Both methods are equivalent if $\beta(\xi) = 1 - 2q(\xi)$, Figure 3.1.

In this work, we are only going to use Filippov method. Boundaries between sliding and crossing regions satisfy $n^T(\xi)f_{\pm}(\xi) = 0$, implying that a trajectory of (2.1) is tangent to \mathcal{M} .

Remark 3.2. *The tangency points play an important role in the nongeneric bifurcations of limit cycles; limit cycles undergo a sliding bifurcation precisely when it passes through one of these points.*

Lemma 3.1. *The equivalent dynamics of PWS (2.1) for $\xi \in \mathcal{M}^s$ during the sliding motion is described by (1.11) if and only if*

$$n^T(\xi)(f_-(\xi) - f_+(\xi)) \neq 0.$$

Proof: If $\xi \in \mathcal{M}$, the solution of (2.1) is also solution of (1.11) for $q = 0$ or $q = 1$, respectively. While if $\xi \in \mathcal{M}^s$, then we get $h(\xi) = 0$ and

$$\begin{aligned} 0 &= \frac{d}{dt}h(\xi) = \frac{\partial h}{\partial \xi} \dot{\xi} = \frac{\partial h}{\partial \xi} (q(\xi)f_+(\xi) + (1 - q(\xi))f_-(\xi)) \\ &= q(\xi)n^T(\xi)(f_+(\xi) - f_-(\xi)) + n^T(\xi)f_-(\xi), \end{aligned}$$

which can be solved for q iff $n^T(\xi)(f_-(\xi) - f_+(\xi)) \neq 0$.

3.2 Sliding bifurcations

Bifurcations due to interactions between limit cycles and the boundary of sliding regions in PWS are called sliding bifurcations. Recently, analytical and numerical investigations of PWS (Filippov system) have shown that there are four fundamental types of sliding bifurcation which are called crossing-sliding, grazing-sliding, switching-sliding, and adding-sliding, see Figure 3.2. For a review and more thorough exposition of this topic where F_s is defined (3.1) by using Utkin method, the reader is referred to [14–17]. Next, we will present a brief description and the analytical conditions that must hold for each case where F_s is defined (1.11) by using Filippov method,

3.2.1 Crossing-sliding Bifurcations

Crossing-sliding bifurcation (Figure 3.2(a)) occurs when the trajectory of a subsystem under the effect of parameter variation crosses the manifold \mathcal{M} transversally (direct crossing) at the boundary of the sliding region $\partial\mathcal{M}_+^s$ (or $\partial\mathcal{M}_-^s$), which means that the flow given by F_s moves locally towards $\partial\mathcal{M}_+^s$ (or $\partial\mathcal{M}_-^s$). Thus, at the crossing-sliding bifurcation point ξ^* where λ is fixed, we must have

$$h(\xi^*) = 0, \quad \nabla h(\xi)|_{\xi^*} \neq 0. \quad (3.2)$$

Without loss of generality, we assume that the boundary bifurcation point lies on $\partial\mathcal{M}_+^s$ (i.e. $q(\xi) = 1$, $F_s(\xi) = f_+(\xi)$). Thus, we have

$$\frac{d(h(\varphi^+(\xi, t)))}{dt}\Big|_{t=0} = 0 \Leftrightarrow (n^T(\xi)f_+(\xi))|_{\xi^*} = 0, \quad (3.3)$$

where φ^\pm represents the flow corresponding to f^\pm . The sliding flow will be forced to leave the sliding region through the boundary $\partial\mathcal{M}_+^s$ if the time derivative of $q(\xi)$ along the flow lines is positive. Hence, we get

$$\frac{d(q(\varphi^+(\xi, t)))}{dt}\Big|_{t=0} = (\nabla q(\xi)f_+(\xi))|_{\xi^*} > 0. \quad (3.4)$$

After substituting $\nabla q(\xi)$ which is defined in (1.13), and taken into account (1.9), we can clearly see (3.4) as

$$(n^T(\xi) \cdot \nabla f_+(\xi) \cdot f_+(\xi))|_{\xi^*} > 0. \quad (3.5)$$

Conditions (3.2) and (3.3) are general conditions that must be satisfied for all cases of sliding bifurcations. These conditions ensure that the bifurcation point is located on the boundary of the sliding motion area, i.e., $\xi^* \in \partial\mathcal{M}_+^s$ and that it is a tangent point.

3.2.2 Grazing-sliding bifurcation

Grazing-sliding bifurcation will take place when the sliding flow moves towards the boundary of sliding $\partial\mathcal{M}_+^s$ and the sliding trajectory tends to leaves \mathcal{M} (see Figure 3.2(b)). In this case the same analytical conditions of crossing-sliding bifurcation hold.

3.2.3 Switching-sliding bifurcation

In this case, the vector field $F_s(\xi)$ must point away from the boundary of the sliding region at the bifurcation point on $\partial\mathcal{M}_+^s$, conditions (3.2) and (3.3) hold as well and at ξ^* we require that the flow leaves the boundary point towards the sliding region, (Figure 3.2(c)), the additional condition is given by

$$(n^T(\xi) \cdot \nabla f_+(\xi) \cdot f_+(\xi))|_{\xi^*} < 0. \quad (3.6)$$

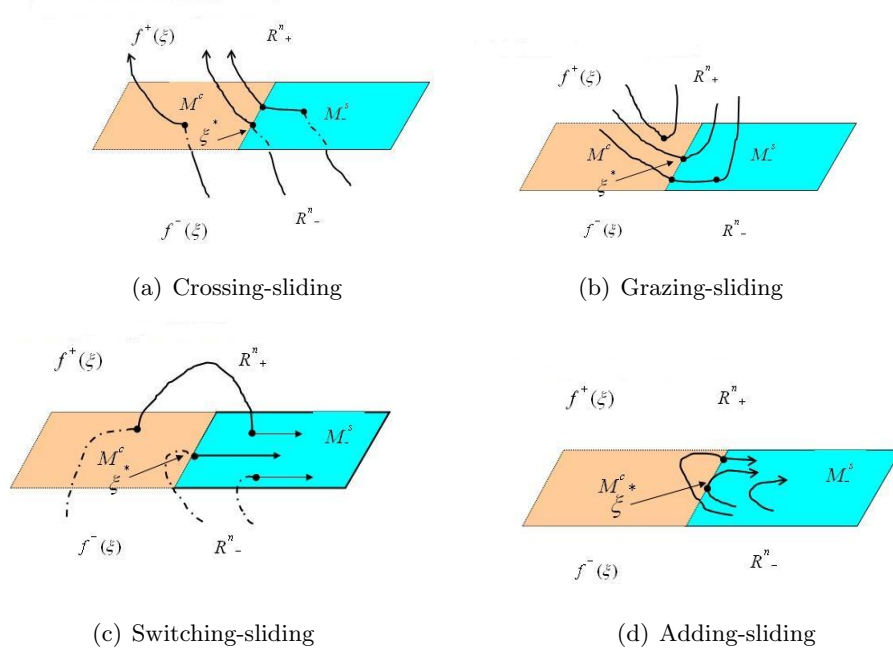


Figure 3.2: Structures of sliding bifurcation

3.2.4 Adding-sliding bifurcation

In this case the segment of the sliding flow lies entirely within the sliding region \mathcal{M}_-^s which is tangential to $\partial\mathcal{M}_-^s$ at the bifurcation point, see Figure 3.2(d), hence the following additional condition

$$(n^T(\xi) \cdot \nabla f_+(\xi) \cdot f_+(\xi))|_{\xi^*} = 0. \quad (3.7)$$

The sliding flow in this case has a local minimum with respect to the boundary $\partial\mathcal{M}_-^s$. Thus, we have

$$(n^T(\xi) \cdot (\nabla f_+(\xi))^2 \cdot f_+(\xi))|_{\xi^*} < 0. \quad (3.8)$$

Remark 3.3. If $\xi^* \in \partial\mathcal{M}_-^s$, then $q(\xi) = 0$, hence $F_s(\xi) = f_-(\xi)$. An analogous analytical conditions of sliding bifurcation is obtained with opposite sign.

A **sliding segment** is a smooth curve which is a trajectory of $\dot{\xi} = F_s(\xi)$, $h(\xi) = 0$, and F_s is given by (1.11) or (3.1).

The question arises, if the trajectory of (2.1) for $\xi \in \mathcal{M}_-^s$, thereby loses/gains a segment of sliding, as well as how and when the trajectory leaves the sliding region through the boundary ?

If $\xi \in \mathbb{R}^n$ and $n^T(\xi)f_{\pm}(\xi) \neq 0$, Filippov [24,25] devised a theory which helps to decide what to do in this situation. At $\xi \in \partial\mathcal{M}_-^s$, such that one of $n^T(\xi)f_{\pm}(\xi) = 0$, (not both) where one of them always occurs immediately at the boundary of sliding area, see Section 1.4. In this situation there are two possibilities:

(i) If $n^T(\xi)f_+(\xi) = 0$, we get $q = 1$ and $F_s = f_+(\xi)$ or $n^T(\xi)f_-(\xi) = 0$, then

we get $q = 0$ and $F_s = f_-(\xi)$. As can be expected the trajectory enters \mathcal{M}_+^c in the case $n^T(\xi)f_+(\xi) = 0$ and enters \mathcal{M}_-^c in the other case $n^T(\xi)f_-(\xi) = 0$.

(ii) The trajectory hits the boundary and thereafter remains on \mathcal{M}_-^s .

In this way, Dieci and Lopez [19] examined second order corrections to the theory of Filippov. We can limit ourselves to a very brief summary of this below.

For $\xi \in \mathcal{M}$, we assume that

$$g_1(\xi) = n^T(\xi)f_-(\xi), \quad g_2(\xi) = n^T(\xi)f_+(\xi), \quad g(\xi) = g_1(\xi)g_2(\xi).$$

With the notation $t = 0^\pm$ means $\lim_{t \rightarrow 0^\pm}$, for t in a right/left neighborhood of $t = 0$, we have

$$g_i(\xi) = A_i + tB_i^\pm + \frac{t^2}{2}C_i^\pm + O(t^3), \quad i = 1, 2,$$

where $A_i = g_i(\xi(0))$, $B_i^\pm = \left[\frac{\partial}{\partial \xi} g_i(\xi(t)) \dot{\xi} \right]_{t=0^\pm}$, $C_i^\pm = \left[(\dot{\xi}(t))^T \frac{\partial^2}{\partial \xi^2} g_i(\xi(t)) \dot{\xi}(t) + \frac{\partial}{\partial \xi} g_i(\xi(t)) \ddot{\xi}(t) \right]_{t=0^\pm}$. Taking into account the properties of the vector field on the four sectors 2.2 and depending on the sign of A_i , B_i^\pm and C_i^\pm many possibilities of motion can be observed [19]. Our main interest here is the situation where the trajectory leaves the boundary in between crossing and sliding regions, hence when the two cases below are satisfied.

Lemma 3.2. [19] *Using the above setting, at $\xi \in \partial\mathcal{M}_-^s$ or $\xi \in \partial\mathcal{M}_+^s$, respectively. The following holds true:*

- i-** *If $A_1 = 0$, $A_2 < 0$, $B_1^- < 0$, then the trajectory leaves $\partial\mathcal{M}_-^s$ and enters \mathcal{M}_-^c with vector field $f_-(\xi)$.*
- ii-** *If $A_2 = 0$, $A_1 > 0$, $B_2^- > 0$, then the trajectory leaves $\partial\mathcal{M}_+^s$ and enters \mathcal{M}_+^c with vector field $f_+(\xi)$.*

3.3 Fundamental matrix solutions

The fundamental matrix solutions on the sliding surface [25, 44] can be estimated from the evolution of the linearized Filippov system (1.11) with respect to the sliding vector field, i.e. for all initial $\tilde{\xi} \in \mathcal{M}^s$, we get

$$\dot{Y}_s = \frac{\partial}{\partial \xi} F_s(\tilde{\xi}) Y_s, \quad Y_s(0) = I,$$

where $Y_s = \frac{\partial}{\partial \xi} \varphi(\tau_s, \tilde{\xi})$, $\varphi(\tau_s, \tilde{\xi})$ is the solution of $\dot{\xi} = F_s(\xi)$ and

$$F_s(\xi) = \frac{n^T(\xi)f_-(\xi) \cdot f_+(\xi) - n^T(\xi)f_+(\xi) \cdot f_-(\xi)}{n^T(\xi)(f_-(\xi) - f_+(\xi))}. \quad (3.9)$$

In order to state the appropriate generalization of Theorem 2.1, we consider the flow given by $\varphi(\tau_-, \xi)$ with respect to \ominus -system of (2.1) reaching \mathcal{M}^s , but not crossing the manifold (i.e. no direct crossing). Rather the motion starts to slide on it beginning at the boundary point $\tilde{\eta}$ at time $\tilde{\tau}$ which is given by equation (2.3).

Thus, we get

$$Y_s = J_s Y_-, \quad J_s = I + \frac{(F_s(\tilde{\tau}_-, \tilde{\eta}) - f_-(\tilde{\tau}_-, \tilde{\eta}))n^T(\tilde{\eta})}{n^T(\tilde{\eta})f_-(\tilde{\tau}_-, \tilde{\eta})}. \quad (3.10)$$

On the other hand, if the trajectory of \oplus -system reaches \mathcal{M}^s coming from \mathcal{M}_+^c , we get the same form of the jump matrix (3.10) due to the attractivity of the sliding manifold. Obviously there is a singularity of the jump matrix ensuring that the motion on \mathcal{M}_-^s will take place on a lower dimensional manifold. Furthermore we cannot uniquely trace the orbit backward in time.

3.3.1 Monodromy matrix in PWS with sliding

Again, the eigenvalues of the monodromy matrix, known as Floquet characteristic multipliers, are used to study the local stability of periodic orbits of a smooth nonlinear system (1.1). In PWS, without loss of generality, we can assume that the periodic orbit of PWS (2.1) without sliding motion starts from $\xi(0) \in \mathcal{M}_-^c$ with the \ominus -system, intersects the manifold at $\tilde{\eta} \in \mathcal{M}_+^c$ and passes over to the \oplus -system, and finally the periodic orbit closes at $\xi(T) = \xi(0)$, where $T = \tau_- + \tau_+$. Thus, one can define the monodromy matrix by

$$Y(T, \xi) = J_+ Y_+(\tau_+, \xi(\tau_-)) J_- Y_-(\tau_-, \xi(0)). \quad (3.11)$$

Note that if the periodic orbit crosses different discontinuity surfaces \mathcal{M}_i , one just has to compose the monodromy matrix out of the state jump matrices for the passage through each subsystem. This strategy will allow us to determine periodic orbits with multiple discontinuity surfaces. Furthermore, the processes described in this strategy also apply to the case of attractive sliding motion, for example the monodromy matrix around an periodic orbit with sliding segment can be obtained by replacing \mathcal{M}_+^c by \mathcal{M}_-^s , i.e.,

$$Y(T, \xi) = Y_s(\tau_s, \xi(\tau_-)) J_s Y_-(\tau_-, \xi(0)), T = \tau_- + \tau_s. \quad (3.12)$$

Note that, the trajectory leaves the separation manifold tangentially, i.e. the corresponding jump matrix is equal to the identity matrix.

The monodromy matrix essentially represents the linearization of the Poincaré map around the periodic orbit, and hence its eigenvalues known as Floquet

multipliers determine the stability of the periodic orbit. The invariant cone is locally attractive if the absolute values of the Floquet multipliers except the trivial one are less than 1.

Lemma 3.3. *For PWS (2.1) without sliding motion the monodromy matrix has at least one eigenvalue equal to 1 (Periodicity) and the dynamics of the orbit is determined by the other eigenvalues μ_j , ($j = 1, \dots, n - 1$). If \mathcal{M}_-^s is involved the monodromy matrix has one eigenvalue equal to 1 in case of an periodic orbit and at least one eigenvalue equal to 0 due to the singularity of J_s . The dynamics of the orbit depends on the remaining eigenvalues μ_j , ($j = 1, \dots, n - 2$).*

3.4 Invariant cones with sliding motion for PWLS

In this section, our objective is to discuss the situation that the invariant cone contains a segment of sliding motion or evolves under the sliding flow towards $\partial\mathcal{M}_-^s$ or $\partial\mathcal{M}_+^s$.

For an initial position in \mathcal{M}_-^s or if the flow of a subsystem of (2.5) arrives at the sliding region \mathcal{M}_-^s , the sliding motion can be observed along the discontinuity surface in phase space. Let $\varphi^s(t_s(\xi), \xi)$ in \mathbf{C}^k , $k \geq 1$, denote the sliding flow generated by

$$\dot{\xi} = F_s = k_1 A^+ \xi + k_2 A^- \xi, \quad (3.13)$$

with $k_1, k_2 \in (0, 1)$, $\xi \in \mathcal{M}_-^s$, and let t_s be the time spent in the \mathcal{M}_-^s region. Then we define the sliding map as

$$\begin{aligned} P_s : \mathcal{M}_-^s &\rightarrow \mathcal{M}_-^s, \\ \xi &\rightarrow P_s(\xi) = \varphi^s(t_s, \xi). \end{aligned}$$

The sliding flow will either stay on \mathcal{M}_-^s for all future times $t_s \rightarrow \infty$ or reach one of the boundaries $\partial\mathcal{M}_\pm^s$ at some time. Furthermore, the sliding trajectory will move along \mathcal{M}_-^s to approach $\partial\mathcal{M}_+^s$ if $\nabla q(\xi) \cdot F_s(\xi) > 0$ or it will come close to $\partial\mathcal{M}_-^s$ if $\nabla q(\xi) \cdot F_s(\xi) < 0$. Thus, t_s depend on the direction of the sliding flow and it can be computed as the time evaluation from ξ^0 to $\partial\mathcal{M}_-^s$ (or to $\partial\mathcal{M}_+^s$) by using the following sliding boundary conditions

$$q(\varphi^s(t_s, \xi)) = 1, \text{ if } \xi \in \partial\mathcal{M}_+^s, \quad (3.14a)$$

$$q(\varphi^s(t_s, \xi)) = 0, \text{ if } \xi \in \partial\mathcal{M}_-^s, . \quad (3.14b)$$

Clearly (3.13) is non-linear in ξ and homogeneous and preserves a linear homogeneity, i.e., if $\varphi^s(t_s, \xi)$ is a solution of (3.13), then $\tilde{\varphi}^s(t_s, \xi) := \lambda \varphi^s(t_s, \xi)$ is a solution as well. Then we have the following lemma.

Lemma 3.4.

For all $\hat{\xi} \in \mathcal{M}_-^s$, $P_s(\hat{\xi}) \in \mathcal{M}_-^s$ and $\varphi^s(t, \hat{\xi}) \in \mathbb{R}^n$, $0 < t < t_s(\hat{\xi})$:

- (i) The function t_s is differentiable in $\hat{\xi}$, $t_s(\lambda\hat{\xi}) = t_s(\hat{\xi})$, and $P_s(\lambda\xi) = \lambda P_s(\xi)$, $0 < \lambda < \infty$.
- (ii) P_s is differentiable in $\hat{\xi}$, and $\frac{\partial P_s}{\partial \xi}(\hat{\xi}) = \left(\frac{\partial \varphi^s}{\partial \xi} + F_s(\xi) \frac{\partial t_s}{\partial \xi} \right)(\hat{\xi})$.

The existence of an invariant cone passing through the sliding region depends on the existence of an “eigenvector” $\bar{\xi} \notin \mathcal{M}_+^s$ of the nonlinear eigenvalue problem

$$P(\bar{\xi}) = \mu_c \bar{\xi},$$

where P is the composition of one or both of (P_-, P_+) and P_s . Without loss of generality, we may assume that the Poincaré map can be expressed as: $P(\bar{\xi}) = P_s \circ P_+ \circ P_-(\bar{\xi})$. In general, it is not possible to obtain in this way an explicit expression for the sub-map P_s due to the nonlinearity of F_s , and only a numerical solution can be obtained. Thus, we will show that it is possible to construct the linearizations of P_{\pm} and P_s . In the present situation, we get a non-smooth map $DP(\bar{\xi}) = DP_s DP_+ DP_-(\bar{\xi})$, where $D = \frac{\partial}{\partial \xi}$, and DP_i is the linearized matrix of sub-maps P_i , $i = (-, +, s)$. In fact, there are many possibilities of flow that passes through \mathcal{M}_-^s to generate an invariant cone. In this Chapter, we will discuss several different scenarios.

In order to study the attractivity of the cone we consider the eigenvalues of the Jacobian $DP(\lambda\bar{\xi})$, which are independent of $\lambda > 0$ due to the properties and linearity of the system: Since the intersection times t_{\pm} and t_s are constant on half-rays, we get the identity

$$P(\lambda\xi) = \lambda P(\xi), \quad 0 < \lambda < \infty.$$

Differentiating this identity with respect to ξ yields $DP(\lambda\xi) = DP(\xi)$, which confirms independency of λ . By differentiating with respect to λ we obtain $DP(\lambda\bar{\xi})\bar{\xi} = P(\bar{\xi}) = \mu_c \bar{\xi}$. Hence μ_c is an eigenvalue of $DP(\bar{\xi})$ with eigenvector $\bar{\xi}$. For the remaining $n - 2$ eigenvalues μ_i we assume

$$|\mu_i| \leq \min\{1, \mu_c\}, \quad i = 1, \dots, n - 2. \quad (3.15)$$

This approach is suitable for the stability analysis of invariant cones, but we will need some facts concerning the Jacobian DP , when P cannot be determined in closed form. The construction of DP is given precisely by the monodromy matrix of the normal variational equations at the period T .

In order to illustrate the theoretical considerations, we consider a class of 3D PWLS.

3.5 Analysis of a class of 3D PWLS

Now we concentrate our attention on PWLS (2.16) in \mathbb{R}^3 . We are interested in the case when the system (2.16) has a sliding motion, thus we write the full dynamical system with one discontinuity surface as:

$$\dot{\xi} \in F(\xi) = \begin{cases} A^+\xi, & \xi \in \mathbb{R}_+^3, \\ F_s(\xi) = q(\xi)A^+\xi + (1 - q(\xi))A^-\xi, & \xi \in \mathcal{M}^s, \\ A^-\xi, & \xi \in \mathbb{R}_-^3. \end{cases} \quad (3.16)$$

where $q(\xi) = \frac{n^T(\xi)A^-\xi}{n^T(\xi)(A^-\xi - A^+\xi)} \in (0, 1)$, consequently we get

$$F_s(\xi) = \frac{n^T(\xi)A^-\xi \cdot A^+\xi - n^T(\xi)A^+\xi \cdot A^-\xi}{n^T(\xi)(A^-\xi - A^+\xi)}. \quad (3.17)$$

To be more precise, we assume that A^\pm are given as

$$A^+ = \begin{pmatrix} \lambda^+ & -\omega^+ & 0 \\ \omega^+ & \lambda^+ & \alpha^+ \\ 0 & 0 & \mu^+ \end{pmatrix}, \quad A^- = \begin{pmatrix} a_{11}^- & a_{12}^- & a_{13}^- \\ a_{21}^- & a_{22}^- & a_{23}^- \\ a_{31}^- & a_{32}^- & a_{33}^- \end{pmatrix}.$$

Then A^+ has eigenvalues $\lambda^+ \pm i\omega^+$, μ^+ , and we assume that A^- has eigenvalues $\lambda^- \pm i\omega^-$, μ^- , and the only equilibrium point is at the origin. The manifold \mathcal{M} is given by $h(\xi) = \xi_1$. This form of A^\pm is used since we can always assume that one of the subsystems is in normal form (here: A^+) and take the other in general form. Already such systems exhibit a rich variety of bifurcation behavior.

3.5.1 Detecting sliding region

The idea of this section is to investigate the existence of stable sliding motion on the manifold. The system (2.16) is said to have an attractive sliding motion if at $\xi \in M^s$, $n^T(\xi)A^+\xi < 0$ and $n^T(\xi)A^-\xi > 0$, where $n^T(\xi)A^+\xi$ and $n^T(\xi)A^-\xi$ be the projection of $A^+\xi$ and $A^-\xi$ onto the normal to the hyperplane M^s . Thus, we get

$$n^T(\xi)A^+\xi = -\omega^+\xi_2, \quad n^T(\xi)A^-\xi = a_{12}^-\xi_2 + a_{13}^-\xi_3.$$

In order to determine the region of attractivity on the sliding manifold, we analyze the domain in \mathbb{R}^3 for which

$$\begin{aligned} (n^T(\xi)A^+\xi)(n^T(\xi)A^-\xi) &\leq 0, \\ \xi_2(a_{12}^-\xi_2 + a_{13}^-\xi_3) &\geq 0, \end{aligned} \quad (3.18)$$

giving the attractivity domain

$$\mathcal{M}_-^s = \{\xi \in \mathbb{R}^3 : \xi_1 = 0, \xi_2 > 0, a_{12}^- \xi_2 + a_{13}^- \xi_3 > 0\}. \quad (3.19)$$

The repulsive domain is given by

$$\mathcal{M}_+^s = \{\xi \in \mathbb{R}^3 : \xi_1 = 0, \xi_2 < 0, a_{12}^- \xi_2 + a_{13}^- \xi_3 < 0\}. \quad (3.20)$$

According to Lemma 2.5, depending on the sign of a_{12}^- and a_{13}^- , the solution of system (2.16) exhibits an attractive/repulsive sliding motion along the surface \mathcal{M} as indicated in the graphs in Figure 3.3.

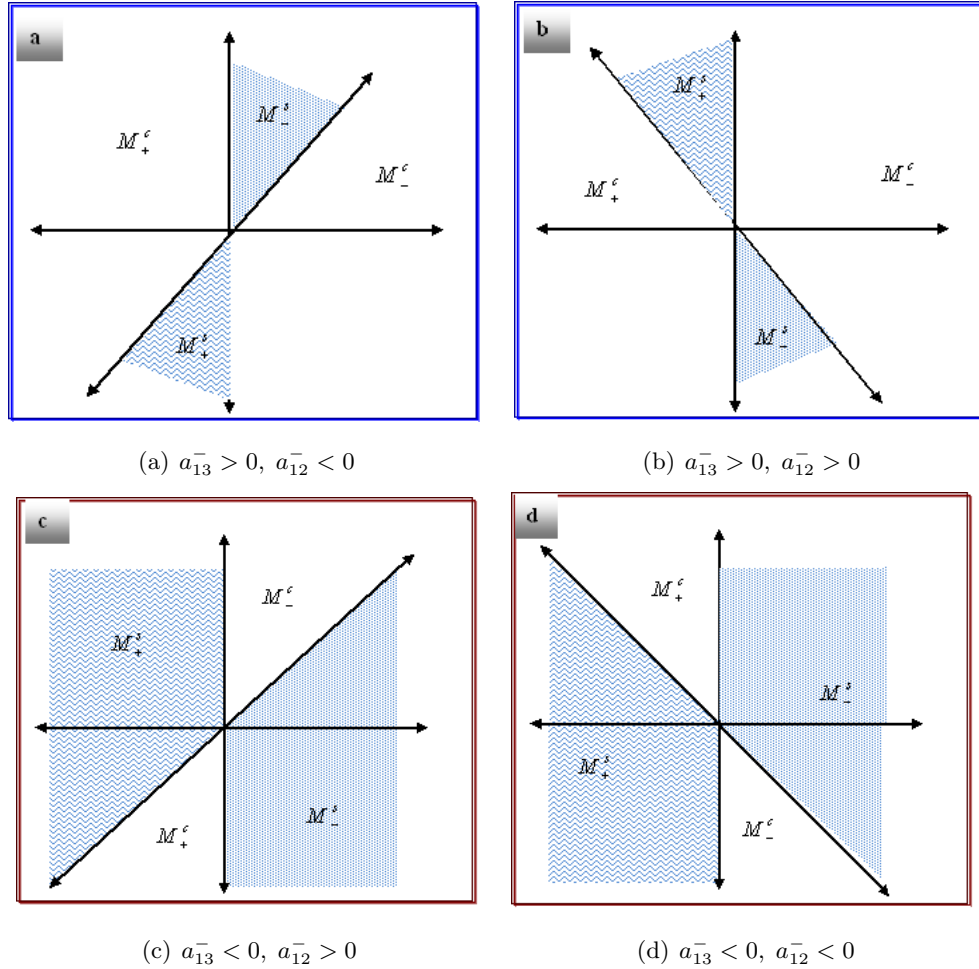


Figure 3.3: Location of attractive sliding motion \mathcal{M}_-^s .

3.5.2 Vector field of sliding motion

If $\xi \in \mathcal{M}^s$, the equivalent dynamics in the sliding region is given by

$$\begin{aligned} \begin{pmatrix} \dot{\xi}_2 \\ \dot{\xi}_3 \end{pmatrix} &= \frac{a_{12}^- \xi_2 + a_{13}^- \xi_3}{(a_{12}^- + \omega^+) \xi_2 + a_{13}^- \xi_3} \begin{pmatrix} \lambda^+ \xi_2 + \alpha^+ \xi_3 \\ \mu^+ \xi_3 \end{pmatrix} \\ &+ \frac{\omega^+ \xi_2}{(a_{12}^- + \omega^+) \xi_2 + a_{13}^- \xi_3} \begin{pmatrix} a_{22}^- \xi_2 + a_{23}^- \xi_3 \\ a_{32}^- \xi_2 + a_{33}^- \xi_3 \end{pmatrix}. \end{aligned} \quad (3.21)$$

We also consider the dynamics on the boundaries $\partial\mathcal{M}_-^s = \mathcal{M}_-^c \cap \mathcal{M}_-^s$ and $\partial\mathcal{M}_+^s = \mathcal{M}_+^c \cap \mathcal{M}_+^s$, respectively

- If $\xi \in \partial\mathcal{M}_-^s$ then $q = 0$, $F_s = A^-\xi$ and $\xi_3 = \frac{-a_{12}^-}{a_{13}^-}\xi_2$. Thus, the dynamics on this boundary is given by $\dot{\xi} = \begin{pmatrix} (a_{22}^- - \frac{a_{23}^-a_{12}^-}{a_{13}^-})\xi_2 \\ (a_{32}^- - \frac{a_{33}^-a_{12}^-}{a_{13}^-})\xi_2 \end{pmatrix}$.
- If $\xi \in \partial\mathcal{M}_+^s$ then $q = 1$, $F_s = A^+\xi$ and $\xi_2 = 0$. Thus, the dynamics on this boundary is given by $\dot{\xi} = \begin{pmatrix} \alpha^+\xi_3 \\ \mu^+\xi_3 \end{pmatrix}$.

This means the dynamics around any point $\xi \in \partial\mathcal{M}_\pm^s$ is significantly distinct, depending on the kind of tangency at this point.

3.5.3 Generalized Poincaré map

The simple choice of the \oplus -system implies: For all $\eta \in \mathcal{M}_+^c$, the function $\mathbf{t}_+(\eta)$ depends on η in a nonlinear way (2.7), and it is determined by the smallest positive solution of the following condition

$$0 = \omega^+(\sigma^{+2} + 1)s^+\eta_2 - \alpha^+(\sigma^+s^+ + c^+ - E^+)\eta_3, \quad (3.22)$$

where $\sigma^+ = \frac{\mu^+ - \lambda^+}{\omega^+}$, $\mathbf{t}_+ = \frac{t_+}{\omega^+}$. Thus, the slope function $n_0(t_+)$ of the initial half-plane is given by

$$n_0(t_+) = \frac{\omega^+(\sigma^{+2} + 1)s^+}{\alpha^+(\sigma^+s^+ + c^+ - E^+)}. \quad (3.23)$$

Further, the sub-Poincaré map is given as

$$P_+(\eta) = \begin{pmatrix} c^+e^{\lambda^+t_+/\omega^+} & \frac{\alpha^+(s^+ - \sigma^+c^+ + \sigma^+e^{\sigma^+t_+})e^{\lambda^+t_+/\omega^+}}{\omega^+(\sigma^{+2}+1)} \\ 0 & e^{\mu^+t_+/\omega^+} \end{pmatrix} \begin{pmatrix} \eta_2 \\ \eta_3 \end{pmatrix}.$$

For the \ominus -system, to be specific we assume that A^- is obtained through a similarity transformation of a suitable Jordan normal form incorporating the desired properties of the eigenvalues:

$$A^- = S^{-1}A_N^-S$$

where

$$A_N^- = \begin{pmatrix} \lambda^- & -\omega^- & 0 \\ \omega^- & \lambda^- & 0 \\ 0 & 0 & \mu^- \end{pmatrix}, \quad S = \begin{pmatrix} 1 & 0 & -1 \\ \frac{a(\delta - \lambda^- \mu^- - \alpha^-) + \mu^- - \lambda^-}{a} & \frac{\omega^-(1 - a\mu^-)}{a} & \alpha^- \\ -\lambda^- \mu^- & -\mu^- \omega^- & \delta \end{pmatrix},$$

where α^- , δ and a are constant parameters.

The general solution of the \ominus -system is given by

$$\xi(t_-) = e^{\lambda^- t_-} \left\{ (c^- S^{-1} e_1 + s^- S^{-1} e_2) \bar{\xi}_1 + (c^- S^{-1} e_2 - s^- S^{-1} e_1) \bar{\xi}_2 \right\} + e^{\mu^- t_-} S^{-1} e_3, \quad (3.24)$$

where $S\xi(0) = \bar{\xi}$. In order to keep the calculations simple, we discuss the situation for $\delta = (\lambda^-)^2 + (\omega^-)^2$, and a suitable parameter α^- , hence

$$A^- = \begin{pmatrix} a_{11}^- & a_{12}^- & a_{13}^- \\ a_{21}^- & a_{22}^- & a_{23}^- \\ a_{31}^- & a_{32}^- & a_{33}^- \end{pmatrix} = \begin{pmatrix} \mu^- + a(\delta - \alpha^-) & -a & a \\ \frac{\delta(1-2a\lambda^-) + a^2(\alpha^- - \delta) + a\alpha^-(2\lambda^- - \mu^-)}{a} & a(\alpha^- - \delta) + 2\lambda^- & \frac{1+a^2(\delta - \alpha^-) - 2a\lambda^-}{a} \\ -\mu^- \delta & 0 & 0 \end{pmatrix}.$$

The return time function $t_-(\xi)$ in (2.6) is determined as the smallest positive root of (we recall from Chapter 2 that $E^- = e^{(\mu^- - \lambda^-)t_-}$, $s^- = \sin(\omega^- t_-)$, $c^- = \cos(\omega^- t_-)$)

$$a[\mu^- \omega^- (c^- - E^-) + (\lambda^- \mu^- - \delta) s^-] \xi_2 + [\omega^- (1 - a\mu^-) (c^- - E^-) + (a(\delta - \lambda^- \mu^-) + \mu^- - \lambda^-) s^-] \xi_3 = 0.$$

Therefore, it is easy to show for all $\xi \in \mathcal{M}_-^c$ that the slope function $m_0(t_-)$ in the initial half-plane is given by

$$m_0(t_-) = - \frac{a[\mu^- \omega^- (c^- - E^-) + (\lambda^- \mu^- - \delta) s^-]}{[\omega^- (1 - a\mu^-) (c^- - E^-) + (a(\delta - \lambda^- \mu^-) + \mu^- - \lambda^-) s^-]}. \quad (3.25)$$

By the general solution (3.24), the Poincaré map for the \ominus -system is given as:

$$P_-(\xi) = \begin{pmatrix} p_1 & p_2 \\ p_3 & p_4 \end{pmatrix} \begin{pmatrix} \xi_2 \\ \xi_3 \end{pmatrix},$$

where

$$p_1 = - \frac{1}{a\omega^-((\omega^-)^2 + (\lambda^- - \mu^-)^2)} \left[e^{\lambda^- t_-} \left((a^2 \delta ((\omega^-)^2 - \alpha^- + (\mu^-)^2 - 2\lambda^- \mu^-) + a^2 (\lambda^-)^2 \delta - a\lambda^- \delta + a\mu^- \lambda^- (2\lambda^- - \mu^- + a\alpha^-)) s^- - a\omega^- (\delta - \mu^- (2\lambda^- - \mu^- + a\alpha^-)) c^- \right) - a^2 \alpha^- \omega^- \mu^- e^{\mu^- t_-} \right],$$

$$p_2 = - \frac{1}{a\omega^-((\omega^-)^2 + (\lambda^- - \mu^-)^2)} \left[e^{\lambda^- t_-} \left((a^2 \delta (\alpha^- + 2\lambda^- \mu^- - (\mu^-)^2 - (\omega^-)^2) + \delta (2a\lambda^- - 1) - (\mu^-)^2 - a^2 \lambda^- \delta + \mu^- \lambda^- (2 + 2a\mu^- - a^2 \alpha^- - 4a\lambda^-)) s^- + a\alpha^- \omega^- (1 - a\mu^-) c^- \right) + a\alpha^- \omega^- (a\mu^- - 1) e^{\mu^- t_-} \right],$$

$$p_3 = -\frac{1}{\omega^-((\omega^-)^2 + (\lambda^- - \mu^-)^2)} \left[a e^{\lambda^- t_-} \left(((\mu^-)^2 \delta - \lambda^- \mu^- \delta) s^- + \omega^- \mu^- \delta c^- \right) - e^{\mu^- t_-} a \omega^- \mu^- \delta \right],$$

$$p_4 = -\frac{1}{\omega^-((\omega^-)^2 + (\lambda^- - \mu^-)^2)} \left[e^{\lambda^- t_-} \left((-a(\mu^-)^2 \delta + \lambda^- (\mu^-)^2 + \mu^- ((\omega^-)^2 - (\lambda^-)^2) + a \lambda^- \mu^- \delta) s^- + (-a \omega^- \mu^- \delta - \omega^- (\mu^-)^2 + 2\mu^- \omega^- \lambda^-) c^- + e^{\mu^- t_-} (a \omega^- \mu^- \delta - \omega^- \delta) \right) \right].$$

In the case $\alpha^+ = 0$, the Poincaré return map (without having sliding motion) can be computed rigorously as

$$P^c(\xi) = \begin{pmatrix} -e^{\lambda^+ t_+} p_1 & -e^{\lambda^+ t_+} p_2 \\ e^{\mu^+ t_+} p_3 & e^{\mu^+ t_+} p_4 \end{pmatrix} \begin{pmatrix} \xi_2 \\ \xi_3 \end{pmatrix}, \quad (3.26)$$

where $P^c = P_+ P_-(\xi)$.

Lemma 3.5.

Under the above hypotheses, the slope transition maps $n_1(t_+)$ with $\xi \in \mathcal{M}_+^c$ and $m_1(t_-)$ with $\xi \in \mathcal{M}_-^c$ are given by

$$n_1(t_+) = \frac{\omega^+(\sigma^{+2} + 1)e^{\sigma^+ t_+} n_0(t_+)}{c^+ \omega^+(\sigma^{+2} + 1) + \alpha^+(s^+ - \sigma^+ c^+ + \sigma^+ e^{\sigma^+ t_+}) n_0(t_+)}, \quad m_1(t_-) = \frac{p_3 + p_4 m_0(t_-)}{p_1 + p_2 m_0(t_-)}.$$

Furthermore $\alpha^+ = 0$ implies that $t_+ = \pi$ and $P^c(\xi) = P_+ P_-(\xi)$. Then, $P^c(\xi) \in \mathcal{M}_-^s$ if $\xi_2 = e_1^T P^c(\xi) > 0$ and $E^+ m_1(t_-) < 1$.

The flow of attractive sliding motion has been defined by $P_s(\xi) : M_-^s \rightarrow M_-^s$, for all $\xi \in \mathcal{M}_-^s$. Due to nonlinearity of equation (3.21), the map P_s must be evaluated by numerical methods solving (3.21) with regard to the boundary equations related to \mathcal{M}_-^s .

The PWS (3.16) possesses an invariant cone if $0 < \mu_c \in \rho(DP(\xi))$. The map DP is a composition of maps DP_\pm and DP_s which is mapped into itself and then we examine whether the map DP has a fixed point. A fixed point of DP will give rise to a periodic orbit of (3.16). However here we note that it is not an easy task to study the existence of fixed-point of DP due to nonlinearity of exists the intersection times t_\pm , the time evolution of sliding segment t_s , and composition of sub-maps.

Coming back now to the structure of A^- , we note that the existence of \mathcal{M}_\pm^s depends on the sign of the parameter a . For $a > 0$ or $a < 0$ the locations of \mathcal{M}_\pm^s are depicted in Figure 3.3a, or Figure 3.3c, respectively.

Lemma 3.6.

If $\xi \in \partial M_-^s$, and (i) in Lemma 3.2 holds, then for the function $t_-(\xi) = \frac{t_-(\xi)}{\omega^-}$ defined in (3.25) and $\sigma^- = \frac{\mu^- - \lambda^-}{\omega^-}$, the following statements hold

- (i) If $\sigma^- \leq 0$, then $t_- \in (\pi, 2\pi)$;
- (ii) If $\sigma^- = 0$, then $t_- = 2\pi$;
- (iii) If $\sigma^- > 0$, the trajectory starting inside \mathcal{M}_-^c given by $\varphi^-(\xi, t_-)$ cannot leave \mathcal{M} for all future times, hence there is no finite return time and thus, there is no invariant cone starting in \mathcal{M}_-^c .

Proof: If $\xi \in \partial\mathcal{M}_-^s$ implies that $m_0(t_-) = m_0(t_-/\omega^-) = 1$ and using (3.25) we can define $\Phi_{\sigma^-}(t_-) = c^- + \sigma^- s^- - e^{\sigma^- t_-}$ where t_- is the return time which defined as smallest root of $\Phi_{\sigma^-}(t_-) = 0$. It can be seen that $\Phi_{-\sigma^-}(-t_-) = \Phi_{\sigma^-}(t_-)$ for any $(\sigma^-, t_-) \in \mathbb{R}$. Furthermore, if $\sigma^- \neq 0$, then we get $\Phi_{\sigma^-}(0) = \Phi'_{\sigma^-}(0) = 0$, $\Phi''_{\sigma^-}(0) = \Phi'_{\sigma^-}(\pi) < 0$, while $\Phi_{\sigma^-}(2\pi) > 0$ iff $\sigma^- \leq 0$ implies (i) and (iii) hold and if $\sigma^- = 0$, then we get $\Phi_0(t_-) = c^- - 1$, satisfies (ii).

Lemma 3.7. *If $\eta \in \partial\mathcal{M}_+^s$, $\alpha^+ \neq 0$, then the function $t_+(\eta)$ defined in (3.22) the following statements hold*

- (i) If $\sigma^+ \leq 0$, then $t_+ \in (\pi, 2\pi)$;
- (ii) If $\sigma^+ = 0$, then $t_+ = 2\pi$;
- (iii) If $\sigma^+ > 0$, the trajectory starting inside \mathcal{M}_+^c given by $\varphi^+(\eta, t_+)$ cannot leave \mathcal{M} for all future times, hence there is no finite return time and thus, there is no invariant cone starting in \mathcal{M}_+^c .

Proof:

If $\eta \in \partial\mathcal{M}_+^s$ and $\alpha^+ \neq 0$, using (3.22) we can define $\Phi_{\sigma^+}(t_+) = \sigma^+ s^+ + c^+ - e^{\sigma^+ t_+}$ which is taken a similar behaviour of $\Phi_{\sigma^-}(t_-)$. Thus, the proof is finished.

Based on the above analysis, we can describe various scenarios of invariant cones with periodic orbits involving sliding segment. To simplify the computation, we set $\alpha^- = \delta - 2\lambda^- + 1$, $a = 1$ in the following. Then the dynamics on \mathcal{M}_-^s is governed by

$$\begin{aligned} \begin{pmatrix} \dot{\xi}_2 \\ \dot{\xi}_3 \end{pmatrix} &= \frac{\xi_3 - \xi_2}{(\omega^+ - 1)\xi_2 + \xi_3} \begin{pmatrix} \lambda^+ \xi_2 + \alpha^+ \xi_3 \\ \mu^+ \xi_3 \end{pmatrix} + \frac{\omega^+ \xi_2}{(\omega^+ - 1)\xi_2 + \xi_3} \begin{pmatrix} \xi_2 \\ 0 \end{pmatrix}, \text{ if } \xi \in \mathcal{M}_-^s, \\ \dot{\xi} &= \begin{pmatrix} \alpha^+ \xi_3 \\ \mu^+ \xi_3 \end{pmatrix}, \text{ if } \xi \in \partial\mathcal{M}_+^s, \quad \dot{\xi} = \begin{pmatrix} \xi_2 \\ 0 \end{pmatrix}, \text{ if } \xi \in \partial\mathcal{M}_-^s. \end{aligned} \tag{3.27}$$

Note that the dynamic on \mathcal{M}_-^s depends only on parameters λ^+ , α^+ and μ^+ . Further, when $\xi^0 \in \partial\mathcal{M}_-^s$ implies $m_0(t_-) = 1$ (i.e., $\xi_3^0 = \xi_2^0$), then we get

$$\begin{aligned} \frac{\xi_2^1}{\xi_2^0} &= -\frac{1}{\omega^-((\omega^-)^2 + (\lambda^- - \mu^-)^2)} \left[e^{\lambda^- t_-} \left((((\lambda^-)^2 - (\omega^-)^2)(1 - \mu^-) + (\mu^-)^2(\lambda^- - 1) \right. \right. \\ &\quad \left. \left. + \mu^- - \lambda^-)s^- + \omega^- (2\lambda^-(\mu^- - 1) + 1 - (\mu^-)^2) \right) c^- \right) \\ &\quad \left. + e^{\mu^- t_-} (2\lambda^- - (\lambda^-)^2 - (\omega^-)^2 - 1)\omega^- \right], \\ \frac{\xi_3^1}{\xi_3^0} &= -\frac{1}{\omega^-((\omega^-)^2 + (\lambda^- - \mu^-)^2)} \left[e^{\lambda^- t_-} \left(\mu^-((\omega^-)^2 - (\lambda^-)^2 + \mu^- \lambda^-)s^- \right. \right. \\ &\quad \left. \left. + \omega^- (2\mu^- \lambda^- - (\mu^-)^2) \right) c^- - e^{\mu^- t_-} ((\lambda^-)^2 + (\omega^-)^2)\omega^- \right], \end{aligned} \tag{3.28}$$

hence,
$$m_1(t_-) = \frac{\xi_3^1}{\xi_2^1} = \frac{p_3 + p_4}{p_1 + p_2}.$$

Also, $\tilde{\xi} \in \partial\mathcal{M}_+^s$ implies that for the line of $\partial\mathcal{M}_+^s$ determined by $(0, \tilde{\xi}_3)$, we get

$$n_1(t_+) = \frac{\omega^+(\sigma^{+2} + 1)e^{\sigma^+ t_+}}{\alpha^+(s^+ - \sigma^+ c^+ + \sigma^+ e^{\sigma^+ t_+})}.$$

3.5.4 One-zonal invariant cone

In this case, according to Figure 3.3a and 3.3c, ($a = 1$) we are led to define the Poincaré return map in two ways as: $P(\xi) = P_s \circ P_-(\xi)$ or $P(\xi) = P_- \circ P_s(\xi)$. Let us start by treating the situation where $P(\xi) = P_- \circ P_s(\xi)$. This means that the flow is coming from \mathcal{M}_-^s where $\xi_3^0 = \mathbf{np} \xi_2^0$, where $\mathbf{np} > 1$ is the slope of initial position of half-rays. If $\lambda^+ \geq 0$ in (3.27), then the trajectory reaches the boundary $\partial\mathcal{M}_-^s$ in forward time. At the boundary point $\tilde{\xi} \in \partial\mathcal{M}_-^s$, the trajectory leaves $\partial\mathcal{M}_-^s$ tangentially or smoothly and continues into \mathcal{M}_-^c under the \ominus -system. The trajectory of a periodic point is called a closed trajectory if $P_- \circ P_s(\xi) - \xi = 0$, which implies that $m_1(t_-) > 1$.

Corollary 3.1. *If $(\lambda^+, \alpha^+) \geq 0$, $\mathbf{np} > 1$ and $\sigma^\pm < 0$. Then the system (3.16) has an invariant cone with a segment of sliding motion living in one-zone if the following conditions hold.*

$$m_1(t_-) = \mathbf{np}.$$

Note that this implies that $\frac{\xi_2^1}{\xi_2^0} = 1$ and $\frac{\xi_3^1}{\xi_3^0} = 1$.

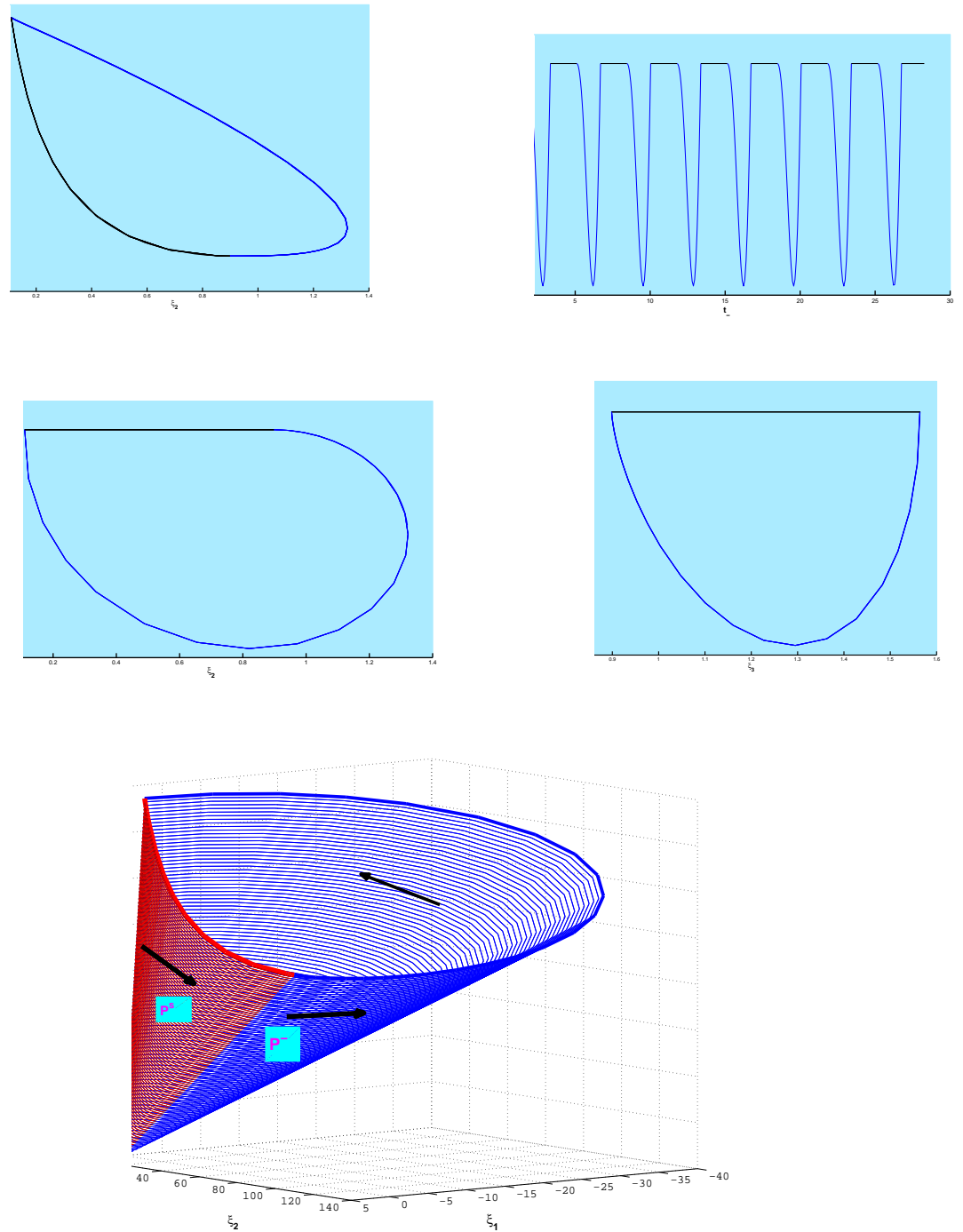


Figure 3.4: Invariant cone (only Sliding) with sliding segment and solution components: $\lambda^+ = 1.3, \mu^+ = -0.5, \omega^+ = 0.9, \alpha^+ = 0, \lambda^- = 1, \mu^- = 0.212, \omega^- = 3.0$.

More precisely, the above corollary leads to $t_- \in (\pi, 2\pi)$, and practically necessary conditions of existence of invariant cone for the present case which can be explicitly written as

$$\begin{aligned} & \left[e^{\lambda^- t_-} \left(((\lambda^2 - \omega^2)(1 - \mu^-) + \mu^{-2}(\lambda^- - 1) + \mu^- - \lambda^-) s^- \right. \right. \\ & \left. \left. + \omega^- (2\lambda^- (\mu^- - 1) + 1 - \mu^{-2}) c^- \right) + e^{\mu^- t_-} (2\lambda^- - \lambda^2 - \omega^{-2} - 1) \omega^- \right] \tilde{\xi}_2 \\ & + \omega^- (\omega^{-2} + (\lambda^- - \mu^-)^2) \xi_2^0 = 0, \end{aligned}$$

$$\begin{aligned} & \left[e^{\lambda^- t_-} \left(\mu^- (\omega^{-2} - \lambda^{-2} + \mu^- \lambda^-) s^- + \omega^- (2\mu^- \lambda^- - \mu^{-2}) c^- - e^{\mu^- t_-} (\lambda^{-2} + \omega^{-2}) \omega^- \right) \right] \tilde{\xi}_2 \\ & + \omega^- (\omega^{-2} + (\lambda^- - \mu^-)^2) \xi_2^0 = 0, \end{aligned}$$

$$\begin{aligned} & \left[e^{\lambda^- t_-} \left(\mu^- (\omega^{-2} - \lambda^{-2} + \mu^- \lambda^-) s^- + \omega^- (2\mu^- \lambda^- - \mu^{-2}) c^- - e^{\mu^- t_-} (\lambda^{-2} + \omega^{-2}) \omega^- \right) \right. \\ & \quad \left. - \left[e^{\lambda^- t_-} \left(((\lambda^2 - \omega^2)(1 - \mu^-) + \mu^{-2}(\lambda^- - 1) + \mu^- - \lambda^-) s^- \right. \right. \right. \\ & \quad \left. \left. + \omega^- (2\lambda^- (\mu^- - 1) + 1 - \mu^{-2}) c^- \right) + e^{\mu^- t_-} (2\lambda^- - \lambda^2 - \omega^{-2} - 1) \omega^- \right] \mathbf{np} = 0. \end{aligned}$$

In order to examine the stability of the periodic orbit, we compute the monodromy matrix which in the present case takes the form

$$Y(T, \xi) = J_s \cdot Y_-(\tilde{t}_-, \xi(\tilde{t}_s)). \quad Y_s(\tilde{t}_s, \xi^0), \quad T = \tilde{t}_- + \tilde{t}_s, \quad (3.29)$$

where \tilde{t}_s is the time spent before the trajectory reaches $\partial\mathcal{M}_-^s$ and \tilde{t}_- is the exact positive solution of (3.25).

An example to illustrate the current scenario can be found in Figure 3.4. By numerical evaluating of $Y(T, \xi)$ in (3.29) for the bifurcating cycle after one period $T = 3.2962$, we find numerically that the multipliers are: $(1.00, 1.43, 0)$, implying that the invariant cone consist of periodic orbit but the motion outside the cone is unstable (center+unstable focus).

3.5.5 Two-zones invariant cones (Crossing + Sliding)

We consider now a trajectory related to the form $P(\xi) = P_s \circ P_+ \circ P_-(\xi)$, see Figure 3.5, which is a composition of three maps. Any trajectory starting in \mathcal{M}_-^c spends a time determined by (3.25) before it reaches \mathcal{M}_+^c . We assume that the trajectory starts at the boundary $\xi^0 \in \partial\mathcal{M}_-^s$ with $m_0(t_-) = 1$. In order to decide at this point if the trajectory will leave $\partial\mathcal{M}_-^s$ to enter \mathcal{M}_-^c or \mathcal{M}_-^s , we can check the sign of B_1^- where $A_2 < 0$, see Lemma 3.2. For our system situation B_1^- is negative and leads to the trajectory entering \mathcal{M}_-^c with the \ominus -system. After some time it reaches the switching manifold at some

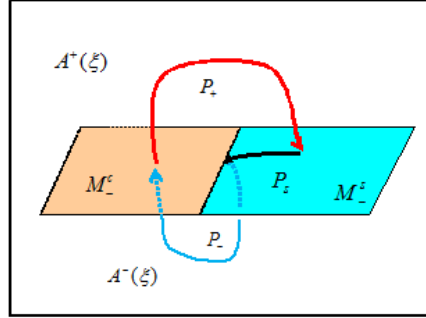


Figure 3.5: Poincaré map structure is a composition of three maps P_{\pm} , P_s .

point in \mathcal{M}_+^c . Note that in view of Lemma 3.6 the return time t_- is uniquely determined. The trajectory after reaching \mathcal{M}_+^c switches to \oplus -system. This trajectory starting in \mathcal{M}_+^c spends a time $t_+ \in \mathcal{M}_+^c$ which is determined in view of Lemma 3.7 before it reaches the switching manifold \mathcal{M} again. At this point there are several possibilities of motion: The trajectory may reach again \mathcal{M}_-^c and moves towards the \ominus -system without sliding motion. This means that the dynamics of the full system can be achieved by studying the map P^c for instance that has been given in (3.26), or under the influence of varying dynamic parameters the trajectory may reach one of \mathcal{M}_{\pm}^s (\mathcal{M}_+^s is less interesting), after reaching \mathcal{M}_-^s the trajectory follows the vector field F_s hence there is sliding governed by (3.27).

Corollary 3.2. *If $\lambda^+ \geq 0$, $m_0(t_-) = 1$ and $\sigma^- < 0$. Then the system (3.16) has an invariant cone with a segment of sliding motion living in two-zones if the following conditions hold.*

- i- $(p_1 + p_2) < 0$ and $(p_3 + p_4) > |p_1 + p_2| > 0$.
- ii- *The solution of (3.27) satisfies the boundary conditions $\xi(t_1) = P^c(\xi^0)$, i.e. $\xi(t_1) \in \mathcal{M}_-^s$, and $\xi(t_2) = \xi^0 \in \partial\mathcal{M}_-^s$, i.e. $m_0(t_-) = 1$, where $t_s \in (t_1, t_2)$.*

Based on the closed-form solution which has been discussed in Section (3.4), the above corollary indicates necessary conditions for two-zones \mathcal{C} involving a sliding segment which are described explicitly as

$$p_1 + p_2 < 0 \Rightarrow \left[((\lambda^2 - \omega^2)(1 - \mu^-) + \mu^{-2}(\lambda^- - 1) + \mu^- - \lambda^-)s^- + \omega^-(2\lambda^-(\mu^- - 1) + 1 - \mu^{-2})c^- + E^-(2\lambda^- - \lambda^2 - \omega^{-2} - 1)\omega^- \right] > 0,$$

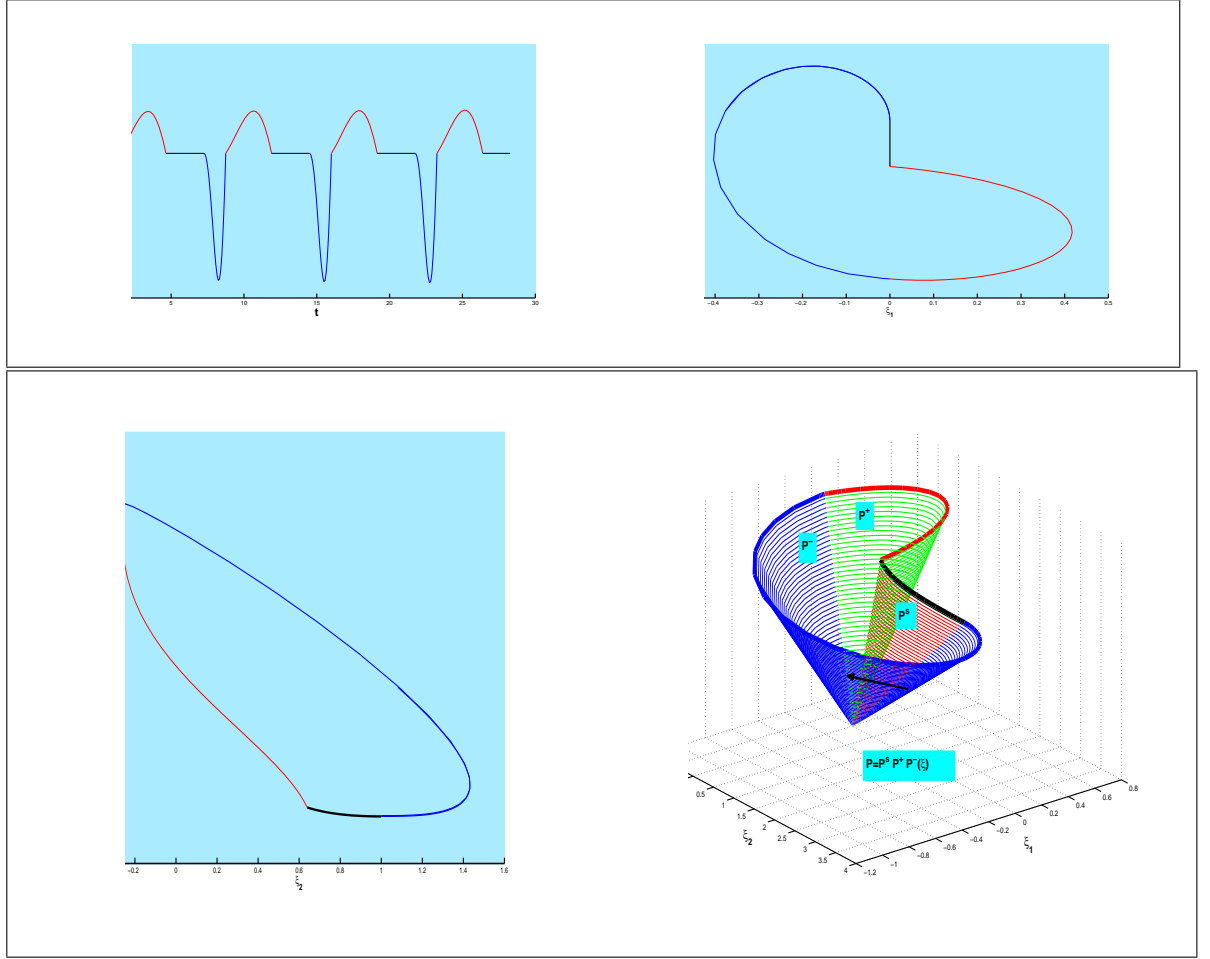


Figure 3.6: Invariant cone (Crossing + Sliding) with sliding segment and solution components: $\lambda^+ = 0.3, \mu^+ = -0.087, \omega^+ = 1.0, \alpha^+ = 0, \lambda^- = 1.0, \mu^- = 0.1, \omega^- = 3.0$.

$$(p_3 + p_4) = \frac{\xi_3^1}{\xi_2^0} > |p_1 + p_2|,$$

where $\frac{\xi_3^1}{\xi_2^0}$ is given by (3.28). It may be also useful to remark that the t_s value is computed by (3.14b). To investigate the stability of invariant cones located using the necessary conditions outlined above, we compute the Monodromy matrix which is of the form

$$Y(T, \xi) = Y_s(\tilde{t}_s, \xi(\tilde{t}_+)) J_s Y_+(\tilde{t}_+, \xi(\tilde{t}_-)) J_- Y_-(\tilde{t}_-, \xi^0), \quad T = \frac{\pi}{\omega^+} + \tilde{t}_- + \tilde{t}_s, \quad (3.30)$$

An example of a two-zone invariant cone together with solution components in the present scenario satisfying the above conditions can be found in Figure 3.6. Numerical evaluation of $Y(T, \xi)$ in (3.30) provides eigenvalues: $(1.00, 0.5635, 0)$ after one period $T = 5.2159$. Thus, the invariant cone is attractive (center+stable focus).

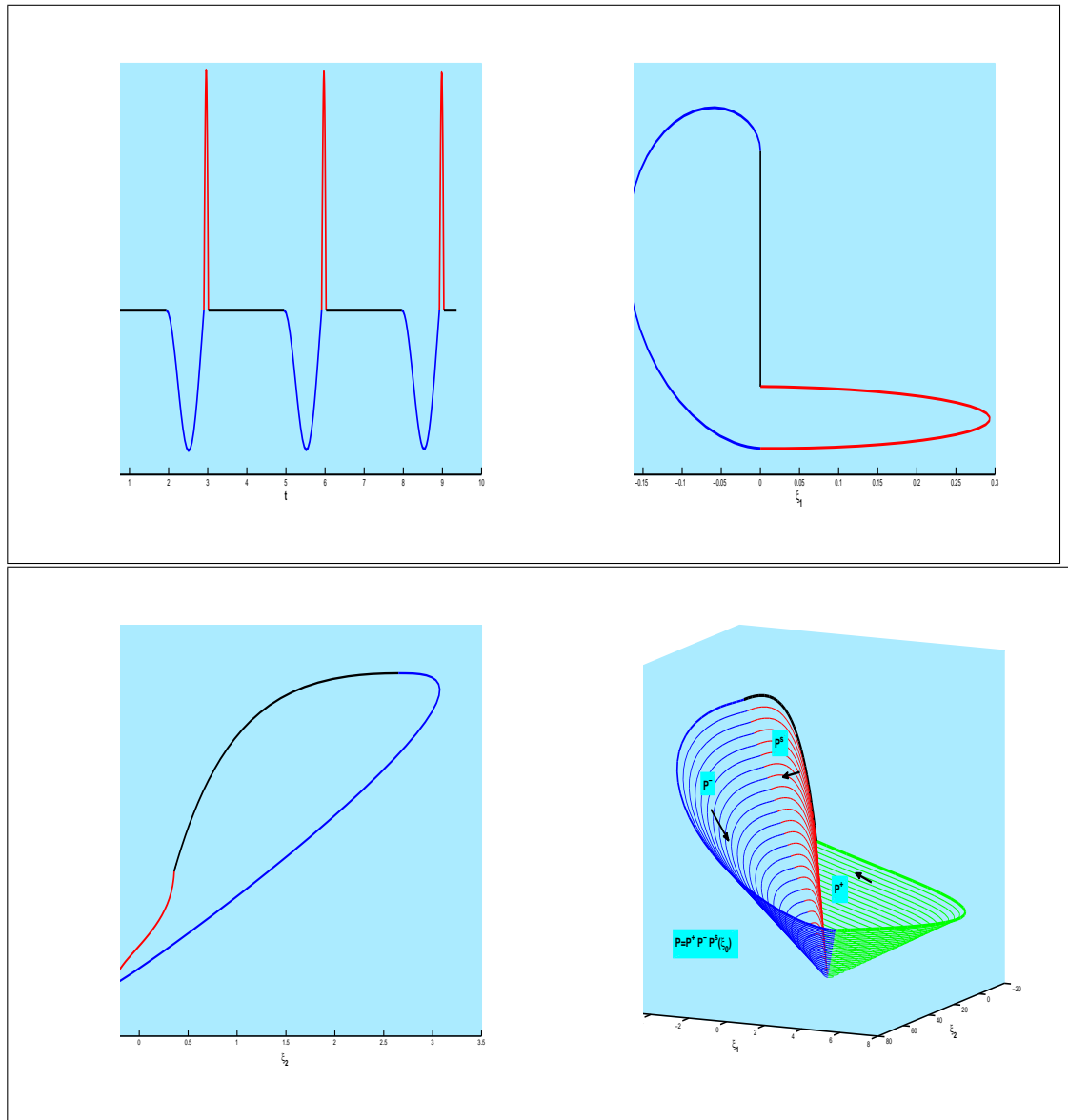


Figure 3.7: Invariant cone (Sliding + Crossing) with sliding segment and solution components: $\lambda^+ = 1.8, \mu^+ = 10.0, \omega^+ = 28.0, \lambda^- = 0.185, \mu^- = -1.0, \omega^- = 5.0$.

3.5.6 Two-zones invariant cones (Sliding + Crossing)

In this case, we consider the mapping structure described by $P(\xi) = P_+ \circ P_- \circ P_s(\xi)$, in a manner similar to that in Figure 3.5. The trajectory is starting at the point ξ^0 where $\mathbf{np} > 1$ reaching the boundary if $\lambda^+ \geq 0$ (set $\alpha^+ = 0$) in finite time. The sliding trajectory on the boundary will vanish and such a motion will switch into the domain \mathcal{M}_-^c which leaving $\partial\mathcal{M}_-^s$ tangentially under \ominus -system; this was already observed during the examination of the one-zonal invariant cone in Figure 3.4. The trajectory in \mathcal{M}_-^c returns to the manifold \mathcal{M}_+^c , i.e., the motion switches from \mathcal{M}_-^c to \mathcal{M}_+^c . Finally the flow in \mathcal{M}_+^c returns to the starting point so that a periodic orbit is achieved. Next, we establish necessary and sufficient conditions for the existence of such a fixed point of P .

Corollary 3.3. *Let $\lambda^+ \geq 0$, $\mathbf{np} > 1$ and $\sigma^- < 0$. Then the system (3.16) has an invariant cone with a segment of sliding motion living in two-zones if the following conditions hold:*

- i- $(p_1 + p_2) < 0$ and $(p_3 + p_4) > |p_1 + p_2|$,
- ii- The solution of (3.27) satisfies the boundary conditions $\xi(0) = \xi^0 \in \mathcal{M}_-^s$, i.e. $\mathbf{np} > 1$, and $\xi(t_2) = \tilde{\xi}$, i.e. $m_0 = 1$, where $t_s \in (0, t_2)$.
- iii- $P^c(\tilde{\xi}) = \xi^0$.

The monodromy matrix is given by

$$Y(T, \xi) = J_s Y_+(\tilde{t}_+, \xi(\tilde{t}_-)) J_- Y_-(\tilde{t}_-, \xi(\tilde{t}_s)) Y_s(\tilde{t}_s, \xi^0), \quad T = \frac{\pi}{\omega^+} + \tilde{t}_- + \tilde{t}_s, \quad (3.31)$$

For example, Figure 3.7 shows a family of periodic trajectories involving a sliding segment generated by the above map P . The eigenvalues of the monodromy matrix are computed to be $(1.00, 0.03, 0)$. Due to size of the second smallest eigenvalue the current invariant cone is attractive.

3.6 Invariant cones: Sliding bifurcation

Here we show the existence of invariant cones for (3.16) which undergo sliding bifurcation. From the results discussed above, there are many opportunities for invariant cones to exhibit sliding bifurcation behaviour due to many possible transitions between crossing and sliding regions through $\partial\mathcal{M}_-^s$ or $\partial\mathcal{M}_+^s$. Thus, we set the parameters according to geometrical consideration.

For **crossing-sliding** bifurcation we will check that the set of analytical conditions is satisfied at the bifurcation point under investigation. For example, let us consider the trajectory starting from \mathcal{M}_-^c , i.e. $\mathbf{np} < 1$ which in forward time reaches the bifurcation point (t_- is determined according to Lemma 3.6). The bifurcation occurs when $\alpha^+ = -1$, $\omega^\pm = 3.0$, $\mu^- = 0.41$, $\lambda^+ = .294$, $\mu^+ = -0.92$ and $\lambda^- = 0.9654$, and the bifurcation point is $\xi^* = (0, -3.2813E - 4, 0.1990)^T$. At this point we get

- (i) $h(\xi^*) = 0$, $\nabla h(\xi)|_{\xi^*} \neq 0$,
- (ii) $(n^T(\xi)A^+\xi)|_{\xi^*} = 1.0938E - 4 \simeq 0$,
- (iii) $(n^T(\xi)A^+A^+\xi)|_{\xi^*} = 0.5970 > 0$.

Thus, at $\xi^* \in \partial\mathcal{M}_+^s$, the system (3.16) satisfies all three conditions and it is simple to show that the existence of an invariant cone depends on the existence of a fixed point of the Poincaré map describing the flow close to the bifurcation point. To illustrate the nature of the change in the dynamics as we pass through a crossing-sliding bifurcation we present in Figure 3.8 an invariant cone and solution components passing through ξ^* . After the bifurcation point the invariant cone acquires a segment of sliding motion due to decreasing values of $\lambda^- \simeq 0.95$. Solution components are depicted in Figure 3.9.

An invariant cone undergoing a **grazing-sliding** bifurcation point is characterized by a trajectory of the subsystem of (3.16) that becomes tangent to the sliding region at $\partial\mathcal{M}_-^s$ or $\partial\mathcal{M}_+^s$. In other words, there is a set of points that does not interact with $\partial\mathcal{M}_-^s$ or $\partial\mathcal{M}_+^s$ and a set of point that hits $\partial\mathcal{M}_-^s$ or $\partial\mathcal{M}_+^s$. If we're going to find evidence of this phenomenon it is appropriate to use an one-zonal invariant cone with sliding segment as discussed in section 3.5.4. Therefore, by varying parameters the sliding segment contained in an invariant cone becomes an infinitesimally small sliding segment that is close to a grazing-sliding bifurcation point. Making things more precise, let us now get back to the \ominus -system in (3.16) and set the parameter values: $\lambda^- = \mu^- = 0$, $\omega^- = 2.0$ and $\xi^0 = (-.4931, 1.609, 1)^T$ i.e. $\mathbf{np} < 1$. An invariant cone passing through the grazing bifurcation point $\xi^* = (0, 1, 1)^T$ is obtained. We indeed find that at ξ^* the following conditions hold:

- (i) $h(\xi^*) = 0$, $\nabla h(\xi)|_{\xi^*} \neq 0$,
- (ii) $(n^T(\xi)A^-\xi)|_{\xi^*} = 0$,
- (ii) $(n^T(\xi)A^-A^-\xi)|_{\xi^*} = -1 < 0$, (Note that ξ^* lies in $\partial\mathcal{M}_-^s$).

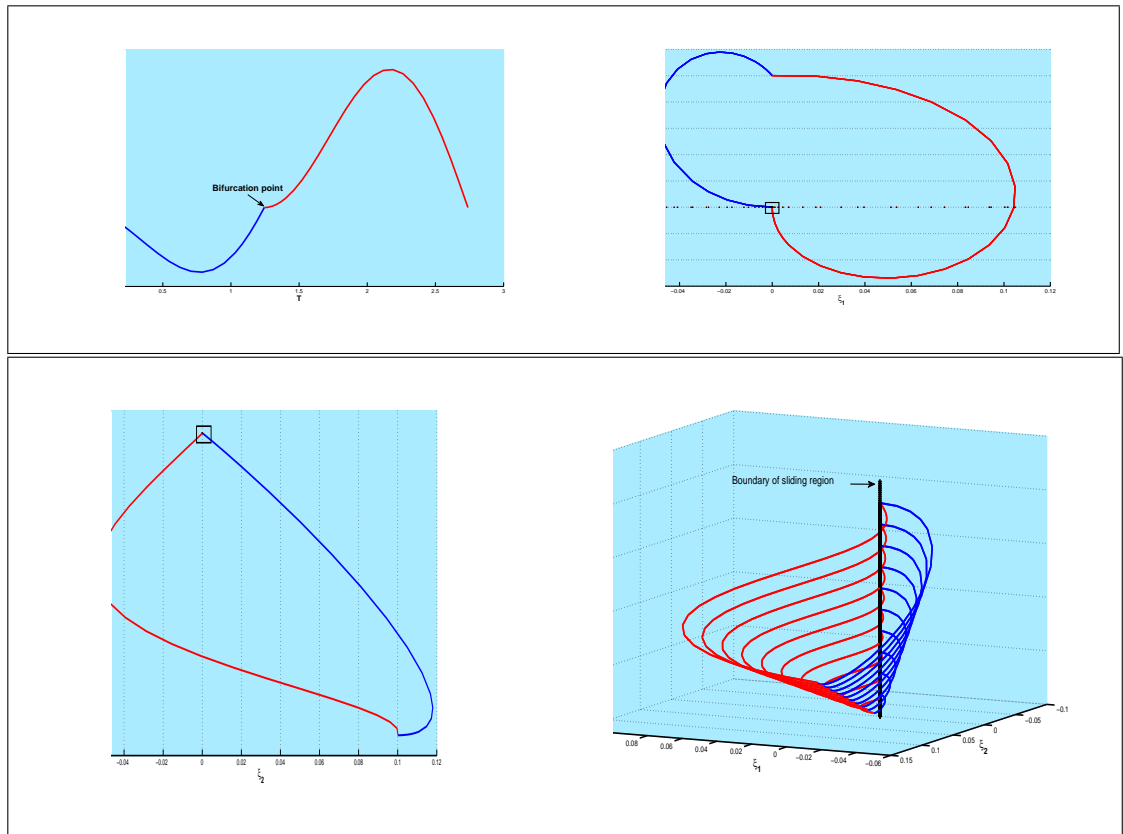


Figure 3.8: Invariant cone and solution components at the crossing-sliding bifurcation point, $\lambda^- = 0.9654$.

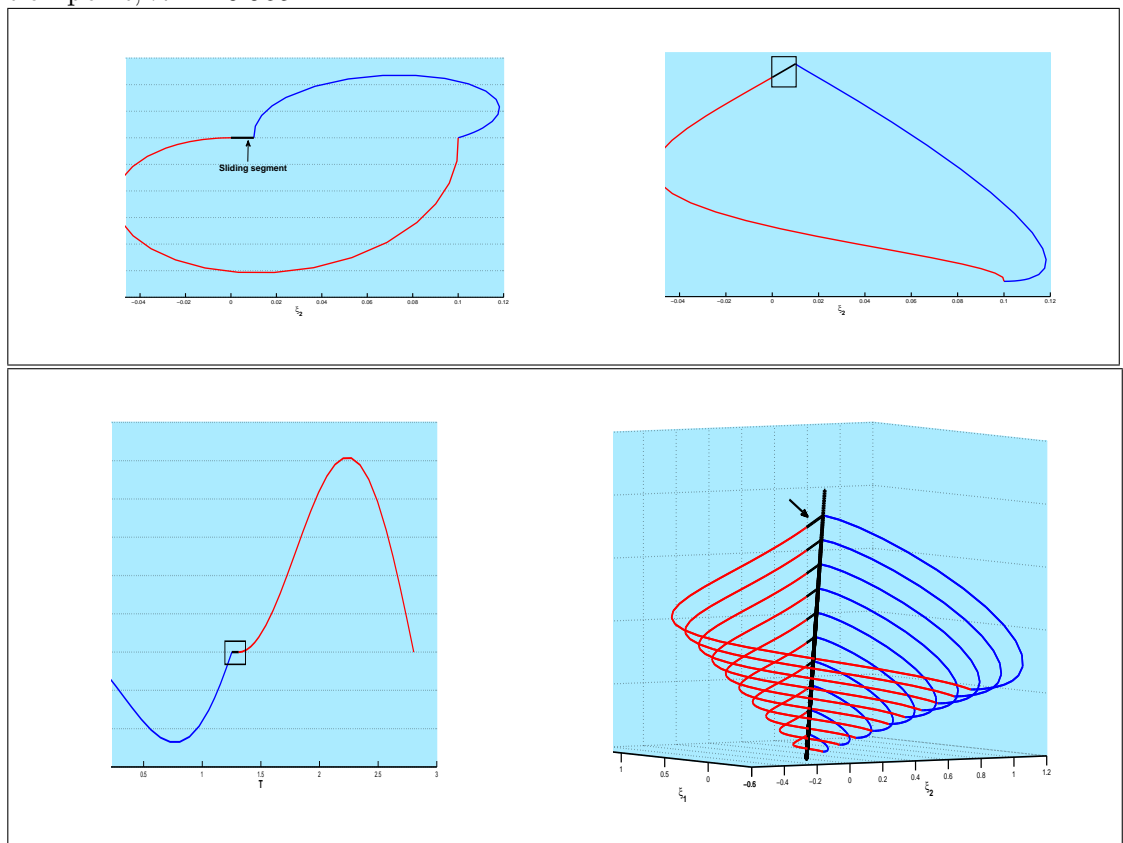


Figure 3.9: Invariant cone and solution components after the crossing-sliding bifurcation point, $\lambda^- = 0.95$.

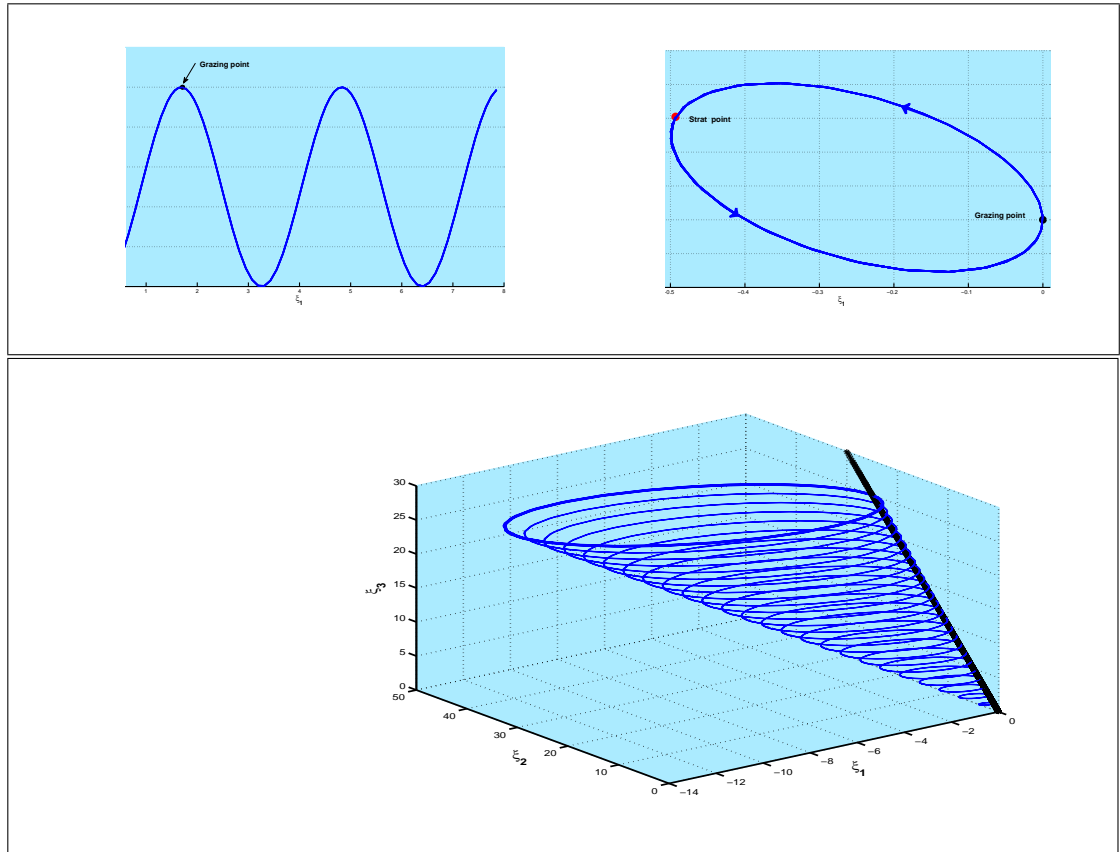


Figure 3.10: One-zonal invariant cone and solution components at grazing-sliding bifurcation point.

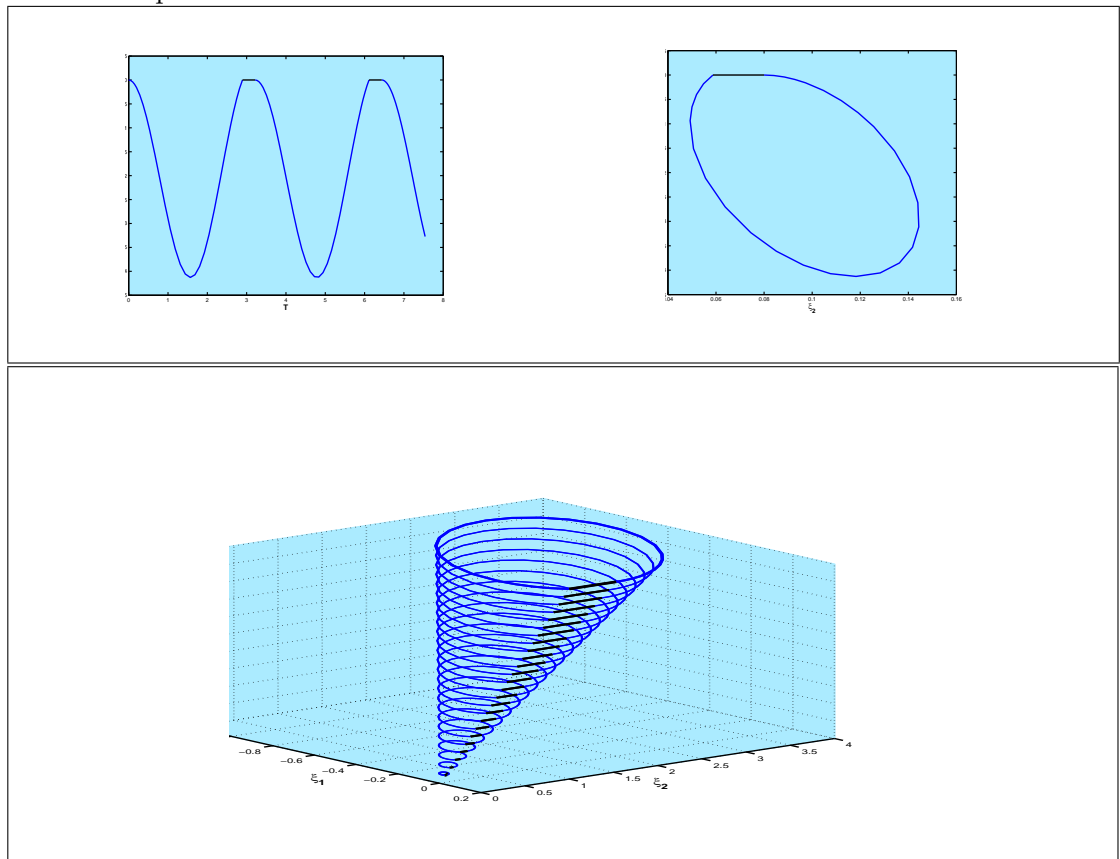


Figure 3.11: One-zonal invariant cone and solution components after grazing-sliding bifurcation point, $\lambda^+ = \mu^+ = \alpha^+ = 0$ and $\omega^+ = 1$

Figure 3.10 shows an invariant cone and related components undergo a grazing bifurcation point. Consequently, for increasing values of the bifurcation parameter λ^- , we see that system (3.16) turns from a no sliding cone into a sliding cone at $\lambda^- = 0$, Figure 3.11. Note that, in the present case, if $\lambda^+ = \mu^+ = \alpha^+ = 0$, the sliding vector (3.27) requires $\omega^+ \neq 0$, and therefore, the explicit solution can be found.

Finally, we present an invariant cone exhibiting *switching-sliding* bifurcation corresponding to the case when the trajectory has a piece of sliding motion in a one-zone orbit. If the system is perturbed, the orbit hits the sliding boundary $\partial\mathcal{M}_+^s$ at the bifurcation point and starting in \mathcal{M}_-^s . For our system, we set the parameter values: $\lambda^+ = \omega^+ = 1$, $\mu^- = \alpha^+ = .1$, $\omega^- = 2$, $\mu^+ = -0.663$, $\lambda^- = 0.35$ and $\xi^0 = (0, 0.5, 0.5)^T$ i.e. $m_0(t_-) = 1$. Hence, an invariant cone passing through the switching-sliding bifurcation point $\xi^* = (0, 0.0003, 0.7129)^T$ is achieved see Figure 3.12. We indeed find that at ξ^* the following conditions hold:

- (i) $h(\xi^*) = 0$, $\nabla h(\xi)|_{\xi^*} \neq 0$,
- (ii) $(n^T(\xi)A^+\xi)|_{\xi^*} \simeq 0$,
- (ii) $(n^T(\xi)A^-A^-\xi)|_{\xi^*} = -0.0719 < 0$.

After the bifurcation event the invariant cone is switching to the \oplus -system and finally slides, see Figure 3.13 where $\mu^+ = -0.1778$, $\lambda^- = 0.45$.

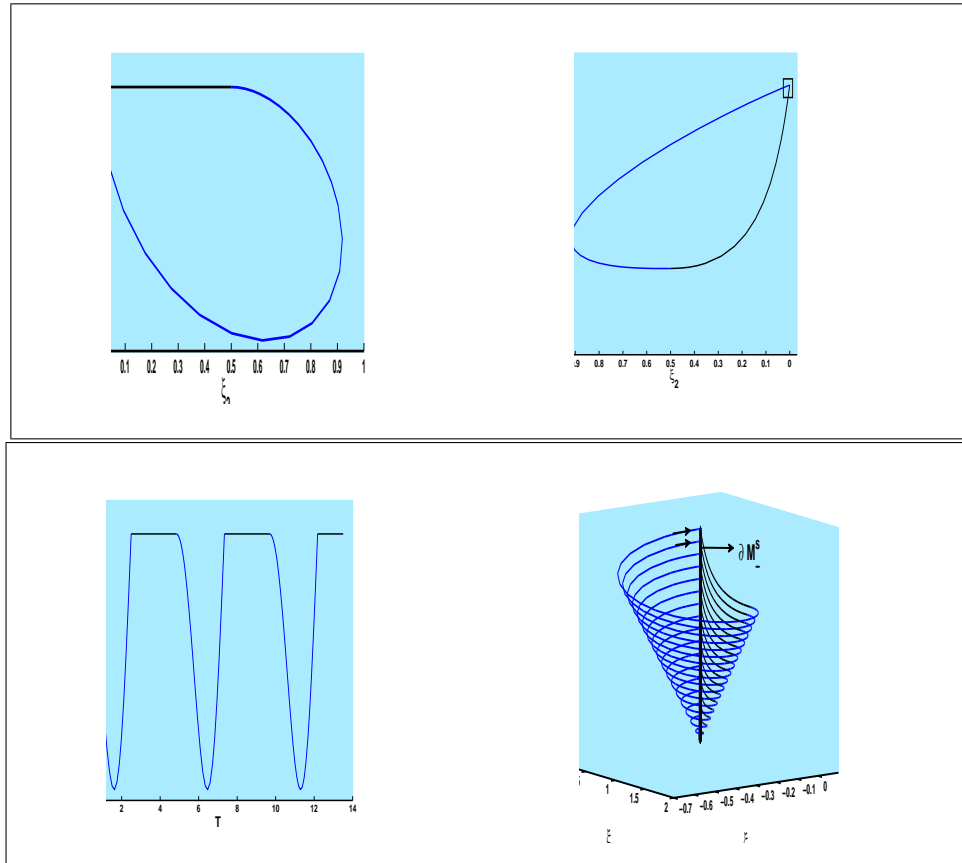


Figure 3.12: Invariant cone and solution components at the switching-sliding bifurcation point.

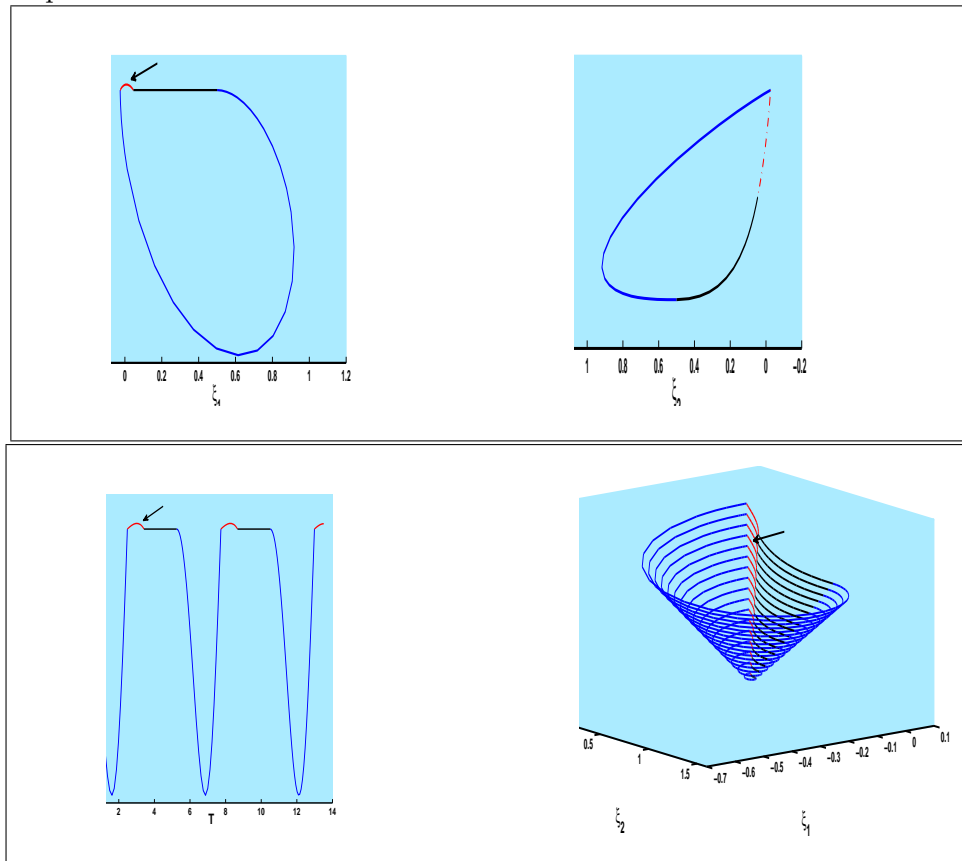


Figure 3.13: Invariant cone and solution components after the switching-sliding bifurcation point

Chapter 4

A 6-dimensional non-smooth brake-system

The aim of our research in this Chapter is to carry out a case study dealing with an automotive brake system under the excitation of a dry friction force, which usually strongly affects the behaviour of the system by introducing non-smoothness to the system. We use an analytical approach to investigate the local behaviour of the phase flow of the smooth system (continuous system) which in some sense converges to the nonsmooth system. We have performed analytical and numerical studies concerning of the cone like manifold for the model, based on the mapping structure and an event function. The normal vector field on the discontinuity surface gives the analytical compatibility criteria for sliding and direct transition of motions. It is shown how the brake system exhibits different types of bifurcation phenomena such as sliding periodic doubling and multiple periodic orbits, in some cases, we observe a sudden transition through discontinuous manifold.

4.1 Introduction

Dry friction is common in many mechanical and structural systems such as squeaking doors, string instruments, squealing railway wheels, brakes and rattling machine tools, valves, hydraulic and pneumatic cylinders, as well as in our everyday life, see [2, 23, 29, 44, 56] for a comprehensive survey. Over the last few decades, this phenomenon plays a key role in the dynamical behaviour of engineering problems because it is a source of self-sustained oscillations termed stick-slip vibrations. Therefore, oscillations induced by dry friction have received a lot of attention from researchers in an attempt to improve the analysis of friction dampers and it is still a very important topic of fundamental research in engineering today.

The theory of dry friction, or Coulomb friction, allows us to estimate the maximum friction forces that can be exerted by dry, contacting surfaces that are stationary relative to each other or the friction forces exerted by the surfaces when they are in relative motion (sliding). Stick-slip may occur at low speeds when the motion of one surface sliding along another becomes discontinuous. So one has to assume slipping between contact surfaces and also situations in which the two surfaces in contact may have zero relative velocity. Dry friction in the system complicates the dynamic analysis of the system due to its nonlinear and nonsmoothness nature. The mathematical modelling induced by dry friction often leads to differential inclusion of Filippov type. Filippov systems, describing systems with friction, can exhibit equilibrium sets, which correspond to the stiction behaviour of those systems and different types of bifurcation phenomena. The discontinuity of these so called slip-stick vibrations makes these systems interesting and a rich bifurcation behaviour under parameter variation is exhibited. Popp and Stelter [56] investigated the motion of four different models including a single-degree-of-freedom nonsmooth oscillator with external excitation that is used to describe the behaviour of stick-slip systems. Beside the well known periodic limit cycle, periodic-doubling and chaotic motions are also possible. In [4] a smoothing procedure is applied to illustrate different bifurcations such as a period-doubling route to stick-slip chaos, stick-slip hyper-chaos as well as quasi-periodic attractors. In [26] a one-dimensional map was introduced for studying bifurcations in a four-dimensional system. Hence, a class of bifurcations leading to the onset of stick-slip motion has been observed. In fact, many investigators [17, 18, 26–28] were working to link standard/nonstandard bifurcations with slip to stick-slip transitions, thus conjecturing that similar abrupt qualitative changes of the system attractors could be observed when slip to stick-slip transitions take place.

As motivation for this work, we consider an automotive brake device as a typical system with dry friction. The noise of the brake systems is an important problem and has received considerable attention from researchers. This attention is due to the economics of the related customer complaints, warranty claims and repairs to disc brake systems, and also due to the difficult nature of the problem. There is a great amount of literature about automotive disc brake, [34, 47, 50, 62, 63, 69] provide a very comprehensive review. More precisely, we consider an automotive brake model which was introduced by Popp [55].

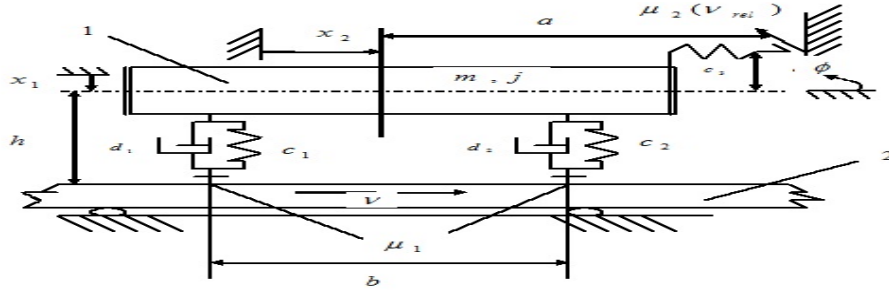


Figure 4.1: Three-degree-of-freedom brake system model

4.2 General description of model

The mechanical system to be investigated, shown schematically in Figure 4.1 is a simple model for a brake system. A brake pad 1 on a rigid frame acts on a brake disc 2. Between brake pad and brake disc there is a relative displacement with constant velocity $v > 0$, thus the frictional forces depend only on the normal force F_n and the kinematic friction μ_2 . The coefficients of the linear viscous dampers are represented by d_1 , d_2 and spring constants are denoted by c_1 , c_2 . Therefore, the brake pad is equipped with three mechanical degrees of freedom:

- Vertical movement x_1 .
- Horizontal movement x_2 .
- Rotation ϕ .

4.2.1 Mathematical model

The equations of motion for the brake model depend on the the relative velocity and are given as in [55]:

$$m\ddot{x}_1 = -(d_1 + d_2)\dot{x}_1 + \frac{b}{2}(d_2 - d_1)\dot{\phi} - (c_1 + c_2)x_1 + \frac{b}{2}(c_2 - c_1)\phi - \mu_2 \text{sgn}(\dot{x}_1 - a\dot{\phi})c_3x_2 \quad (4.1a)$$

$$m\ddot{x}_2 = (d_1 + d_2)\mu_1\dot{x}_1 + \frac{\mu_1 b}{2}(d_1 - d_2)\dot{\phi} + (c_1 + c_2)\mu_1x_1 - c_3x_2 + \frac{\mu_1 b}{2}(c_2 - c_1)\phi, \quad (4.1b)$$

$$\begin{aligned}
\mathbf{j}\ddot{\phi} = & \left(\frac{b}{2}(d_2 - d_1) + (d_1 + d_2)h\mu_1\right)\dot{x}_1 - \left(\frac{b^2}{4}(d_1 + d_2) + \frac{bh\mu_1}{2}(d_2 - d_1)\right)\dot{\phi} \\
& - \left(\frac{b}{2}(c_1 - c_2) - (c_1 + c_2)h\mu_1\right)x_1 + c_3sx_2 - \left(\frac{b^2}{4}(c_1 + c_2) + \frac{bh\mu_1}{2}(c_2 - c_1)\right)\phi \\
& + \mu_2\text{sgn}(\dot{x}_1 - a\dot{\phi})c_3ax_2.
\end{aligned} \tag{4.1c}$$

The covering is connected with a brake holder through a velocity depending friction force $F(\nu_{rel})$ acting on the contact surfaces, where ν_{rel} is the relative velocity between the contacting surfaces. Stick-slip motion is intimately related to the nature of the frictional force and is often attributed to the difference between the static and kinematic coefficients of friction. Initially, this system is modelled by simple Coulomb's law $F(\nu_{rel}) = F_n\mu_2\text{sgn}(\nu_{rel})$, $\nu_{rel} = \dot{x}_1 - a\dot{\phi}$ where μ_2 is the coefficient of kinematic friction, the friction force acts in a direction opposite to the motion. If a more realistic form of the friction force with a typically nonlinear characteristic will be taken, nonlinear terms have to be added. Therefore, a different version of the dynamic friction coefficient $\mu_2(\nu_{rel})$ is given by

$$\mu_2(\nu_{rel}) := \begin{cases} \frac{\alpha_1}{1+\gamma_1|\nu_{rel}|} + \beta_1 + \eta\nu_{rel}^2, & \nu_{rel} > 0 \\ \frac{-\alpha_1}{1+\gamma_1|\nu_{rel}|} - \beta_1 - \eta\nu_{rel}^2, & \nu_{rel} < 0. \end{cases} \tag{4.2}$$

where the kinematic friction is an approximation of the measured friction characteristic, γ_1 is a shape coefficient, α_1 may vary in interval $(0, 1)$. To avoid unrealistic changes of sign in the friction force, η is positive because the dynamic friction force is usually assumed to be increasing for large values of the relative velocity, see [27, 52, 56].

4.2.2 Simplification and reduction

System (4.1) contains six unknown variables $(x_1, \dot{x}_1, x_2, \dot{x}_2, \phi, \dot{\phi})$ and 13 parameters. It is clear, that an exact analytic solutions is unavailable. For that reason we fix some parameters to simplify the problem for a start. To simplify the analysis, we set the parameters $c := c_1 = c_2$ and $d := d_1 = d_2$. Under this assumption the system (4.1) is reduced to the following

$$m\ddot{x}_1 = -2d\dot{x}_1 - 2cx_1 - \mu_2\text{sgn}(\dot{x}_1 - a\dot{\phi})c_3x_2, \tag{4.3a}$$

$$m\ddot{x}_2 = 2d\mu_1\dot{x}_1 + 2c\mu_1x_1 - c_3x_2, \tag{4.3b}$$

$$\mathbf{j}\ddot{\phi} = 2dh\mu_1\dot{x}_1 - \frac{db^2}{2}\dot{\phi} + 2ch\mu_1x_1 + c_3sx_2 - \frac{cb^2}{2}\phi + \mu_2\text{sgn}(\dot{x}_1 - a\dot{\phi})c_3ax_2 \tag{4.3c}$$

Table 4.1: parameters are presented in [55]

Description	Unit	Value	Remark
m	kg	0.3	weighed, rounded
\mathbf{j}	kgm ²	$3 \cdot 10^{-4}$	from m and geometry
a	m	$58 \cdot 10^{-3}$	measured
b	m	$50 \cdot 10^{-3}$	estimated
h	m	$8 \cdot 10^{-3}$	measured
s	m	$1 \cdot 10^{-3}$	measured
μ_1	1	0.4	static friction
μ_2	1	0.15	kinetic friction
c_1, c_2	Nm ⁻¹	$18 \cdot 10^8$	spring coefficients
c_3	Nm ⁻¹	$13 \cdot 10^7$	Spring constant, estimated
d_1, d_2	Nsm ⁻¹	657.3	damping coefficients

which still contains 11 parameters, Table 4.1.

Our approach to such a problem is to view it as a non-smooth system. Hence, using the following transformation and scaling of t described as:

$$z_1 := x_1, \quad z_2 := x_2, \quad z_3 := x_1 - a\phi, \quad z_4 := \mu_1 x_1, \quad z_5 := \dot{x}_2, \quad z_6 := \dot{x}_2 - a\dot{\phi}, \quad t \rightarrow ma\mu_1 t,$$

where $a, m, \mu_1 > 0$, it seems natural to expect that such a scaling should have no effect on solution behaviour of the model system.

To be specific, we rewrite (4.3) by using the above transformation as an equivalent six-dimensional system as follows:

$$\dot{z} = \begin{cases} A^+ z, & h(z) > 0, \\ A^- z, & h(z) < 0, \end{cases} \quad (4.4)$$

with the simple form of the matrices

$$A^\pm = \begin{pmatrix} 0 & 0 & 0 & \mathbf{a} & 0 & 0 \\ 0 & 0 & 0 & 0 & \mathbf{b} & 0 \\ 0 & 0 & 0 & 0 & 0 & \mathbf{b} \\ -\mathbf{c} & \mp\alpha & 0 & -\mathbf{d} & 0 & 0 \\ \mathbf{c} & \gamma & 0 & \mathbf{d} & 0 & 0 \\ \mathbf{e} & \mp\beta & \mathbf{g} & \mathbf{h} & 0 & \mathbf{f} \end{pmatrix}, \quad (4.5)$$

where A^\pm are constant matrices containing various parameters; the system has a unique standard equilibrium at the origin. Note that the elements of the

matrices are constant functions of eleven parameters i.e.

$$\begin{aligned}\mathbf{a} &= ma, \quad \mathbf{b} = ma\mu_1, \quad \mathbf{c} = 2ac\mu_1^2, \\ \alpha &= ac_3\mu_1^2\mu_2, \quad \mathbf{d} = 2ad\mu_1, \quad \gamma = -ac_3\mu_1, \\ \mathbf{e} &= -2ac\mu_1 + \frac{acmb^2\mu_1 - 4a^2cmh\mu_1^2}{2\mathbf{j}}, \\ \beta &= \frac{a^3c_3m\mu_1\mu_2 - a^2c_3sm\mu_1}{\mathbf{j}}, \\ \mathbf{g} &= \frac{-ab^2cm\mu_1}{2\mathbf{j}}, \quad \mathbf{f} = \frac{-ab^2dm\mu_1}{2\mathbf{j}}, \\ \mathbf{h} &= -2ad + \frac{ab^2dm - 4a^2dhm\mu_1}{2\mathbf{j}}.\end{aligned}$$

The general structure is given by the observation that A^+ and A^- only differ in two entrances due to the simple (piecewise constant) form of the friction force. In a typical situation such as in the special case given by Table 4.1, The structure of the eigenvalues is that all eigenvalues of A^\pm are complex which A^- stable (i.e. only eigenvalues with negative real part) and A^+ has two eigenvalues with positive real part and four eigenvalues with negative real part. Hence there is an interplay of damping and excitation or mathematically there is interaction between stable and unstable behaviour.

The discontinuity surface in the phase space is defined as $\mathcal{M} := \{z \in \mathbb{R}^6 | h(z) = z_6 = 0\}$.

4.3 Smooth system

The setting $\alpha = \beta = 0$ in (4.4) leads to $A = A^\pm$, hence a smooth system:

$$\dot{z} = Az, z \in \mathbb{R}^6. \quad (4.6)$$

For small values of α and β the system is of the form $A^\pm(\alpha, \beta) = A + \alpha B^\pm + \beta C^\pm$ as discussed in Chapter 2. In fact this example has stimulated to consider problems of that form. The methods developed there however do not apply in the present situation since the brake system typically exhibits stick-slip transition. Furthermore, due to the fast movement that occurs between the two sides, the brake system will involve multiple crossings with sliding motion. We shall here first concentrate on the situation $\alpha = \beta = 0$. The eigenvalues and eigenvectors of A play a significant role in determining the behavior of linear system (4.6) near an equilibrium point.

Lemma 4.1. *The matrix A has the following complex eigenvalues*

$$\mathbf{l} \pm i \mathbf{m}, \quad \pm i \mathbf{n}, \quad \mathbf{k} \pm i \mathbf{o},$$

with corresponding complex eigenvectors

$$V(j, 1) \mp iV(j, 2), V(j, 3) \mp iV(j, 4), V(j, 5) \mp iV(j, 6), j = 1, \dots, 6,$$

where the eigenvector matrix V is computed as follows :

$$V = \begin{pmatrix} 0 & 0 & 0 & 0 & \frac{\mathbf{ak}}{\mathbf{k}^2 + \mathbf{o}^2} & \frac{\mathbf{ao}}{\mathbf{k}^2 + \mathbf{o}^2} \\ 0 & 0 & 0 & \frac{\mathbf{b}}{\mathbf{n}} & \frac{\mathbf{bkV}(3,5) - \mathbf{boV}(3,6)}{\mathbf{k}^2 + \mathbf{o}^2} & \frac{\mathbf{bkV}(3,6) + \mathbf{boV}(3,5)}{\mathbf{k}^2 + \mathbf{o}^2} \\ \frac{\mathbf{bl}}{\mathbf{l}^2 + \mathbf{m}^2} & \frac{\mathbf{bm}}{\mathbf{l}^2 + \mathbf{m}^2} & 0 & 0 & \frac{\mathbf{bkV}(6,5) - \mathbf{boV}(6,6)}{\mathbf{k}^2 + \mathbf{o}^2} & \frac{\mathbf{bkV}(6,6) + \mathbf{boV}(6,5)}{\mathbf{k}^2 + \mathbf{o}^2} \\ 0 & 0 & 0 & 0 & 1 & 0 \\ 0 & 0 & 1 & 0 & \frac{(\mathbf{ac} + \mathbf{kd})(\mathbf{k}^2 - \mathbf{o}^2 - \gamma\mathbf{b}) + 2\mathbf{kdo}^2}{(\mathbf{k}^2 - \mathbf{o}^2 - \gamma\mathbf{b}) + 4\mathbf{k}^2\mathbf{o}^2} & \frac{2\mathbf{ko}(\mathbf{ac} + \mathbf{kd}) - \mathbf{od}(\mathbf{k}^2 - \mathbf{o}^2 - \gamma\mathbf{b})}{(\mathbf{k}^2 - \mathbf{o}^2 - \gamma\mathbf{b}) + 4\mathbf{k}^2\mathbf{o}^2} \\ 1 & 0 & 0 & 0 & \frac{(\mathbf{hk} - \mathbf{ae})(\mathbf{k}^2 - \mathbf{o}^2 - \mathbf{kf} - \mathbf{bg}) + \mathbf{oh}(2\mathbf{ko} - \mathbf{of})}{(\mathbf{k}^2 - \mathbf{o}^2 - \mathbf{kf} - \mathbf{bg}) + (2\mathbf{ko} - \mathbf{of})^2} & \frac{\mathbf{K}}{(\mathbf{k}^2 - \mathbf{o}^2 - \mathbf{kf} - \mathbf{bg}) + (2\mathbf{ko} - \mathbf{of})^2} \end{pmatrix},$$

$$\mathbf{l} = \frac{\mathbf{f}}{2} = \frac{-ab^2dm\mu_1}{4\mathbf{j}},$$

$$\mathbf{m} = \frac{1}{2}\sqrt{-(\mathbf{f}^2 + 4\mathbf{bg})} = \frac{abm\mu_1}{4\mathbf{j}}\sqrt{8\mathbf{j}c - b^2d^2},$$

$$\mathbf{n} = \sqrt{-\gamma\mathbf{b}} = \sqrt{ma^2c_3\mu_1^2},$$

$$\mathbf{k} = \frac{-\mathbf{d}}{2} = -ad\mu_1,$$

$$\mathbf{o} = \frac{1}{2}\sqrt{4\mathbf{ac} - \mathbf{d}^2} = a\mu_1\sqrt{2mc - d^2},$$

$$\mathbf{K} = (2\mathbf{ko} - \mathbf{of})(\mathbf{hk} - \mathbf{ae}) - \mathbf{oh}(\mathbf{k}^2 - \mathbf{o}^2 - \mathbf{kf} - \mathbf{bg}).$$

The general solution of (4.6) is given by:

$$\begin{aligned} z(t) = & e^{\mathbf{lt}} [a_1 (\cos(\mathbf{mt})V(j, 1) + \sin(\mathbf{mt})V(j, 2)) + a_2 (-\sin(\mathbf{mt})V(j, 1) + \cos(\mathbf{mt})V(j, 2))] \\ & + a_3 (\cos(\mathbf{nt})V(j, 3) + \sin(\mathbf{nt})V(j, 4)) + a_4 (-\sin(\mathbf{nt})V(j, 3) + \cos(\mathbf{nt})V(j, 4)) \\ & + e^{\mathbf{kt}} [a_5 (\cos(\mathbf{ot})V(j, 5) + \sin(\mathbf{ot})V(j, 6)) + a_6 (-\sin(\mathbf{ot})V(j, 5) + \cos(\mathbf{ot})V(j, 6))], \end{aligned} \quad (4.7)$$

the integration constants can be computed from the initial value $z(0) = V\vec{a}$, where $\vec{a} = [a_1, a_2, a_3, a_4, a_5, a_6]^T$.

The following result establishes the existence of periodic orbits.

Theorem 4.1.

The linear system (4.6) has a stable periodic orbit in the (z_2, z_5) -plane with period $T = \frac{2\pi}{\mathbf{n}}$. In addition to this periodic orbit, there are two other periodic orbits if $d = 0$, namely, one of them in the (z_3, z_6) -plane with period $T = \frac{2\pi}{\mathbf{m}}$ and another in the plane spanned by the the last two columns of V .

With regard to an investigation of the perturbed system (4.4) we consider the Poincaré map of (4.6). Since the general solution of the linear system is known

explicitly the Poincaré map is known. It is of the following structure:

$$P(z) = \begin{pmatrix} p_{11} & 0 & 0 & p_{14} & 0 \\ p_{21} & p_{22} & 0 & p_{24} & p_{25} \\ p_{31} & 0 & p_{33} & p_{34} & p_{35} \\ p_{41} & 0 & 0 & p_{44} & 0 \\ p_{51} & p_{52} & 0 & p_{54} & p_{55} \end{pmatrix} \begin{pmatrix} z_1 \\ z_2 \\ z_3 \\ z_4 \\ z_5 \end{pmatrix}, \quad (4.8)$$

the elements used in P are given in Appendix A.

The eigenvalues of P are computed as (where t is taken as a parameter):

- $\bar{\mu}_1 = e^{lt} \left(\cos(\mathbf{m}t) - \frac{1}{\mathbf{m}} \sin(\mathbf{m}t) \right)$,
- $\bar{\mu}_{2,3} = \cos(\mathbf{n}t) \pm i \sin(\mathbf{n}t)$,
- $\bar{\mu}_{4,5} = e^{\mathbf{k}t} \left[\cos(\mathbf{o}t) \pm i \frac{1}{\mathbf{o}} \left(\sin(\mathbf{o}t) (2\mathbf{k}^2 \sin(\mathbf{o}t) - 2\mathbf{k}\mathbf{o} \cos(\mathbf{o}t) + \mathbf{o}^2 \sin(\mathbf{o}t)) \right)^{1/2} \right]$.

A periodic orbit corresponds to a fixed point of P , hence an eigenvalue equal to one. There are two possibilities; they depend on the presence of damping effects:

- (i) If $d = 0$ (the case without any damping, hence $\mathbf{l} = \mathbf{k} = 0$). If $\mu_1 = 1$ then $T = \frac{2\pi}{\mathbf{m}}$, and if $\mu_2 = \mu_3 = 1$ then $T = \frac{2\pi}{\mathbf{o}}$ and if $\mu_4 = \mu_5 = 1$ then $T = \frac{2\pi}{\mathbf{n}}$. Hence, the linear system (4.6) has 3 periodic orbits corresponding to those fixed points of P .
- (ii) $d > 0$ (presence of damping). If $\mu_4 = \mu_5 = 1$ then $T = \frac{2\pi}{\mathbf{n}}$, therefore, the linear system (4.6) has a periodic orbit in the (z_2, z_5) -plane.

For a specific situation we fix all parameters in Table 4.1 and consider the case with damping. The real parts of the eigenvalues of A are always negative with $|\mathbf{l}| > 9.53$, $|\mathbf{k}| > 15.23$. Consequently, the two parts of the general solution (4.7) converge by a factor of e^{lt} and $e^{\mathbf{k}t}$ very quickly to 0 for increasing t , Figure 4.2. Furthermore, the periodic orbit is generated by a fixed point of P in the (z_2, z_5) -plane at $T = \frac{2\pi}{\mathbf{n}}$. Since all eigenvalues of A have non-positive real part, the equilibrium point 0 is stable.

These two cases may indicate that in our smooth system, it is possible to have a transition from one type of motion to the other one via the effect of friction damping d . This effect of damping clearly shows when we consider the nonsmooth system.

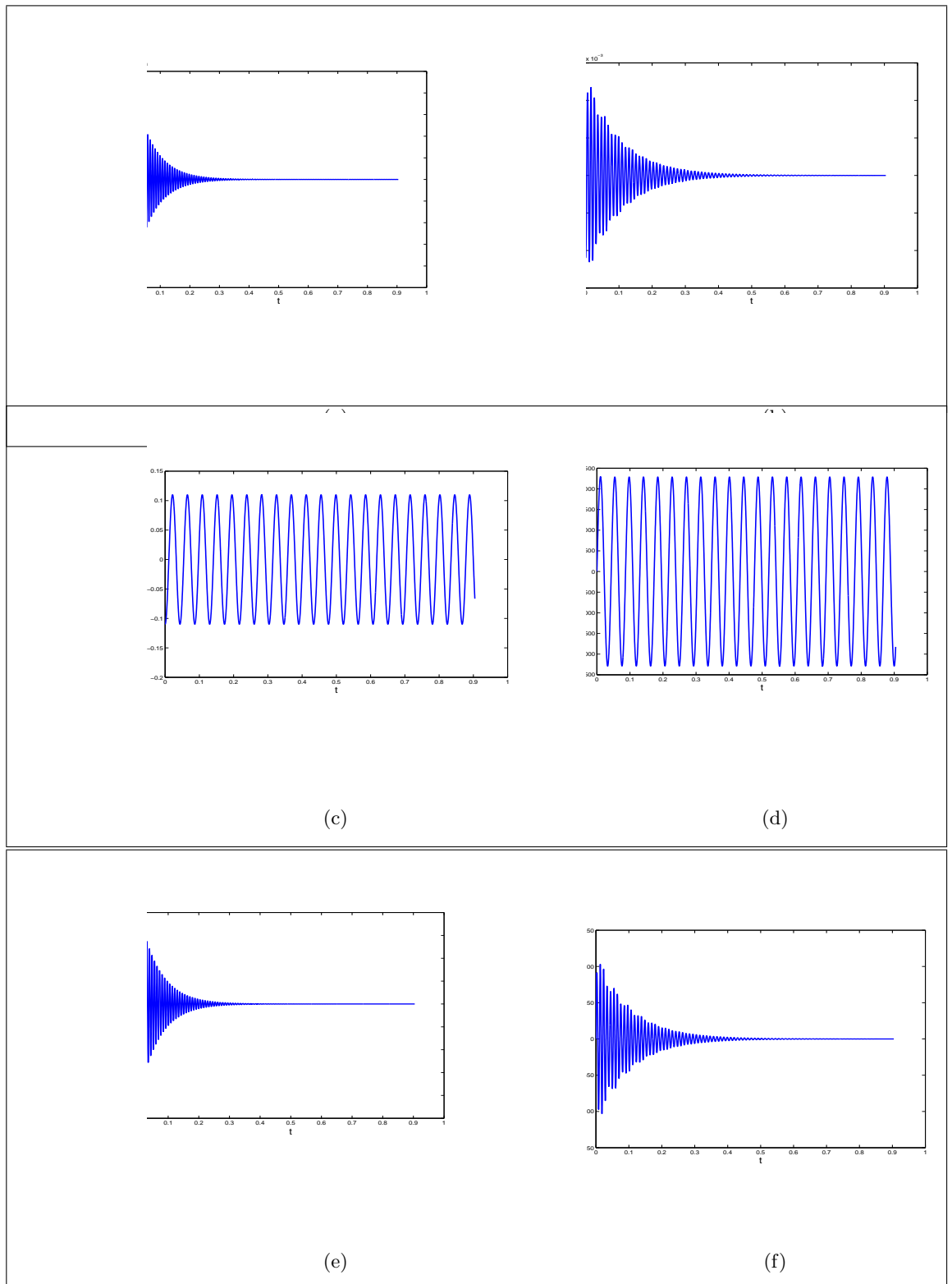


Figure 4.2: Solution components behaviour with presence of damping and time increases, there is only one periodic orbit in (z_2, z_5) -plane for the coefficients as in Table 4.1

4.4 Non-smooth model

It is clear that a lack of smoothness for the model is due to the presence of (α, β) . In PWLS, it is useful to know the direction of flow of the vector field as well as when the trajectory reaches \mathcal{M} . We will discuss the vector-field on \mathcal{M} in two main cases, namely direct crossing through \mathcal{M} or sliding motion on \mathcal{M} where the sliding surface is particularly important with regard due to the friction coefficient.

4.4.1 Detecting crossing and sliding regions

In this section we demonstrate the existence of a crossing and sliding mode from the point of view of a Filippov system. Let $\Upsilon(z) = \mathbf{e}z_1 + \mathbf{g}z_3 + \mathbf{h}z_4$. The direct crossing in \mathcal{M}^c for $z_6 = 0$ occurs if both quantities $[n^T(z)f^\pm(z)]$ have the same sign. Therefore, the crossing region $\mathcal{M}^c := \{z \in \mathcal{M} | \Upsilon(z)^2 - (\beta z_2)^2 > 0\}$ is divided into two main region regions, namely

$$\begin{aligned}\mathcal{M}_+^c &:= \{z \in \mathcal{M}^c | \Upsilon(z) > \beta z_2\}, \\ \mathcal{M}_-^c &:= \{z \in \mathcal{M}^c | \Upsilon(z) < \beta z_2\}.\end{aligned}$$

In a similar way, we can define the sliding mode region as $\mathcal{M}^s := \{z \in \mathcal{M} | \Upsilon(z)^2 - (\beta z_2)^2 \leq 0\}$ which is divided into two main region regions, namely

$$\begin{aligned}\mathcal{M}_-^s &:= \{z \in \mathcal{M}^s | \Upsilon(z) < \beta z_2\}, \\ \mathcal{M}_+^s &:= \{z \in \mathcal{M}^s | \Upsilon(z) > \beta z_2\},\end{aligned}$$

where we use the notation \mathcal{M}_-^s to represent the attractive sliding motion and \mathcal{M}_+^s to represent repulsive sliding motion.

It is well-known that the solutions of (4.4) connect standard solutions in \mathcal{M}_\pm^c and sliding solutions on \mathcal{M}^s .

Sliding trajectories are solutions of

$$\dot{z} = F_s(z), z \in \mathcal{M}^s$$

where $F_s(z) = q(z)f^+(z) + (1 - q(z))f^-(z)$ and $q(z) = \frac{1}{2} + \frac{\Upsilon(z)}{2\beta z_2}$.

Therefore, we obtain an explicit definition of the dynamics along \mathcal{M}^s , namely

$$\dot{z} = \begin{pmatrix} \mathbf{a}z_4 \\ \mathbf{b}z_5 \\ 0 \\ -(\mathbf{c} + \frac{\alpha\mathbf{e}}{\beta})z_1 - \frac{\alpha\mathbf{g}}{\beta}z_3 - (\mathbf{d} + \frac{\alpha\mathbf{h}}{\beta})z_4 \\ \mathbf{c}z_1 + \gamma z_2 + \mathbf{d}z_4 \end{pmatrix}.$$

Additionally, the dynamics along the boundary of the sliding regions is expressed as:

* $z \in \partial\mathcal{M}_-^s$ implies $q = 0$, $F_s(z) = A^-z$, $z_6 = 0$ and $z_2 = -\frac{\Upsilon(z)}{\beta}$, i.e.,

$$\dot{z} = \begin{pmatrix} \mathbf{a}z_4 \\ \mathbf{b}z_5 \\ 0 \\ -\mathbf{c}z_1 - \frac{\alpha\Upsilon(z)}{\beta} - \mathbf{d}z_4 \\ \mathbf{c}z_1 - \frac{\gamma\Upsilon(z)}{\beta} + \mathbf{d}z_4 \end{pmatrix}.$$

** $z \in \partial\mathcal{M}_+^s$ implies $q = 1$, $F_s(z) = A^+z$, $z_6 = 0$ and $z_2 = \frac{\Upsilon(z)}{\beta}$, i.e.,

$$\dot{z} = \begin{pmatrix} \mathbf{a}z_4 \\ \mathbf{b}z_5 \\ 0 \\ -\mathbf{c}z_1 - \frac{\alpha\Upsilon(z)}{\beta} - \mathbf{d}z_4 \\ \mathbf{c}z_1 + \frac{\gamma\Upsilon(z)}{\beta} + \mathbf{d}z_4 \end{pmatrix}.$$

Remark 4.1. *If $\beta = 0$ then there is only a direct transition of the flow of (4.4) through \mathcal{M} in forward time due to $\mathcal{M}^s = \{\phi\}$, hence β is a key parameter determining the sliding motion of \mathcal{M} .*

If $z \in \mathcal{M}_-^s$ then the systems trajectory enters the attractive sliding region, but this does not assert that it stays there. The trajectory may leave the sliding mode due to the fact that the equilibrium point of F_s can be unstable or stable with a small domain of attraction (the sliding surface \mathcal{M}^s can change from being attractive to be repulsive), [25]. However, if this happens, the trajectory may eventually return to \mathcal{M}_-^s .

4.4.2 Construction of Poincaré maps

Our results are based on the existence of invariant cones for the brake system (4.3). In order to be able to discuss the existence of invariant cones and their stability of PWLS (4.4) where $\alpha \neq 0$ and $\beta \neq 0$, we construct the Poincaré map. Without loss of generality, we assume $z \in \mathcal{M}_-^c$ and that the trajectory given by $\varphi^-(t_-(z), z)$ crosses \mathcal{M} transversally (i.e., $\mathcal{M} = \mathcal{M}_-^c$) or slides on it (i.e., $\mathcal{M} = \mathcal{M}_-^s$) at the time $t_-(z)$. Hence, we can find the map

$$\begin{aligned} P_-(z) &: \mathcal{M}_-^c \rightarrow \mathcal{M}, \\ z &\rightarrow \varphi^-(t_-(z), z) = P_-(z) \end{aligned}$$

where $\varphi^-(t_-(z), z) = e^{t_-(z)A^-}z$ and $t_-(z)$ is computed as

$$t_-(z) = \inf\{t > 0 \mid e_6^T e^{t(\xi)A^-} z = 0\}. \quad (4.9)$$

In a similar way, for all $z \in \mathcal{M}_+^c$, the trajectory given by $\varphi^+(t_+(z), z)$ crosses \mathcal{M} transversally or slides on it. Then, we get

$$\begin{aligned} P_+(z) &: \mathcal{M}_+^c \rightarrow \mathcal{M}, \\ z &\rightarrow \varphi^+(t_+(z), z) = P_+(z) \end{aligned}$$

where $\varphi^+(t_+(z), z) = e^{t_+(z)A^+} z$ and $t_+(z)$ is computed as

$$t_+(z) = \inf\{t > 0 \mid e_6^T e^{t(\xi)A^+} z = 0\}. \quad (4.10)$$

Fortunately, one can observe that the sliding vector field is linear due to our simple choice of friction force. Hence, for an initial value $z \in \mathcal{M}_-^s$ the trajectory is given by $\varphi^s(t_s(z), z) = e^{t_s(z)A_s} z$ where t_s is the time spent during sliding before it reaches one point of $\partial\mathcal{M}_\pm^s$ and A_s is given as $A_s = \frac{\partial}{\partial z} F_s$. Moreover, we can define the map

$$\begin{aligned} P_s(z) &: \mathcal{M}_-^s \rightarrow \partial\mathcal{M}_-^s, \\ z &\rightarrow \varphi^s(t_s(z), z) = P^s(z). \end{aligned}$$

The map P_s satisfies Lemma 2.3 (replace P_- by P_s) and t_s is computed via system (3.14).

In effect, this procedure is similar to that which has been described in detail in the previous two chapters. The existence of exactly one positive eigenvalue $\bar{\mu}$ of P that is given as the composition of partial Poincaré maps leads to existence of invariant cone. The remaining eigenvalues determine the dynamics on the cone.

4.5 Case $\alpha = 0, \beta \neq 0$

In this case the non-smoothness depends only on one parameter β , but we will show that the dynamics of the system can be quite different from that in the smooth system.

Lemma 4.2. *The matrices A^\pm share identical eigenvalues of A , but their eigenvectors differ by V_β such that*

$$V^\pm = V \mp V_\beta, \quad (4.11)$$

where

$$V_\beta = \beta \begin{pmatrix} 0 & 0 & 0 & 0 & 0 & 0 \\ 0 & 0 & 0 & 0 & 0 & 0 \\ 0 & 0 & \frac{-\mathbf{b}^2 \mathbf{f}}{(\mathbf{n}^2 + \mathbf{b}\mathbf{g})^2 + (\mathbf{n}\mathbf{f})^2} & \frac{\mathbf{b}^2(\mathbf{n}^2 + \mathbf{b}\mathbf{g})}{(\mathbf{n}^2 + \mathbf{b}\mathbf{g})^2 + (\mathbf{n}\mathbf{f})^2} & 0 & 0 \\ 0 & 0 & 0 & 0 & 0 & 0 \\ 0 & 0 & 0 & 0 & 0 & 0 \\ 0 & 0 & \frac{\mathbf{b}(\mathbf{n}^2 + \mathbf{b}\mathbf{g})}{(\mathbf{n}^2 + \mathbf{b}\mathbf{g})^2 + (\mathbf{n}\mathbf{f})^2} & \frac{\mathbf{b}\mathbf{n}\mathbf{f}}{(\mathbf{n}^2 + \mathbf{b}\mathbf{g})^2 + (\mathbf{n}\mathbf{f})^2} & 0 & 0 \end{pmatrix}, \quad (4.12)$$

Hence the general solution of $\dot{z} = A^\pm z$, $z \in \mathcal{M}_\pm^c$ can be obtained by replacing $V = V^\pm$ in (4.7).

Lemma 4.3. *The Poincaré section is replaced by the discontinuity surface \mathcal{M} . By using Lemma 4.2 we obtain the following structure for the Poincaré map for the \ominus -system (the elements a_{ij} are given in Appendix B):*

$$P_-(z) = \begin{pmatrix} a_{11} & 0 & 0 & a_{14} & 0 \\ a_{21} & a_{22} & 0 & a_{24} & a_{25} \\ a_{31} & 0 & a_{33} & a_{34} & a_{35} \\ a_{41} & 0 & 0 & a_{44} & 0 \\ a_{51} & a_{52} & 0 & a_{54} & a_{55} \end{pmatrix} \begin{pmatrix} z_1 \\ z_2 \\ z_3 \\ z_4 \\ z_5 \end{pmatrix}. \quad (4.13)$$

The return time $t_-(z)$ is defined as the smallest positive root of

$$a_{61}z_1 + a_{62}z_2 + a_{63}z_3 + a_{64}z_4 + a_{65}z_5 = 0. \quad (4.14)$$

Furthermore, the Poincaré map P_+ and the return time $t_+(z)$ for the \oplus -system can be obtained by replacing $\beta = -\beta$ in P_- and equation (4.14), respectively.

To obtain a preliminary illustration of the behaviour without sliding motion we present the following theorem.

Theorem 4.2. *We assume that no sliding motion can take place on \mathcal{M} . Without loss of generality, the first return Poincaré map is a composition of P_- and P_+ defined by $P(z) = P_+P_-(z)$. Then the nonsmooth system (4.4) has at least 3 invariant cones in the case without any damping.*

Proof:

It can be shown by direct computation that the Poincaré map $P = P_+P_-(z)$ has five eigenvalues explicitly written when $d = 0$ as:

$$\bar{\mu}_1 = \cos(\mathbf{m}t_-) \cos(\mathbf{m}t_-),$$

$$\bar{\mu}_{2,3} = \cos(\mathbf{n}t_+) \cos(\mathbf{n}t_-) - \sin(\mathbf{n}t_+) \sin(\mathbf{n}t_-) \pm i(\cos(\mathbf{n}t_+) \sin(\mathbf{n}t_-) + \cos(\mathbf{n}t_-) \sin(\mathbf{n}t_+)).$$

$$\bar{\mu}_{4,5} = \cos(\mathbf{o}t_+) \cos(\mathbf{o}t_-) - \sin(\mathbf{o}t_+) \sin(\mathbf{o}t_-) \pm i(\cos(\mathbf{o}t_+) \sin(\mathbf{o}t_-) + \cos(\mathbf{o}t_-) \sin(\mathbf{o}t_+)).$$

In order to have an invariant cone consisting of periodic orbits one of the above eigenvalues have to equal one. We distinguish 3 cases:

- (i) $\cos(\mathbf{m}t_-)\cos(\mathbf{m}t_+) = 1$. Then $t_{\pm} = \frac{\pi}{\mathbf{m}}$ and there is a degenerate (flat) cone within the (z_3, z_6) -plane.
- (ii) $(\cos(\mathbf{n}t_+)\cos(\mathbf{n}t_-) - \sin(\mathbf{n}t_+)\sin(\mathbf{n}t_-)) = 1$ and $(\cos(\mathbf{n}t_+)\sin(\mathbf{n}t_-) + \cos(\mathbf{n}t_-)\sin(\mathbf{n}t_+)) = 0$. Then $t_{\pm} = \frac{\pi}{\mathbf{n}}$ and there is a flat cone within the (z_2, z_5) -plane.
- (iii) $(\cos(\mathbf{o}t_+)\cos(\mathbf{o}t_-) - \sin(\mathbf{o}t_+)\sin(\mathbf{o}t_-)) = 1$ and $(\cos(\mathbf{o}t_+)\sin(\mathbf{o}t_-) + \cos(\mathbf{o}t_-)\sin(\mathbf{o}t_+)) = 0$. Then $t_{\pm} = \frac{\pi}{\mathbf{m}}$ and there is a flat cone within the (z_1, z_4) -plane.

The remaining eigenvalues of P for each case of (i)-(iii) determine the stability of the corresponding periodic orbit.

In general, the trajectory may intersect the manifold with zero time (direct crossing) or with non-zero time (sliding motion) \mathbf{n} -times before closing on itself. We describe the solution of invariant cones involving several crossing of the manifold in:

Lemma 4.4. *Consider a generalized Poincaré mapping structure for a periodic motion without sliding motion as:*

$$P^{\mathbf{n}}(z) = (P_i \circ P_j)^{\mathbf{n}}(z), \quad i, j \in \{+, -\}, i \neq j, n = 2, \dots$$

$$P^{\mathbf{n}}(z) = z.$$

or with sliding motion

$$P^{\mathbf{n}}(z) = (P_i \circ P_k \circ P_j)^{\mathbf{n}}(z), \quad i, j, k \in \{+, -, s\}, i \neq j \neq k, \mathbf{n} = 2, \dots$$

$$P^{\mathbf{n}}(z) = z.$$

Then, the corresponding invariant cone consists of periodic orbits without or with sliding motion, respectively.

Stick-slip occurs if the trajectory enters and leaves frequently the sliding surface \mathcal{M}_-^s . In this case, the equilibrium point of F_s can be unstable or stable with a small region of attraction, hence the trajectory may leave \mathcal{M}_-^s to enter \mathcal{M}^c due to the loss of attractivity of \mathcal{M}^s . This means that, when the relative velocity increases and attends its maximum value (slip state). Then, the manifold becomes attractive, and the trajectory returns to \mathcal{M}_-^s and then decreases to the minimum value of relative velocity (stick state). This is repeated continuously. For instance see Figure 4.7

4.6 Simulation results

In this section, we present numerical results of PWS (4.4) for different parameters. The numerical results presented show the occurrence of different types of motion.

It is noteworthy that for numerical simulation of PWS it is essential to record the transitions between different vector fields through the manifold \mathcal{M} . Such transitions are called events and are triggered by zero crossings of scalar valued event functions. Hence, it is possible to locate numerically where the discontinuity occurs and numerical solution for t_{\pm} and t_s are achieved with high accuracy. Further, the conditions of regions \mathcal{M}_{\pm}^c and \mathcal{M}_{\pm}^s providing the location of nonsmooth events corresponding to different vector fields are computed as accurately as possible. The ODE solvers of MATLAB contain routines for detecting zero crossings of event functions with high accuracy. We use a fourth-order Runge-Kutta algorithm for dissipative systems in order to perform simulations for our system.

Now, in order to present the influence of friction and of the parameters values, we restrict our-self to the case *without sliding* motion. For $\alpha = 0$, Theorem 4.2 provided that there is at least one fixed point of P in the (z_2, z_5) -plane, with $t_{\pm} = \frac{\pi}{\mathbf{n}}$. For $\alpha \neq 0$, small we expect that the system exhibits a rich dynamics when simulation due to deformation of eigenvalues with varying of parameters.

For instance, we fix all parameters in Table 4.1 and choose the kinetic coefficient smaller than the static one (i.e., $\mu_2 \ll \mu_1$). The main reason for choosing μ_2 is that this choice rapidly restores the spring to a more relaxed length. A change of this parameter changes the control parameters α , β (i.e. the friction force). The parameter β in turn causes the existence of sliding and crossing regions.

In Figure 4.3(c) an invariant cone consisting of periodic orbits without sliding motion is shown. Further, there is a sudden transition from \mathcal{M}_{+}^c to \mathcal{M}_{-}^c due to the strong effect of the spring constant c . Figure 4.3(a) the fixed point can be computed by $P(z) = P^{+}P^{-}P^{+}(z) = z$ without damping effect $d = 0$. In Figure 4.3(d), we shall take the same parameters values, but we choose our starting point in the attractive sliding motion $\xi \in \mathcal{M}_{-}^s$, we show that there is sudden transition after segment of sliding from negative to positive side of z_6 . It is obvious that a significant amount of time is spent outside the discontinuity surface, since the sliding motion disappears in the system with forward time.

Moreover, if we move only the spring parameter c to the value indicated in Table 4.1 we show that the system has 4-periodic orbit without sudden transition between \mathcal{M}_{\pm}^c and no sliding motion, Figure 4.4.

If we consider $\alpha = 0$ and $\beta \neq 0$ (all other parameters fixed) there is quite a difference in motion between the smooth system and PWS (case 4.5). The smooth system (4.6) has flat cone with periodic orbit in the (z_2, z_5) -plane, but in PWS this cone is developed to govern other aspects of motion such as invariant cone consisting of sliding segment and a periodic orbit involving multiple crossing due to the fast movement that occurs between the two sides. For instance, an invariant cone involving an double-periodic orbit with sliding segment can be shown in Figure 4.5 with $d = 467.9$. However, it is interesting to notice that the numerical evidence shows that there is a transition from double-periodic to a 3-periodic at $d = 468.9$ as shown in Figure 4.6. It indicates that damping plays an important role in periodic stick-slip phenomena

Finally, it should be pointed out that in the general situation such as $\alpha \neq 0, \beta \neq 0$, and for special choice that kinetic friction equal to static $\mu_2 = \mu_1 = 0.4$, the complex behavior in the brake system is revealed to multiple sliding periodic. Within this multiple periodic is governed by an attractor of 4-periodic orbits involving sliding. The importance of this stick-slip phenomena is revealed in Figure 4.7 after some transition we show the small slip length.

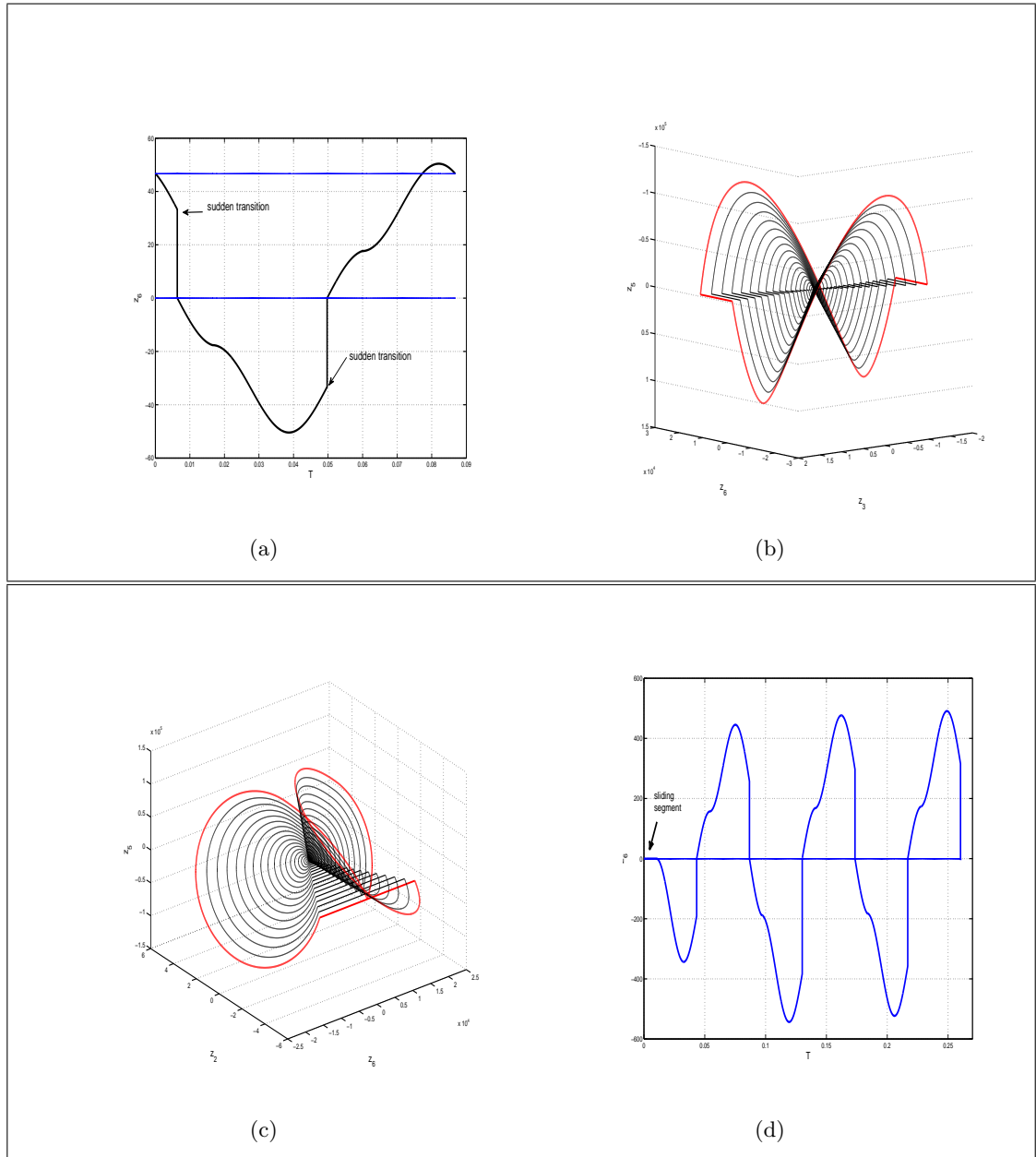


Figure 4.3: Invariant cone and periodic time series with fix all parameters in Table 4.1 and $\mu_2 = 0.00014$ is quite small, $c = 1.8E7$, $d = 0$ where (a)-(c) without sliding $z \in \mathcal{M}_+^c$, (d) starting point $z \in \mathcal{M}_-^s$

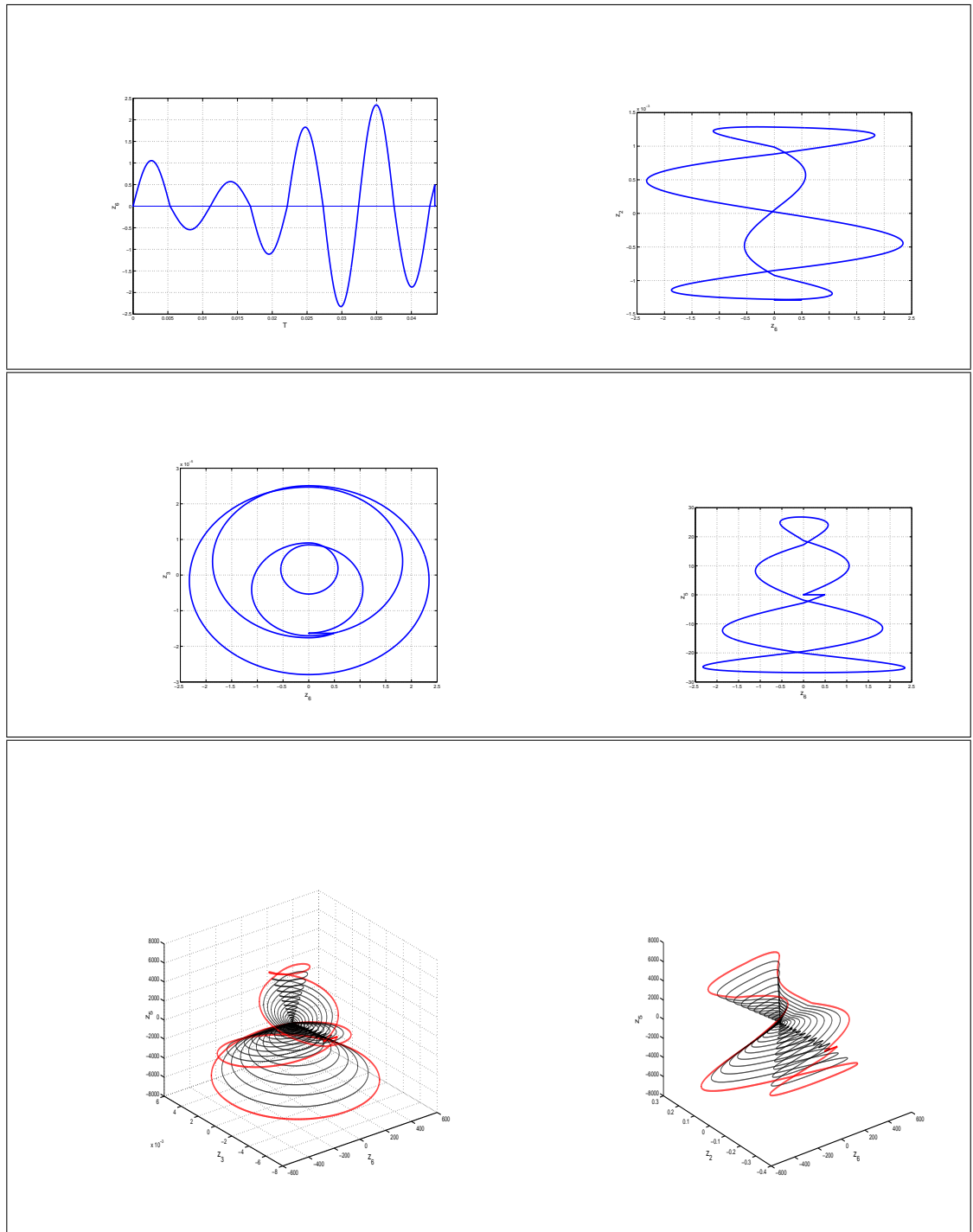


Figure 4.4: Invariant cones and solution components, existence of 4-periodic orbit due to spring parameter without sliding motion.

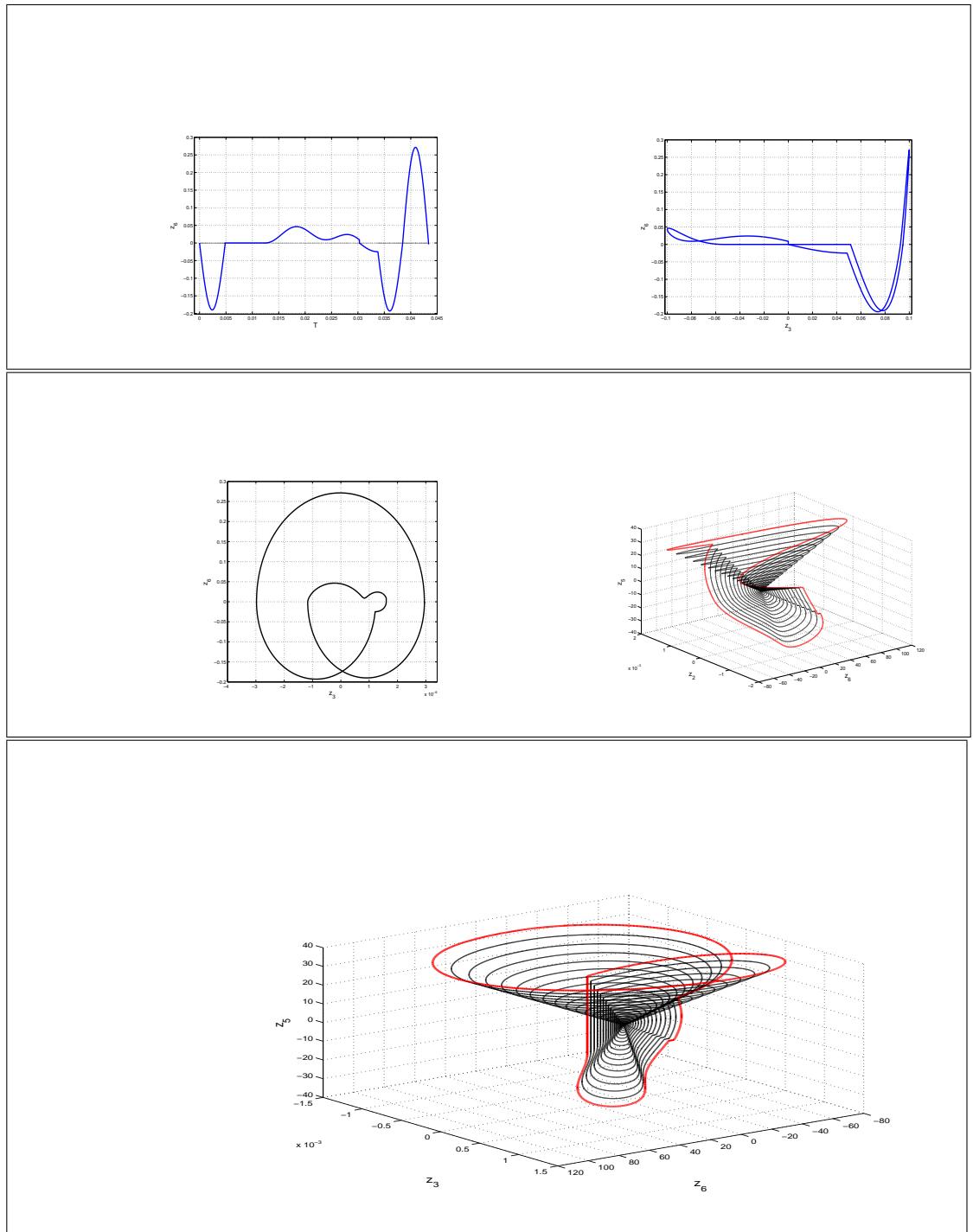


Figure 4.5: Invariant cones and solution components, existence of double-sliding periodic orbit when $d = 467.9$.

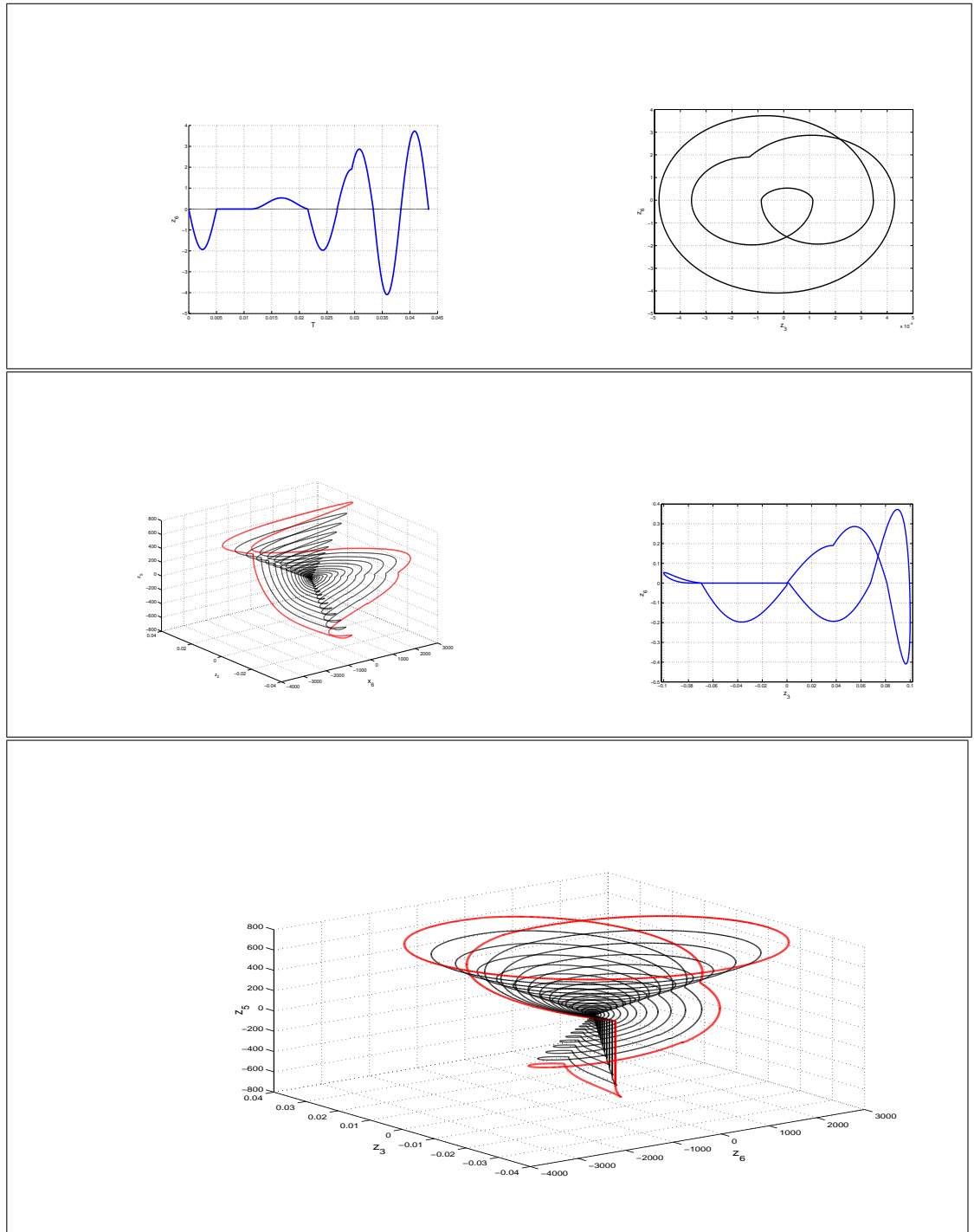


Figure 4.6: Invariant cones and solution components, existence of 3-sliding periodic orbit when $d = 468.9$.

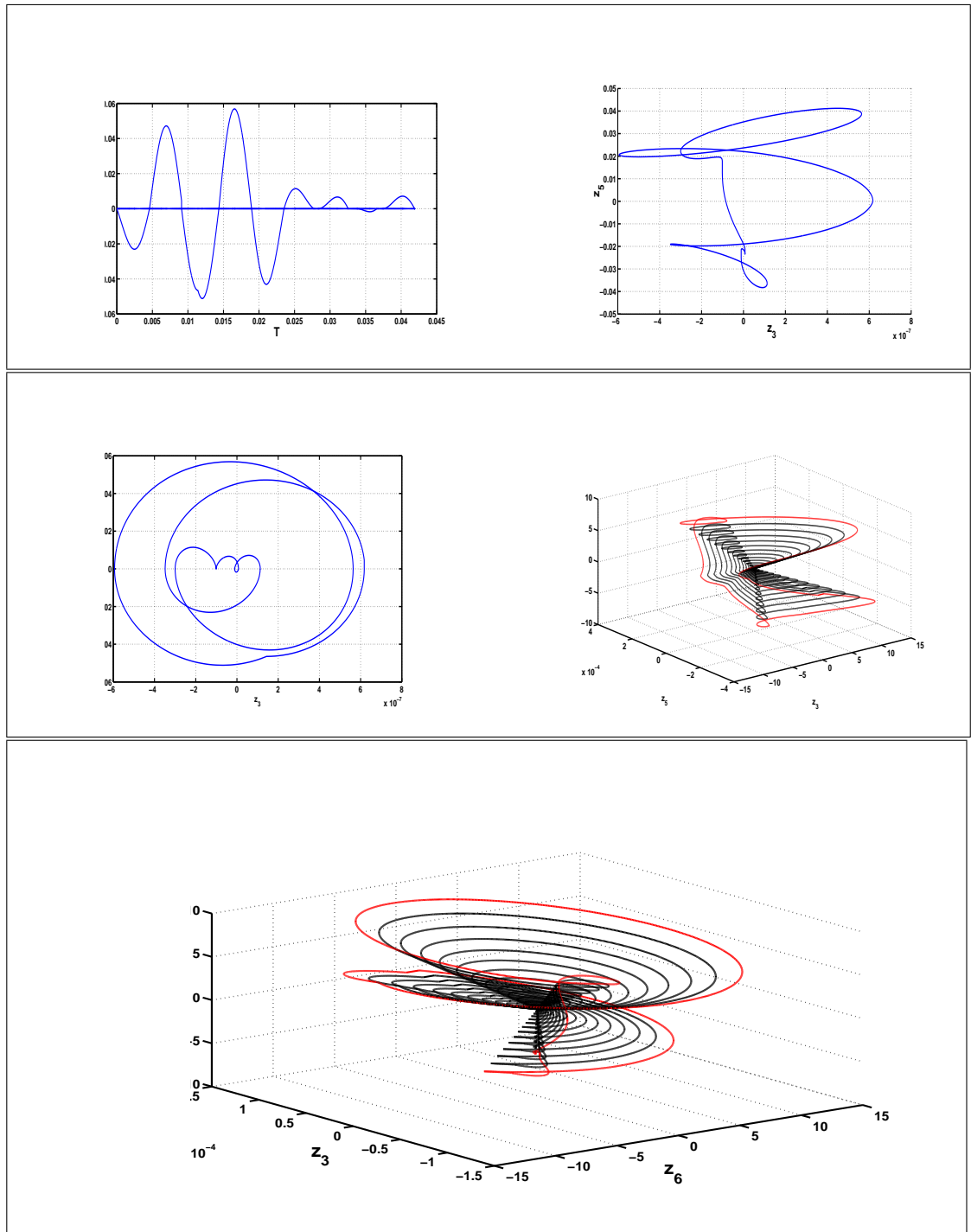


Figure 4.7: Invariant cones and solution components, existence of 4-sliding periodic orbit when $\alpha \neq 0, \beta \neq 0$.

Chapter 5

Invariant manifold for PWS

The aim of this chapter is to obtain a similar reduction to lower dimensional system for PWS as has been achieved for smooth system via the center manifold approach. In PWLS the invariant sets are given as invariant cones which have been discussed in previous chapters. For nonlinear perturbations of PWLS the invariant sets are deformations of those cones. The generation of invariant manifolds and a bifurcation analysis establishing periodic orbits are demonstrated. Hence, we present a class of nonlinear PWS having a cone-like invariant "manifold" carrying the essential dynamics of the full system. We explain the theoretical results by numerical examples, the analytical results included in the chapter confirm accurately the observed behavior.

5.1 Introduction

It is well known that the asymptotic behavior of high dimensional smooth systems can be described by corresponding systems of lower dimensional via center manifold analysis. In the context of bifurcations of equilibria and stability analysis, center manifold theory is a well established and mathematically proven procedure to reduce the dimension of dynamical systems. The lower dimensional systems are further simplified by normal form theory, allowing for a mainly analytical and numerical analysis of the bifurcation. This technique is crucial for understanding complex dynamical systems of high dimension. However in PWS a lack of smoothness does not admit a dimensional reduction surface. Hence a natural question arises: *How it is possible to reduce PWS to a lower-dimensional invariant manifold?* For PWLS the notion of an invariant cone appeared generalizing the focus to an object on a cone consisting of periodic orbits or orbits spiraling "in" respectively "out" of zero. In the case of smooth systems the cone reduces to an object which can be regarded

as a flat, degenerated cone. It is the key observation to view that cone as a generalized invariant “manifold” determining the dynamics. In fact it is the main result of this chapter to establish that even for nonlinear perturbations of piecewise linear systems there is a cone-like invariant “manifold” carrying the essential dynamics of the full system under appropriate conditions. In that way a reduction procedure to a two-dimensional surface has been established for nonsmooth systems allowing a bifurcation and stability analysis of a reduced system.

For simplicity, let us consider PWS with the separation manifold define by a hyperplane $\mathcal{M} := \{\xi \in \mathbb{R}^n | e_1^\top \xi = \xi_1 = 0\}$, written in the form

$$\dot{\xi} = \begin{cases} f_+(\xi), & \xi_1 > 0, \\ f_-(\xi), & \xi_1 < 0 \end{cases} \quad (5.1)$$

with smooth functions $f_+, f_- : \mathbb{R}^n \rightarrow \mathbb{R}^n$. In order to give the statements of the main results, we also introduce the following hypotheses.

The hypotheses on the PWS (5.1) are the following:

(a) We assume that

$$\begin{aligned} f_+(\xi) &= A^+ \xi + g_+(\xi) \\ f_-(\xi) &= A^- \xi + g_-(\xi) \end{aligned}$$

with constant matrices A^\pm and nonlinear C^k -parts $g_\pm(\xi) = o(\|\xi\|)$, $k \geq 1$.

(b) Direct transition between \mathbb{R}_-^n and \mathbb{R}_+^n through \mathcal{M} , hence, without loss of generality, $\xi \in \mathcal{M}_-^c$.

(c) Existence of μ_c and $\bar{\xi}$ such that $P(\bar{\xi}) = \mu_c \bar{\xi}$ for linear PWS.

(d) The attractivity condition (2.8) for (5.1) is satisfied.

The main result is the following theorem which has been obtained in a cooperation with D. Weiss and T. Küpper and which has already been presented in [66]. For a better understanding of the results and the following application we include an abbreviated version of the proof using subtle estimates essentially due to D. Weiss.

Theorem 5.1. [66]

Under the previous hypotheses on the corresponding PWLS and g_\pm , there exists a sufficiently small δ and a C^1 -function $h : [0, \delta) \rightarrow \mathcal{M}$ satisfying $h(0) = 0$ and $\frac{\partial}{\partial u} h(0) = \bar{\xi}$ such that

$$\{h(u) \mid 0 \leq u < \delta\}$$

is locally invariant and attractive under the Poincaré map of system (1). For $k = 2$ the function h is C^k in case of $\mu_c \geq 1$ and $C^{\min(k,j)}$ in case of $\mu_c < 1$ and $\alpha < \mu_c^j$.

The first idea we use in the proof is to decompose the Poincaré maps of PWLS and PWNS into a linear part and a nonlinearity. The Poincaré map \mathcal{P} for PWNS will be written using properties of the Poincaré map of PWLS, P . In that way, we are able to use the approach relying on Hadamard's graph transformation.

5.2 Properties of PWLS

We first decompose P using the derivative at $\bar{\xi}$ and an appropriate nonlinear term Q as

$$P(\xi) = P'(\bar{\xi})\xi + Q(\xi).$$

Using the properties of P we immediately obtain $Q(\bar{\xi}) = 0$, $Q'(\bar{\xi}) = 0$ and

$$\begin{aligned} Q(\lambda\xi) &= \lambda Q(\xi), \\ Q'(\lambda\xi) &= Q'(\xi), \quad 0 < \lambda < \infty. \end{aligned}$$

Hence, the function Q' is constant on half-rays. Differentiating the second equation with respect to ξ gives

$$Q^{(j+1)}(\lambda\xi)\lambda^j = Q^{(j+1)}(\xi), \quad 0 < \lambda < \infty,$$

for $j \geq 1$, again indicating possible difficulties for $\lambda \rightarrow 0$. On the other hand we find vanishing derivatives of the return time t_- applied in the direction of the ray leading to corresponding results for derivatives of Q .

Lemma 5.1. *For $j \geq 1$ we get $Q^{(j+1)}(\lambda\xi)\xi = 0$ for $\xi \in \mathcal{M}_-^c$ and $P_-(\xi) \in \mathcal{M}_+^c$.*

Proof. The statement follows due to $Q^{(j+1)}(\xi) = P^{(j+1)}(\xi)$, $P'_-(\xi)\xi = P_-(\xi)$ and

$$\begin{aligned} P_-^{(j+1)}(\lambda\xi)\xi &= 0, \\ P_+^{(j+1)}(P_-(\lambda\xi))P_-(\xi) &= 0, \end{aligned}$$

which is guaranteed by Lemma 2.3. \square

To simplify matters we linearly transform the coordinates of system (5.1) by a constant matrix

$$\begin{pmatrix} 1 & 0 \\ 0 & T \end{pmatrix}, \quad T \in \mathbb{R}^{(n-1) \times (n-1)}$$

to get $\bar{\xi} = e_2 \in \mathbb{R}^n$ and

$$P'(\bar{\xi}) = \begin{pmatrix} \mu_c & 0 \\ 0 & A^s \end{pmatrix}, \quad (5.2)$$

where the eigenvalues of the matrix A^s are exactly the μ_r , $r = 1, \dots, n-2$. Note that \mathcal{M} remains the separating plane, and that the transformation of the last $(n-1)$ components is independent of ξ_1 .

We decompose

$$P = \begin{pmatrix} P_c \\ P_s \end{pmatrix}, \quad \xi = \begin{pmatrix} y \\ z \end{pmatrix}$$

according to the blocks in (5.2), so that y is a scalar and $z \in \mathbb{R}^{n-2}$. Due to assumption (2.8) we can choose a norm on \mathbb{R}^{n-2} such that

$$\|A^s\| =: \alpha < \min\{1, \mu_c\}.$$

On \mathbb{R}^{n-1} we define a norm by

$$\|\xi\| = \max\{|y|, \|z\|\}.$$

Remark 5.1. *Due to the properties of the derivative of Q we are able to obtain an estimate for Q' in a neighborhood of the vector $\bar{\xi}$:*

$$\|Q'(\xi)\| \leq L_\varepsilon, \quad \xi \in S_\varepsilon(\bar{\xi}),$$

$S_\varepsilon(\bar{\xi}) := \{(y, z)^T \in \mathcal{M} \mid y > 0, \|z/y\| \leq \varepsilon\}$, for some constant L_ε with $L_\varepsilon \rightarrow 0$ for $\varepsilon \rightarrow 0$.

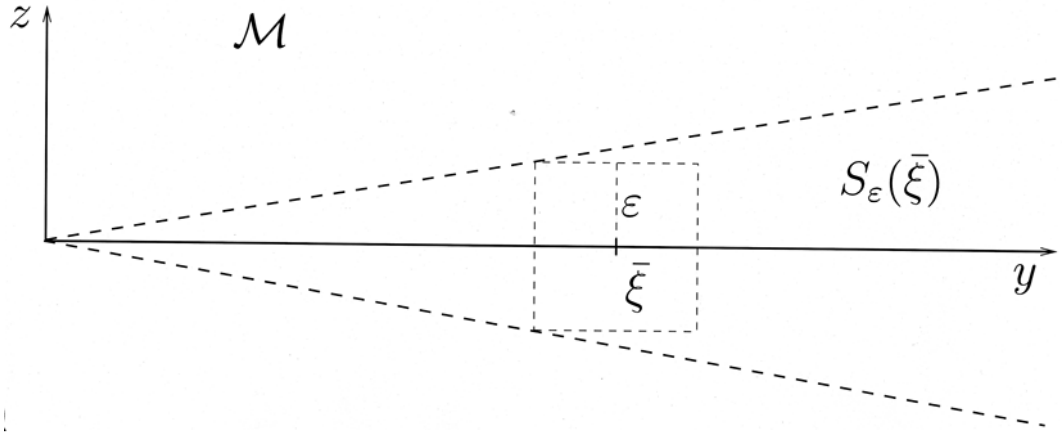
We now use the property of the sector $S_\varepsilon(\bar{\xi})$ to obtain an estimate relating relations of P_c and P_s , hence the approximation property mentioned in Remark 2.3. For $\xi \in S_\varepsilon(\bar{\xi})$ we know $\|z\|/y \leq \varepsilon$ and hence $\|\xi\| = y$ for $\varepsilon < 1$. According to Remark 5.1 and $Q(y, 0) = 0$ we know

$$\begin{aligned} \|P_s(\xi)\| &\leq \|A^s z\| + \|Q(\xi)\| \\ &\leq (\alpha + L_\varepsilon)\varepsilon y, \\ P_c(\xi) &\geq (\mu_c - L_\varepsilon\varepsilon)y. \end{aligned} \quad (5.3)$$

Combining these two estimates we see

$$\frac{\|P_s(\lambda\xi)\|}{P_c(\lambda\xi)} \leq \frac{\alpha + L_\varepsilon}{\mu_c - L_\varepsilon\varepsilon}\varepsilon < \varepsilon \quad (5.4)$$

for sufficiently small ε . Additionally we get $\alpha + L_\varepsilon < 1$ for small values of ε . Hence (5.3) shows the local attractivity of the cone \mathcal{C} , whereas (5.4) guarantees that in case of contracting spiraling on \mathcal{C} solutions close to the cone converge faster to the cone than to the origin.

Figure 5.1: ε -sector of the cone in \mathcal{M} .

5.3 The piecewise nonlinear system (PWNS)

As we are interested to prove the existence of a local manifold we use the usual techniques of “cut-off and scale” and without restriction we end up with a piecewise nonlinear system of the form

$$\dot{\xi} = \begin{cases} A^+\xi + g_+(\xi), & \xi_1 > 0, \\ A^-\xi + g_-(\xi), & \xi_1 < 0, \end{cases} \quad (5.5)$$

where the nonlinear perturbations g_{\pm} are C^k -maps, $k \geq 1$, defined on the whole phase space \mathbb{R}^n with $\text{supp } g_{\pm} \subset \{\xi \in \mathbb{R}^n \mid \|\xi\| \leq \delta\}$ and $g_{\pm} = o(\|\xi\|)$, $\|\xi\| \rightarrow 0$. Obviously we find a constant $o(1)$ depending on the scaling parameter δ with $\|g_{\pm}\| + \|g'_{\pm}\| \leq o(1)$, $\delta \rightarrow 0$.

A global invariant manifold of system (5.5) gives a local invariant manifold of system (5.1).

5.3.1 The Poincaré map

The Poincaré maps \mathcal{P}_- , \mathcal{P}_+ and $\mathcal{P} = \mathcal{P}_+(\mathcal{P}_-(\xi))$ will be defined on sectors $S_{\varepsilon}(\bar{\xi})$ resp. $S_{\varepsilon_{\eta}}(\bar{\eta})$ as long as $\varepsilon, \varepsilon_{\eta}$ and δ are sufficiently small.

We decompose the Poincaré map of system (5.5) using the Poincaré map of the PWLS:

$$\mathcal{P}(\xi) = P(\xi) + R(\xi), \quad R(\xi) := \mathcal{P}(\xi) - P(\xi).$$

Due to the compact support of the perturbations g_{\pm} depending on δ , we know $R(\xi) = 0$ for $\|\xi\| \geq \text{const} \cdot \delta$, const sufficiently large. In this section we will

study further properties of the remaining term R .

A crucial step in the definition of \mathcal{P}_- , \mathcal{P}_+ , relies on the definition and properties of the intersection times τ_{\pm} of PWNS (5.5), which in case of the \ominus -system is given by (we omit the $(-)$ -indices)

$$\begin{aligned}\tau_-(\xi) &= \inf\{\tau > 0 \mid F(\tau, \xi) = 0\}, \\ F(t, \xi) &= e_1^T [e^{At}\xi + \int_0^t e^{A(t-s)}g(y(s, \xi))ds],\end{aligned}$$

where $y(t, \xi)$ is the solution of $\dot{y} = Ay + g(y)$, $y(0) = \xi$. Applying Gronwall's Lemma it is obvious, that we have $y(t, \xi) = e^{At}\xi + o(\|\xi\|)$ for $t \in [0, T]$. The existence of C^k -functions τ_{\pm} for initial values close to the cone is guaranteed by the Implicit Function Theorem due to the transversality condition (2.8) and the hypothesis on the perturbations g_{\pm} (see proof of Lemma 5.2). Furthermore we know that $\tau_{\pm}(\xi)$ is "close" to $t_{\pm}(\xi)$ for small perturbations g_{\pm} :

$$\begin{aligned}e_1^T A^- e^{t^* A^-} \xi [t_-(\xi) - \tau_-(\xi)] &= \\ e_1^T \int_0^{\tau_-(\xi)} e^{A^-(\tau_-(\xi)-s)} g_-(y_-(s, \xi)) ds &\end{aligned}$$

with intermediate time t^* . Due to the transversality condition (2.8) and the hypothesis on g_- we find

$$\tau_-(\xi) - t_-(\xi) = o(1) \tag{5.6}$$

for $\delta \rightarrow 0$ or $\|\xi\| \rightarrow 0$. Differentiating the equations defining $t_-(\xi)$ and $\tau_-(\xi)$ with respect to ξ and using (2.8) and the properties of g_- we find $\tau'(\xi) = \mathcal{O}(\|\xi\|^{-1})$ and with (5.6) additionally

$$\tau'_-(\xi) - t'_-(\xi) = o(\|\xi\|^{-1}) \tag{5.7}$$

for $\delta \rightarrow 0$ or $\|\xi\| \rightarrow 0$.

Remark 5.2. *In case of $k \geq 2$ we assume without loss of generality $g_{\pm} = \mathcal{O}(\|\xi\|^2)$. Thus we can replace the o -terms in (5.6) and (5.7) by $\mathcal{O}(\|\xi\|)$ and $\mathcal{O}(1)$ respectively. Similarly we conclude*

$$\tau''_-(\xi) - t''_-(\xi) = \mathcal{O}(\|\xi\|^{-1}).$$

All o - and \mathcal{O} -terms are independent of ε .

Corresponding to Lemma 2.3 we get

Lemma 5.2. *The intersection time τ_- is C^k in $S_\varepsilon(\bar{\xi})$, ε suitably small. Let $\xi \in S_\varepsilon(\bar{\xi})$ with $\|\xi\| = 1$. For $0 \leq j \leq k$ we get*

$$\tau_-^{(j)}(\lambda\xi) = \mathcal{O}(\lambda^{-j}), \quad 0 < \lambda.$$

In case of $k \geq 2$ we gain one power of λ in direction of the ray ξ :

$$\tau_-^{(j+1)}(\lambda\xi)\xi = \mathcal{O}(\lambda^{-j}), \quad 0 < \lambda.$$

Similar results hold for τ_+ .

Proof. Let ε and δ be sufficiently small, so that transversality of the perturbed vectorfields is still given. Application of the Implicit Function Theorem implies the existence of $\tau_-(\xi)$ for $\xi = (1, z)^T$, $\|z\| \leq \varepsilon$. The existence on $S_\varepsilon(\bar{\xi})$ can be concluded applying the Contraction-Mapping Theorem to the operator $t \rightarrow t - \frac{1}{\lambda\beta}F(t, \lambda\xi)$ for $\lambda > 0$, where $e_1^T A^- e^{\tau_-(\xi)A^-} \xi = \beta > 0$.

The statements about τ_- and τ'_- are given by (5.6), (5.7) and Lemma 2.3 in case of $k = 1$. Let $k \geq 2$. By (5.7), Remark 5.2 and Lemma 2.3 we find $\tau'(\lambda\xi)\xi = \mathcal{O}(1)$.

The statement for higher derivatives follows inductively by differentiating $F(\tau(\xi), \xi) = 0$ with respect to ξ , by the transversality condition (2.8) and by the observation $\frac{\partial}{\partial t}F(\tau(\lambda\xi), \lambda\xi) = \mathcal{O}(\lambda)$. \square

Lemma 5.3. *The remaining term R is C^k in $S_\varepsilon(\bar{\xi})$. Furthermore there is a constant K_δ independent of ε with $K_\delta \rightarrow 0$ for $\delta \rightarrow 0$ and*

$$\|R(\xi)\| + \|R'(\xi)\| \leq K_\delta, \quad \xi \in S_\varepsilon(\bar{\xi}).$$

Let $\xi \in S_\varepsilon(\bar{\xi})$ with $\|\xi\| = 1$. In case of $k = 2$ we get

$$R''(\lambda\xi) = \mathcal{O}(1), \quad 0 < \lambda < \infty.$$

Proof. Since the intersection times τ_\pm are C^k the same holds for the remaining term R . Using $\mathcal{P}_\pm(\xi) = e^{A^\pm \tau_\pm} \xi + \int_0^{\tau_\pm} e^{A^\pm(\tau_\pm - s)} g_\pm(y_\pm(s, \xi)) ds$ we get

$$\begin{aligned} R(\xi) &= [e^{A^+ \tau_+} e^{A^- \tau_-} - e^{A^+ t_+} e^{A^- t_-}] \xi \\ &\quad + e^{A^+ \tau_+} \int_0^{\tau_-} e^{A^-(\tau_- - s)} g_-(y_-(s, \xi)) ds \\ &\quad + \int_0^{\tau_+} e^{A^+(\tau_+ - s)} g_+(y_+(s, \mathcal{P}_-(\xi))) ds, \end{aligned}$$

$\tau_- = \tau_-(\xi)$, $\tau_+ = \tau_+(\mathcal{P}_-(\xi))$, $t_- = t_-(\xi)$, $t_+ = t_+(\mathcal{P}_-(\xi))$. Obviously the Lemma is true for the last two terms. For the first term we write equivalently

$$\begin{aligned} [e^{A^+ \tau_+} e^{A^- \tau_-} - e^{A^+ t_+} e^{A^- t_-}] \xi &= \\ e^{A^+ \tau_+} [e^{A^- \tau_-} - e^{A^- t_-}] \xi & \\ + [e^{A^+ \tau_+} - e^{A^+ t_+}] e^{A^- t_-} \xi. & \end{aligned}$$

By differentiating $[e^{A^- \tau^-} - e^{A^- t^-}] \xi$ with respect to ξ and using (5.6), (5.7) and Remark 5.2 it is easy to conclude that the Lemma holds for this term and thus for R . \square

5.3.2 Hadamard's Graph Transform

Using the explicit form of P leads to the composition of \mathcal{P} which we can use to define Hadamard's graph transformation:

$$\mathcal{P}(\xi) = \begin{pmatrix} \mu_c & 0 \\ 0 & A^s \end{pmatrix} \xi + \mathcal{R}(\xi),$$

$\mathcal{R}(\xi) := Q(\xi) + R(\xi)$. Obviously the remaining term \mathcal{R} is C^k in $S_\varepsilon(\bar{\xi})$ and we get

$$\|\mathcal{R}'(\xi)\| \leq L_{\varepsilon, \delta} := L_\varepsilon + K_\delta, \quad (5.8)$$

so that $L_{\varepsilon, \delta}$ can be made as small as necessary by setting ε and δ suitably small.

We will prove the existence of a smooth function $H : [0, \infty) \rightarrow \mathbb{R}^{n-2}$ with $H(0) = 0$, which satisfies the invariance condition

$$H(\mathcal{P}_c(y, H(y))) = \mathcal{P}_s(y, H(y)) \quad (5.9)$$

for $y \geq 0$ using Hadamard's Graph Transform $T : D \rightarrow D$ defined by

$$[TH](\zeta) := \mathcal{P}_s(y, H(y)), \quad \zeta \geq 0, \quad (5.10)$$

and $\zeta = \mathcal{P}_c(y, H(y))$. Obviously, a fixed point of the operator T vanishes at $y = 0$ and fulfills the invariance condition (5.9).

In case of $k = 1$ we define D as a set of maps $H : [0, \infty) \rightarrow \mathbb{R}^{n-2}$, satisfying $H(0) = 0$, $\|H\|_\infty \leq \varepsilon$, $\text{graph}(H) \subset S_\varepsilon(\bar{\xi})$, i.e. $(y, H(y)) \in S_\varepsilon(\bar{\xi})$ for all $y \geq 0$ and $\|H(y_1) - H(y_2)\| \leq \varepsilon|y_1 - y_2|$ for $y_1, y_2 \geq 0$.

Due to Remark 5.1, Lemma 5.3 and the following Lemma 5.4 the existence of a fix-point of the operator T can be proved quite similar to [36]. We only have to make use of $Q(\bar{\xi}) = 0$ and to guarantee $\text{graph}(\tilde{H}) \subset S_\varepsilon(\bar{\xi})$ for $\tilde{H} = TH$, which can easily be seen: We will show

$$\mathcal{P}(S_\varepsilon(\bar{\xi})) \subset S_\varepsilon(\bar{\xi})$$

which holds for ε and δ sufficiently small. For $\xi \in S_\varepsilon(\bar{\xi})$ we get similar to (5.3)

$$\begin{aligned} \|\mathcal{P}_s(\xi)\| &\leq \|A^s z\| + \|Q(\xi)\| + \|R(\xi)\| \\ &\leq (\alpha + L_\varepsilon + K_\delta \varepsilon^{-1}) \varepsilon y, \\ \mathcal{P}_c(\xi) &\geq (\mu_c - L_\varepsilon \varepsilon - K_\delta) y. \end{aligned}$$

Combining these two estimates we get for sufficiently small ε and δ as in (5.4)

$$\frac{\|\mathcal{P}_s(\xi)\|}{\mathcal{P}_c(\xi)} \leq \frac{\alpha + L_\varepsilon + K_\delta \varepsilon^{-1}}{\mu_c - o(\varepsilon) - K_\delta} \varepsilon \leq \varepsilon.$$

Lemma 5.4. *For each $\zeta \geq 0$ and each $H \in D$ there is a unique $y = \omega(\zeta, H)$ with*

$$\mathcal{P}_c(y, H(y)) = \zeta.$$

Furthermore the function $\omega(\cdot, H)$ is Lipschitz-continuous with constant $1/(\mu_c - L_{\varepsilon, \delta})$.

Proof. Since

$$\begin{aligned} & |\mathcal{R}_c(y_1, H(y_1)) - \mathcal{R}_c(y_2, H(y_2))| \\ & \leq L_{\varepsilon, \delta} \max\{|y_1 - y_2|, \|H(y_1) - H(y_2)\|\} \\ & \leq L_{\varepsilon, \delta} |y_1 - y_2|, \end{aligned} \tag{5.11}$$

the function $\mathcal{P}_c(\cdot, H(\cdot))$ given by $\mathcal{P}_c(y, H(y)) = \mu_c y + \mathcal{R}_c(y, H(y)) \geq 0$ is strictly monotonically increasing as long as $L_{\varepsilon, \delta} < \mu_c$. Hence there exists such a function $\omega(\cdot, H)$. Using (5.11) a second time we find $|\zeta_1 - \zeta_2| \geq \mu |y_1 - y_2| - L_{\varepsilon, \delta} |y_1 - y_2|$. \square

The differentiability of the fix-point $H = TH$ can be shown as in [12]. To prove $H'(0) = 0$ we use Lemma 5.4 and the invariance condition (5.9) to conclude

$$\begin{aligned} & \limsup_{\zeta \rightarrow 0} \frac{\|H(\zeta)\|}{|\zeta|} \\ & \leq \frac{1}{\mu_c - L_{\varepsilon, \delta}} \limsup_{y \rightarrow 0} \frac{\|A^s H(y) + \mathcal{R}_s(y, H(y))\|}{|y|} \\ & \leq \frac{\alpha + L_{\varepsilon, \delta}}{\mu_c - L_{\varepsilon, \delta}} \limsup_{y \rightarrow 0} \frac{\|H(y)\|}{|y|}. \end{aligned}$$

For $k = 2$ we define D as a set of C^1 -maps $H : [0, \infty) \rightarrow \mathbb{R}^{n-2}$, satisfying the additional conditions

- $\|H\|_{1, \infty} := \max\{\|H\|_\infty, \|H'\|_\infty\} \leq \varepsilon,$
- $\|H'(y_1) - H'(y_2)\| \leq L'|y_1 - y_2|$

for all $y_1, y_2 \geq 0$, where the Lipschitz-constant L' will be determined later. D is a Banach space with respect to the norm $\|\cdot\|_{1, \infty}$.

Additionally to Lemma 5.4 we need

Lemma 5.5. *The function $y = \omega(\cdot, H)$ is continuously differentiable with*

$$|y'_1 - y'_2| \leq K|\zeta_1 - \zeta_2| \quad (5.12)$$

for $y'_i := \frac{\partial}{\partial \zeta} \omega(\zeta_i, H)$, where the constant K is independent of L' for $(\varepsilon + L_{\varepsilon, \delta})L' \leq \text{const.}$ Furthermore for $y_i := \omega(\zeta, H_i)$ and $y'_i := \frac{\partial}{\partial \zeta} \omega(\zeta, H_i)$ we find

$$|y_1 - y_2| + |y'_1 - y'_2| \leq K_{\varepsilon, \delta} \|H_1 - H_2\|_{1, \infty}$$

for some constant $K_{\varepsilon, \delta}$ with $K_{\varepsilon, \delta} \rightarrow 0$ for $\varepsilon, \delta \rightarrow 0$.

Proof. Obviously the function $\omega(\cdot, H)$ is C^1 together with \mathcal{P} and H . Differentiating $\zeta = \mathcal{P}_c(y, H(y))$ gives

$$1 = \mu_c y' + \mathcal{R}'_c(y, H(y)) \begin{pmatrix} 1 \\ H'(y) \end{pmatrix} y'.$$

Setting $y'_i := y'(\zeta_i)$, $i = 1, 2$, and using the abbreviations $\mathcal{R}'_j := \mathcal{R}'(y_j, H(y_j))$, $H'_j := H'(y_j)$, $j = 1, 2$, we estimate

$$\begin{aligned} \mu |y'_1 - y'_2| &\leq \left\| \mathcal{R}'_1 \begin{pmatrix} 1 \\ H'_1 \end{pmatrix} y'_1 - \mathcal{R}'_2 \begin{pmatrix} 1 \\ H'_2 \end{pmatrix} y'_2 \right\| \\ &\leq \left\| \mathcal{R}'_1 \begin{pmatrix} 1 \\ H'_1 \end{pmatrix} (y'_1 - y'_2) \right\| \\ &\quad + \left\| \mathcal{R}'_1 \begin{pmatrix} 0 \\ H'_1 - H'_2 \end{pmatrix} y'_2 \right\| \\ &\quad + \left\| [\mathcal{R}'_1 - \mathcal{R}'_2] \begin{pmatrix} 1 \\ H'_2 \end{pmatrix} y'_2 \right\|, \end{aligned}$$

where the first term can be estimated by $L_{\varepsilon, \delta} |y'_1 - y'_2|$, the second term by $L_{\varepsilon, \delta} L' |y_1 - y_2| |y'_2|$ and the third using Lemma 5.1 and 5.3:

$$\left\| [\mathcal{R}'_1 - \mathcal{R}'_2] \begin{pmatrix} 1 \\ H'_2 \end{pmatrix} \right\| \leq K |y_1 - y_2|.$$

More precisely we get

$$\begin{aligned} &\left\| [\mathcal{R}'_{i,1} - \mathcal{R}'_{i,2}] \begin{pmatrix} 1 \\ H'_2 \end{pmatrix} \right\| \\ &= \left\| \mathcal{R}''_{i,*} \left(\begin{pmatrix} 1 \\ H'_* \end{pmatrix}, \begin{pmatrix} 1 \\ H'_2 \end{pmatrix} \right) \right\| |y_1 - y_2| \end{aligned}$$

with intermediate value y^* , where \mathcal{R}_i is the i th component of \mathcal{R} and $\mathcal{R}_{i,*}' := \mathcal{R}_{i,*}'(y^*, H(y^*))$, $H_*' := H'(y^*)$. Finally

$$\begin{aligned} \left\| Q_{i,*}' \left(\begin{pmatrix} 1 \\ H_*' \end{pmatrix}, \begin{pmatrix} 1 \\ H_2' \end{pmatrix} \right) \right\| &= \mathcal{O}(\varepsilon)L', \\ \left\| R_{i,*}' \left(\begin{pmatrix} 1 \\ H_*' \end{pmatrix}, \begin{pmatrix} 1 \\ H_2' \end{pmatrix} \right) \right\| &= \mathcal{O}(1), \end{aligned}$$

prove the first statement.

We now set $y_i := \omega(\zeta, H_i)$, i.e.

$$\zeta = \mathcal{P}_c(y_i, H_i(y_i)) = \mu_c y_i + \mathcal{R}_c(y_i, H_i(y_i)).$$

Hence

$$\begin{aligned} \mu_c |y_1 - y_2| &\leq \|\mathcal{R}(y_1, H_1(y_1)) - \mathcal{R}(y_2, H_2(y_2))\| \\ &\leq L_{\varepsilon, \delta} [|y_1 - y_2| + \|H_1 - H_2\|_\infty] \end{aligned}$$

and therefore

$$|y_1 - y_2| \leq \frac{L_{\varepsilon, \delta}}{\mu_c - L_{\varepsilon, \delta}} \|H_1 - H_2\|_\infty.$$

For $y_i' := \frac{\partial}{\partial \zeta} \omega(\zeta, H_i)$ and $\mathcal{R}_{k,i}' := \mathcal{R}(y_i, H_k(y_i))$, $H_{k,i} = H_k(y_i)$ we get

$$\begin{aligned} \mu_c |y_1' - y_2'| &\leq \left\| \mathcal{R}'_{1,1} \begin{pmatrix} 1 \\ H'_{1,1} \end{pmatrix} y_1' - \mathcal{R}'_{2,2} \begin{pmatrix} 1 \\ H'_{2,2} \end{pmatrix} y_2' \right\| \\ &\leq \left\| \mathcal{R}'_{1,1} \begin{pmatrix} 1 \\ H'_{2,1} \end{pmatrix} y_1' - \mathcal{R}'_{2,2} \begin{pmatrix} 1 \\ H'_{2,2} \end{pmatrix} y_2' \right\| \\ &\quad + \frac{L_{\varepsilon, \delta}}{\mu_c - L_{\varepsilon, \delta}} \|H'_1 - H'_2\|_\infty \\ &\leq \left\| \mathcal{R}'_{2,1} \begin{pmatrix} 1 \\ H'_{2,1} \end{pmatrix} y_1' - \mathcal{R}'_{2,2} \begin{pmatrix} 1 \\ H'_{2,2} \end{pmatrix} y_2' \right\| \\ &\quad + \left\| [\mathcal{R}'_{1,1} - \mathcal{R}'_{2,1}] \begin{pmatrix} 1 \\ H'_{2,1} \end{pmatrix} \right\| \|y_1'\| \\ &\quad + \frac{L_{\varepsilon, \delta}}{\mu_c - L_{\varepsilon, \delta}} \|H'_1 - H'_2\|_\infty, \end{aligned}$$

where the first term is already estimated above. For the second term we find

$$\begin{aligned} & \left\| [\mathcal{R}'_{i,1,1} - \mathcal{R}'_{i,2,1}] \begin{pmatrix} 1 \\ H_{2,1} \end{pmatrix} \right\| \\ &= \left\| \mathcal{R}''_i(y_1, z^*) \left(\begin{pmatrix} 0 \\ H_{1,1} - H_{2,1} \end{pmatrix}, \begin{pmatrix} 1 \\ H_{2,1} \end{pmatrix} \right) \right\| \\ &\leq [\mathcal{O}(\varepsilon) + \mathcal{O}(\delta)] \|H'_1 - H'_2\|_\infty \end{aligned}$$

with intermediate value z^* . More precisely:

$$\begin{aligned} & \left\| Q''_i(y_1, z^*) \left(\begin{pmatrix} 0 \\ H_{1,1} - H_{2,1} \end{pmatrix}, \begin{pmatrix} 1 \\ H_{2,1} \end{pmatrix} \right) \right\| \\ &\leq \mathcal{O}(\varepsilon) \|H'_1 - H'_2\|_\infty \\ & \left\| R''_i(y_1, z^*) \left(\begin{pmatrix} 0 \\ H_{1,1} - H_{2,1} \end{pmatrix}, \begin{pmatrix} 1 \\ H_{2,1} \end{pmatrix} \right) \right\| \\ &\leq \mathcal{O}(\delta) \|H'_1 - H'_2\|_\infty \end{aligned}$$

for $y_1 = \mathcal{O}(\delta)$. □

In the following we will prove that $T : D \rightarrow D$ is a contraction. Defining $\tilde{H} := TH$ for $H \in D$ gives

$$\tilde{H}(\zeta) = \mathcal{P}_s(y, H(y)), \quad y = \omega(\zeta, H).$$

Clearly, \tilde{H} is a continuously differentiable function with $\tilde{H}(0) = 0$. Further we get with $Q(y, 0) = 0$, Remark 5.1 and Lemma 5.3

$$\begin{aligned} \|\tilde{H}(\zeta)\| &\leq \|A^s\| \|H(y)\| + \|\mathcal{R}(y, H(y))\| \\ &\leq (\alpha + L_\varepsilon + K_\delta \varepsilon^{-1}) \varepsilon. \end{aligned}$$

Using $Q'(y, 0) = 0$, Lemma 5.1 and 5.3 we find

$$\begin{aligned} \|\tilde{H}'(\zeta)\| &\leq \|A^s\| \|H'(y)\| \|y'\| \\ &\quad + \|\mathcal{R}'(y, H(y)) \begin{pmatrix} 1 \\ H'(y) \end{pmatrix}\| \|y'\| \\ &\leq \frac{\alpha + \mathcal{O}(\varepsilon) + K_\delta \varepsilon^{-1}}{\mu_c - L_{\varepsilon, \delta}} \varepsilon. \end{aligned}$$

Eventually we can guarantee

$$\|\tilde{H}\|_{1, \infty} \leq \varepsilon$$

for ε and δ sufficiently small.

Indeed, \tilde{H}' is Lipschitz continuous: For $\zeta_1, \zeta_2 \geq 0$ we define $y_1 := \omega(\zeta_1, H)$ and $y_2 := \omega(\zeta_2, H)$. Then

$$\begin{aligned} \|\tilde{H}'(\zeta_1) - \tilde{H}'(\zeta_2)\| &\leq \|A^s\| \|H'_1 y'_1 - H'_2 y'_2\| \\ &\quad + \|\mathcal{R}'_1 \begin{pmatrix} 1 \\ H'_1 \end{pmatrix} y'_1 - \mathcal{R}'_2 \begin{pmatrix} 1 \\ H'_2 \end{pmatrix} y'_2\|. \end{aligned}$$

The first term of the right-hand side can be estimated by

$$\begin{aligned} \|H'_1 y'_1 - H'_2 y'_2\| &\leq \|H'_1(y'_1 - y'_2)\| \\ &\quad + \|H'_1 - H'_2\| |y'_2| \\ &\leq \varepsilon |y'_1 - y'_2| + L' |y_1 - y_2| |y'_2| \end{aligned}$$

whereas the second term is already estimated in the proof of Lemma 5.5. We then arrive at

$$\begin{aligned} \|\tilde{H}'(\zeta_1) - \tilde{H}'(\zeta_2)\| &\leq (\alpha\varepsilon + L_{\varepsilon,\delta}) |y'_1 - y'_2| \\ &\quad + (\alpha L' + L_{\varepsilon,\delta} L' + \mathcal{O}(1)) |y_1 - y_2| |y'_2|, \end{aligned}$$

where the \mathcal{O} -term is independent of L' . Using Lemma 5.5 we eventually get

$$\begin{aligned} \|\tilde{H}'(\zeta_1) - \tilde{H}'(\zeta_2)\| &\leq \frac{\alpha L' + L_{\varepsilon,\delta} L' + \mathcal{O}(1)}{(\mu_c - L_{\varepsilon,\delta})^2} |\zeta_1 - \zeta_2|, \end{aligned}$$

where the \mathcal{O} -term is still independent of L' . Choosing L' sufficiently large and ε, δ small we end up with

$$\|\tilde{H}'(\zeta_1) - \tilde{H}'(\zeta_2)\| \leq L' |\zeta_1 - \zeta_2|$$

which proves $T(D) \subset D$.

For any $H_1, H_2 \in D$ we define $\tilde{H}_i = TH_i$ and y_i, y'_i as in Lemma 5.5. Then by definition (5.10) and Lemma 5.5 we find

$$\begin{aligned} \|\tilde{H}_1(\zeta) - \tilde{H}_2(\zeta)\| &\leq \|A^s\| \|H_{1,1} - H_{2,2}\| + \|\mathcal{R}_{1,1} - \mathcal{R}_{2,2}\| \\ &\leq \alpha(\varepsilon |y_1 - y_2| + \|H_1 - H_2\|_\infty) \\ &\quad + L_{\varepsilon,\delta} (|y_1 - y_2| + \|H_1 - H_2\|_\infty) \\ &\leq [\alpha + o(1)] \|H_1 - H_2\|_{1,\infty} \end{aligned}$$

for $\varepsilon, \delta \rightarrow 0$.

Furthermore we get

$$\begin{aligned} \|\tilde{H}'_1(\zeta) - \tilde{H}'_2(\zeta)\| &\leq \|A^s\| \|H'_{1,1}y'_1 - H'_{2,2}y'_2\| \\ &\quad + \|\mathcal{R}'_{1,1} \begin{pmatrix} 1 \\ H'_{1,1} \end{pmatrix} y'_1 - \mathcal{R}'_{2,2} \begin{pmatrix} 1 \\ H'_{2,2} \end{pmatrix} y'_2\|, \end{aligned}$$

where the first term can be estimated by

$$\begin{aligned} &\|H'_{1,1}y'_1 - H'_{2,2}y'_2\| \\ &\leq \|H'_{1,1}\| \|y'_1 - y'_2\| \\ &\quad + (\|H'_{1,1} - H'_{1,2}\| + \|H'_{1,2} - H'_{2,2}\|) \|y'_2\| \\ &\leq \varepsilon |y'_1 - y'_2| \\ &\quad + \frac{1}{\mu_c - L_{\varepsilon,\delta}} (L'|y_1 - y_2| + \|H'_1 - H'_2\|_\infty) \end{aligned}$$

and the second term is already estimated in the proof of Lemma 5.5:

$$\begin{aligned} &\|\mathcal{R}'_{1,1} \begin{pmatrix} 1 \\ H'_{1,1} \end{pmatrix} y'_1 - \mathcal{R}'_{2,2} \begin{pmatrix} 1 \\ H'_{2,2} \end{pmatrix} y'_2\| \\ &\leq \frac{L_{\varepsilon,\delta}}{\mu_c - L_{\varepsilon,\delta}} \|H'_1 - H'_2\|_\infty \\ &\quad + o(1) \|H_1 - H_2\|_{1,\infty} \end{aligned}$$

for $\varepsilon, \delta \rightarrow 0$. Finally we end up with

$$\begin{aligned} &\|\tilde{H}'_1(\zeta) - \tilde{H}'_2(\zeta)\| \\ &\leq \frac{\alpha + L_{\varepsilon,\delta} + o(1)}{\mu_c - L_{\varepsilon,\delta}} \|H_1 - H_2\|_{1,\infty} \end{aligned}$$

for $\varepsilon, \delta \rightarrow 0$.

Since $\alpha < \min\{1, \mu - c\}$ we can guarantee that T is a contraction for ε, δ sufficiently small, hence by the Contraction-Mapping Theorem there is a fixed point defining the invariant graph.

Remark 5.3. *Theorem 5.1 holds even in case of $k = 3$. The proof depends crucially on Lemma 5.2, which guarantees*

$$\begin{aligned} R'''(\lambda\xi)\xi &= \mathcal{O}(\lambda^{-1}), \\ R'''(\lambda\xi)\xi^2 &= \mathcal{O}(1), \quad 0 < \lambda < \infty. \end{aligned}$$

5.4 Bifurcation

Once the existence of $H(y) = a_1y + a_2y^2 + \dots$, has been established, we can use H to determine the dynamics on $\{h(y) = (y, H(y)) \mid 0 \leq y < \delta\}$.

For example to determine periodic solutions we consider the fixed point equation $\mathcal{P}(\xi) = \xi$, reduced to the first component

$$\mu_c y + \mathcal{R}_c(y, H(y)) = y, \quad (y \geq 0).$$

Dividing by y we obtain

$$\mu_c - 1 = \mathcal{R}_c(y, H(y))/y. \tag{5.13}$$

Solutions $y > 0$ of (5.13) then lead to periodic orbits.

5.5 Class of PWNS

We illustrate the results by class of PWNS where the PWLS is designed according to setting parameters in general situation presented in Chapter 2 as: $\beta^\pm = \sigma^+ = \alpha^+ = 0, k^\pm = \gamma^\pm = 1, \sigma^- = -\delta, \alpha^- = \alpha$. Hence, the \oplus -system is taken in normalized form $A^+ = A_N^+$ and the \ominus -system is give by

$$A^- = (S^-)^{-1} A_N^- S^-, \quad (S^-)^{-1} = \begin{pmatrix} 1 & \frac{-\alpha(\alpha+1)}{2} & -\alpha \\ -\delta & 1 & 0 \\ 0 & -\delta & 1 \end{pmatrix},$$

with suitable parameters α and δ . Further we have chosen a nonlinearity such that the solution is explicitly known for comparison.

Hence we consider the system

$$\dot{\xi} = A^\pm \xi + g_\pm(\xi), \quad \pm e_1^T \xi > 0, \quad (5.14)$$

where

$$g_+(\xi) = \rho_+ \begin{pmatrix} 0 \\ 0 \\ \xi_1^2 + \xi_2^2 \end{pmatrix}, \quad g_-(\xi) = \rho_- \begin{pmatrix} \xi_3^2 \\ 0 \\ 0 \end{pmatrix}.$$

Note that the eigenvalues of A^\pm are given by $\lambda^\pm \pm i\omega^\pm, \mu^\pm$, and the existence of a *direct crossing* domain is guaranteed by (2.2).

For $\eta = (y, z)^T \in \mathcal{M}_+^c$, we have $t_+ := \tau_+(\eta) = \pi/\omega^+$ independent of the nonlinearity g_+ and therefore

$$\mathcal{P}_+(y, z) = \begin{pmatrix} -e^{\lambda^+ t_+} y \\ e^{\mu^+ t_+} z + G_3 y^2 \end{pmatrix},$$

where $G_3 = \rho_+(e^{2\lambda^+ t_+} - e^{\mu^+ t_+})/(2\lambda^+ - \mu^+)$.

Since there are still many parameters involved we illustrate various situations for a special choice of parameters.

5.5.1 Case I: $\alpha = \rho_- = 0$

In this case, PWNS (5.14) ensures that a simple situation will be considered, where we have only direct crossing between half spaces and $\tau_\pm = t_\pm$ independent of the nonlinearity g_\pm and ξ . For $\xi = (y, z)^T \in \mathcal{M}_-^c$ the intersection time is constant, i.e. $\tau_-(\xi) = \pi/\omega^-$, and the map \mathcal{P}_- is given by

$$\mathcal{P}_-(y, z) = \begin{pmatrix} e^{\lambda^- \pi/\omega^-} & 0 \\ \delta(e^{\lambda^- \pi/\omega^-} + e^{\mu^- \pi/\omega^-}) & e^{\mu^- \pi/\omega^-} \end{pmatrix} \begin{pmatrix} y \\ z \end{pmatrix}.$$

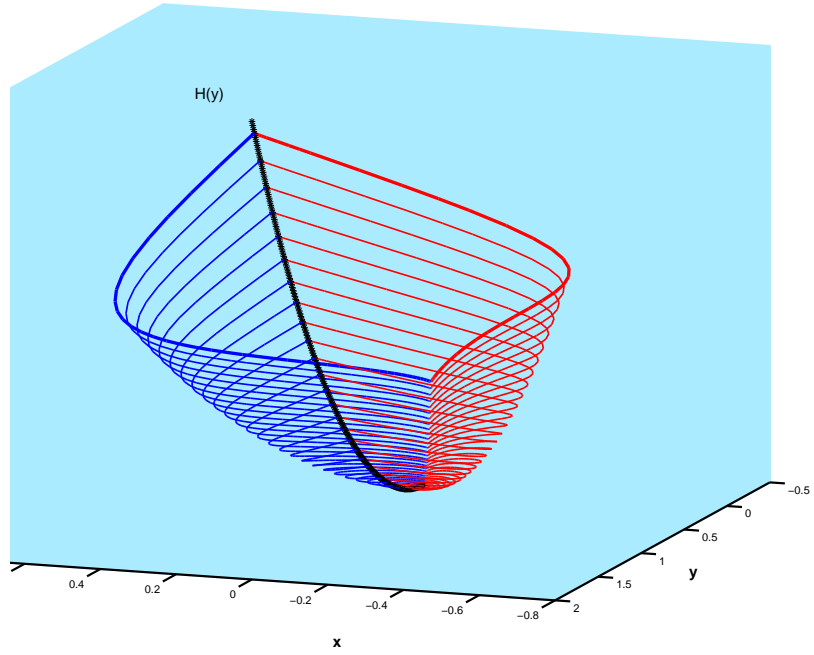


Figure 5.2: An attractive \mathcal{C} with invariant graph $H(y)$ of PWNS.

For $\xi \in \mathcal{M}_-$, then $\mathcal{P}(y, z) = \mathcal{P}_+(\mathcal{P}_-(y, z))$ we obtain

$$\mathcal{P}(y, z) = \begin{pmatrix} \mu_c & 0 \\ d & \mu_1 \end{pmatrix} \begin{pmatrix} y \\ z \end{pmatrix} + \begin{pmatrix} 0 \\ G_3 \mu_c y^2 \end{pmatrix},$$

with

$$\mu_c = e^{\lambda^- \pi / \omega^- + \lambda^- \pi / \omega^-}, \quad d = \delta e^{\mu^+ \pi / \omega^+} (e^{\lambda^- \pi / \omega^-} + e^{\mu^- \pi / \omega^-}), \quad \mu_1 = e^{\mu^- \pi / \omega^- + \mu^+ \pi / \omega^+}.$$

Attractivity of the cone is then guaranteed if $|\mu_1| < \min\{1, \mu_c\}$ and the invariant “eigenvector” $\bar{\xi}$ satisfying $P(\bar{\xi}) = \mu_c \bar{\xi}$ in PWLS is chosen as $\bar{\xi} = (\bar{y}, \bar{z})^T = (1, m)^T$ with $m = d / (\mu_c - \mu_1)$.

By Theorem 5.1, we know there exists a local invariant set tangent to the cone at 0 which is generated by a graph of the form $H(y) = my + a_2 y^2 + \mathcal{O}(y^3)$. Using $Q(\bar{\xi}) = 0$, $Q'(\bar{\xi}) = 0$ and $g_{\pm} = \mathcal{O}(\|\xi\|^2)$, we obtain

$$\begin{aligned} Q(y, H(y)) &= \mathcal{O}(y^3), \\ R(y, H(y)) &= \begin{pmatrix} b_1 \\ b_2 \end{pmatrix} y^2 + \mathcal{O}(y^3). \end{aligned}$$

where $b_1 = 0$, $b_2 = \mu_c G_3$. To determine the coefficient a_2 we substitute H into the equation representing the invariance condition; hence

$$H(\mathcal{P}_c(y, H(y))) = \mathcal{P}_s(y, H(y)), \quad (5.15)$$

then, we deduce that

$$a_2 = \frac{b_2}{\mu_c^2 - \mu_1}.$$

The generation of an invariant cone is given by using the graph function $H(y) = my + \frac{b_2}{\mu_c^2 - \mu_1}y^2$ and for a periodic orbit we set $\mu_c = 1$. An attractive invariant cone for PWNS (5.14) which is generated by $H(y)$ is shown in Figure 5.2 with parameters set as $\omega^\pm = 1.0, \lambda^+ = -\lambda^- = 1.0, \mu^- = -0.5, \mu^+ = 0.02, \rho_+ = 12.3$.

5.5.2 Case II: $\delta = 0, \alpha = 1$

In this case, the existence of an invariant cone for PWLS has been fully investigated in Chapter 2 and [39]. The PWNS (5.14) has direct crossing if $\xi_2[-2\omega^-\xi_2 + (\lambda^- - \mu^- - \omega^-)\xi_3 + \rho_-\xi_3^2] < 0$, see 2.2.

For $\xi = (y, z)^T \in \mathcal{M}_-^c$ the intersection time $\tau_-(\xi) = \tau_-$ is determined as smallest positive root of equation

$$0 = -2sye^{\lambda^-\tau_-} + [(c-s)e^{\lambda^-\tau_-} - e^{\mu^-\tau_-}]z + G_1(\tau_-)z^2 \quad (5.16)$$

with

$$\begin{aligned} G_1(\tau_-) &= \rho_- \frac{(\mu^- - \kappa)(s - c) + 2\omega^-c}{(\lambda^- - 2\mu^-)^2 + \omega^{-2}} e^{\lambda^-\tau_-} \\ &\quad + \rho_- \frac{2\mu^- - \lambda^- - \omega^-}{(\lambda^- - 2\mu^-)^2 + \omega^{-2}} e^{2\mu^-\tau_-}, \end{aligned}$$

where we have used the abbreviations $s := \sin(\omega^-\tau_-)$ and $c := \cos(\omega^-\tau_-)$. Further the map \mathcal{P}_- is given by

$$\mathcal{P}_-(y, z) = \begin{pmatrix} (c+s)e^{\lambda^-\tau_-} & \alpha se^{\lambda^-\tau_-} \\ 0 & e^{\mu^-\tau_-} \end{pmatrix} \begin{pmatrix} y \\ z \end{pmatrix} + \begin{pmatrix} G_2(\tau_-)z^2 \\ 0 \end{pmatrix},$$

where

$$\begin{aligned} G_2(\tau_-) &= \rho_- \frac{(\lambda^- - 2\mu^-)s - \omega^-c}{(\lambda^- - 2\mu^-)^2 + \omega^{-2}} e^{\lambda^-\tau_-} \\ &\quad + \rho_- \frac{\omega^-}{(\lambda^- - 2\mu^-)^2 + \omega^{-2}} e^{2\mu^-\tau_-}. \end{aligned}$$

For $\xi \in \mathcal{M}_-^c$, then $\mathcal{P}(y, z) = \mathcal{P}_+(\mathcal{P}_-(y, z))$ we obtain

$$\mathcal{P}(y, z) = \begin{pmatrix} \mu_1(\tau_-) & d(\tau_-) \\ 0 & \mu_c(\tau_-) \end{pmatrix} \begin{pmatrix} y \\ z \end{pmatrix} + \begin{pmatrix} -G_2(\tau_-)e^{\lambda^+t_+}z^2 \\ G_3[((c+s)y + \alpha sz)e^{\lambda^-\tau_-} + G_2(\tau_-)z^2]^2 \end{pmatrix}$$

with

$$\begin{aligned}\mu_1(\tau_-) &= -(c+s)e^{\lambda^-\tau_-+\lambda^+t_+}, \\ d(\tau_-) &= -se^{\lambda^-\tau_-+\lambda^+t_+}, \\ \mu_c(\tau_-) &= e^{\mu^-\tau_-+\mu^+t_+}.\end{aligned}$$

We write $\mathcal{P}(y, z)$ as

$$\mathcal{P}(y, z) = \begin{pmatrix} \mu_1 & d \\ 0 & \mu_c \end{pmatrix} \begin{pmatrix} y \\ z \end{pmatrix} + \mathcal{R}(y, z),$$

with $\mu_1 = \mu_1(t_-(\bar{\xi}))$, $d = d(t_-(\bar{\xi}))$, $\mu_c = \mu_c(t_-(\bar{\xi}))$; further $t_-(\bar{\xi})$ is determined as smallest positive root of

$$0 = -2\bar{s} + \alpha[\bar{c} - \bar{s} - e^{(\mu^- - \lambda^-)t_-}]m, \quad (5.17)$$

where we have used the abbreviations $\bar{s} = \sin(\omega^-t_-(\bar{\xi}))$, $\bar{c} = \cos(\omega^-t_-(\bar{\xi}))$, and the invariant ‘‘eigenvector’’ $\bar{\xi}$ satisfying $P(\bar{\xi}) = \mu_c\bar{\xi}$ is chosen as $\bar{\xi} = (\bar{y}, \bar{z})^T = (1, m)^T$ with $m = (\mu_c - \mu_1)/d$.

Note that we want to consider the situation that $\mu_c \approx 1$; again attractivity of the cone is then guaranteed if $|\mu_1| < \min\{1, \mu_c\}$. By Theorem 1, the invariant graph is tangent to the cone at 0 which is taken of the form $H(y) = my + a_2y^2 + \mathcal{O}(y^3)$. Using $Q(\bar{\xi}) = 0$, $Q'(\bar{\xi}) = 0$ and $g_{\pm} = \mathcal{O}(\|\xi\|^2)$, we obtain

$$\begin{aligned}Q(y, H(y)) &= \mathcal{O}(y^3), \\ R(y, H(y)) &= \begin{pmatrix} b_1 \\ b_2 \end{pmatrix} y^2 + \mathcal{O}(y^3).\end{aligned}$$

After lengthy computations we obtain

$$\begin{aligned}b_1 &= -\left[\bar{G}_2 - \frac{e_2^T A^- \bar{\eta}}{e_1^T A^- \bar{\eta}} \bar{G}_1\right] e^{\lambda^+t_+} m^2, \\ b_2 &= -\frac{e_3^T A^- \bar{\eta}}{e_1^T A^- \bar{\eta}} \bar{G}_1 e^{\mu^+t_+} m^2 + G_3 \bar{\eta}_2^2,\end{aligned}$$

where $\bar{\eta} = P_-(\bar{\xi})$ and $\bar{G}_j = G_j(t_-(\bar{\xi}))$, $j=1,2,3$.

To determine the coefficient a_2 we substitute H into the equation representing the invariance condition; hence

$$H(\mathcal{P}_1(y, H(y))) = \mathcal{P}_2(y, H(y)),$$

which leads to

$$\begin{aligned}m\mu_c y + m(da_2 + b_1)y^2 + a_2\mu_c^2 y^2 \\ = m\mu_c y + \mu_c a_2 y^2 + b_2 y^2 + \mathcal{O}(y^3),\end{aligned}$$

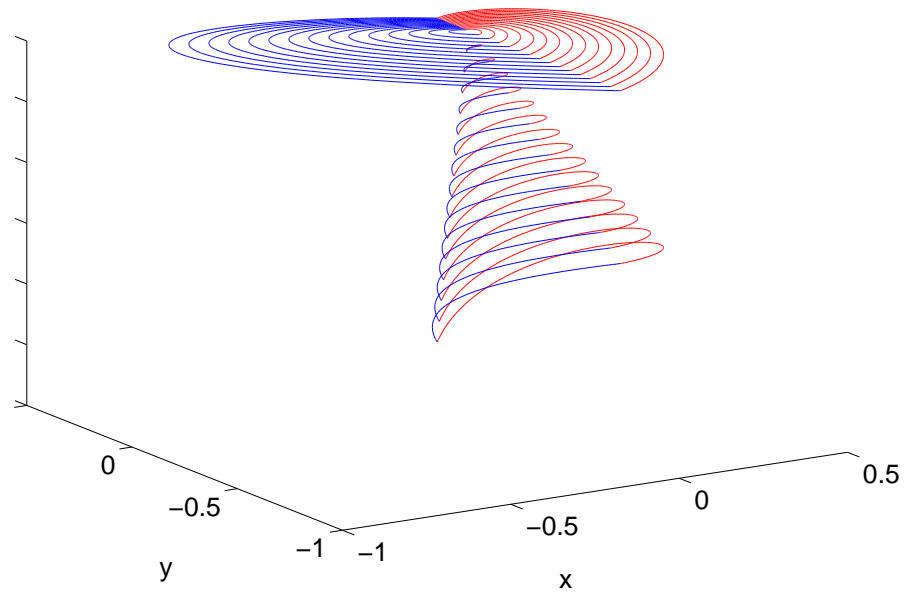


Figure 5.3: Two attractive invariant cones of PWLS for $\mu^- = \mu_0^-$.

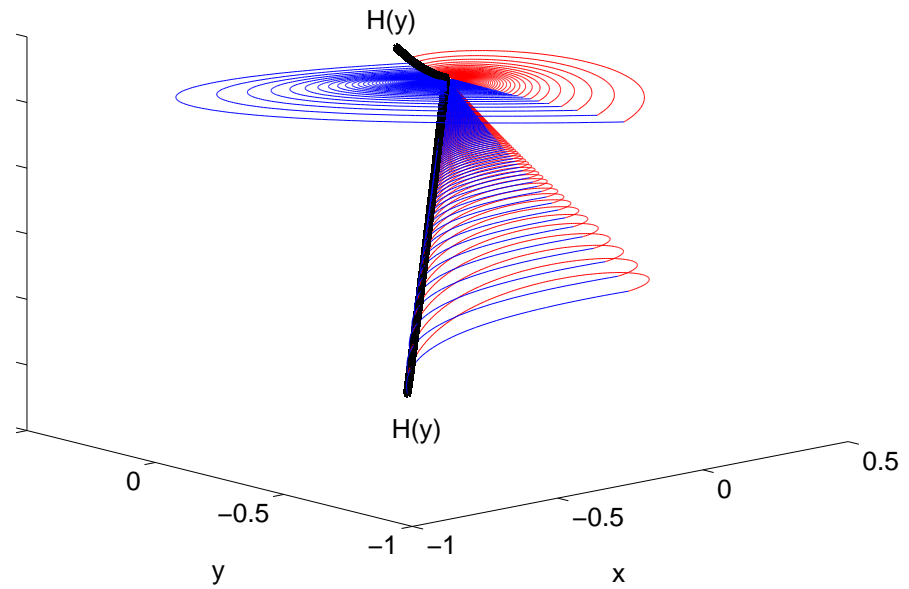


Figure 5.4: Two generalized center manifolds of PWNS ($\rho^- = -0.01, \rho^+ = 0.1$) for $\mu^- = \mu_0^-$.

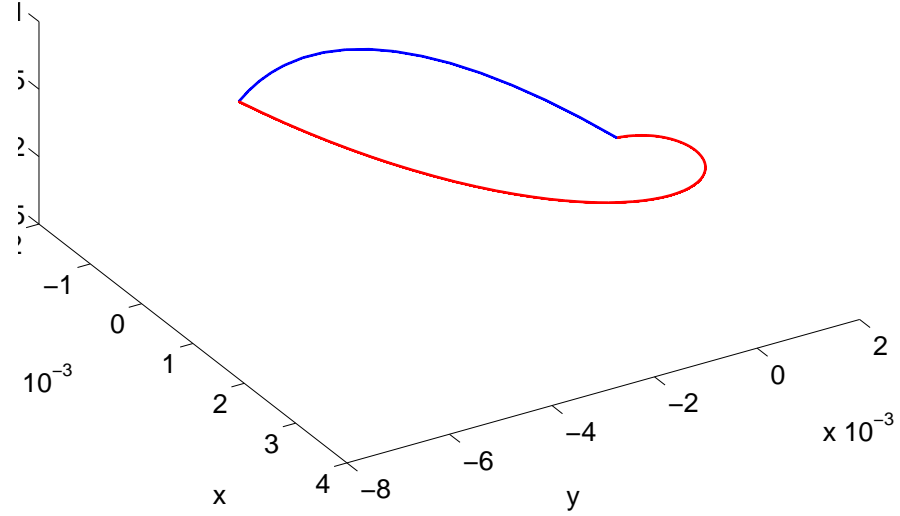


Figure 5.5: Stable periodic orbit of PWNS for $\mu^- = -1.06 > \mu_0^-$.

and thus

$$a_2 = \frac{b_2 - mb_1}{\mu_c^2 - \mu_1}.$$

Finally we can use the expression for $H(y)$ to study bifurcation of periodic orbits by determining fixed points of the reduced system

$$\begin{aligned} \mathcal{P}_1(y, H(y)) := \mu_c y + \frac{db_2 - \mu_c(1 - \mu_c)b_1}{\mu_c^2 - \mu_1} y^2 \\ + \mathcal{O}(y^3). \end{aligned}$$

Thus the fixed point is approximately given by

$$y^* \approx \frac{1 - \mu_c}{db_2 - \mu_c(1 - \mu_c)b_1} (\mu_c^2 - \mu_1).$$

Using this general form various situations can be derived by a special choice of parameters. The simulation is done with parameters set at $\lambda^+ = -0.5$, $\lambda^- = 0.5$, $\mu^+ = 0.2$, $\alpha = 0.5$, $t_+ = \pi$, $w^+ = w^- = 1.0$, $\rho_- = -0.01$, $\rho_+ = 0.1$ and bifurcation parameter μ^- close to $\mu_0^- := -\mu^+ t_+ / t_-(\bar{\xi}) \approx -1.0604$, where $t_-(\bar{\xi}) \approx 0.5928$ is determined by

$$0 = -2\bar{s} + \alpha[\bar{c} - \bar{s} - e^{-(\mu^+ t_+ + \lambda^- t_-(\bar{\xi}))}]m,$$

where $m = \frac{1 - \mu_1}{d}$. We get $\mu(\mu_0^-) = 1$ and $\frac{\partial}{\partial \mu^-} \mu(\mu_0^-) > 0$. For this set of values in PWLS (i.e. $\rho_- = \rho_+ = 0$), the phase space contains two attractive invariant cones (Figure 5.3), likewise there are two generalized center manifolds of

PWNS (5.14), Figure 5.4. These attractive cones are given by $\bar{\xi} = (0, 1, 0)^T$ and $\bar{\xi} = (0, 1, m)$ with eigenvalues $\mu_1 = 1, \mu_c \approx 0.0671$ and $\mu_c = 1, \mu_1 \approx -0.3881$ respectively and are separated by a nonattractive cone. Recall, that the existence of two attractive cones is not possible in continuous PWLS (see [10] Theorem 2). A periodic orbit on the manifold generated by Hopf bifurcation is shown in Figure 5.5.

Chapter 6

Summary and future work

Es ist besser, einige Fragen zu haben als alle Antworten zu wissen

James Thurber (1894 - 1961)

The main goal of this thesis was to develop rigorous mathematical techniques to investigate the existence of cone-like invariant manifolds for nonsmooth systems. The crossing and sliding regions have been determined by means of a vectors field evaluation without knowledge about the existence of solutions for PWS. Therefore, the general behavior on \mathcal{M} and non-existence of an \mathcal{C} were obtained for different classes of PWS.

It was shown that the existence of \mathcal{C} played an important role in describing the dynamical behavior for PWS. The dynamics on \mathcal{C} in the phase space \mathbb{R}^n was collected into 3 cases as: (i) Stable focus type, (ii) Center focus type (iii) Unstable focus type. Hence the dynamics on \mathcal{C} behaved like a classical center manifold and we have used it to explain paradoxical situations concerning stability.

To find all possible invariant cones, numerical procedure and theoretical results were combined via the construction of Poincaré return map. A generalized Poincaré map for PWS exhibiting a strongly attracting \mathcal{C} and describing the dynamics on \mathcal{C} was introduced that allowed us to describe explicitly the systems behavior close to the bifurcation point. The mechanism to determine attractivity of the original system and various ways to generate invariant cones were investigated that yields a complete analysis of dynamics for 3D linear PWS. The existence of multiple invariant cones were found for 3D PWLS which is completely different correspond to smooth systems . An interpretation for this situation in terms of generalized center manifolds is that there are locally multiple generalized center manifolds at the same time.

Further, have shown how to generalize the notion of an invariant cone when sliding motion takes place on \mathcal{M} . A generalized Poincaré map also has been

used to predict analytically the scenarios following a sliding bifurcation with the notion of \mathcal{C} . The existence of an \mathcal{C} and non-standard bifurcations have been reported for different values of the system parameters such as: Invariant cones exhibiting *crossing-sliding*, *grazing-sliding* and *switching-sliding* bifurcation. Also as specific applications, an automotive brake with dry friction has been proposed and investigated; the dynamics of this system offers much interest because it is a simple representation of a mechanical model containing non-smooth characteristics; its response exhibits different types of bifurcation phenomena. The discontinuities have been transformed into discontinuities of the vector field and therefore the system model is converted into a Filippov system. The existence of invariant cones, nonsmooth phenomena such as sliding periodic doubling and multiple periodic orbits, and the possibility of more complex bifurcation scenarios have been identified and discussed; theoretical predictions and numerical tools were used.

The existence of cone-like invariant manifolds as an extension to nonlinear perturbations of certain n -dimensional PWS under appropriate conditions in the case without sliding motion carrying the essential dynamics of the full system has also been proved. A class of PWNS for which multiple cones exist has been proposed and investigated to illustrate a technique for generalized center manifold reduction and associated bifurcation. It was shown that the generalized Hopf-bifurcation provided a well established way to generate periodic orbits for PWNS.

This following will be topic in future work:

- It should be possible to extend the results of this thesis to non-homogeneous and affine linear PWS, i.e., an investigation concerning the existence, uniqueness and bifurcations of invariant cones in both cases.
 - In this thesis, we have only considered a single discontinuity surface, but the existence of \mathcal{C} and its stability for a system whose vector fields lead to several manifolds including manifolds of various dimensions requires further attention.
 - More complicated invariant cones for PWS may exhibit catastrophic bifurcation.
 - Development of numerical methods for computing cone-like invariant manifolds and their dynamics for non-linear PWS .
 - Reduction of PWS to lower-dimensional invariant manifolds when the sliding motion is involving.
-

- The existence of invariant cones and sliding-bifurcation are important aspects of the analysis which should be carried out for non-linear perturbation of the brake system.

Chapter 7

Appendix

7.1 Appendix A

$$\begin{aligned} p_{11} &= \frac{e^{kt}}{V(1,6)} (\cos(\mathbf{ot})V(1,6) - \sin(\mathbf{ot})V(1,5)), \\ p_{14} &= \frac{e^{kt}}{V(1,6)} (V(1,6)(\cos(\mathbf{ot})V(1,5) + \sin(\mathbf{ot})V(1,6)) + V(1,5)(\sin(\mathbf{ot})V(1,5) \\ &\quad - \cos(\mathbf{ot})V(1,6))), \end{aligned}$$

$$p_{21} = -\frac{1}{V(1,6)} [V(1,6) \cos(\mathbf{nt}) + V(5,6)V(2,4) \sin(\mathbf{nt}) - e^{kt} (\cos(\mathbf{ot})V(2,6) - \sin(\mathbf{ot})V(2,5))],$$

$$p_{22} = \cos(\mathbf{nt}),$$

$$\begin{aligned} p_{24} &= \frac{1}{V(1,6)} [(V(5,6)V(1,5) - V(1,6)V(5,5))V(2,4) \sin(\mathbf{nt}) + (V(2,6)V(1,5) - \\ &\quad V(1,6)V(2,5)) \\ &\quad \cos(\mathbf{nt}) + e^{kt} (V(1,6)V(2,5) \cos(\mathbf{ot}) + V(1,6)V(2,6) \sin(\mathbf{ot}) - V(1,5)(\cos(\mathbf{ot})V(2,6) \\ &\quad - \sin(\mathbf{ot})V(2,5))], \end{aligned}$$

$$p_{25} = V(2,4) \sin(\mathbf{nt}),$$

$$\begin{aligned} p_{31} &= e^{lt} \left[\frac{-V(6,6)}{V(1,6)} (\cos(\mathbf{mt})V(3,1) + \sin(\mathbf{mt})V(3,2)) + \frac{V(3,1)V(2,4)V(6,6) - V(2,4)V(6,3)}{V(2,4)V(1,6)V(3,2)} \right. \\ &\quad \left. (\cos(\mathbf{mt})V(3,2) - \sin(\mathbf{mt})V(3,1)) \right] + \frac{e^{kt}}{V(3,2)} (\cos(\mathbf{ot})V(3,6) - \sin(\mathbf{ot})V(3,5)), \end{aligned}$$

$$p_{33} = \frac{e^{lt}}{V(3,2)} (\cos(\mathbf{mt})V(3,2) - \sin(\mathbf{mt})V(3,1)),$$

$$\begin{aligned} p_{34} &= \frac{e^{lt}}{V(3,2)V(1,6)V(2,4)} \left[(\cos(\mathbf{mt})V(3,1) + \sin(\mathbf{mt})V(3,2)) (V(2,4)V(1,6)V(6,6) \right. \\ &\quad \left. - V(2,4)V(6,6)V(1,5)) - \frac{1}{V(2,4)V(1,6)V(3,2)} (V(3,1)V(2,4)V(1,6) - V(1,6)V(2,4)V(6,5) \right. \\ &\quad \left. + V(2,4)V(6,6)V(1,5) - V(3,1)V(2,4)V(1,5)) (\cos(\mathbf{mt})V(3,2) - \sin(\mathbf{mt})V(3,1)) \right] \end{aligned}$$

$$+ \frac{e^{kt}}{V(1,6)} \left[V(1,6) (\cos(\mathbf{ot})V(3,5) + \sin(\mathbf{ot})V(3,6)) - V(1,5) (\cos(\mathbf{ot})V(3,6) - \sin(\mathbf{ot})V(3,5)) \right],$$

$$p_{35} = \frac{e^{lt}}{V(3,2)} \left[V(3,2) (\cos(\mathbf{mt})V(3,1) + \sin(\mathbf{mt})V(3,2)) - V(3,1) (\cos(\mathbf{mt})V(3,2) - \sin(\mathbf{mt})V(3,1)) \right],$$

$$p_{41} = -\frac{e^{kt} \sin(\mathbf{ot})}{V(6,1)}$$

$$p_{44} = \frac{e^{kt}}{V(1,6)} (V(1,6) \cos(\mathbf{ot}) + V(1,5) \sin(\mathbf{ot})),$$

$$p_{51} = -\frac{V(5,6) \cos(\mathbf{nt})}{V(1,6)} + \frac{V(2,6) \sin(\mathbf{nt})}{V(1,6)V(2,4)} + \frac{e^{kt}}{V(1,6)} (\cos(\mathbf{ot})V(5,6) - \sin(\mathbf{ot})V(5,5)),$$

$$p_{52} = -\frac{\sin(\mathbf{nt})}{V(3,2)},$$

$$p_{54} = \frac{e^{lt}}{V(3,2)V(1,6)V(2,4)} \left[-V(1,6) (\cos(\mathbf{mt})V(1,5) + \sin(\mathbf{mt})V(1,6)) (V(2,4)V(1,6)V(6,5) - V(2,4)V(6,5)V(1,5)) + V(2,4)V(1,6) (V(1,5)V(6,5) - V(3,5) + V(3,6) - V(3,1)V(6,6)) (\cos(\mathbf{mt})V(3,2) - \sin(\mathbf{mt})V(3,1)) \right]$$

$$+ \frac{e^{kt}}{V(1,6)} \left[V(1,6) (\cos(\mathbf{ot})V(3,5) + \sin(\mathbf{ot})V(3,6)) - V(1,6) (\cos(\mathbf{ot})V(3,6) - \sin(\mathbf{ot})V(3,5)) + \frac{V(5,6)V(6,1) - V(6,1)V(5,6)}{V(1,6)} \cos(\mathbf{nt}) - \frac{V(2,6)V(1,5)}{V(1,6)V(2,4)} \frac{-V(1,6)V(2,5)}{V(1,6)V(2,4)} \sin(\mathbf{nt}) + \frac{e^{kt}}{V(1,6)} \left[V(1,6) (\cos(\mathbf{ot})V(5,5) + \sin(\mathbf{ot})V(5,6)) - V(1,6) (\cos(\mathbf{ot})V(5,6) - \sin(\mathbf{ot})V(5,5)) \right] \right]$$

$$p_{55} = \cos(\mathbf{nt}),$$

$$p_{63} = -\frac{e^{lt} \sin(\mathbf{mt})}{V(3,2)},$$

7.2 Appendix B

$$a_{11} = \frac{e^{kt_-}}{V^-(1,6)} (\cos(\mathbf{ot}_-)V^-(1,6) - \sin(\mathbf{ot}_-)V^-(1,5)),$$

$$a_{14} = \frac{e^{kt_-}}{V^-(1,6)} (V^-(1,6) (\cos(\mathbf{ot}_-)V^-(1,5) + \sin(\mathbf{ot}_-)V^-(1,6)) + V^-(1,5) (\sin(\mathbf{ot}_-)V^-(1,5) - \cos(\mathbf{ot}_-)V^-(1,6))),$$

$$a_{21} = -\frac{1}{V^-(1,6)} [V^-(1,6) \cos(\mathbf{nt}_-) + V^-(5,6)V^-(2,4) \sin(\mathbf{nt}_-) - e^{kt_-} (\cos(\mathbf{ot}_-)V(2,6) - \sin(\mathbf{ot}_-)V^-(2,5))],$$

$$a_{22} = \cos(\mathbf{nt}_-),$$

$$a_{24} = \frac{1}{V^-(1,6)} \left[(V^-(5,6)V^-(1,5) - V^-(1,6)V^-(5,5))V^-(2,4) \sin(\mathbf{nt}_-) + (V^-(2,6)V^-(1,5) - V^-(1,6)V^-(2,5)) \cos(\mathbf{nt}_-) + e^{\mathbf{kt}_-} (V^-(1,6)V^-(2,5) \cos(\mathbf{ot}_-) + V^-(1,6)V^-(2,6) \sin(\mathbf{ot}_-) - V^-(1,5)(\cos(\mathbf{ot}_-)V^-(2,6) - \sin(\mathbf{ot}_-)V^-(2,5))) \right],$$

$$a_{25} = V^-(2,4) \sin(\mathbf{nt}_-),$$

$$a_{31} = e^{\mathbf{lt}_-} \left[\frac{-\left(V(2,4)V(6,6) - V(2,4)V(6,4)V(5,6) - V(6,4)V(2,6)\right)}{V(1,6)V(2,4)} \left(\cos(\mathbf{mt})V(3,1) + \sin(\mathbf{mt})V(3,2) \right) + \frac{-V(3,1)V(2,4)V(6,2) + V(3,1)V(2,4)V(6,6) - V(3,1)V(6,4)V(2,6) - V(2,4)V(3,6) + V(3,4)V(2,6) + V(2,4)V(3,3)V(5,6)}{V(2,4)V(1,6)V(3,2)} \left(\cos(\mathbf{mt})V(3,2) - \sin(\mathbf{mt})V(3,1) \right) \right]$$

$$\frac{-V(5,6) \left(\cos(\mathbf{nt}_-)V(3,2) + \sin(\mathbf{nt}_-)V(3,4) \right)}{V(1,6)} - \frac{V(2,6) \left(\cos(\mathbf{nt}_-)V(3,4) - \sin(\mathbf{nt}_-)V(3,3) \right)}{V(1,6)V(2,4)}$$

$$e^{\mathbf{kt}_-} \frac{\left(\cos(\mathbf{nt}_-)V(3,6) - \sin(\mathbf{ot}_-)V(3,5) \right)}{V(1,6)},$$

$$a_{32} = e^{\mathbf{lt}_-} \left[-\frac{V(6,2)}{V(2,4)} \left(\cos(\mathbf{mt}_-)V(3,1) + \sin(\mathbf{mt}_-)V(3,2) \right) + \left(V(3,1)V(6,4)V(1,6) - V(3,4)V(1,6) \right) \left(\cos(\mathbf{mt}_-)V(3,2) - \sin(\mathbf{mt}_-)V(3,1) \right) + \frac{\cos(\mathbf{nt}_-)V(3,4) - \sin(\mathbf{nt}_+)V(3,3)}{V(2,4)}, \right]$$

$$a_{33} = \frac{e^{\mathbf{lt}_-}}{V^-(3,2)} \left(\cos(\mathbf{mt}_-)V^-(3,2) - \sin(\mathbf{mt}_-)V^-(3,1) \right),$$

$$a_{34} = -\frac{e^{\mathbf{lt}_-}}{V^-(1,6)V^-(2,4)} \left(V^-(2,4)V^-(1,6)V^-(6,5) - V^-(2,4)V^-(6,6)V^-(1,6) \right)$$

$$+ V^-(2,4)V^-(6,3)V^-(5,6)V^-(1,6) - V^-(2,4)V^-(6,3)V^-(1,6)V^-(5,6)$$

$$+ V^-(6,4)V^-(2,6)V^-(1,6) - V^-(6,4)V^-(1,6)V^-(2,6) \left(\cos(\mathbf{nt}_-)V^-(3,1) + \sin(\mathbf{nt}_-)V^-(3,2) \right)$$

$$\frac{1}{V^-(2,4)V^-(1,6)V^-(3,1)} \left[V^-(2,4)V^-(3,3)V^-(1,6)V^-(5,6) + V^-(3,1)V^-(4,2)V^-(1,6)V^-(6,6) - V^-(2,4)V^-(1,6)V^-(3,6) \right]$$

$$+ V^-(2,4)V^-(3,6)V^-(1,5) + V^-(3,4)V^-(1,6)V^-(2,5) - V^-(3,4)V^-(2,6)V^-(1,5) - V^-(3,1)V^-(2,4)V^-(6,6)V^-(1,5)$$

$$- V^-(3,1)V^-(2,4)V^-(6,3)V^-(1,6)V^-(5,5) - V^-(2,4)V^-(3,3)V^-(5,6)V^-(1,5)$$

$$+ V^-(3,1)V^-(6,4)V^-(2,6)V^-(1,5) - V^-(3,1)V^-(6,4)V^-(1,6)V^-(2,6)$$

$$+ V^-(3,1)V^-(2,4)V^-(6,3)V^-(5,6)V^-(1,6) \left[\cos(\mathbf{nt}_-)V^-(3,1) \right]$$

$$- \sin(\mathbf{nt}_-)V^-(3,2) \left. \right] + \frac{\left(V^-(5,6)V^-(1,5) - V^-(1,6)V^-(5,6) \right) \left(\cos(\mathbf{nt}_-)V^-(3,3) + \sin(\mathbf{nt}_-)V^-(3,4) \right)}{V^-(1,6)}$$

$$+ \frac{\left(V^-(2,6)V^-(1,6) - V^-(1,6)V^-(2,6) \right) \left(\cos(\mathbf{nt}_-)V^-(3,2) - \sin(\mathbf{nt}_-)V^-(3,1) \right)}{V^-(1,6)V^-(2,4)} + e^{\mathbf{kt}_-} \left[\cos(\mathbf{ot}_-)V^-(3,5) \right]$$

$$+ \sin(\mathbf{ot}_-)V^-(3,6) - \frac{V^-(1,5)}{V^-(1,6)} \left(\cos(\mathbf{ot}_-)V^-(3,6) \right)$$

$$- \sin(\mathbf{ot}_-)V^-(3,6) \left. \right],$$

$$a_{35} = e^{\mathbf{lt}_-} \left(-V^-(6,3) \left(\cos(\mathbf{mt}_-)V^-(3,1) + \sin(\mathbf{mt}_-)V^-(3,2) \right) \right)$$

$$+ \frac{\left(-V^-(2,4)V^-(3,3)V^-(1,6) + V^-(3,1)V^-(2,4)V^-(6,3)V^-(1,6) \right) \left(\cos(\mathbf{mt}_-)V^-(3,2) - \sin(\mathbf{mt}_-)V^-(3,1) \right)}{V^-(2,4)V^-(1,6)V^-(3,2)}$$

$$+ (\cos(\mathbf{nt}_-)V^-(2, 3) + \sin(\mathbf{nt}_-)V^-(3, 4)),$$

$$a_{41} = -\frac{e^{\mathbf{kt}_-} \sin(\mathbf{ot}_-)}{V^-(6,1)}$$

$$a_{44} = \frac{e^{\mathbf{kt}_-}}{V^-(1,6)} (V^-(1, 6) \cos(\mathbf{ot}_-) + V^-(1, 5) \sin(\mathbf{ot}_-)),$$

$$a_{51} = -\frac{V^-(5,6) \cos(\mathbf{nt}_-)}{V^-(1,6)} + \frac{V^-(2,6) \sin(\mathbf{nt}_-)}{V^-(1,6)V^-(2,4)} + \frac{e^{\mathbf{kt}_-}}{V^-(1,6)} (\cos(\mathbf{ot}_-)V^-(5, 6) - \sin(\mathbf{ot}_-)V^-(5, 5)),$$

$$a_{52} = -\frac{\sin(\mathbf{nt}_-)}{V^-(3,2)},$$

$$a_{54} = \frac{(V^-(5,5)V^-(1,6) - V^-(1,6)V^-(5,6)) \cos(\mathbf{nt}_-)}{V^-(1,6)} - \frac{(V^-(2,6)V^-(1,5) - V^-(1,6)V^-(2,5)) \sin(\mathbf{nt}_-)}{V^-(2,4)V^-(1,6)}$$

$$\frac{e^{\mathbf{kt}_-}}{V^-(1,6)} (\cos(\mathbf{ot}_-)V^-(5, 6) + \sin(\mathbf{ot}_-)V^-(5, 6) - V^-(1, 6)(\cos(\mathbf{ot}_-)V^-(5, 6) - \sin(\mathbf{ot}_-)V^-(5, 5))),$$

$$a_{55} = \cos(\mathbf{nt}_-),$$

Bibliography

- [1] V. Acary, B. Brogliato, *Numerical Methods for Nonsmooth Dynamical Systems. Applications in Mechanics and Electronics*. Springer Verlag, 2008.
- [2] B. Armstrong-Hélouvry, P. Dupont, C. Canudas de Wit, A survey of models, analysis tools and compensation methods for the control of machines with friction, *Automatica*, 30 (7)(1994)1083-1138.
- [3] J. Awrejcewicz, C. Lamarque, *Bifurcation and Chaos in Nonsmooth Mechanical Systems*, World Scientific, Singapore, 2004.
- [4] J. Awrejcewicz, P. Olejnik, Regular and chaotic stick-slip dynamics in a self-excited two-degree-of-freedom system with friction, *Int. J. Bifur. Chaos* 13(4) (2003)843-861.
- [5] S. Banerjee, G. Verghese, *Nonlinear Phenomena in Power Electronics*, IEEE Press, New York, 2001.
- [6] S. Barnett, R. G. Cameron, *Introduction to mathematical control theory* , New York: Oxford University Press, 1985.
- [7] B. Brogliato, *Nonsmooth Mechanics-Models, Dynamics and Control*, Springer-Verlag, London, 1999.
- [8] V. Carmona, E. Freire, E. Ponce, F. Torres, On simplifying and classifying piecewise linear systems, *IEEE Trans. Circuits Systems I, Fund. Theory Appl.*, 49 (2002)609-620.
- [9] V. Carmona, E. Freire, E. Ponce and F. Torres, Invariant manifolds of periodic orbits for piecewise linear three-dimensional systems. *IMA J. APPL.Math*, 69 (2004)71-91.
- [10] V. Carmona, E. Freire, E. Ponce, F. Torres, Bifurcation of invariant cones in piecewise linear homogeneous systems. *Int. J. Bifur. Chaos* 15 (8) (2005) 2469-2484.

-
- [11] V. Carmona, E. Freire, J. Ros, F. Torres, Limit cycle bifurcation in 3d continuous piecewise linear systems with two zones. Application to Chua's circuit, *Int. J. Bifur. Chaos* 15(10)(2005)3153-33164.
- [12] S.N. Chow, K. Lu, C^k center unstable manifolds, *Proc. Roy. Soc. Edinburgh*, 108A, (1988) 303-320.
- [13] F. Dercole, A. Gragnani, S. Rinaldi, Bifurcation analysis of piecewise smooth ecological models, *Theoretical Population Biology*, 72 (2007) 197-213.
- [14] M. di Bernardo, C. Budd, A. R. Champneys, P. Kowalczyk, *Piecewise-smooth Dynamical Systems: Theory and Applications*. Applied Mathematics Series vol. 163, Springer-Verlag, 2008.
- [15] M. di Bernardo, C. Budd, A. R. Champneys, P. Kowalczyk, A. B. Nordmark, G. Olivar and P.T. Piiroinen, Bifurcations in Nonsmooth Dynamical Systems, *SIAM Review*, 50(4), (2008) 629-701.
- [16] M. di Bernardo, S. J. Hogan, Discontinuity-induced bifurcations of piecewise smooth dynamical systems, *Phil. Trans. R. Soc. A* 368 (2010)4915-4935.
- [17] M. di Bernardo, K. H. Johansson, F. Vasca, Self-oscillations and sliding in relay feedback systems: Symmetry and bifurcations. *Int. J. Bifur. Chaos* 11(4)(2001)1121-1140.
- [18] M. di Bernardo, P. Kowalczyk, Sliding bifurcation: A novel mechanism for the sudden onset of chaos in dry friction oscillators, *Int. J. Bifur. Chaos* 13 (10) (2003) 2935-2948.
- [19] L. Dieci, L. Lopez, Sliding motion in Filippov differential systems: Theoretical results and a computational approach, *SIAM Journal on Numerical Analysis*, 47 (2009) 2023-2051.
- [20] L. Dieci, L. Lopez, On Filippov and Utkin sliding solutions of discontinuous systems, *Applied and Industrial Mathematics in Italy III*, World Scientific, (2009) 323-330.
- [21] L. Dieci, L. Lopez, Fundamental matrix solutions of piecewise smooth differential systems, special Issue of *Mathematics and Computers in Simulation*, 81 (2011) 932-953.
- [22] M. Fečkan, Bifurcation of periodic and chaotic solutions in discontinuous systems, *Archivum Mathematicum*, 34 (1)(1998)73-82
-

-
- [23] B. Feeny, A. Guran N. Hinrichs, K. Popp, A historical review on dry friction and stick-slip phenomena, *App. Mech. Rev.*, 51 (1998) 321-344.
- [24] A. F. Filippov, Differential equations with discontinuous right-hand side, *American Mathematical Society Translations*, 2(42)(1964)199-231.
- [25] A. F. Filippov, *Differential equations with discontinuous right-hand sides*, Mathematics and Its Applications, Kluwer Academic, Dordrecht, Netherlands, 1988.
- [26] U. Galvanetto, Bifurcations and chaos in a four-dimensional mechanical system with dry-friction, *J. Sound Vibr.* 204 (1997)690-695.
- [27] U. Galvanetto, Some discontinuous bifurcations in a two block stick-slip system, *J. Sound Vibr.* 284 (2001) 653-669.
- [28] U. Galvanetto, S. R. Bishop, Dynamics of a simple damped oscillator undergoing stick-slip vibrations, *Meccanica* 178 (1998)291-306.
- [29] J. Guckenheimer, P. Holmes, *Nonlinear Oscillations, Dynamical Systems, and Bifurcations of Vector Fields*. Springer-Verlag, New York, 1983.
- [30] W. Heemels, B. Brogliato, The complementarity class of hybrid dynamical systems, *European J. Control*, 9 (2003) 311-319.
- [31] N. Hinrichs, M. Östreich, K. Popp, On the modelling of friction oscillators, *J. Sound Vibr* 216(3) (1998)435-459.
- [32] H. A. Hosham, Bifurcations in nonsmooth high-dimensional brake system, Proceedings of 2nd International Symposium Rare Attractors and Rare Phenomena in Nonlinear Dynamics RA'11 May (16)17 - 20, 2011, Rīga - Jūrmala, Latvia.
- [33] H. B. Keller, *Numerical solution of bifurcation and nonlinear eigenvalue problems*, Applications of Bifurcation Theory, P.H. Rabinowitz, ed., New York, London, 1977.
- [34] N. M. Kinkaid, O. M. O'Reilly, P. Papadopoulos, Automotive disc brake squeal. *J. Sound. Vib.* 267 (2003) 105-66.
- [35] B. Krauskopf, H.M. Osinga, J. Galán-Vioque, *Numerical Continuation Methods for Dynamical Systems: Path following and boundary value problems*, Springer-Verlag, 2007.
-

-
- [36] Y. A. Kuznetsov, http://www.math.uu.nl/people/kuznet/NLDV/Lect10_11.pdf and <http://www.math.uu.nl/people/kuznet/NLDV/Lect12.pdf>, [14.04.2010].
- [37] Y. A. Kuznetsov, *Elements of Applied Bifurcation Theory*, 2nd Edition, Springer, Berlin, 1998.
- [38] T. Küpper, Invariant cones for non-smooth systems, *Mathematics and Computers in Simulation*, 79 (2008) 1396-1409.
- [39] T. Küpper, H. A. Hosham, Reduction to invariant cones for non-smooth systems, special Issue of *Mathematics and Computers in Simulation*, 81 (2011) 980-995.
- [40] T. Küpper, H. A. Hosham, K. Dudtschenko, The dynamics of bells as impacting system, to appear in *J. Mech. Eng. Sci.* (2011)
- [41] T. Küpper, S. Moritz, Generalized Hopf bifurcation of nonsmooth planar systems. *R. Soc. Lond. Philos. Trans. Ser. A Math. Phys. Eng. Sci.* 359 (2001) 2483-2496.
- [42] V. Krivan, S. Diehl, Adaptive omnivory and species coexistence in tri-trophic food webs. *Theor. Popul. Biol.* 67 (2005)85-99.
- [43] V. Krivan, J. Eisner, Optimal foraging and predator-prey dynamics, III. *Theor. Popul. Biol.* 63 (2003)269-279.
- [44] R. I. Leine and H. Nijmeijer, *Dynamics and Bifurcations of Non- Smooth Mechanical Systems*. Berlin, Germany: Springer-Verlag, 2004.
- [45] R. I. Leine, D. H. van Campen, Bifurcation phenomena in non-smooth dynamical systems, *European Journal of Mechanics A/Solids*, 25 (2006)595-616.
- [46] T. Ma , S. Wang, *Bifurcation Theory and Applications*, Series A: Monographs and Treatises, World Scientific Series on Nonlinear Science vol. 53, World Scientific Publishing Co. Pte. Ltd., Hackensack, NJ 2005.
- [47] M. R. Nishiwaki, Review of study on brake squeal, *Japan Society of Automobile Engineering Review*, 11 (1990) 48-54.
- [48] A. B. Nordmark, Non-periodic motion caused by grazing incidence in an impact oscillator, *J. Sound Vibr* 145 (2) (1991) 279-297.
-

-
- [49] A. B. Nordmark, P. T. Piiroinen, Simulation and stability analysis of impacting systems with complete chattering, *Nonlinear Dynamics* 58(1)(2009)85-106.
- [50] N. R. North, Disc brake squeal, Proceedings of IMechE, C38/76,(1976) 169-176.
- [51] J. M. Ortega, W. C. Rheinboldt, *Iterative Solution of Nonlinear Equations in Several Variables*, Academic Press, New York 1970.
- [52] M. Östreich, N. Hinrichs, K. Popp, Bifurcation and stability analysis for a non-smooth friction oscillator. Arch. Appl. Mech. 66 (1996) 301-314.
- [53] F. Pfeiffer, C. Glocker, *Multibody dynamics with unilateral contacts*, Wiley Series in Nonlinear Science, Wiley, 1996.
- [54] S. S. Pilyugin, P. Waltman, Multiple limit cycles in the chemostat with variable yield, *Math. Biosci.* 182 (2003) 151-166.
- [55] K. Popp, Private communication.
- [56] K. Popp, P. Stelter, Stick-slip vibrations and chaos, *Phil. Trans. R. Soc. London/A*, (1990) 89-105.
- [57] S.J. Schreiber, R.N. Lipcius, R.D. Seitz, W.C. Long, Dancing between the devil and deep blue sea: the stabilizing effect of enemy-free and victimless sinks. *Oikos* 113 (2006) 67-81.
- [58] R. Seydel, *Practical Bifurcation and Stability Analysis; From Equilibrium to Chaos*, IAM 5, Springer-Verlag, New York, 1994.
- [59] S. W. Shaw, P. J. Holmes, A periodically forced piecewise linear oscillator, *J. Sound Vibr.* 90(1) (1983) 129-155.
- [60] H. L. Trentelman, A. A. Stoorvogel, M.L.J. Hautus, *Control Theory for Linear Systems*, Springer, London, 2001.
- [61] V. I. Utkin. *Sliding Modes in Control Optimization*, Springer-Verlag, New York, 1992.
- [62] S. Yang, R. F. Gibson, Brake vibration and noise: reviews, comment, and proposals, *Int. J. Mater Product. Technol.* 12 (1997)496-513.
- [63] F. H. Yang, W. Zhang, J. Wang, Sliding bifurcations and chaos induced by dry friction in a braking system, *Chaos, Solitons and Fractals* 40 (2009) 1060-1075.
-

-
- [64] N. van de Wouw, R. I. Leine, Attractivity of equilibrium sets of systems with dry friction, *Int. J. Nonlin. Dyn. Chaos Engin. Syst.* 35 (2004) 19-39.
- [65] L. N. Virgin, C. J. Begley, Grazing bifurcations and basins of attraction in impact-friction oscillator, *Physica D* 130 (1999)43-57.
- [66] D. Weiss, T. Küpper, H. A. Hosham, Invariant manifolds for nonsmooth systems, *Physica D: Nonlinear Phenomena*, to appear in (2011).
- [67] S. Wiggins, *Introduction to Applied Nonlinear Dynamical System and Chaos*, 2nd edition, Springer-Verlag, New York, 2003.
- [68] C. W. Wu, L. O. Chua, On the Generality of the Unfolded chua's Circuit, *Int. J. Bifur. Chaos*, (6) (1996)801-832.
- [69] W. Zhang, S. P. Yang, M. Ye, *Periodic oscillations and bifurcations of nonlinear systems*. Beijing: Science Press; 2002.
- [70] Z. Zhusubalyev, E. Mosekilde, *Bifurcations and Chaos in Piecewise-smooth Dynamical Systems*, Singapore: World Scientific. 2003.
- [71] Y. Zou, T. Küpper, Generalized Hopf bifurcation emanated from a corner, *Nonlin. Anal. TAM.* 62 (1)(2005)1-17.
- [72] Y. Zou, T. Küpper, Generalized Hopf bifurcation for nonsmooth planar dynamical systems: the corner case, *Notheast. Math. J.* 17 (4) (2001) 383-386.
- [73] Y. Zou, T. Küpper, Generalized Hopf bifurcation emanated from a corner for piecewise smooth planar systems, *Non. Anal.* 62 (2005) 1-17.
- [74] Y. Zou. T. Küpper, W. J. Beyn, Generalized Hopf bifurcation for planar Filippov systems continuous at the origin. *J. Nonlin. Sci.* 16(2)(2006) 159-177.
-

Eigenständigkeitserklärung

Ich versichere, dass ich die von mir vorgelegte Dissertation selbständig angefertigt, die benutzten Quellen und Hilfsmittel vollständig angegeben und die Stellen der Arbeit - einschließlich Tabellen, Karten und Abbildungen -, die anderen Werken im Wortlaut oder dem Sinn nach entnommen sind, in jedem Einzelfall als Entlehnung kenntlich gemacht habe; dass diese Dissertation noch keiner anderen Fakultät oder Universität zur Prüfung vorgelegen hat; dass sie - abgesehen von unten angegebenen Teilpublikationen - noch nicht veröffentlicht worden ist sowie, dass ich eine solche Veröffentlichung vor Abschluss des Promotionsverfahrens nicht vornehmen werde. Die Bestimmungen der Promotionsordnung sind mir bekannt. Die von mir vorgelegte Dissertation ist von Herr Prof. Dr. Tassilo Küpper betreut worden.

Köln, den 26.04.2011 Hany Bakit

LEBENS LAUF

Hany A. Hosham Bakit

Persönliche Daten:

- Name: Hany Albadrey Hosham, Bakit.
- Wissenschaftlicher Name: H. A. Hosham .
- Geschlecht: männlich.
- Geburtsdatum: Januar, 20, 1975.
- Geburtsort: Assiut, Ägypten.
- Aktuelle Adresse: Hahnenstr. 23, 50354 Hürth. Deutschland .
- E-mail: hbakit@math.uni-koeln.de or hanyalbadrey@yahoo.com.

Akademischer Hintergrund :

- 1994-1998: B.Sc in der Mathematik.
- 1998-1999: Militärdienst.
- 2000-2001: Pre-Master.
- 2002-2004: M. Sc. (Angewandten Mathematik), Das Thema heißt "Finite-Difference Methods and Similarity Solutions for Solving Some Problems in Fluid Dynamics." Betreut von Prof. Dr. I. A. Hassanien and Prof Dr. A. A. Salama , Universität Assiut, Ägypten.
- 2004- 2007: PhD-Programm mit dem Titel "On some problems in magneto-thermoelastic" (nicht abgeschlossen). Betreut von Prof. Dr. A. M. Abd-Alla and Prof. Dr. A. A. Salama.
- 2007 bis Jetzt, PhD-Programm mit dem Titel (Cone-like invariant manifolds for nonsmooth systems), Betreut von Prof. Dr. Dr. h.c. Tassilo Küpper, Universität zu Köln, Deutschland.

Forschungsschwerpunkte:

- Bifurkationstheorie, Nicht-glatte dynamische Systeme und Anwendungen.
- Numerische Lösungen von partiellen und gewöhnlichen Differentialgleichungen (mit Anwendung in der Fluidodynamik und thermoelastische).
- Implizite Finite-Differenzen-Methoden.

- Gruppentheorie mit Anwendung in der partiellen Differentialgleichungen.

Tätigkeiten

- 2000-2004 Studentische Hilfskraft Fachbereich Mathematik, Universität Assiut, Ägypten.
- 2000-2007 Wissenschaftliche Mitarbeiter, Fachbereich Mathematik, Universität Assiut, Ägypten.
- 2007-2011 Stipendiat in der Promotionsförderung.
- 1.4.2011 Wissenschaftliche Mitarbeiter, Universität zu Köln, Deutschland.

Liste der Veröffentlichungen

- H. A. Hosham, Fourth-Order Finite Difference Method for Solving Burgers' Equation, Applied Mathematics and Computation, 170 (2005), 781-800 (with I. A. Hassanien, A. A. Salama). This article is one of the "ScienceDirect TOP 25 hottest Articles (Oct. 2005).
 - H. A. Hosham, Analytical and Numerical Solutions of Generalized Burgers' Equation Via Buckingham's Pi-Theorem, Conidian Journal of Physics, 83 (2005) 1035-1049 (with I. A. Hassanien, A. A. Salama).
 - H. A. Hosham, Group Theoretic Method Analysis for Unsteady Boundary Layer Flow Near a Stagnation Point, Taiwanese Journal of Mathematics, 9 (2005) 639-660 (with I. A. Hassanien, A. A. Salama).
 - H. A. Hosham, An Implicit Finite-Difference Method for Solving the Transient Coupled Thermoelastic of an Annular Fin, Applied Mathematics – Information Sciences, 1 (2007), 79-93. (with A. M. Abd-Alla, A. A. Salama, M. R. Abd-El-Salam).
 - Hany A. Hosham, A Numerical Solution of Magneto-Thermo elastic Problem in Non-Homogenous Isotropic Cylinder by the Finite Difference Method, Applied Mathematical Modelling, 31, 8 (2007) 1662-1670 .(with M.R. Abd-El-Salam, A.M. Abd-Alla).
 - H. A. Hosham, Reduction to Invariant Cones for Non-smooth Systems, Mathematics and Computers in Simulation, 81, (5)(2011) 980-995. With (T. Küpper).
-

- H. A. Hosham, Invariant manifolds for nonsmooth systems, *Physica D: Nonlinear Phenomena*, to appear (2011), with (T. Küpper and D. Weiß).
- H. A. Hosham, The dynamics of bells as impacting system, *J. Mech. Eng. Sci.*, to appear (2011), with (T. Küpper and K. Dudtschenko).
- H. A. Hosham, Bifurcations in nonsmooth high-dimensional brake system, *Proceeding of 2nd International Symposium Rare Attractors and Rare Phenomena in Nonlinear Dynamics RA'11* May (16)17 - 20, 2011, Rīga - Jūrmala, Latvia.

Konferenzen und Netzwerktreffen Präsentationen:

- Egyptian Mathematics Society with Department of Mathematics: February 2002, Assiut University, Egypt.
- Workshop Bifurcations in Dynamical Systems with Applications: Department of Mathematics, Bielefeld University, May 19 - May 21, 2008.
- Workshop SDS2008, Structural Dynamical systems computational Aspects. Hotel Porto Giardino, Monopoli, Italy, June 17-20, 2008. "Reduction to an invariant two-dimensional "manifold" for a six-dimensional non-smooth Brake-system"
- Dobbiaco Summer School, ODEs with Discontinuous Right-Hand Side: Theory and Applications. DOBBIACO (BOLZANO - ITALY) JUNE 22 - 26, 2009.
- Oberwolfach Meeting on Nonsmooth System, November (2007, 2008, 2009).
- The 8th AIMS Conference on Dynamical System, Differential Equations and Applications, Dresden, Germany, May 25 - 28, 2010.
"On Dynamics and Bifurcations of 3D Piecewise Systems"
- The 8th AIMS Conference on Dynamical System, Differential Equations and Applications, Dresden, Germany, May 25 - 28, 2010.
"On Dynamics and Bifurcations of 3D Piecewise Systems"
- Workshop SDS2010, Structural Dynamical systems computational Aspects. Hotel Porto Giardino, Monopoli, Italy, June 8-11, 2010.
"Invariant cones for systems with sliding motion"

- 2nd International Symposium Rare Attractors and Rare Phenomena in Nonlinear Dynamics RA'11 May (16)17 - 20, 2011, Rīga - Jūrmala, Latvia.

” Bifurcations in nonsmooth high-dimensional brake system”